A SYSTEMS ENGINEERING APPROACH TO ENVIRONMENTAL
RISK MANAGEMENT: A CASE STUDY OF DEPLETED URANIUM
AT TEST AREA C-64, EGLIN AIR FORCE BASE, FLORIDA

THESIS

Charles M. Carter, Captain, USAF
Kristina M. Fortmann, Major, USAF
Stephen W. Hill, Captain, USAF
Robert M. Latin, Captain, USAF
Edward J. Masterson, Captain, USAF
Joseph A. Roh, Captain, USAF
Sujay R. Setlur, 2nd Lieutenant, USAF

AFIT/GSE/ENY/94D-1

DEPARTMENT OF THE AIR FORCE

AIR UNIVERSITY

AIR FORCE INSTITUTE OF TECHNOLOGY

Wright-Patterson Air Force Base, Ohio

AFIT/GSE/ENY/94D-1

A SYSTEMS ENGINEERING APPROACH TO ENVIRONMENTAL
RISK MANAGEMENT: A CASE STUDY OF DEPLETED URANIUM
AT TEST AREA C-64, EGLIN AIR FORCE BASE, FLORIDA

THESIS

Charles M. Carter, Captain, USAF
Kristina M. Fortmann, Major, USAF
Stephen W. Hill, Captain, USAF
Robert M. Latin, Captain, USAF
Edward J. Masterson, Captain, USAF
Joseph A. Roh, Captain, USAF
Sujay R. Setlur, 2nd Lieutenant, USAF

AFIT/GSE/ENY/94D-1

Accesion For

NTIS CRA&I	☒
DTIC TAB	☐
Unannounced	☐
Justification	

By _____

Distribution /

Availability Codes

| Dist | Avail and / or Special |
| A-1 | |

Approved for public release; distribution unlimited

AFIT/GSE/ENY/94D-1

A SYSTEMS ENGINEERING APPROACH TO ENVIRONMENTAL RISK

MANAGEMENT: A CASE STUDY OF DEPLETED URANIUM AT TEST AREA

C-64, EGLIN AIR FORCE BASE, FLORIDA

THESIS

Presented to the Faculty of the Graduate School of Engineering

of the Air Force Institute of Technology

Air University

In Partial Fulfillment for the Degree of

Master of Science in Systems Engineering

Charles M. Carter   Kristina M. Fortmann   Stephen W. Hill   Robert M. Latin
Captain, USAF   Major, USAF   Captain, USAF   Captain, USAF

Edward J. Masterson   Joseph A. Roh   Sujay R. Setlur
Captain, USAF   Captain, USAF   2nd Lieutenant, USAF

December 1994

Preface

Environmental restoration is an area of concern in an environmentally conscious world. Much effort is required to clean up the environment and promote environmentally sound methods for managing current land use. In light of the public consciousness with the latter topic, the United States Air Force must also take an active role in addressing these environmental issues with respect to current and future USAF base land use.

This thesis uses the systems engineering technique to assess human health risks and to evaluate risk management options with respect to depleted uranium contamination in the sampled region of Test Area (TA) C-64 at Eglin Air Force Base (AFB). The research combines the disciplines of environmental data collection, DU soil concentration distribution modeling, ground water modeling, particle resuspension modeling, exposure assessment, health hazard assessment, and uncertainty analysis to characterize the test area. These disciplines are required to quantify current and future health risks, as well as to recommend cost effective ways to increase confidence in health risk assessment and remediation options.

Usually the systems engineering approach is applied to the design of military-industrial systems. This thesis is unique in that it uses the systems methodology to tackle an environmental problem, rather than using conventional approaches outlined by the Environmental Protection Agency. Another unique aspect of this thesis is that the human health risk is probabilisticaly characterized, providing the decision maker with a more complete picture of potential risks and uncertainties. The result of the research is

ii

Last but not least, we extend special thanks to all our family and friends. Without their support, this thesis would not have been possible.

Table of Contents

List of Figures

List of Tables

Table   Page

AFB	Air Force Base
API	Armor Piercing Incendiary
ARAR	Applicable or Relevant and Appropriate Requirements
BIER	Biological Effects of Ionizing Radiation
CDF	Cumulative Density Function
CDM	Chief Decision Maker
CERCLA	Comprehensive Environmental Response, Compensation, and Liability Act
Ci	Curie
DI	Design Investigation
DQO	Data Quality Objectives
DU	Depleted Uranium
EPA	Environmental Protection Agency
F	Fahrenheit
FD	Finite Difference
FE	Finite Element
FORM	First Order Reliability Method
FS	Feasibility Study
ft	Feet
g	Grams
GW	Groundwater

HEAST	Health Effects Assessment Summary Table
HHEM	Human Health Evaluation Manual
hr	Hour
HRA	Health Risk Assessment
in	Inch
L	Liter
LFA	Lower Floridan Aquifer
LHS	Latin Hypercube Sampling
LOAEL	Lowest Observable Adverse Effect Level
m	Meter
min	Minute
MODFLOW	Modular Flow Model
MOE	Measure of Effectiveness
MT3D	Modular Transport Model
NCRP	National Council on Radiation Protection and Measurement
NESHAPS	National Emission Standards for Hazardous Air Pollutants
OA	Observational Approach
PDF	Probability Density Function
ppb	Parts Per Billion
ppm	Parts Per Million
PRG	Preliminary Redemption Goal

PTC	Princeton Transport Code
RA	Remedial Action
RCA	Radiation Control Area
RD	Remedial Design
RfD	Reference Dose
RI	Remediation Investigation
ROD	Record of Decision
S&GA	Sand and Gravel Aquifer
SAFER	Streamlined Approach to Environmental Restoration
sec, s	Second
TA	Test Area
TQ	Total Quality
UFA	Upper Floridan Aquifer
UNSCEAR	United Nations Scientific Committee on the Effects of Atomic Radiation
wk	Week
wt	Weight

AFIT/GSE/ENY/94D-1

Abstract

This case study used the systems engineering technique to determine human health risk and to provide risk management guidelines with respect to depleted uranium (DU) contamination at test area (TA) C-64 in Eglin Air Force Base (AFB), Florida. The United States Air Force (USAF) used TA C-64 to test warheads and new weapons concepts with solid and liquid explosives. Throughout the thesis, we applied a systems engineering methodology consisting of the following steps: defining the problem, setting objectives, developing alternatives, modeling alternatives, evaluating alternatives, selecting alternatives, and planning for implementation. We arrived at prudent decisions for each facet of our thesis using these steps. The case study combined the disciplines of environmental data collection, DU soil concentration distribution analysis, and uncertainty analysis to characterize the test area. Specifically, we performed kriging on available soil data to determine the present state of DU contamination around the radiation control area (RCA) which surrounds the target butt. We used the results from this analysis to determine the probability of contaminant infiltration into the groundwater and air transport pathways. The output of the TA's characterization supported the human health risk assessment. We performed Monte Carlo simulation analysis to determine residential and occupational health risks to humans with respect to present and future land use. Results from this analysis indicated that the carcinogenic risks ranged from approximately 10E-5 to 10E-10; the non-carcinogenic risks were statistically

insignificant. The main pathway of concern was the inhalation pathway for current occupational land use scenarios. We used this as a basis for risk management decisions. Various alternative solutions were explored for TA C-64. For the residential land use scenario, a trade off between two remediation options lead to the selection of a soil cleaning technique including volume reduction. For the occupational land use scenario, further air sampling was recommended to reduce the uncertainty in the analysis.

Assessing and managing risk will continue to be a complicated field of study, but we believe insights from the discipline of systems engineering can provide powerful resources to help work through this complicated process.

A SYSTEMS ENGINEERING APPROACH TO ENVIRONMENTAL RISK MANAGEMENT: A CASE STUDY OF DEPLETED URANIUM AT TEST AREA C-64 AT EGLIN AIR FORCE BASE, FLORIDA

I. Introduction

Assessing and managing environmental risk is a growing, complicated field of study. The government and private industry have wrestled with creating a reasonable method of doing this without overestimating the danger (leading to overspending) or underestimating the danger (leading to harmful effects). We believe a systems engineering approach can provide a good framework for risk assessment and management.

In this thesis, we will develop a systems engineering methodology for risk assessment and risk management and apply it to an environmental case study. Specifically, we will study depleted uranium (DU) existing on the test area (TA) C-64 at Eglin Air Force Base (AFB), Florida. In this chapter, we will first develop our theory of systems engineering and will then conclude with an overview of background information relevant to the TA C-64 case study.

1.1 Systems Engineering Background and Terminology

Systems engineering is an interdisciplinary field that has been applied to many

different areas of study. This field emphasizes a logical, systematic approach to problem-solving. Arthur D. Hall provided the first comprehensive work on the subject in the early sixties (32) and many other authors have modified or added to this early work. Almost all authors in the field use the same basic approach to solving problems, involving an iterative step-by-step process. Over the last thirty years, a number of tools and techniques to help with this approach have also been developed.

We centered our study on the seven-step systems engineering approach presented by Gil Mosard (49), with modifications as needed to fit our environmental application. The content of Mosard's steps are included in most authors' presentations (64), but we preferred the way he divided and worded his process. The seven steps are: *1) defining the problem, 2) setting objectives, 3) developing alternatives, 4) modeling alternatives, 5) evaluating alternatives, 6) selecting an alternative, and 7) planning for implementation.* We will now discuss each of these steps individually.

1.1.1 Defining the Problem. In this step, our goal is to provide a description of the situation so that we can set preliminary objectives and do an analysis. For this, we require two things: a good description of the system (or environment of interest) and a well-formulated problem definition.

System Description. A variety of techniques are available to help the systems engineer develop a description of the system. Two tools that are particularly helpful are interaction matrices (65) and concept maps (54). Major elements of this description include the boundaries of the system and the interactions between elements of the system.

Problem Formulation. Once the systems engineer has an understanding of the system, the specific problem needs to be defined and described as completely as possible. Hill and Warfield (37) developed 'twelve products of problem definition' as useful tools to help the systems engineer analytically and completely describe the problem. With a well-defined problem, the systems engineer can narrow the possible solutions and avoid tackling too much or too little in the final analysis. As the problem comes into focus, the systems engineer may also find it helpful to break the problem up into sub-problems as well as to isolate subjective from more objective elements.

This first step is not easy. In fact, a very large portion of the total work in applying the systems engineering process should be spent on this step alone. The problem definition should provide a good understanding of the conditions of the environmental area of concern and of the final goal of the project.

1.1.2 Setting Objectives. In this step, our goal is to develop measurable objectives against which we can compare the alternative solutions we will define in later steps. These objectives are essential to defining what is important to the solution and thereby allowing us to gear our research towards evaluating how different alternative solutions stack up against those measures. In other words, the problem definition helps us determine the right question, while objective setting enables us to determine the right answer. Two tasks are useful in setting objectives: develop a list of objectives and define specific measurements.

List of Objectives. When developing the objectives, the systems engineer should ensure that the desired solution is completely described. This step is a creative one;

brainstorming can be a useful tool to generate a full list of possible objectives. Once a comprehensive list of objectives is created, the systems engineer can eliminate redundant or unimportant ones. Also, if any of the objectives on the list are sub-objectives, or means to other objectives, the systems engineer can use these to develop a hierarchical structure of objectives. Hall (32) provides excellent procedural guidelines to help develop objectives and includes a list of certain kinds of objectives that appear frequently in engineering. This is a good source to check objectives against for completeness.

Measurements. Once the major objectives have been identified, the systems engineer should develop measurements or dimensions of these objectives. This is often difficult, but necessary in order to provide a standard way of comparing how well different alternative solutions meet the objectives.

Although we have only covered two steps, these two take a large amount of the work on any given project. After all, the better we know our problem and what is important to us in a solution, the easier it will be to select the best alternative.

Up to this point we have been concerned primarily with what the problem is and the reasons for solving it. We have sought to understand the current state of the environment as well as the desired state and which objectives we wish to pursue with the most intensity. Now, in the remaining steps, we will start developing, modeling, evaluating, selecting, and implementing alternative solution(s) to attain our objectives and sub-objectives.

1.1.3 Developing Alternatives. Mosard (49) describes this step as "developing a set of activities designed to accomplish an objective." Again, there are several steps

involved: list all possible alternative solutions and then reduce the list to a manageable size.

Generate List of Alternatives. The systems engineer can initially use brainstorming and other creative techniques to develop a list of all possible alternative solutions. In this step, the systems engineer wants to be uncritical and initially consider all possible solutions, so that he or she can be reasonably confident that the best solution is included on the list.

Reduce List of Alternatives. Once a comprehensive list has been developed, the systems engineer can go through and discard impossible solutions (outside of the known constraints) or solutions obviously dominated by other solutions according to the objectives. The systems engineer concludes the process by selectively weeding the possible solutions until only two to five solutions remain for each sub-problem. Beyond this number, analysis of the different solutions would be too time-consuming.

1.1.4 Modeling Alternatives. Now that we have generated a list of alternatives, we want to develop descriptive models that will predict how these alternatives will measure up against our objectives. Modeling is a vast field and is specific to the area of study, so we will not discuss specific modeling techniques here. However, there are some general principles that are helpful to direct the modeling process.

First, the systems engineer should do only the modeling necessary to analyze the elements of the alternatives relevant to the objectives. This is one strength of setting objectives early so that we can focus our modeling process. Second, the systems engineer should choose a model which provides the desired measurements of the objectives for

comparison with other alternatives. Finally, the systems engineer should optimize and refine the alternatives as they are modeled and areas of improvement become apparent.

1.1.5 Evaluating Alternatives. In this step, we want to evaluate the alternatives with respect to the objectives. This should be straightforward if the modeling and objective-setting steps have been done well. One additional consideration in this step is to estimate the probability of different future conditions. Often, alternatives will perform differently depending on the type of conditions present in the future environment. We want to take these different possible future scenarios into account as we evaluate the alternatives.

1.1.6 Selecting an Alternative. At this point in the process, we have several alternatives and we know how well they meet our objectives depending on the future conditions. From this data, we need to choose an alternative to implement. Although this is the role of the chief decision maker (CDM), the system engineer can provide some help. One important portion of this step is to assign relative weights to the different objectives according to their importance to the CDM. In the words of Mosard (49), "The primary task in selecting an alternative is to combine and structure the important evaluation information with the evaluation criteria weights of the CDM so that the decision-making process is precise, thorough, and explicit." Once the weights are developed, the systems engineer compares the alternatives and, along with the CDM, selects the best one.

1.1.7 Planning for Implementation. In this final step, we focus on the activities necessary to implement the selected alternative. Depending on the situation, this could

involve scheduling resources, communicating results of the solution, marketing the solution, etc. A variety of software packages are available to help with scheduling for implementation. This step is often overlooked and the engineering work is stopped after a 'study' has been done with no one to carry out the plan for implementation. The actual marketing and communicating of the results can be a bit more difficult, but is necessary, nonetheless.

1.1.8   General Systems Engineering Discussion. We would like to finish this discussion of the system engineering approach with a few comments.

First, systems engineering is an interdisciplinary field of study; therefore, it is important to consult with experts from the different disciplines involved throughout the process. Systems engineering provides a great framework for tackling problems, but expertise in specific areas is still a requirement for a good design.

Second, the steps of this process are highly iterative; as work continues on the project, the problem may need modification or the objectives may need clarification. This is to be expected.

Third, the seven steps we chose to discuss here provide a framework for the system engineering process. They can be modified as needed to fit our specific application. These steps are meant to be a helpful tool in the solution process, not an anchor around the neck of the systems engineer!

Fourth and finally, we conclude this section by noting that individual phases or stages of an engineering problem can also go through the seven-step process, which allows for focusing in on the best solution for each phase, rather than trying to generate a

more complicated overall solution. Hall presented this idea in his morphological box as shown, with steps slightly modified, in Figure 1.1. The figure shows the seven steps of the systems engineering process along one axis of a cube, the relevant disciplines along another axis, and the different phases of an engineering process along the third axis. Hall used this to describe how the system engineering process can be used for each different phase of a military-industrial problem, which may help discover more possible solutions than could be found by merely listing them. In other words, this box is just a graphical form of visualizing the various problem phases.

1.2   TA C-64 Case Study Background and Terminology

In this section, we provide an overview of background information relevant to the

Plan implementation
Select alternative
Evaluate alternatives
Model alternatives
Develop alternatives
Set objectives
Define problem

Program Planning
Project Planning
System Development
Production
Distribution
Operation
Retirement

Social Science   Engineering   Law   Medicine
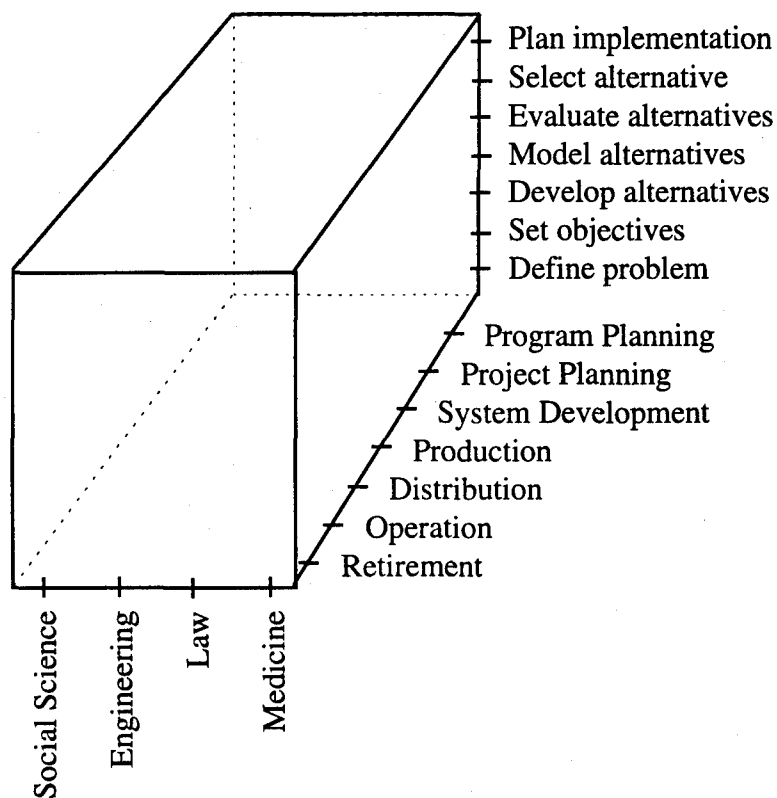
Figure 1.1 Morphological Box

TA C-64 case study. We include a brief description of the test area, including site operations and characteristics, and conclude with a discussion of the contaminant.

1.2.1 Site Description

Site Operations. The Terminal Effects and Experimentation Facility, TA C-64A/B/C is located on a 250-acre cleared area approximately 20 miles north of the main complex of Eglin AFB, situated in the panhandle area of northwest Florida. The test area is used for testing warheads and new weapons concepts with solid and liquid explosives. The test area we used for this study, TA C-64, has two gun bays and associated target butts used for projectile ballistics experiments (2).

The two target butts are located within a radiation control area (RCA) which is built up with a clay layer to bind any DU present, to provide a firm surface for heavy equipment to operate on, and to provide a level area around the gun butts. The smaller of the two gun butts is used with a single barrel gun which is laser boresighted for firing single rounds at a hardened target; the larger gun butt is used with a GAU-8 gun which fires up to 4200 rounds per minute into a sand pile. The smaller gun butt is completely enclosed except for an opening in the long narrow tube through which the bullets are shot. The larger gun butt has one opening approximately five feet across through which the bullets are shot into sand (27).

TA C-64 has been used for service life testing of 30 millimeter armor piercing incendiary (API) rounds since the late 1970's with a total of over 16,000 rounds fired to date (27). Each API round contains about 0.75 lb (340 g) of DU as a conventional munitions component.

The target butts are cleaned periodically by wetting down and sifting the sand to remove excess residue resulting from ballistics testing. Sand sifting operations are conducted with a wind speed restriction of five or less miles per hour. Airborne particulate counters are set up downwind of the operation, two within and three outside the RCA. Interviews with personnel on site during the sifting operations indicate that historically no plumes or puffs of dust have been measured or visually observed during sifting operations (27).

Site Physical Characteristics. Figure 1.2 shows an overview of the Eglin AFB land ranges, including TA C-64. A brief discussion of the geology, soil type, surface streams and weather are provided below. More detailed descriptions of these characteristics are provided in Appendix B.

Geology. The Eglin AFB geologic setting is one of coastal plain sediments (8:5; 12:2). These sediments consist of mainly sand, clay, limestone, and dolomite and range in thickness from 1500 ft in the northeast of Eglin AFB to greater than 2500 ft in the southwest of Eglin AFB. Below the coastal plain sediments is a thick sequence of limestones, dolostones, and shales.

At the surface is the *sand-and-gravel aquifer* made up of Holocene to Pliocene sands and Citronelle formation. Below the sand-and-gravel aquifer is the *Pensacola confining bed* made up of Miocene series soils which are Miocene coarse clastics, intracoastal formations, the Alum Bluff Group and Pensacola Clay. The Pensacola confining bed separates the sand-and-gravel aquifer from the next aquifer, the *Upper Floridan aquifer*, which consists of Tampa Limestone equivalent and Chickasawhay, also

of the Miocene series. The lowest aquifer, the *Lower Floridan aquifer*, is made up of

Ocala limestone of the Eocene series and is separated from the Upper Floridan aquifer by

the *Bucatunna Clay confining bed*. Finally the Lisbon and Tallahatta Formation, also of

the Eocene series, forms the lowest confining unit, the *Lisbon-Tallahatta confining unit*.

Surface water. There are numerous surface streams on Eglin AFB; the

Titi, Bull, and Ramer streams border on TA C-64. A study of nearby Turkey

Creek revealed that mean monthly flow varied little throughout the year which

was fairly representative of other streams in the study area (8). Little variation in

the mean monthly flow shows a close interaction between the surface streams and

groundwater.
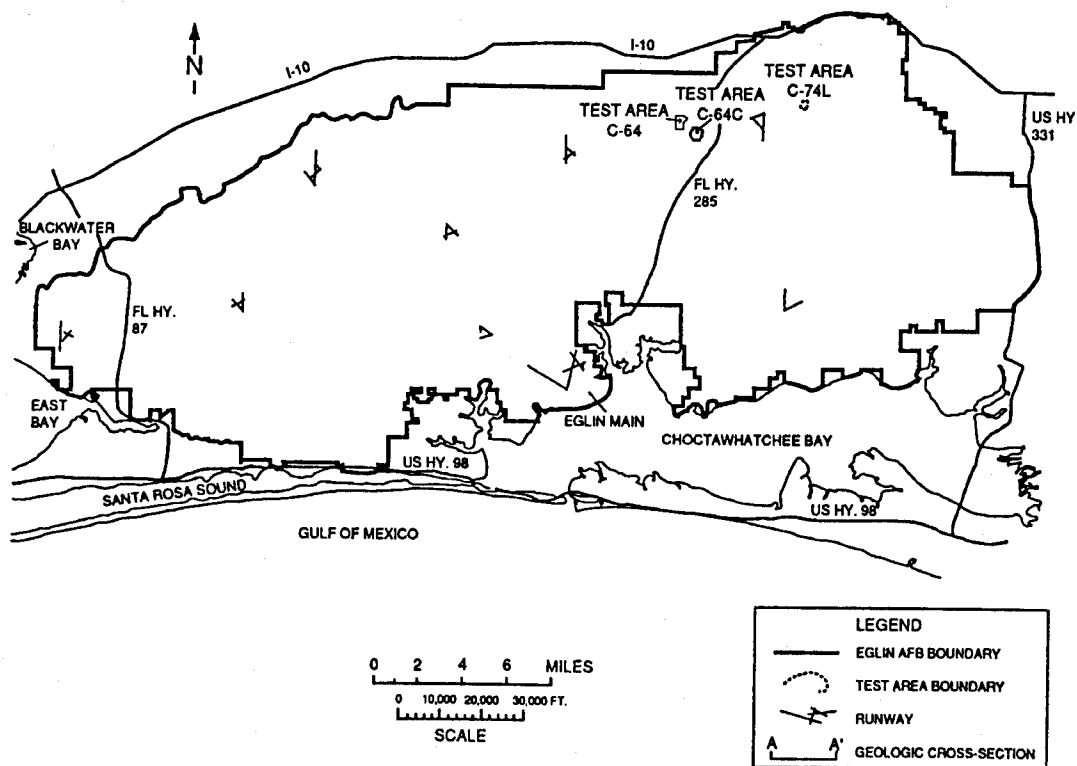
Figure 1.2 Eglin AFB Land Range (12)

Weather. As reported by Barr and others (8) the annual rainfall since 1941

ranged from a low of 31.01 inches in 1954 to a high of 95.43 inches in 1975 with an

average annual rainfall at the National Weather Service Station at Niceville, Florida of

64.1 inches. The mean wind speed ranges from 5.2 to 8.7 knots. Winds historically are

calm 11% of the time, less than 5 knots 45% of the time, less than 10 knots 85%, and less

than 15 knots 98.5% of the time (41).

1.2.2   Contaminant Description

Physical Characteristics. DU is a waste product from the enrichment process of

natural uranium. DU also has the same chemical and metallurgical properties as natural

uranium and is about three times as dense as steel (3).

DU is an effective penetrator because the kinetic energy it carries when fired is

transformed into high levels of thermal energy on impact. The slug becomes molten,

causing intense burning. It also will break up and oxidize producing shrapnel, and

uranium oxide dust particles which can be inhaled, ingested or implanted.(6).

Health Effects. DU can adversely affect the human body in two distinct and

significant ways. The first is the radiological effect in the form of low level radiation.

The second is the toxicological or poisonous effect of DU in its elemental state or by DU

compounds formed with other elements. Research on the health risks associated with DU

have mostly been radiological and well documented due to extensive studies by various

government agencies and the nuclear power industry (66). Toxicological effects of DU

on human health are not well defined and little research has been published on the subject

(1).

Contaminant in Local Area. Soil sampling in the vicinity of the RCA indicates that varying levels of DU contamination exist in the soil on the test area (12). Permit monitoring soil samples are taken once per quarter; water run-off samples are taken once per significant rain event. The soil samples are taken at surveyed points out to a 180 ft (55 m) radius from the target butt area; several surveyed points outside 180 ft (55 m) are sampled randomly.

1.3   Thesis Roadmap

This thesis will use the systems engineering methodology to develop a risk management plan for the Eglin AFB TA C-64 site for DU. In Chapter 2, we will review current environmental risk management methods and compare them to the systems engineering approach. In Chapter 3, we begin our application of systems engineering to the case study with an overall problem definition and setting of objectives. From here, the case study is broken into sub-problems which are discussed in Chapter 4, Site Characterization; Chapter 5, Risk Assessment; and Chapter 6, Risk Management. Chapter 7 presents our conclusions and recommendations with respect to the TA C-64 case study and the usefulness of applying the systems engineering approach to environmental risk management.

In this chapter, we develop the details of our environmental risk management problem, we look at other existing and proposed methodologies, and we contrast these methods with the systems engineering methodology.

2.1 Problem Details

2.1.1 What is the problem? Our purpose in this research was two-fold: to compare systems engineering to other environmental risk management methods existing or proposed today and then to apply systems engineering to a specific case study to demonstrate its effectiveness as an environmental risk management tool. The contaminated site we chose was test area (TA) C-64 located on Eglin Air Force Base (AFB) in Florida. The site is contaminated with depleted uranium (DU) as a by-product of ballistic rounds service-life testing. We discuss this test area in greater detail in the Introduction (Chapter 1).

We limited the scope of our investigation to organic and procedural methods for environmental risk management and did not consider law enforcement or mandate issues. Although comparison between SE and other existing or proposed environmental risk management methods will be conducted in a general sense, it is not our intent to evaluate the TA C-64 case study by methods other than the SE methodology. Evaluation by other methods may be material for further thesis work.

2.1.2 Why is this problem important? Exploring new methods of optimizing or refining environmental risk management could ultimately save resource and enhance

public trust. Environmental laws and the actual task of implementing risk management are highly complex and relevant to our society today. Below, we discuss both of these aspects of the problem to explain why this is an important issue to explore.

First, the United States has developed an extensive set of environmental laws to assist with the task of environmental risk management. For our purposes, we borrow the following definition for environmental law: "an organized way of using all of the laws in our legal system to minimize, prevent, punish, or remedy the consequences of actions which damage or threaten the environment, public health and safety." These laws encompass "a *system* of statutes, regulations, guidelines, factual conclusions, and case-specific interpretations which relate one to another" (5:1). Therefore, we note that there is a higher level of complexity inherent to the large and interrelated system of environmental law than for a simpler topic. In addition to being complex, environmental law also exhibits "a higher level of incertitude than most other areas because of its newness and changeability" (5:23).

Complexity and incertitude not withstanding, there are substantive mandates and enforcement methods which require private, business, and government organizations to be aware of and comply with environmental law (5:18). In fact, one of the difficulties faced by the site manager today is that compliance with the law yesterday does not prohibit liability under a changed law today. For example, under the Comprehensive Environmental Response, Compensation, and Liability Act of 1980 (CERCLA), companies have already been penalized by having to "perform extensive and costly

cleanups without regard to when the original disposal took place or the fact that a company may have exercised due care in handling hazardous materials" (5:267).

Secondly, the task of accomplishing environmental risk management is multidimensional and interactive, covering social and political as well as technical issues. In fact, the "critical questions of environmental practice...are often resolved not through scientific and engineering disciplines, but through argument and procedural determinations." (5:35). The site manager must be able to include all facets of these issues to provide an effective environmental risk management plan.

Thus, we conclude that the site manager faces a challenging task to be effective in developing environmental risk management options for a contaminated site. If systems engineering proves to be an effective methodology for environmental risk management, then it will be a useful addition to the existing arsenal of methods available to the site manager of a contaminated site.

2.2   *Existing or Proposed Solutions*

In this section, we will discuss methods currently recommended for environmental risk management. We will describe and critique these methods, as well as compare them to the systems engineering process.

2.2.1   *Techniques Currently Available to Solve the Problem.* We found a variety of laws which deal with aspects of environmental risk management. These laws cover a multitude of topics such as generating, handling, storing, reporting on, transporting, and cleaning up hazardous wastes, among others. We chose to profile

CERCLA as the law which most comprehensively deals with the process of environmental risk management at a contaminated site. CERCLA was designed for the "cleanup of inactive hazardous waste sites and the distribution of cleanup costs among the parties who generated and handled hazardous substances at these sites" (5:268). Although our case study involves an active site (still in operation) with a radionuclide contaminant (CERCLA excludes certain nuclear releases, (5:272)), we felt this law was the most comparable to the systems engineering methodology. We do not intend to imply that we consider the TA C-64 site as a potential CERCLA site.

In addition to looking at CERCLA as a representative of existing environmental law, we profile a recently proposed method for environmental risk management: the Streamlined Approach For Environmental Restoration (SAFER). SAFER is intended to meet the following objectives: enhance focus on planning and scoping activities; link data collection directly to decision-making needs; explicitly recognize and manage uncertainty; learn as planning and remediation proceed, and apply immediately; converge early on a remedy; and assure participation and consensus of key stakeholders (29). This method is currently being evaluated by the EPA at several sites.

Both of these approaches contain elements of systems engineering, but are highly tailored to the task of environmental risk management through remediation. We further describe these methods below.

2.2.1.1   CERCLA.   CERCLA defines two types of action for environmental risk management: removal actions which deal with environmental emergencies and remedial actions which deal with long range, permanent clean-ups.

Remedial actions have much greater administrative requirements than removal actions (5:275). We describe the more detailed remedial action here using a traditional engineering pattern of study, design, and build (15:1).

Study. The study phase of the remedial action starts with site identification and an initial evaluation. This phase entails a review of existing data, a site inspection if required, and possible further investigation if warranted (5:276). In this phase, the scope, objectives, budget, and operating assumptions are defined (15:1) and all state and federal applicable or relevant and appropriate requirements (ARAR) are identified.

As early as possible in the scoping process, preliminary remediation goals (PRG) are defined. PRGs generally come from either ARARs or from a health risk assessment (HRA) using readily available data. PRGs gives designers and decision makers a picture of long-term clean-up goals for use when evaluating possible remedial methods; these goals should be updated continually throughout the study and design process (57:1).

The study phase concludes with the remedial investigation (RI) portion of the remediation investigation/feasibility study (RI/FS) which, in turn, determines the scope of the remedial action (5:277). The RI portion of the study characterizes the extent and nature of the contaminants, the nature of the site, the type of threat posed by the contaminant to human health, as well as other features.

Design. The information in the RI is used during the FS portion of the RI/FS study to develop and evaluate a range of remedial alternatives. Developing alternatives starts with identifying potential treatment technologies and requirements. These alternatives are screened, with technological feasibility and action-specific ARARs in

mind, to reduce the number requiring detailed analysis while preserving a range of options. A process of detailed analysis further refines the alternatives using the EPA's nine criteria summarized in Figure 2.1 (57:4).

CERCLA Section 121 sets forth additional criteria specifying statutory clean-up level requirements for remedial actions as shown in Figure 2.2 (5:279).

Based on these criteria, an alternative is selected by the client and documented via an EPA Record of Decision (ROD). The ROD also finalizes the level to which the

```
                        ┌──────────────┐
                        │     EPA      │
                        │  9-Criteria  │
                        └──────┬───────┘
        ┌──────────────────────┼──────────────────────┐
┌───────────────┐      ┌───────────────┐      ┌───────────────┐
│   Threshold   │      │   Balancing   │      │   Modifying   │
│   Criteria    │      │   Criteria    │      │   Criteria    │
└───────────────┘      └───────────────┘      └───────────────┘
```

Threshold Criteria	Balancing Criteria	Modifying Criteria
1. Overall Protection of Human Health and Environment	3. Short-Term Effectiveness	8. State Acceptance
2. Compliance of ARARs	4. Long-Term Effectiveness	9. Community Acceptance
	5. Reduction of Toxicity Mobility, or Volume Through Treatment	
	6. Implementability	
	7. Cost	

Figure 2.1 EPA Nine Criteria
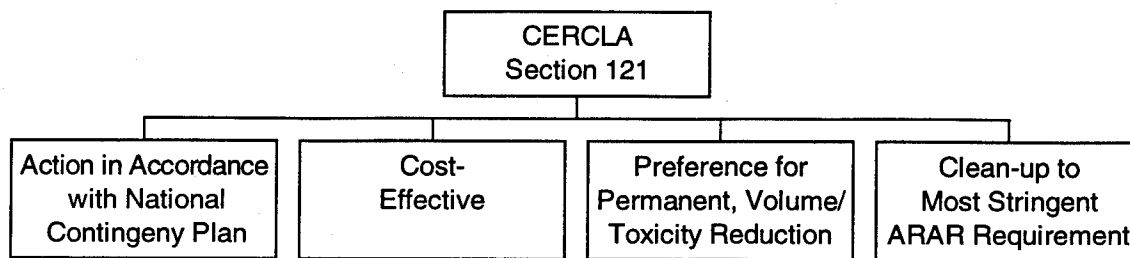
Figure 2.2 CERCLA Section 121 Criteria

contaminant will be cleaned. During the ROD process, there is an opportunity to enter

public comment into the process.

After a remedial action is chosen, the Remedial Design (RD) is started to provide

a detailed design of the physical cleanup process. Further data is collected from the field

and, if needed, further treatability studies are conducted; these tasks are referred to as the

design investigation (DI). At this point, supporting activities are started as needed.

Build. With the remedial action design in hand, the build step is started. This

step covers the actual construction and operation of the remediation activities.

Supplemental site investigations are conducted as needed and incorporated into the

remediation. Testing of the technology effectiveness would also be conducted as needed.

2.2.1.2   SAFER. SAFER is a methodology developed by a joint DOE-

industry team to combine the EPA's Data Quality Objective methodology of site

characterization and Observational Approach of site remediation.

DQO is a process originating from the Total Quality (TQ) approach to

management and decision analysis with an emphasis on facilitating customer-supplier

communications (53; 44). The DQO methodology identifies the environmental problem

and the decisions or actions required, defines the quantity and quality of data needed to solve the problem, and offers a mechanism for determining 'how clean is clean' (29). DQO primarily fits into the RI step of the current EPA methodology and is primarily a data acquisition/sampling planning tool. DQO addresses the following topics (53): the decision the customer needs the data to resolve, why the customer needs a specific type and quality of data, and how the customer plans to use the data to make a defensible decision.

The Observational Approach characterizes the site only enough to understand the most likely conditions expected to be encountered. Likely deviations from the expected are thought out and means to detect these deviations put in place during the remediation. If measured values do not match expected values, then the contingency plans are fully developed and implemented. This allows on the site management of the uncertainty inherent in remediation projects.

The SAFER approach was developed to logically combine the strong points of OA (managing uncertainty) and DQO (data collection planning) and provide site characterization and remediation faster, cheaper, and safer. SAFER is intended to meet the following objectives (29): enhance focus on planning and scoping activities; link data collection directly to decision-making needs; explicitly recognize and manage uncertainty; learn as planning and remediation proceed, and apply immediately; converge early on remedy; and assure participation and consensus of key stakeholders.

SAFER can be organized into three phases; planning, assessment and selection, and implementation.

Planning: The planning step makes a preliminary characterization of the site, develops remedial objectives, and identifies the most probable site conditions and possible deviations from these conditions. A decision rule is established to ensure data collection is coordinated with remediation decisions. Converging on the decision rule early in well understood remedial projects is one of the streamlining goals of SAFER, and a planned advance over conventional EPA thinking. The last important aspect of planning is to come to an understanding of acceptable uncertainty and tolerances on the decision errors by the stakeholders.

Assessment and selection: The assessment and selection phase of SAFER signals the start of field work. Sampling is conducted to sufficiently characterize the site in order to make informed risk-management decisions. As data is collected the remedial team starts evaluating possible decision rules for technology evaluation, linked with the quantity of data available. A manageable number of remedial technologies are evaluated in detail. At this point in the SAFER process the most probable site conditions are determined along with a list of reasonable deviations and contingency plans. A decision on the appropriate method of remediation is then made.

Implementation: The start of the implementation phase is a full development of the remedial design. Contingency plans are developed only in detail appropriate to the probability of occurrence, lead time required to implement, impact of occurrence and cost (29). Integral to this approach is developing a monitoring plan to detect deviations in sufficient time to manage them.

DOE is currently implementing SAFER at three sites in the US (30). By combining the stronger site characterization of DQO and management of uncertainty of OA the SAFER method holds great promise for improved contamination remediation.

2.2.2   *Performance of Techniques Currently Available to Solve the Problem*

Up to this point, we have summarized CERCLA as an example of current environmental law which deals with environmental risk management. We also discussed the SAFER method as a more recent approach now under test. We now comment on the performance of these techniques with respect to environmental risk management.

2.2.2.1   CERCLA. Several critiques can be made with respect to CERCLA. The following are based on those provided by Glickman (31:5-6).

Lengthy process. Since CERCLA was enacted in 1980, over 1,300 sites have been listed on the EPA's National Priority List (NPL). Of these, only 51 sites have subsequently been deleted from the list. This is due to the evolving technologies and processes involved, the long time spans covered by operation and maintenance requirements, and the shear complexity of many of the NPL sites. Never the less, the result is reduced public confidence in and support for the program (31:5).

Unreasonable clean-up requirements. CERCLA incurs unreasonably high expenditures of resources to achieve "far greater permanence and far less residual risk" than was previously required (5:279). This results from strict adherence to requirements for cleaning-up to residential standards regardless of proposed future land uses and from pressing ahead with clean-ups in the absence of efficient or cost-effective technologies.

To avoid or mitigate such liabilities, parties engage in expensive law suits and hiring of consultants, resulting in further EPA expenditure of CERCLA funds.

2.2.2.2 *SAFER*. SAFER is not well proven itself, but is based on two well-established methods. It has a very reasonable method of handling uncertainty "real time" instead of extensive up-front sampling and application of highly conservative safety factors like CERCLA. SAFER improves on OA by adding the sample of DQO, which is a much smarter limited-sampling theory than CERCLA recommends. It also incorporates iteration through the process as needed.

2.3 *Summary of Remaining Problem*

Although CERCLA provides a comprehensive method of dealing with environmental risk management as applied to site clean-up, it is less flexible and more cumbersome than systems engineering. CERCLA attempts to apply one comprehensive clean-up process as well as one set of strict clean-up requirements to all sites. The result is excess time and resources required to accomplish site clean-ups. While SAFER is a potential remedy to some of these problems, it is as yet an unproved method. Systems engineering has a proven track record in several other fields and is proposed as a third potential method of developing environmental risk management alternatives.

2.3.1 *Strengths of new approach.* Systems engineering is an iterative process, which allows the systems engineer to refine the problem, objectives, and alternatives throughout the project. This iteration occurs within and between steps of the process to allow optimization of the objectives and solutions. Systems engineering also allows

flexibility in the environmental risk management process. For example, the problem definition and objective criteria can be tailored to the specific requirements for each site. Also, analysis techniques and decision making tools from other disciplines are more easily integrated into the process. Finally, systems engineering is applicable to any site regardless of whether there are any legal requirements for environmental risk management. With liability for clean-up being legally interpreted as retroactive, system engineering allows the site manager to address environmental risk management before outside agencies become involved.

2.3.2   Application of new approach.   Our purpose in this research was two-fold. Overall, we compared systems engineering to other environmental risk management methods existing or proposed today. Specifically, we compared our process to CERCLA and SAFER as presented above. We then applied systems engineering to a specific case study, DU contamination at TA C-64, to demonstrate its effectiveness as an environmental risk management tool.

In this chapter, we apply the systems engineering process that we will be using for the remainder of the thesis. We begin with an overall definition of the problem and setting of objectives in order to lay a foundation for the rest of the case study.

3.1   Defining the Problem

We used a combination of systems engineering tools to accomplish this step. We started with an interaction matrix to identify the relevant elements, followed by a concept map to clarify the system element interactions, and concluded with development of a problem definition using the twelve products (37). We also noted that future factors may affect the final choice of a solution.

3.1.1   Interaction Matrix. The interaction matrix is a tool that enables the systems engineer to understand which elements of a system interact with each other. To begin understanding the problem and the systems involved, we generated an initial list of all the elements we thought to be involved in our system. From this list, we developed a matrix of their interactions with each other (see Figure 3.1). The 'X' symbols in the figure were placed in the appropriate squares to indicate the existence of interaction between column and row elements. This matrix served as an intermediate step in developing the concept map or a diagram of the system to attain a sense of scope.

3.1.2   Concept Map. Although the interaction matrix was helpful in describing specific interactions, the concept map presents this information in a format that is easier to understand (54). We took the information from the interaction matrix and displayed it

in a chart with connecting lines indicating the direct relationships. This technique was used to develop the concept map shown in Figure 3.2. The concept map acted like an undirected flow chart, which exposed the nature of our thesis (i.e., the best estimate at this stage for what needed to be done to attain the risk management goal). This map served as a good tool to show the web that bounded the elements of the study.

Although the concept map appears to have a logical flow, it is not intended to be a flow chart of the process; not all of the lines connecting relevant elements of the problem are unidirectional. For instance, the relationship between EPA regulations and sampling requirements is a directed relationship, i.e. the EPA regulations contribute to the sampling requirements but not vice versa. The relationship between the sample data and the models, however, is not unidirectional. The models use the initially available data to predict DU concentrations. The models themselves though, through uncertainty analysis or sensitivity analysis, may then indicate a need for additional samples in order to provide the level of detail required. This feeds back to the left on the concept map as additional sampling requirements. Therefore, during the systems engineering process, information related to elements of the concept map may flow back and forth several times before any conclusions are made.

3.1.3   Twelve Products.   Once we gained some understanding of the system and its elements, we used 'twelve products' of problem definition to develop a specific understanding of our problem (65:66).

Product 1. Well-Conceived Title. This should be a clear, easy-to-understand label to identify the effort. For our project, the problem was stated as follows: determine the

	Elements	1	2	3	4	5	6	7	8	9	10	11	12	13	14	15	16	17	18	19	20	21	22	23
1	Source Strength						X																	
2	Topography						X												X					
3	Geology							X																
4	Transport Mechanism						X	X											X	X				
5	Exposure Scenarios						X			X											X			
6	Sampling Requirements													X	X	X							X	X
7	GW Flow Model								X				X										X	X
8	GW Mod Sens. Analysis											X												
9	Land Use																				X			
10	DU Remediation Tech.																X							
11	Future Sampling Plan																X							X
12	GW Model Output																				X			
13	Site History																							
14	EPA Regulations																X							
15	SAFER																							
16	Risk Management																				X			
17	DU Surf. Model Output																		X		X			
18	DU Surf. Model																						X	
19	Uncertainty																					X	X	
20	Risk Assessment																					X		
21	Biological effect of DU																							
22	Available Samples																							X
23	New Samples																							

GW: Groundwater

Figure 3.1 Interaction Matrix for TA C-64 Environmental Analysis
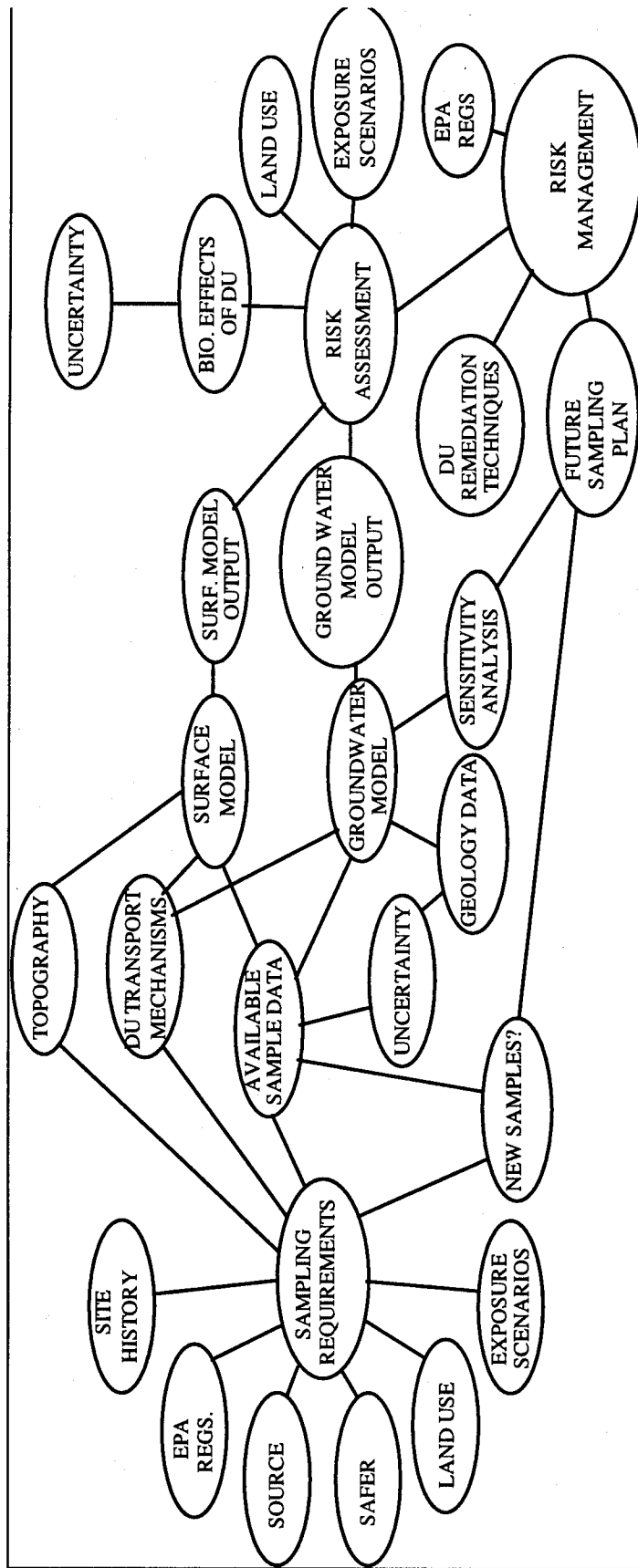
Figure 3.2 Concept Map for TA C-64 Environmental Analysis

health risks associated with TA C-64 in its current state, provide management alternatives to reduce uncertainties and potential DU exposure based on the current land use plan, and limit these risks in the future.

Product 2. Descriptive Scenario.. This provides a detailed understanding of the background, previous solution attempts, and motivation to address the problem. For the top-level problem definition being developed in this chapter, we provided sufficient background in the Introduction (Chapter 1). Further description of the scenario occurs in subsequent chapters.

Product 3. Relevant Disciplines. This covers what knowledge areas are required for the process. In our case, we identified the following disciplines: geology, hydrology, mathematics, physics, nuclear science, health physics, risk assessment, and risk management.

Product 4. Scope. Scope is defined as the limitations of the project, symptoms that will be ignored, and related problems that will not be addressed. This product includes identifying future environmental factors which might effect our solution (environmental meaning outside the system in this case). Scope could include changes in environmental laws and regulations; changes in the land use of the range and of areas near the range; and changes in the levels of risk acceptable to the public. We defined the scope for our case study as follows.

1) limit sources of DU to those originating from the target butts and vicinity;

2) address only DU contamination in the sand-and-gravel aquifer, air and soil;

3) apply health risk assessment exclusively to humans;

4) use existing biological data to determine human response to DU exposure; and

5) consider residential land use as the only potential future factor.

Product 5. Societal Sectors. This is primarily relevant to large scale engineering projects. We considered the following societal sectors to have a potential impact or interest in our case study: the local communities, regulators, scientific community, and the military.

Product 6. Problem-Solving Actors. These can be identified as individuals and groups who will be involved in the decision making process. We limited the list to the following problem-solving actors: our sponsor, our advisor, and ourselves.

Product 7. Needs. This product explains generally what is meant by an effective solution; the needs should not be task oriented but functionally oriented. For this problem, the solution we are looking for addresses the following needs:

1) characterization of the DU contamination at TA C-64,

2) assessment of human health risk due to the DU contamination,

3) generation of a plan to mitigate risk to acceptable levels, and

4) description of the statistical confidence in the results.

Product 8. Alterables. Alterables are defined as those things that the designer is able to change or control. We developed the following potential alterables which could affect our solution:

1) future sampling options (i.e. type, location, frequency),

2) site operations (i.e. worker exposure time, weather restrictions),

3) site access (i.e. restrict to public), and

4) remediation technology (i.e. physical barriers, clean up).

Product 9. Constraints. Constraints are those things that the designer cannot control. We identified several overall constraints to our study as listed below:

1) current operation of TA will continue for the foreseeable future,

2) the solution must obey laws of handling and transporting DU or uranium waste, and

3) future residential populations must have complete access to the site for full lifetime.

Product 10. Relevant Problem Elements. This product provides some initial partitioning of the problem into related sub-problems. We identified three basic sub-problems:

1) site characterization,

2) risk assessment, and

3) risk management.

Because each of these sub-problems involves detailed consideration, we decided to attack each one with its own seven-step systems engineering process.

Product 11. Subjective Elements. This product provides a preliminary identification of subjective elements that can influence the project. We identified one major element which we considered to be subjective: the level of acceptable risk.

Product 12. Relevant Element Interactions. This identifies the major interactions between the various products above, particularly needs, constraints, actors, and alterables. We did not find this product necessary for our overall problem definition.

3.2   Setting Objectives

For the overall problem, we developed a list of objectives that defined our ideal solution. After several iterations through the systems engineering process, we developed the objective criteria presented in Figure 3.3.

As can be seen in Figure 3.3, our overall goal was to develop the best risk management plan for TA C-64. As we can see, site characterization is a sub-objective to risk assessment, which in-turn, is a sub-objective to the risk management objective. Specific sub-objective measurables for the site characterization and risk assessment sub-problems are developed in the appropriate sections of Chapters 4 and 5. Objective measurables for the overall solution of risk management are developed in Chapter 6.

```
                          ┌──────────────┐
                          │  Best Risk   │
                          │  Management  │
                          └──────────────┘
┌──────────────┐ ┌──────────────┐ ┌──────────────┐ ┌──────────┐ ┌──────────────┐
│Widely Accepted│ │Widely Accepted│ │  Best Risk   │ │  Least   │ │    Best      │
│  Risk Level   │ │    Method     │ │  Assessment  │ │Resources │ │ Effectiveness│
└──────────────┘ └──────────────┘ └──────────────┘ └──────────┘ └──────────────┘
┌──────────────┐ ┌──────────────┐ ┌──────────────┐ ┌──────────┐ ┌──────────────┐
│  Compatable   │ │Widely Accepted│ │  Best Site   │ │  Least   │ │    Least     │
│ to Situation  │ │    Method     │ │Characterization│ │  Cost   │ │    Time      │
└──────────────┘ └──────────────┘ └──────────────┘ └──────────┘ └──────────────┘
                  ┌──────────┐ ┌──────────┐ ┌──────────────┐
                  │  Least   │ │  Least   │ │    Best      │
                  │  Cost    │ │  Time    │ │ Performance  │
                  └──────────┘ └──────────┘ └──────────────┘
```
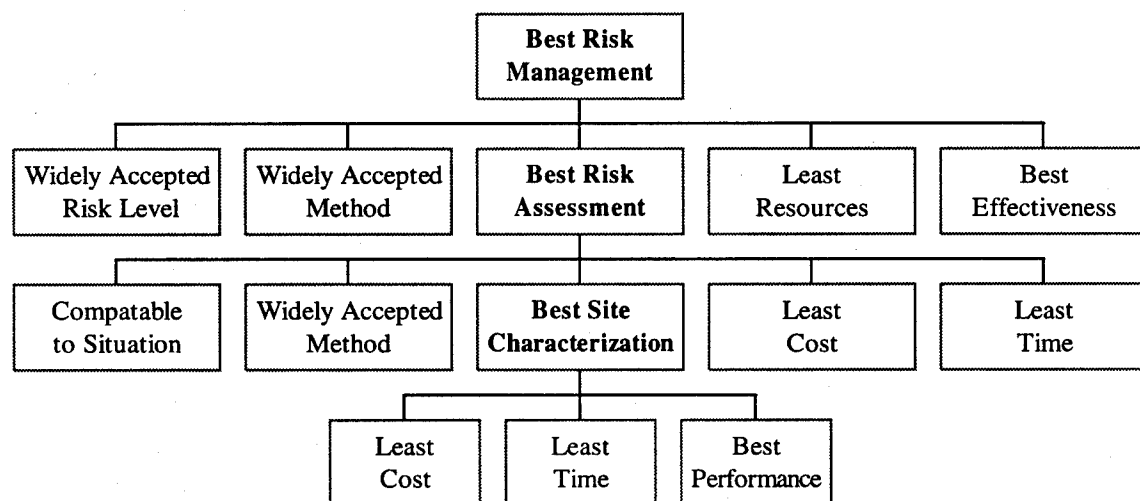
Figure 3.3 Overall Objective Criteria

3.3 Case Study Roadmap

We have now developed an understanding of our system, the problem we want to solve, and the objectives we wish to attain. At this point the study breaks down into a morphological analysis which means to decompose a general problem or system into its basic variables.

Hall's morphological box from the Introduction was modified to fit our application. We used two of the axes, systems engineering steps and project phases, and applied it to our case study. The third axis collapsed to the single discipline of environmental risk management. We also modified the project phases from a typical military-industrial problem to reflect our three sub-problems: site characterization, risk assessment, and risk management. This activity matrix is shown in Figure 3.4.

Hall described his analysis in the following manner: "One of the distinct merits of morphological analysis is that it helps to find more solutions than could be found by
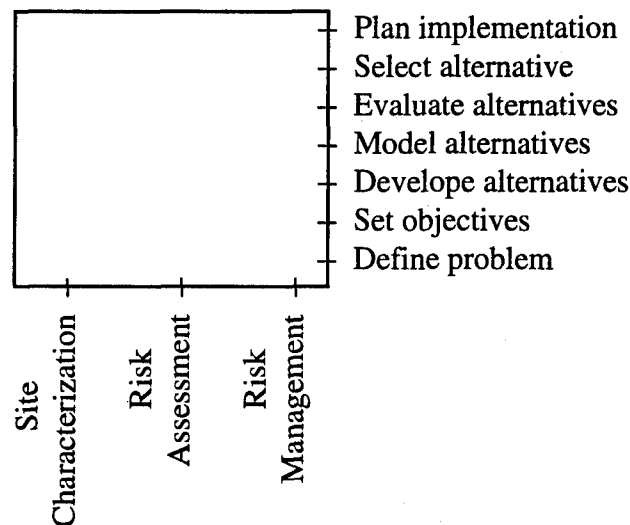
Figure 3.4 Environmental Risk Management Morphological Interaction Matrix

merely listing them" (33). The three phases we chose for analysis seemed the best way to decompose the problem for our analysis. Additional phases could be added or some phases could be subdivided; the point is that this matrix allows us to find individual solutions for each phase. The planning for implementation step of each phase will be the representation of the solution of that phase for input to the next. Now we will develop the seven step process for each phase starting with site characterization in Chapter 4.

Site characterization is important in laying the foundation for the human health

risk assessment and risk management. We sub-divided the site environment into three

areas of concern for DU contaminant analysis: soil, groundwater, and air (Figure 4.1).

This chapter is divided into three sections. The soil section characterizes the

present state of DU contamination in the soil and its output supports the groundwater and

air analyses. The groundwater section analyzes the amount of DU contaminant that

penetrates into the groundwater. Finally, the air section characterizes the amount of DU

resuspended in the air over the test area. The outputs of these three sections are expressed
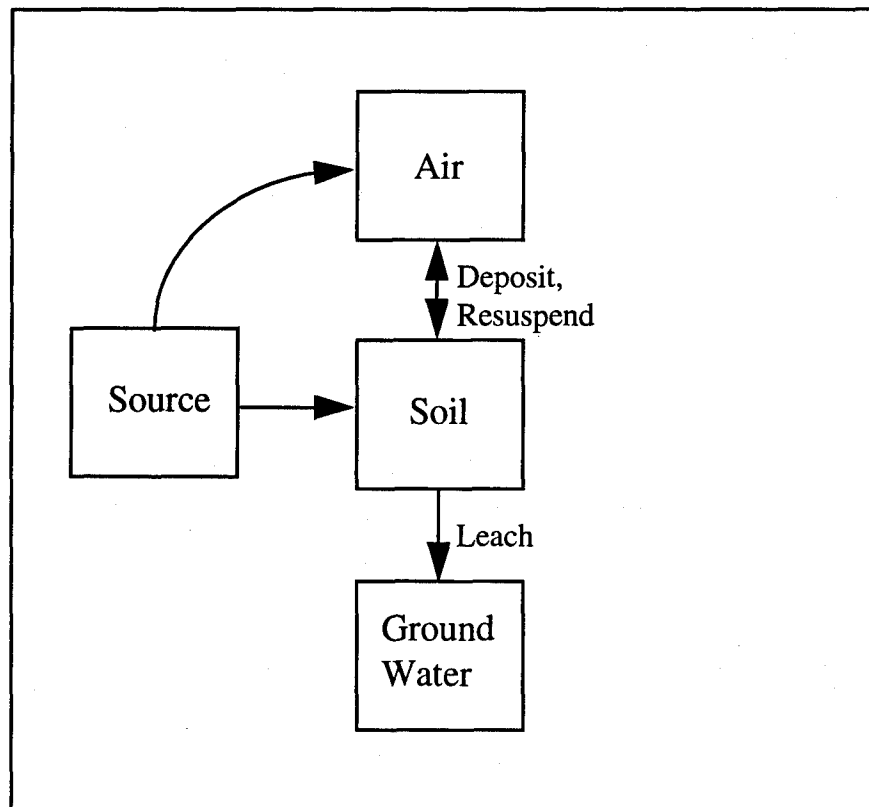
Figure 4.1 DU Areas of Concern

in terms of probability density functions (pdfs) describing DU concentrations and serve as inputs into the health risk assessment presented in Chapter 5.

4.1   Soil

In this section, the sub-problem of characterizing the DU concentration in the soil on the surface of TA C-64 is addressed. The method that best met our objectives for conducting this soil analysis was selected and then used to obtain the desired information.

4.1.1   Defining the Problem.   Several tools were used to select a model for developing concentration levels of DU in the soil. Of the twelve products developed in Chapter 3, we further detailed the *descriptive scenario*, *need* and *constraint* products for this section.

Product 2. Descriptive Scenario.   Soil sampling for DU at TA C-64 began in August of 1978 (12). Since the most likely area for elevated levels of DU was near the RCA, a sampling scheme was devised which has a higher sampling density in this area. The primary purpose for starting the sampling program was to meet permit compliance requirements. This sampling scheme was not conducive to simple statistical analysis, however, since the average of the samples was not an accurate indicator of the average concentration in the region.

TA C-64 sample locations were marked by cement markers and stakes along lines radiating outward from the target butt in a pattern resembling spokes of a wheel (see Figure 4.2). Radial lines were numbered clockwise from north. The stakes were placed 60 ft (18 m), 180 ft (55 m), and 300 ft (91 m) from the center of the larger target butt

along odd numbered radials and 120 ft (37 m), 240 ft (73 m), and 360 ft (110 m) from the

target butt along even numbered radials. The sample points are labeled with a distance

number and direction number. For example, sample point 2-4 is 120 ft (37 m) (or 2 times

60 ft) from the target butt in direction 4. Sample points 0-0, 1-1, 1-3, 1-5, 1-15, and 2-2

are located inside the RCA.

Soil samples were measured in units of micrograms of DU per gram of soil (μg/g)

through 1986. Starting in 1987, the measurements were in units of picoCurie (pCi) of

emitted radiation per gram of soil (pCi/g). The accuracy of the measurements was on the
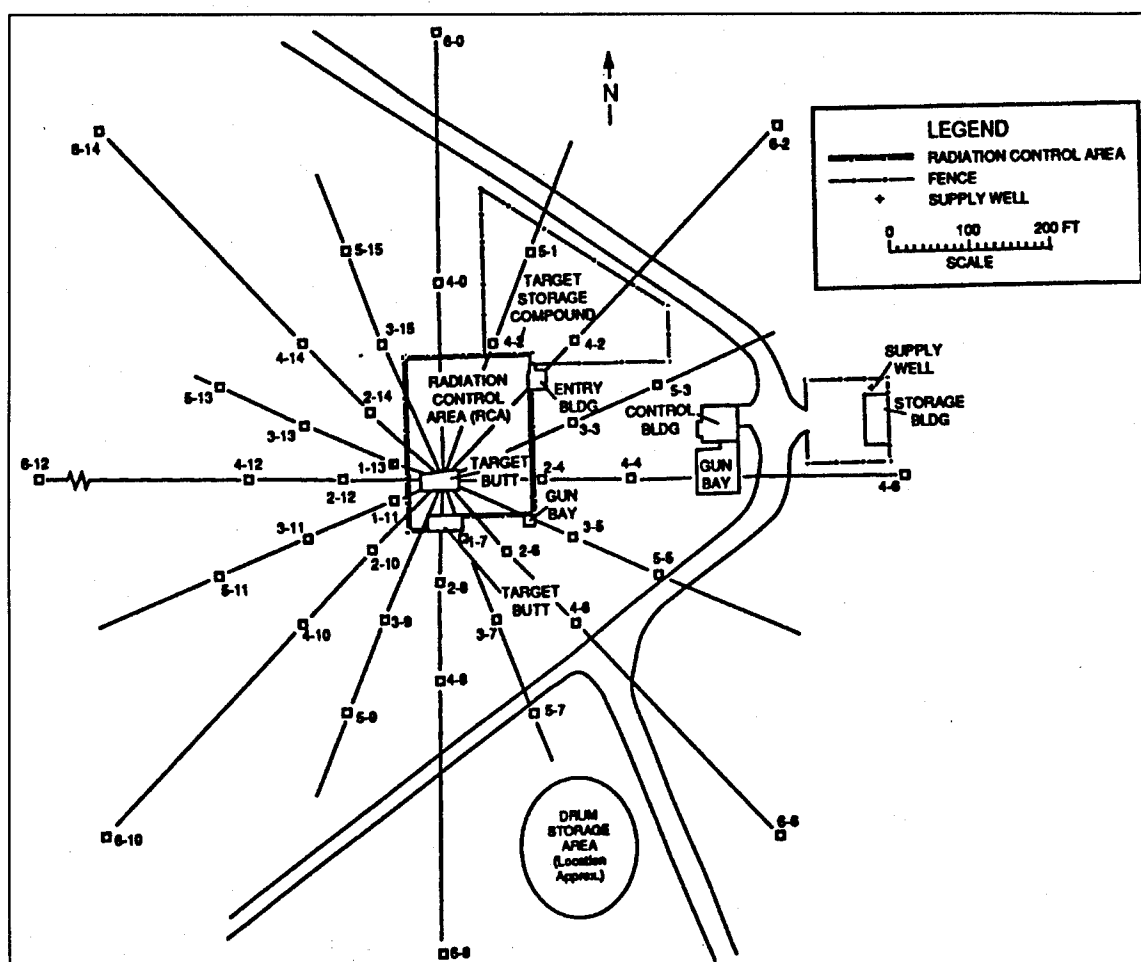
Figure 4.2 Surveyed Sample Locations at TA C-64

order of 2 to 3 micrograms or 1 pCi. We converted all data to pCi/g for our soil analysis. All values originally reported as less than 1.00 pCi/g (i.e. background) were set equal to 1.00 pCi/g. This was a purposefully a conservative estimate to allow for the experimental error and accuracy in the measurements.

For the period of October 1979 to January 1989, sample data were available out to 180 ft (55 m). Starting in April 1989, sample data were available out to 360 ft (110 m), although for two dates, the data were available only out to 240 ft (73 m). Generally speaking, sample radiation levels beyond 180 ft (55 m) were at or near background levels. Naturally occurring background levels in the area were approximately 1 pCi/g (50). After 1982, sampling within the RCA was discontinued as it was recognized that this area was contaminated with levels of DU to a level that clearly required control (above 35 pCi/g (25:18)). The last set of samples in the RCA showed an average concentration of 3028 pCi/g.

Prior to 1984, samples were measured once per year. After this, samples were taken roughly quarterly, except for 1984 and 1992, when only three samplings were completed. The most recent data we used were from March of 1994.

The full set of sample data used in this analysis is presented in Appendix A.

Product 7. Needs. The method chosen for soil surface DU concentration characterization needed to provide sufficient detail to support the health risk assessment. As the health risk assessment requirements developed, we refined this need to specify that the concentration characterization be statistically based and include confidence intervals.

As the site characterization analyses progressed, we added the need to predict the level of DU in unsampled areas to support these models.

Product 9. Constraints. We constrained our model to using available data, i.e. no additional sampling would be completed to support the model. Because existing data on DU concentrations and transport mechanisms were limited, no temporal analysis was done to predict future DU concentrations.

4.1.2   Setting Objectives. We considered the following objective criteria in determining which of the candidate models to select:

1) best ability to accurately predict DU concentration,

2) least time to acquire or develop the model,

3) least time to learn the model,

4) least cost to purchase model, and

5) least cost related to using the model.

4.1.3   Developing Alternatives. Given our stated objectives, we first developed a simple, back-of-the-envelope, calculation alternative using conservative assumptions. If these *rough order calculations* met our objectives, then further detailed analysis would not be necessary. Next, we developed more complex alternatives as described below for predicting contaminant values at unknown locations based on sampling data.

Polynomial surface approximation (62). With this method, a polynomial surface is found using a least squares method. This method provides an estimate for values between sample points; however, it does not provide any confidence bounds on the results.

Method of polygons (62). With this graphical technique, polygons are constructed around each sample point. The polygons are smaller in heavily sampled areas and larger around isolated sample points. With this technique, the predicted value at points in each polygon is equal to the value of the sample point within the polygon. Although this method has been used with reasonable success in predicting the average concentration over a block, it is not particularly accurate for point predictions. Additionally, this method does not provide any statistical confidence limits.

Weighting factor (20). Weighting factors are developed for each sample point in determining the value at an unknown point. In general, large weighting factors are assigned to sample points near the point where a prediction is desired, and small weighting factors are assigned to sample points far from that point. The sum of the weighting factors should equal unity. Schemes for determining weighting factors have been based on the distance each sample point is from the prediction point, as well as the distance squared and other algebraic relations. These weighting schemes are based on engineering judgment.

Kriging (20). In 1951, a South African mining engineer named D.G. Krige began developing empirical methods for predicting ore reserves based on sampled data. His work was expanded on by G. Matheron, who in 1963 introduced a spatial prediction method he called 'kriging' (rhymes with bridging). The mathematical theory associated with kriging was developed by Matheron at the Fountainbleau Mining School in France, under the heading of 'regionalized variables' (42). Like some of the previously mentioned methods, kriging involves determining weighting factors for each sample point

which are used to make a prediction at a point where the value is unknown. The weighting factors are determined after a thorough examination of the spatial correlation between sample points and result in the best linear unbiased estimator for the concentration at unknown points (where 'best' is defined as having the minimum error variance). Thus, at each location where it is desired to know the concentration of DU, kriging provides an unbiased prediction as well as the variance in the prediction.

4.1.4 Modeling, Evaluating, and Selecting Alternative(s). Often when using the systems engineering process, there is no candidate solution (alternative) which is clearly superior to the rest. If this is the case, the alternatives are evaluated and ranked based on the established objectives. When there is one alternative which is equal to or better than the other alternatives in each category of the objective criteria, it is unnecessary to perform this comparison. This is referred to as a *dominant solution.*

For the soil analysis, kriging is a dominant solution. The kriging method was the only one which met all the identified needs. Additionally, kriging could be performed on the currently available data, so no additional samples were required which met one of our constraints. The kriging analysis also would not require any purchase of software, so there was no cost associated with this option.

4.1.5 Planning for Implementation. Before we develop the kriging model for our soil sample data, a discussion of the terminology and assumptions associated with semi-variograms (a tool used in kriging) and kriging is in order.

Background/Theory: Let $z(\mathbf{x})$ represent the concentration of DU at position $\mathbf{x}$ ($\mathbf{x}$ is a two dimensional vector representing East/West and North/South distances from the

target butt). At each sample point, the value of the function z(**x**) is known. In kriging, information on the spatial relationship between the sample points and the values at these points, are combined to create a function known as the semi-variogram. The semi-variogram is a function which describes the variance of the difference in value between two points, Var(z(**x**)-z(**y**)), and is sometimes called the spatial variation function. For example, consider the set of samples shown in Figure 4.3.
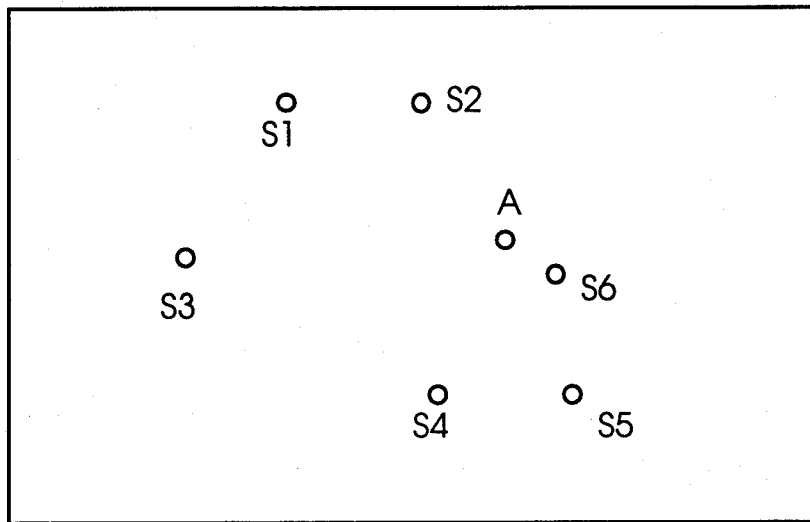
Figure 4.3 Example Sample Points

In this example, we know the value at each of the samples points, S1-S6, and would like an estimate of the value at position A. It is reasonable to assume that the value at position A would not be very different than that at S6, since the two points are close to each other. If the observed value at S3 were different from that at S6, we would expect the value at S3 to have some influence on the estimate at point A, but not as much influence as point S6. In other words, the difference in value between two positions in

the area of concern depends on the distance between the points and their relative orientation.

Let 'h' represent the distance and relative orientation between points. In statistical terms, the distribution of the difference in value between two points depends only on h. Therefore, the mean difference in sample value, m(h), and the variance of the difference in sample value, γ(h), are functions of h only. This assumption, that the two parameters depend only on the relative distance and orientation, is referred to as the 'intrinsic hypothesis' (20).

If we have a set of sample pairs with the same h (for example, the pairs S1-S2 and S4-S5, which are at the same distance apart with both pairs oriented in an East/West direction) then we can determine an experimental value for m(h) and γ(h) for that specific h. With n pairs of points at a specific value of h, we can write Equations (4.1) and (4.2):

$$m(\mathbf{h}) = \frac{1}{n} \sum [z(\mathbf{x}) - z(\mathbf{x}+\mathbf{h})] \qquad (4.1)$$

$$\gamma(\mathbf{h}) = \frac{1}{2n} \sum [z(\mathbf{x}) - z(\mathbf{x}+\mathbf{h})]^2 \qquad (4.2)$$

If m(h) equals zero, then we expect no difference in value at a distance h apart. In other words, there is no 'trend'. It is convenient mathematically if m(h) equals zero, however this is not always the case. There are techniques for dealing with trend which we will discuss later, but for now let us assume there is no trend and further discuss the semi-variogram. Note, if the two in the denominator of Equation (4.2) is brought to the left side, then the quantity 2γ(h) is equal to the variance (as a function of h) and is called

the variogram. The equations involved in the kriging analysis use $\gamma(\mathbf{h})$ so it is easier to just find the semi-variogram.

Semi-variogram Model: Ideally, a semi-variogram should start with a value of zero, since we expect that if we sample two points a distance zero apart, we would obtain the same value. The semi-variogram will increase as **h** increases until a distance is reached where the value at one point is no longer affected by the value at another point. This distance is called the range of influence, usually denoted by 'a'. The semi-variogram value at this point is called the sill value and is usually denoted by 'C'.

Several 'classical' semi-variogram models have been developed. Kriging is normally done by fitting one of the classical semi-variogram models to the experimentally obtained semi-variogram. The three most common classical semi-variograms are the spherical model, the exponential model, and the Gaussian model (see Figure 4.4).

——— =spherical model   —— —— =exponential model   —— — =Gaussian model
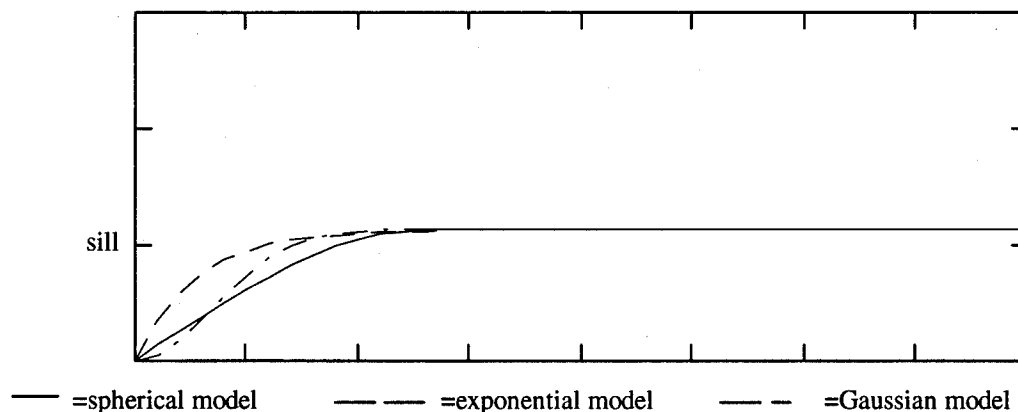
Figure 4.4 Classical Semi-Variogram Models

The *spherical model* is defined by Equation (4.3):

$$\gamma(\mathbf{h}) = C \cdot \left[\frac{3\mathbf{h}}{2a} - \frac{\mathbf{h}^3}{2a^3} \right] \qquad h \leq a$$

$$\gamma(\mathbf{h}) = C \qquad\qquad\qquad h \geq a \tag{4.3}$$

where the sill 'C' is equivalent to the ordinary sample variance and the range parameter 'a' can be found by extending a line along the initial slope of the experimental semi-variogram until it reaches the sill value. This distance is said to be 2/3 of the range, so consequently 'a' is 3/2 of this distance. In this model, the semi-variogram value rises quickly and then levels off beyond the range of influence. Beyond the range of influence, the semi-variogram value equals the sill value. This model was derived on theoretical grounds (20) and is widely used.

The *exponential model* is given by Equation (4.4):

$$\gamma(\mathbf{h}) = C \cdot \left(1 - e^{\left(\frac{-\mathbf{h}}{a} \right)} \right) \tag{4.4}$$

where the parameter 'a' is found by setting '3a' equal to the distance where the semi-variogram value is 95% of the sill. This model rises more slowly than the spherical model and never quite reaches the sill value. The sill is approached asymptotically as **h** approaches infinity.

Another commonly used model is the *Gaussian model* (42). The Gaussian model is given by Equation (4.5):

$$\gamma(\mathbf{h}) = C \cdot \left(1 - e^{\left(\frac{-\mathbf{h}^2}{a^2} \right)} \right) \tag{4.5}$$

where 'a' is $1/\sqrt{3}$ of the distance of 95% of the sill. Like the exponential model, this model reaches it's sill asymptotically.

These purely graphical techniques have been defended with the evidence of much empirical work (42). Since these techniques have been used for predicting the concentration of ore, which was subsequently mined, the accuracy of the predictions can be evaluated. This method of direct checking of the estimations has led to the acceptance of these graphical techniques.

There are several properties of the sample data which can effect the kriging analysis: nugget effect, isotropy, stationarity, lognormal data, and random variation. We discuss these effects below. We also provide an example to illustrate some of these effects.

Nugget Effect. Occasionally, construction of an experimental semi-variogram will indicate that the variance at a distance zero is not zero. Although no pairs of points were compared at zero distance, the semi-variogram constructed on the data may have a classical semi-variogram shape but intersects the 'y' axis at some number above zero (see Figure 4.5).

This indicates that observed values do not always gradually change in value as one moves a short distance. In mining, this is usually due to nuggets of desired material affecting the sample results. If the nugget effect is equal to the sill value, then the semi-variogram looks like a straight line. This is equivalent to saying that knowing the value at one point does not help us predict the value at other points nearby any better than
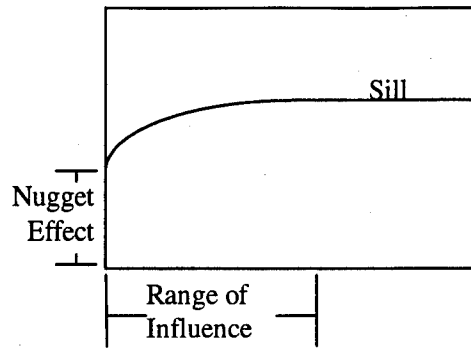
Figure 4.5 Nugget Effect on Semi-Variogram
Shape

information based on the entire sample variance. In this case, we have gained no

information by conducting a spatial analysis of the data.

  Isotropy. The equations in kriging are simplified if the semi-variogram

depends only on the distance between two points and not on the direction. That is, if we

obtained the same semi-variogram by analyzing all points that are oriented east and west

of each other, as we obtained by analyzing all points north and south of each other, then

this condition is known as 'isotropy'. It indicates uniformity in every direction. In some

cases, it is inappropriate to assume isotropy. If, for example, one is interested in the

salinity of the water in a river which runs south and joins the ocean. The difference in

values 100 feet apart in a north-south direction would likely be higher than the difference

in value between two points 100 feet apart in an east-west direction.

  Stationarity. Another important concept in the application of kriging is

stationarity. A stochastic process is said to have stationarity of order two if it has a

constant mean and it covariance function, $C(\mathbf{x},\mathbf{y})$, depends only on the difference vector $\mathbf{h}$

equals (**x-y**) and not on the particular **x** and **y** chosen (42). The variogram is directly

related to the covariance function by Equation (4.6):

$$\gamma(\mathbf{h})=C(0)-C(\mathbf{h}) \qquad (4.6)$$

where C(0) is the covariance of two points a distance zero apart. Thus, in a case with no

trend where the mean is constant, stationarity of the second degree implies that the semi-

variogram applies equally to the entire region which will be analyzed. This is also called

'intrinsic stationarity' (42).

Random Variation: The value z(**x**) at each point can be thought of as having two

components: $\mu(\mathbf{x})$ which is the expected value at that point and $\varepsilon(\mathbf{x})$ which is a random

variation about that point, such that z(**x**) equals $\mu(\mathbf{x})$ plus $\varepsilon(\mathbf{x})$. If $\mu(\mathbf{x})$ is constant, then

there is no trend and the differences in values at different positions are only due to the

random component $\varepsilon(\mathbf{x})$.

Lognormal Data. Although the theory of kriging does not presume or depend on

any specific distribution of the sample data, a few 'side effects' arise if the underlying

data comes from a lognormal distribution (20). For a lognormal distribution, the standard

deviation is directly proportional to its mean. Thus, the variance is proportional to the

square of the mean of the samples. If experimental semi-variograms were constructed on

different sets of samples within the deposit, this 'proportional effect' could have a radical

effect on the individual experimental semi-variograms. It is desirable if this situation

arises to take the log of the data and perform the kriging analysis on the normalized data.

Example: To illustrate the concepts of trend and stationarity, it is useful to consider the following simple example. The curves in Figure 4.6 represent a hypothetical grade of ore versus distance along a certain path.

If samples are taken every five feet and the equation for m($\mathbf{h}$) is used to find m(5) (the average difference in grade between two samples 5 feet apart), the results for curves A and B will show that the average difference in grade as one moves 5 feet in either direction is zero. This is equivalent to saying that $\mu(\mathbf{x})$ is a constant for curves A and B, and the value is just as likely to go up as down at a distance $\mathbf{h}$ from a known sample
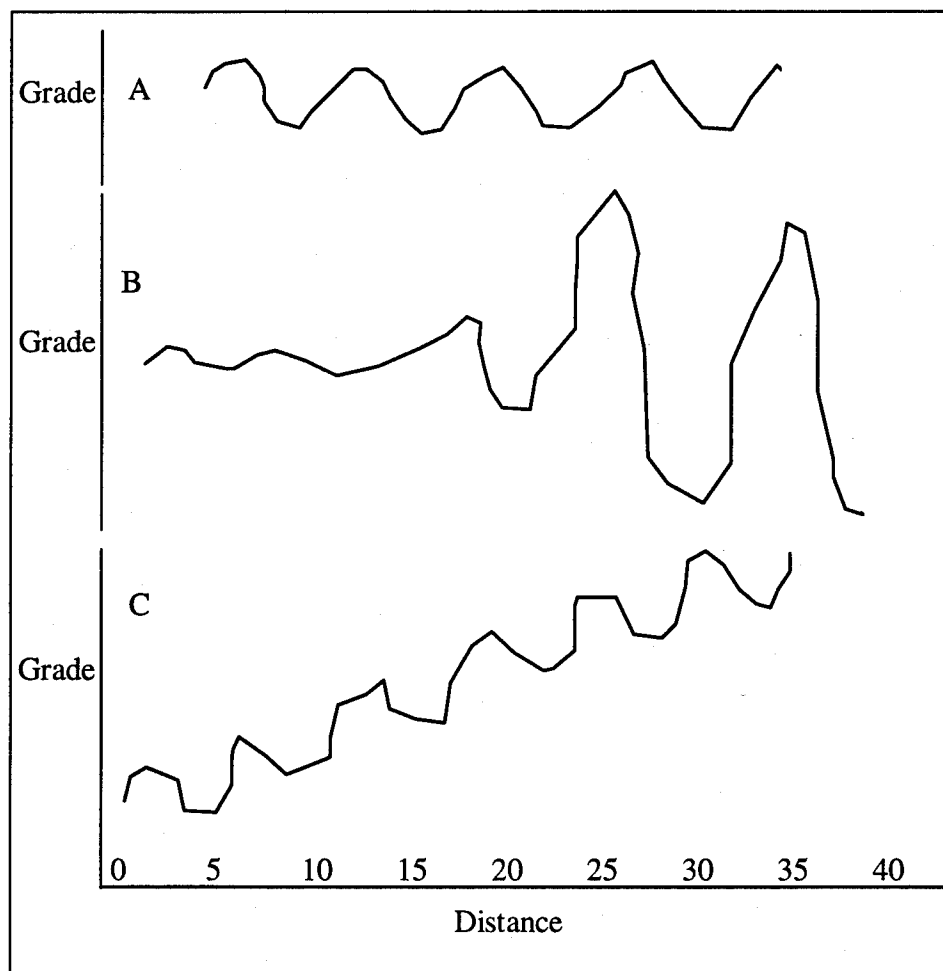
Figure 4.6 Example Ore Grade Data Values

point. For curve C, m(**h**) will not equal zero, $\mu(x)$ increases to the right. Curve A and curve B have no trend, while curve C has what appears to be a linear trend.

Curve A also exhibits second degree stationarity. The variance in the difference between sample values 5 feet apart is the same throughout the curve. To actually show this would require calculating a semi-variogram for the left half of the region and one for the right half , and then showing that they are the same. If we did this for curve B, we would find that the variance of the difference in values at samples 5 feet apart is much greater on the right side than on the left side. Therefore, there is not second degree stationarity for curve B. The semi-variogram for curve C would show greatly increasing values as **h** increases indicating the presence of a trend. In this example, the shape of the curve was given. In a real situation, the determination of whether there is a trend or whether the semi-variogram will apply to the entire region of concern, must be made based on the sample data.

As mentioned earlier, there are methods of dealing with trend. In case C above, if the trend is known, or calculated by assuming a linear drift in $\mu(x)$, and finding a linear equation to approximate the change, then kriging can still be performed. At each sample location, the value for $\mu(x)$ at that point can be subtracted from the observed value, resulting in the value of $\varepsilon(x)$ for each location. A variogram can now be constructed based on these residual values, $\varepsilon(x)$, and the kriging technique can be applied to predict the residual at unknown locations, $\varepsilon(y)$. This value is then added to the expected value at **y**, $\mu(y)$, to estimate z(**y**). The kriging in this case is done using the residual values. If the linear equation that approximates the trend, or drift in $\mu(x)$, is found by a least squares

method, then the expected value of $\varepsilon(\mathbf{x})$ at any point is zero. As long as we can assume that the semi-variogram applies equally over the entire region of concern, then we have satisfied the conditions for stationarity. This again is an example of the intrinsic hypothesis which underlies the use of a semi-variogram to predict the values at unknown locations.

Kriging Model: In kriging, the predicted value at an unknown point is determined by a linear combination of weighting factors and the known sample values. This is shown in Equation (4.7):

$$\hat{z}(\mathbf{x}) = \sum_{i=1}^{n} w_i S_i \qquad (4.7)$$

where S_i = value of sample i.

The weighting factors, w_i, are normalized such that their sum equals unity. Setting the sum of the weighting factors equal to one as shown Equation (4.8) ensures an unbiased estimator:

$$\sum_{i=1}^{n} w_i = 1 \qquad (4.8)$$

There is also a variance associated with each estimate. If the weighting was equally distributed among the n sample points, the variance in the estimation error would be as shown in Equation (4.9):

$$\sigma^2 = \frac{\sum_{i=1}^{n} \left(S_i - \hat{z}(\mathbf{x}) \right)^2}{n} \qquad (4.9)$$

Using the information contained in the semi-variogram, and accounting for unequal weighting, this can be written as shown in Equation (4.10):

$$\sigma^2 = \sum_{i=1}^{n} w_i \gamma(S_i, \mathbf{x}) \qquad (4.10)$$

where $\gamma(S_i, \mathbf{x})$ is the semi-variogram value between each sample point and the unknown point.

The objective of kriging is to find the weighting factors such that the variance in the estimation error is minimized. These can be found by setting the derivative of the error variance with respect to w_i equal to zero (Equation (4.11)).

$$\frac{\partial(\sigma^2)}{\partial(w_i)} = 0 \qquad (4.11)$$

While this will result in the weighting factors which minimize the variance (providing the 'best' solution according to our objective criteria), the weighting factors will not necessarily add up to one. The additional constraint that the sum of the weighting factors equals one, which makes the estimate unbiased, can be included by adding another unknown, a Lagrange multiplier, to the equation. To find the best linear unbiased estimator, the following quantity must be minimized as shown in Equation (4.12):

$$\sigma^2 - \lambda(\sum w_i - 1) \qquad (4.12)$$

After differentiating and simplifying, the following system of equations results (Equation (4.13)):

$$w_1\gamma(S_1,S_1)+w_2\gamma(S_1,S_2)+\ldots+w_n\gamma(S_1,S_n)+\lambda=\gamma(S_1,x)$$
$$w_1\gamma(S_2,S_1)+w_2\gamma(S_2,S_2)+\ldots+w_n\gamma(S_2,S_n)+\lambda=\gamma(S_2,x)$$
$$\vdots$$
$$\vdots \qquad\qquad (4.13)$$
$$w_1\gamma(S_n,S_1)+w_2\gamma(S_n,S_2)+\ldots+w_n\gamma(S_n,S_n)+\lambda=\gamma(S_n,x)$$
$$w_1+w_2+\ldots w_n=1$$

where the values to the right of the equals sign are the semi-variogram values between each sample and the unknown point. The other terms in the equation are semi-variogram values between different pairs of sample points. The only unknowns in this set of n +1 equations are the w_i and λ. In matrix notation, this can be written as Equation (4.14):

$$\Gamma w = \gamma_x \qquad \text{or} \qquad w = \Gamma^{-1}\gamma_x \qquad (4.14)$$

Once the optimal weighting factors have been determined, the estimate and error variance at the unknown point can be determined by:

$$\hat{z}(\mathbf{x}) = w^T\mathbf{S} \qquad (4.15)$$

$$\sigma^2 = w^T\gamma_x + \lambda \qquad (4.16)$$

Kriging Model implementation. At this point, we are ready to calculate soil DU concentrations using the kriging model we developed.

Data Preparation. The kriging analysis was designed to provide a snapshot of the current state of the soil. Although data have been collected since 1979, not all of the data were analyzed. The last cleaning/sifting operation took place in September of 1990. During that operation, according to site workers, a large piece of equipment was dropped on the ground near the south end of the RCA causing a significant amount of dust to blow in the air (27). Because of this incident and the fact

that some DU may have been distributed due to the sifting operation, we analyzed only

data taken since November 1990. None of the data from before that time were

considered.

A quick look at the complete set of sample data indicated that at distances beyond

180 ft (55 m) from the target butt, the DU concentration was below the level of detection

(approximately 1 pCi/g). The average concentration of samples taken at 180 ft (55 m),

120 ft (37 m), and 60 ft (18 m) was 1.93 pCi/g, 5.24 pCi/g, and 13.25 pCi/g, respectively.

The intrinsic hypothesis underlying kriging was that the semi-variogram applied

throughout the region (intrinsic stationarity). Before going further, we had to decide in

what area we were going to assume intrinsic stationarity. It was obvious that a semi-

variogram constructed based on the data within 180 ft (55 m) from the target butt would

not apply to the region outside of 180 ft (55 m). Since the concentration of DU outside of

180 ft (55 m) was essentially at background level, an experimental semi-variogram based

on this data would yield γ(h) equal to zero. Based on the fact that values began changing

at the 180 ft (55 m) sample points and based on the shape of the RCA, we assumed

stationarity within a square block 360 ft by 360 ft (110 m by 110 m) with the target butt at

the center. We constructed the semi-variogram based only on data from within this

region. Twenty sample points were located within this region.

At each sampling location, the reported sample results varied from sampling

quarter to sampling quarter. The variance differed for each sample location but, in

general, sample results for a particular location were consistent. For this analysis, we

assumed that the average concentration in an area was not actually changing quarterly and

that the variation in sample results was due to localized pockets (nuggets). We were interested in predicting the average of DU concentration sample values taken at each sample point since the last cleaning for use as input to our model. The average was chosen since it was an unbiased estimator and because the average value was slightly higher than the median value at almost all locations so it was more conservative.

No sample data from within the RCA were considered in the analysis. The RCA is surrounded by an elevated asphalt covered berm and is graded so rainfall will drain toward a low point within the RCA. By design, the berm caused a discontinuity in the concentration of DU within the area. Very high values of DU have been observed inside the RCA only a short distance from sample points outside the RCA where low values were observed. Therefore, our predictions for the concentration at unsampled locations outside the RCA were based on observed samples taken from outside the RCA.

A histogram of the sample data showed the data were highly skewed to the right (many low values and few high values). We tested the data for lognormality using the Chi-square and Anderson-Darling (goodness-of-fit) tests. With an alpha of 0.1, the critical Chi-square value was 14 as compared to a Chi-square test statistic for our data of 0.4, i.e. less than the critical value. Also, the 'goodness of fit' test picked the lognormal curve fit as the best fit to our data. Therefore, to avoid the side effects associated with lognormal data, the log of the data was taken. Figure 4.7 shows histograms of the original sample data and the log of the sample data.
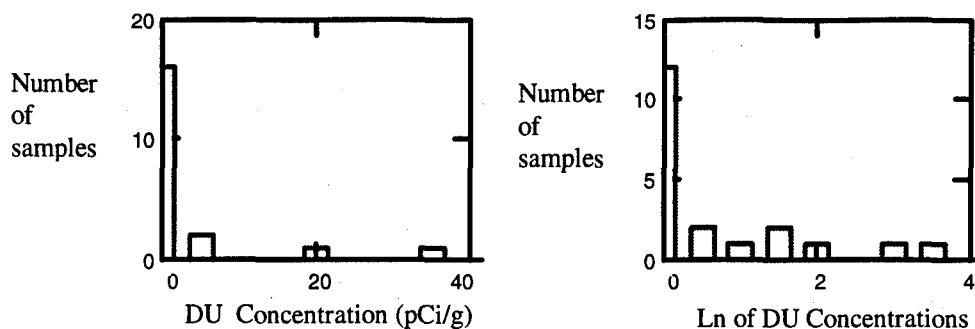
Figure 4.7 TA C-64 DU Soil Concentration Data Histograms

There was still a large spike in the histogram of the logged data, but this spike was due to the large number of values that were reported as 1 pCi/g, the limit of detection of DU. The actual values would range between 0.0 and 1.0 and would not show up as a large spike in the histogram.

Semi-variogram Calculation. The next step was to construct a semi-variogram. In our case, the samples were taken along grid lines pointing radially outward, resulting in very few pairs of points having similar distance and directional alignment. In this case, the semi-variogram value obtained was not particularly reliable because it was based on a very small sample set. Much more data could be combined if we assumed that the covariance between two points depended only on the distance between the two points. For this reason, and the fact that there was no information leading us to suspect a non-isotropic distribution of the DU, we assumed an isotropic region.

Figure 4.8 is a scatterplot of all possible pairs of points among the twenty samples used in this analysis (the complete data set used is given in Appendix A). This is a plot of

the distance **h** versus the point-to-point variance, W, where W is described by Equation (4.17):

$$W = \frac{1}{2}\big(g(x) - g(y)\big)^2 \qquad\qquad (4.17)$$

Data points for the semi-variogram were found by looking at each distance where pairs of points were found, and taking the average of the value W at that point.

Even with the isotropic assumption, there were distances with only a few pairs of points. Clark (20) suggests combining data from nearby points to form a single point on the semi-variogram. This eliminates overemphasizing a particular pair of points. Using this technique, the data in the scatterplot were combined to yield the an experimental semi-variogram shown in Figure 4.9.

This experimental semi-variogram appears to rise initially and then level off and maintain a similar value for the remaining region. The fact that the experimental semi-variogram did not continue to increase indicates that there was not a significant trend in the region being analyzed.

Point to Point Variance, W (pCi/g)^2

Distance Between Sample Points (ft)
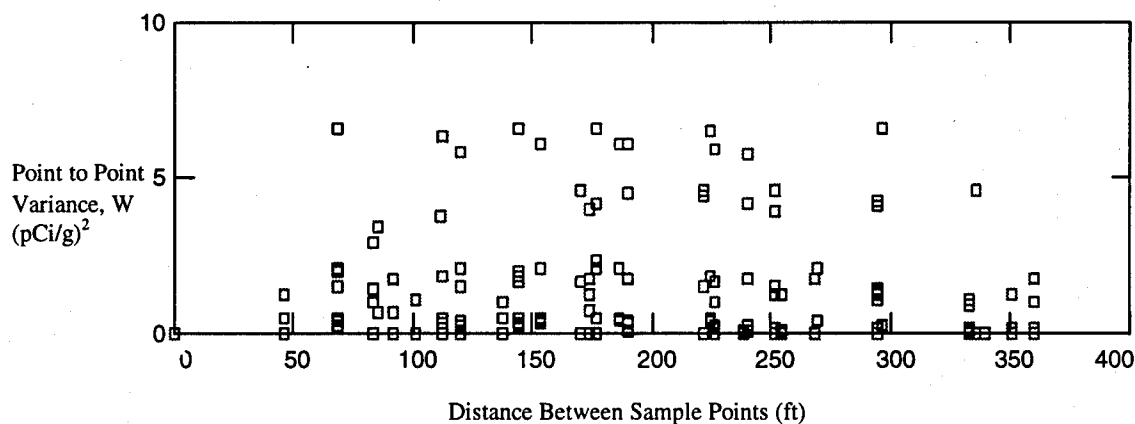
Figure 4.8 TA C-64 Soil Concentration Data Semi-Variogram
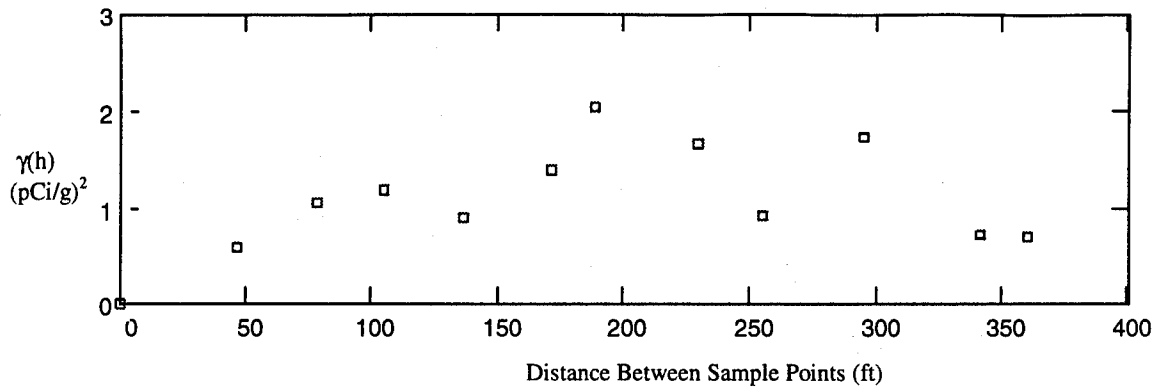
Figure 4.9 Experimental Semi-Variogram

At this point, we fit the experimental semi-variogram with each of the classical semi-variogram shapes using the methods described above, resulting in the classical semi-variograms shown in Figure 4.10. These semi-variograms assumed no nugget effect. This meant that we expected the average concentration to change gradually with no discontinuities.

The Gaussian model appeared to be the best fit for the experimental semi-variogram based on visual interpretation of the graph. For all subsequent calculations
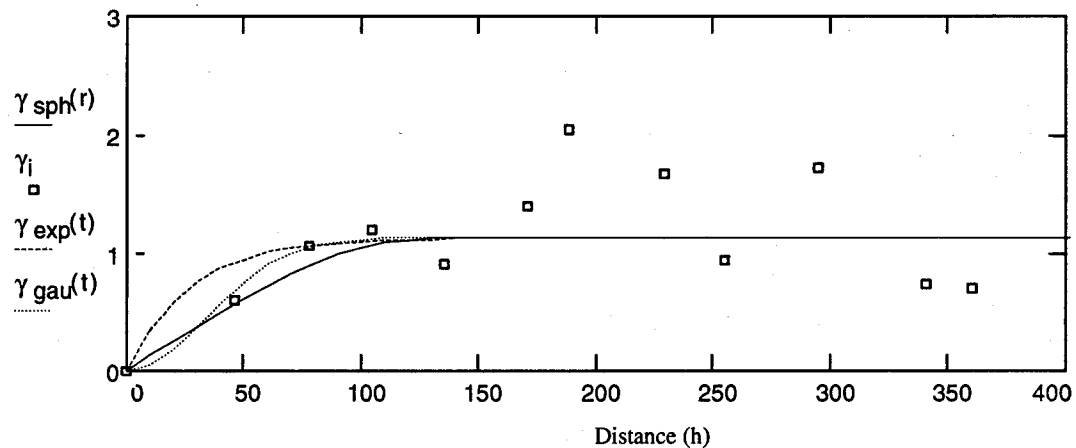
Figure 4.10 Curve Fit to Semi-Variogram

used in this analysis, the Gaussian semi-variogram relationship given by Equation (4.18) was used:

$$\lambda(\mathbf{h}) = 1.1245\left(1 - e^{\left(-\frac{\mathbf{h}^2}{47.6035^2}\right)}\right) \qquad (4.18)$$

Since we now had a semi-variogram model, which we assumed applied over the entire 360 ft by 360 ft (110 m by 110 m) area of concern, we now applied the kriging system of equations.

For each point where a prediction of the concentration was desired, we solved the kriging system of equations to find weighting factors. To accomplish this, we wrote a program in MathCad 5.0 Plus® (47), which is included in Appendix A. We initially chose to estimate the concentration at 30 ft (9 m) intervals, both the East/West and the North/South directions. At each point, the kriging system of equations results in a mean (μ) and a standard distribution (σ) for the concentration. Since we took the log of the original sample data, the mean and standard deviation calculated for each point described the underlying normal distribution. The predicted concentration of DU at each point is given by the lognormal pdf given in Equation (4.19):

$$f(\mathrm{x}) = \frac{1}{\mathrm{x}\sqrt{2\pi\sigma^2}} e^{\left(\frac{-(\ln \mathrm{x} - \mu)^2}{2\sigma^2}\right)} \qquad (4.19)$$

The mean, variance, median, and the lognormal pdf 95% upper bound for the concentration of DU are given by given by Equations (4.20) through (4.23), respectively:

$$E(x) = e^{\left(\mu + \frac{\sigma^2}{2}\right)} \qquad (4.20)$$

$$Var(x) = e^{(2\mu+\sigma^2)}\left(e^{\sigma^2} - 1\right) \tag{4.21}$$

$$median(\mathbf{x}) = e^{\mu} \tag{4.22}$$

$$95\% \text{ Upper Bound} = e^{(\mu+1.645\sigma)} \tag{4.23}$$

Figure 4.11 shows a typical pdf for DU concentration. This pdf is for the concentration of DU at 'x' equals 40 ft (12 m) and 'y' equals -50 ft (-15 m).

A plot of the average for each DU concentration pdf is shown in Figure 4.12. This plot does not incorporate the uncertainty associated with positions that are far from known sample points. Because kriging is an 'exact interpolator', the estimate at a known sample point is exactly equal to the reported sample result.

The real value of kriging came when looking at confidence limits. Figure 4.13 shows a prediction for the 95% upper bound at each location. As one might expect, the highest upper bound values are in the region where the highest sample values were obtained. The highest values are in the vicinity of sample point 1-7 (x=23.0 ft, y=-55.4 ft).
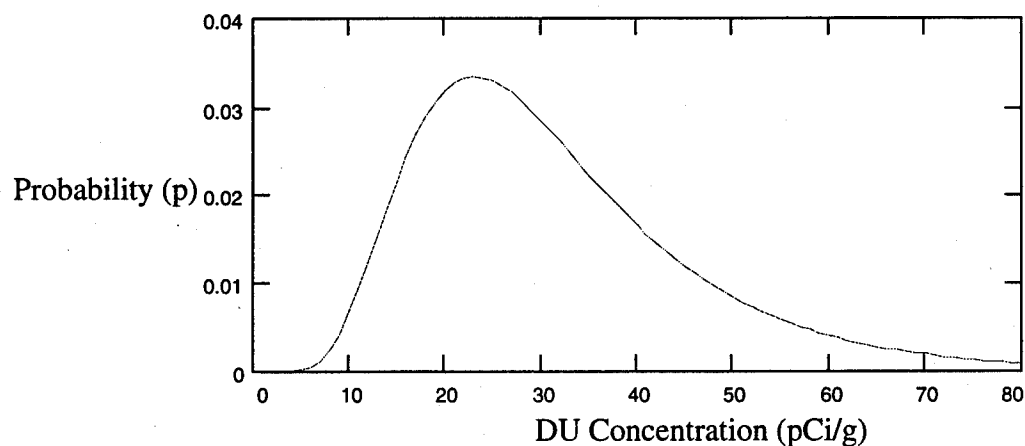
Figure 4.11 Typical pdf for DU Concentration (x=40 ft, y=-50 ft)

The previous plots were a result of using the kriging equations to obtain an estimate every 30 ft (9 m). To better characterize the region where higher concentrations have been observed, the kriging system of equations were used to make predictions at 10 ft (3 m) intervals for a region going from 0-140 ft (0-43 m) in the 'x' direction and -90 to 10 ft (-27 to 3 m) in the 'y' direction. The surface plots for the average and 95% upper bound, at each location, are shown in Figure 4.14 and Figure 4.15, respectively. Tables for the mean and standard deviation defining the distribution at each location are included in Appendix A.

The kriging analysis provided a table of pdf parameters available for health risk assessment and was used as input to the groundwater and air DU concentration models (Appendix A).
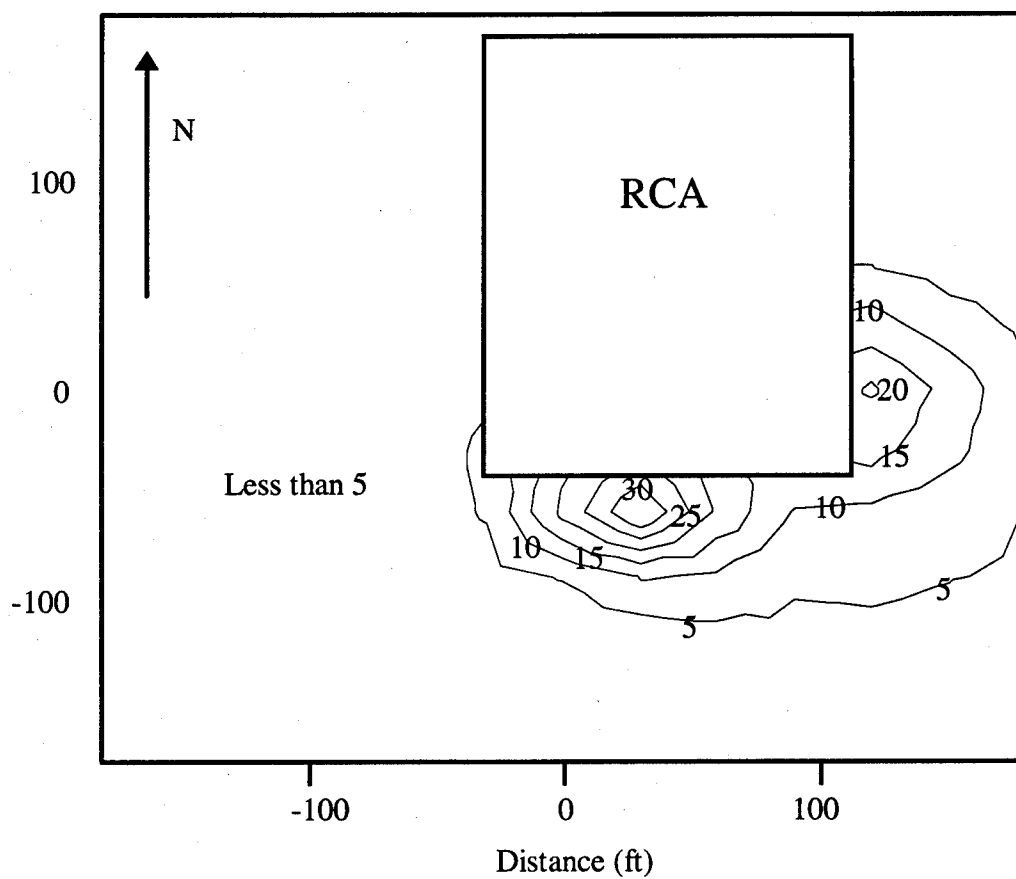
Figure 4.12 DU Soil Concentration (pCi/g): Kriging Plot
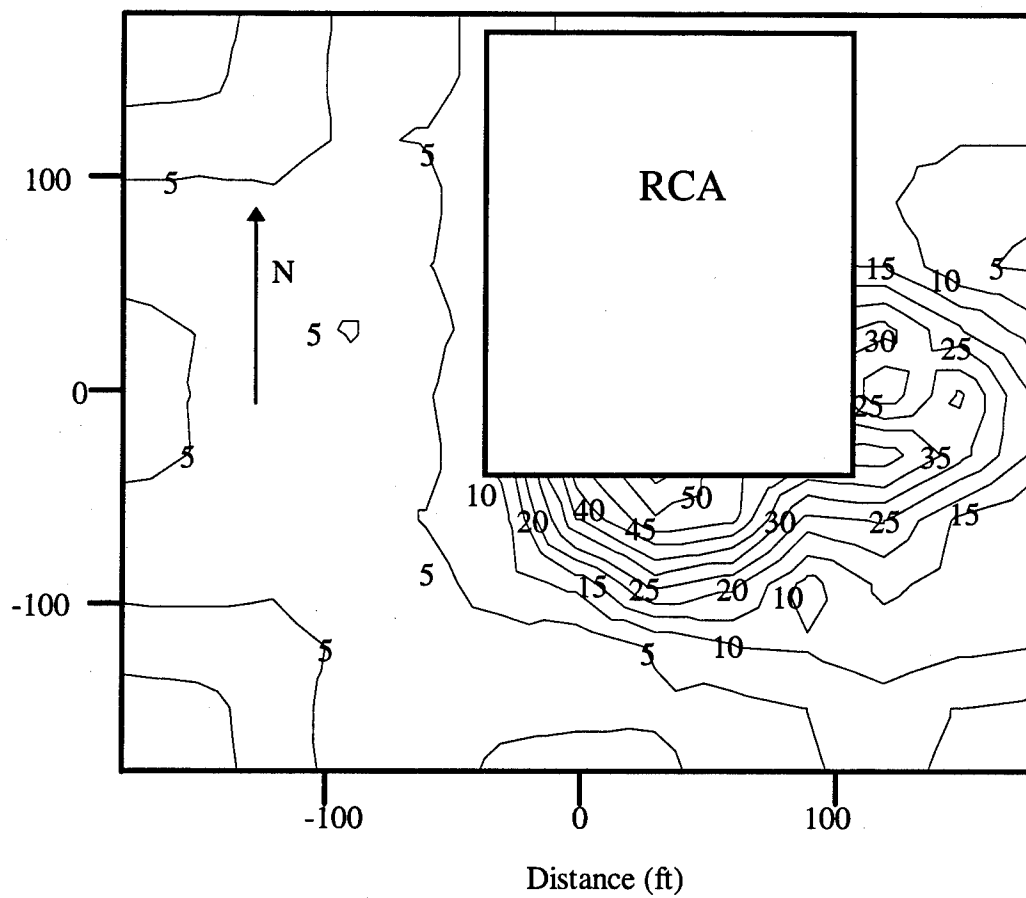
Figure 4.13 DU Soil Concentration (pCi/g): 95% Upper Bound:
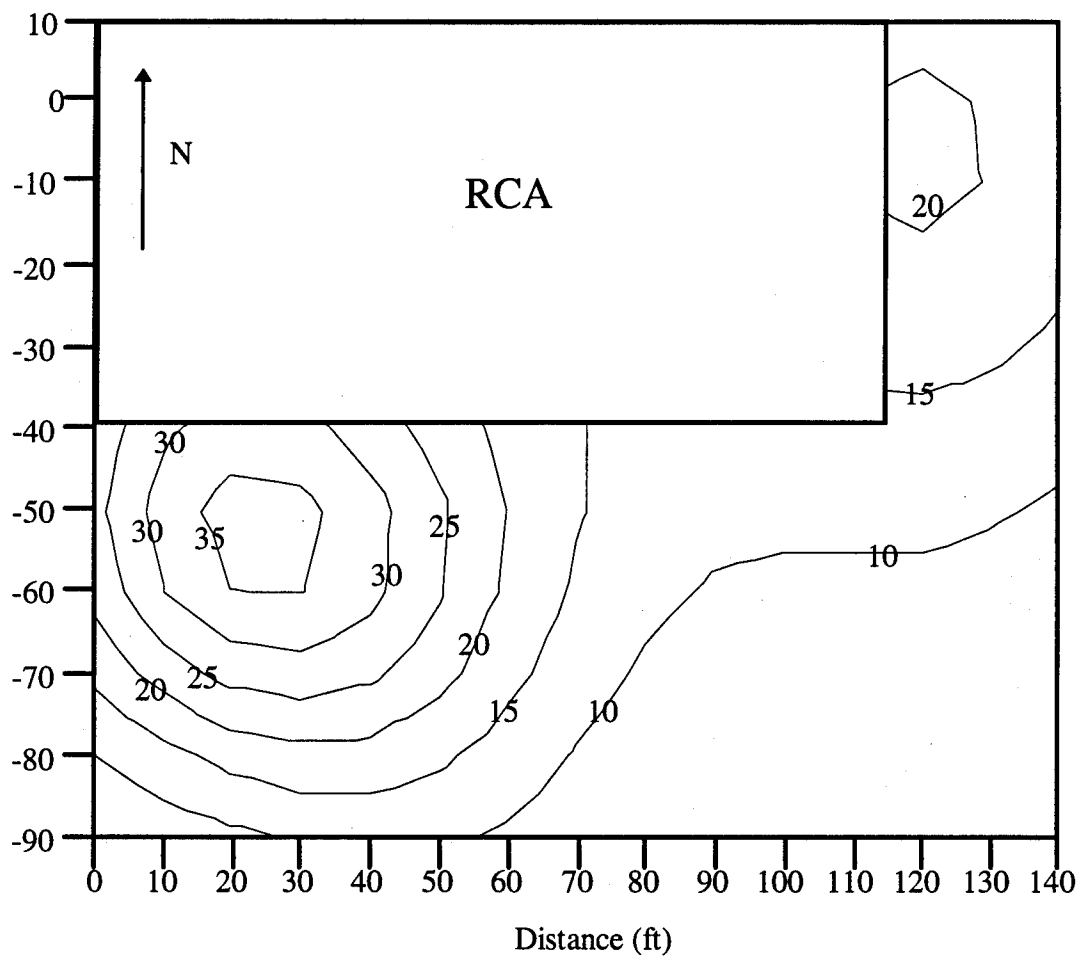
Figure 4.14 DU Soil Concentration (pCi/g): Kriging Plot based on h = 10 ft
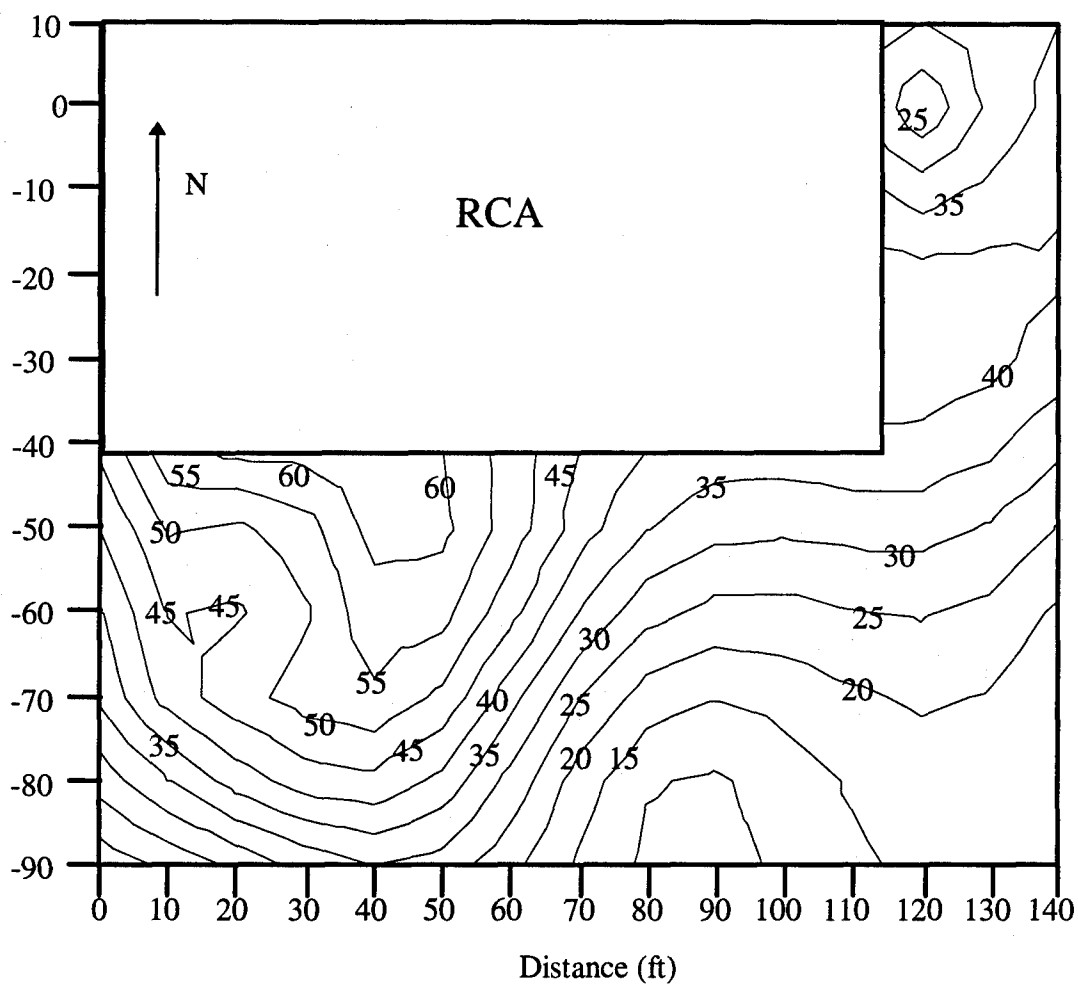
Figure 4.15 DU Soil Concentration (pCi/g): 95% Upper Bound based on h = 10 ft

4.2   Groundwater

In this section, the sub-problem of characterizing the DU concentration in the groundwater under the surface of TA C-64 is addressed. The methods that best met our objectives for conducting this groundwater analysis were selected and then used to obtain the desired information.

4.2.1   Defining the Problem.   Several tools were useful in helping select a model for estimating concentration levels of DU in the groundwater. We used a portion of the twelve products and an interaction matrix in our systems engineering approach to solving this problem.

Product 2.   Descriptive Scenario. We defined two major systems for our analysis: the groundwater flow and the DU transport mechanism. We further broke these down into subsystems. For the groundwater flow, we defined four subsystems as follows:

1) unsaturated groundwater flow zone (vadose zone),

2) sand-and-gravel aquifer,

3) Pensacola confining bed, and

4) Upper Floridan aquifer.

These subsystems are shown in Figure 4.16 . This figure is a cross sectional view of the TA C-64 and vicinity map (Figure 4.17). The cross-section line is indicated by the line C-C' in Figure 4.17.

For the second major system, DU transport, we defined the following three subsystems:
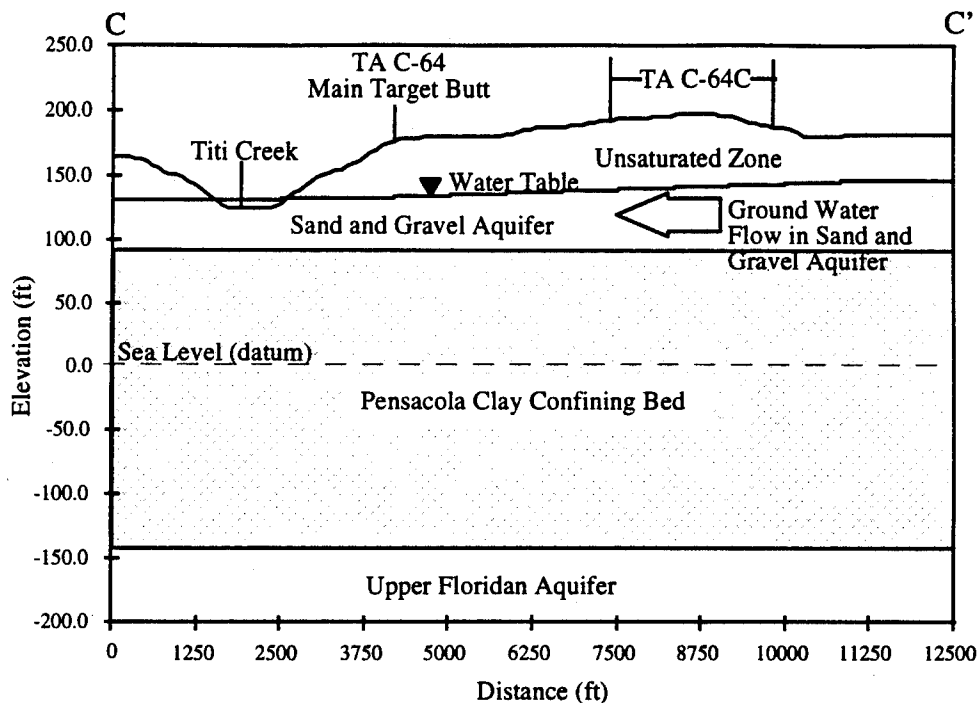
Figure 4.16 Cross-sectional view of TA C-64C and vicinity

1) transport mechanism for DU,

2) transportation rates for DU, and

3) concentration of DU in the sand-and-gravel aquifer.

The groundwater flow and DU transport major systems and their associated

subsystems are summarized in Table 4.1, with their locations in this document. The

systems engineering steps for attaining and implementing appropriate groundwater flow

models including DU transport without respect to concentration are detailed in Appendix

B. The systems engineering steps for obtaining DU concentration in the groundwater

are presented here in full, since the output from this analysis has a more direct impact in

assessing human health risks.
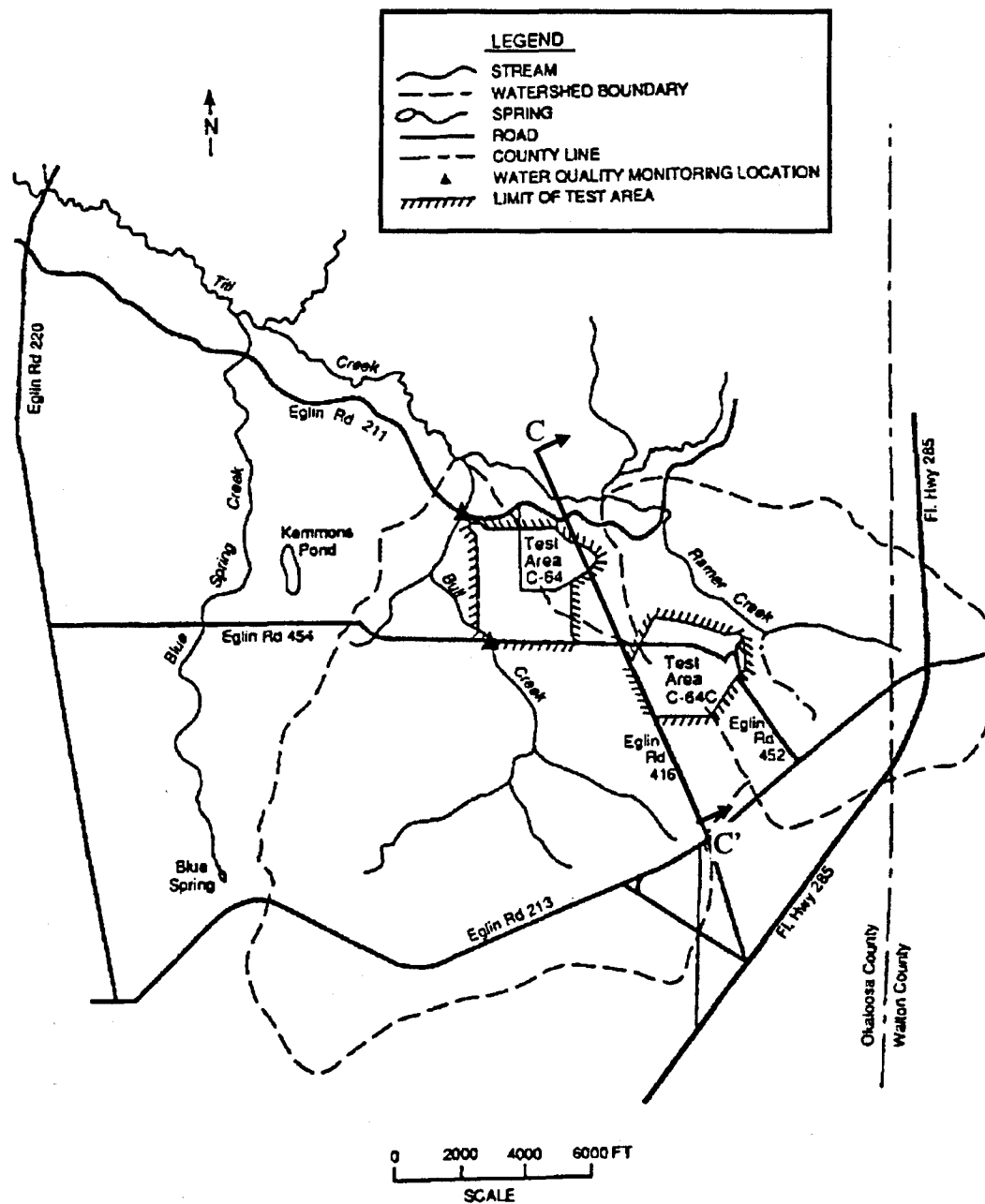
Figure 4.17 Map of TA C-64 and vicinity (12:23)

Groundwater Flow	DU Transport
1) Unsaturated vadose zone (Appendix B) 2) Sand-and-gravel aquifer (Appendix B) 3) Pensacola confining bed (Appendix B) 4) Upper Floridan aquifer (Appendix B)	1) Transport Mechanism for DU (not modeled) 2) Transportation rates for DU (Appendix B) 3) Concentration of DU in the sand-and-gravel aquifer (Section 4.2)

Table 4.1 Groundwater Major Systems and Subsystems Summary

Product 3. Relevant Disciplines. For the groundwater study, we required a working knowledge of chemistry and groundwater hydrology. We used techniques from these disciplines to calculate concentration; retardation; and groundwater hydrology for groundwater flow around TA C-64.

Product 4. Scope. We only considered the groundwater around TA C-64. This included the area between Ramer and Bull Creek to the west and east, respectively, and Titi Creek to the north and the beginnings of Ramer and Bull Creek to the south (see Figure 4.17). Well head data from site TA C-64C was used as representative data for the sand-and-gravel aquifer.

Products 7, 8, and 9. Needs, Alterables, and Constraints. The needs (products) of this section were to provide DU concentrations in the groundwater within the vicinity of TA C-64. We identified the following alterable parameters: the methods and models used for the groundwater flow analysis (in Appendix B); the modeling paradigms (i.e. theoretical or empirical) and software programs; and the numerical values assigned to

modeled parameters for the DU concentration analysis. A major constraint for the DU concentration model selection process was that publicly and scientifically accepted standards of analysis, which gave a reasonably accurate characterization with respect to the available data (i.e., an intelligent guess re-affirmed by analysis), should be used.

Interaction Matrix. Table 4.2 below is a directed interaction matrix showing how the major systems and subsystems effect each other. DU is affected by both the water used to transport it and the medium through which it travels. The groundwater is also affected by the medium through which it travels, and the aquifers affect each other through the relative piezometric head difference between adjacent aquifers and the leakage rate between them. An example of reading the directed interaction matrix is provided as follows: in the first row, we see that groundwater affects DU; the second row shows that DU affects none of the other subsystems; the third row shows that vadose zone affects groundwater, DU, and the sand-and-gravel aquifer subsystems; and so on.

As seen from the interaction matrix, the Pensacola confining bed was included with the aquifers because we were interested in potential leakage (interaction) of

	GW	DU	Vadose	S&GA	UFA	LFA
GW		>				
DU						
Vadose	>	>		>		
S&GA	>	>	>		>	
UFA	>	>		>		>
LFA	>	>			>	
Abbreviations:						
GW: groundwater UFA: Upper Floridan aquifer						
S&GA: sand-and-gravel aquifer LFA: Lower Floridan aquifer						

Table 4.2 Interaction Matrix for Groundwater Section

groundwater from the sand-and-gravel aquifer into the Upper Floridan aquifer through the confining bed. The Upper Floridan aquifer provides the potable (drinking) water to Okaloosa and Walton counties, including Fort Walton Beach.

4.2.2   Setting Objectives. We developed the objective criteria chart (Figure 4.18) as a decision making tool. We used the chart to help determine how well the needs we defined above were met by the alternatives evaluated.

We broke down the objective criteria into three, more specific sub-criteria: least effort, least money, and best availability (accuracy being a constraint). *Least effort* was further specified by the following objective sub-criteria: training time (in days), model simplicity (subjective - meets thesis objectives), flexibility (subjective - functional with data available), and execution time (in minutes and seconds). *Least money* was made-up of the following sub-criteria: product and training cost, both measured in dollars. Finally, *best availability* was measured as how long it would take us to acquire the given product in days (including in-house approval, ordering, and shipping time). Note: It was recognized that accuracy was of major importance for our systems engineering problem. It was handled as a constraint in the groundwater section. Accuracy was not an objective because, there was no field data available for the test area from which to compare calculated values with reality. The flexibility objective insures that the model selected was appropriate for the data available.

4.2.3   Developing and Modeling Alternatives. We identified two general methods for gathering the information for this study: active and passive. We defined active methods as those involving further data gathering activities such as drilling sample

4-37

wells and testing groundwater samples for DU concentration in the sand-and-gravel

aquifer; measuring water head values; or testing the soil at TA C-64 to define

conductivity, leakage, and water drying/re-wetting curves. Earlier in this process, we

decided that no additional testing of TA C-64 to provide groundwater information would

be possible, and so we did not further consider active methods.

The second method, passive, we defined as using existing data from TA C-64

along with data from other sources (other sites, studies and previous laboratory work) to

provide the information we required. We defined two passive methods of determining

the DU concentration: analytical and numerical. We developed alternative models for

evaluation using each of these two methods as outlined below.

Analytical Method. We defined an analytical method of finding the DU

concentration in the groundwater under the kriged area in the sand-and-gravel aquifer by
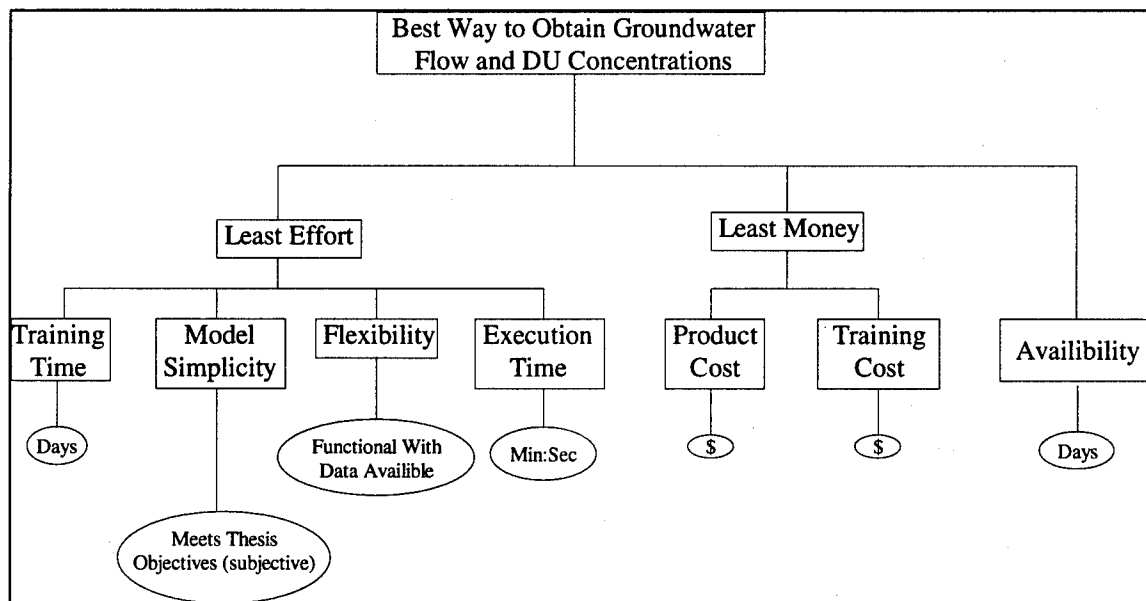
Figure 4.18 Groundwater Objective Criteria

estimating the total amount of DU in the soil around the RCA (excluding the RCA), placing a percentage (from a TA C-64C study) of that DU into the groundwater, and calculating the groundwater DU concentration. The DU within the RCA was excluded because a 3 ft. thick confining layer of clay under the RCA effectively isolates the DU from entering the groundwater.

Numerical Method. For this method, we evaluated numerical methods in the form of computer programs. We considered the following computer programs for DU transport and groundwater flow (presented in Appendix B): SWIFT III®, Geoflow®, SWENT®, Princeton Transport Code (PTC)®, Modular Flow Model (MODFLOW)®, Modular Transport Model (MT3D)® and Infil®. Of these seven programs, SWIFT III®, SWENT®, and MODFLOW® use finite difference methods to solve motion and mass balance equations. Geoflow® and PTC® use both finite difference and finite element methods to solve the motion and mass balance equations. MT3D® is a contaminant transport model that supplements MODFLOW®. Infil® is a program developed to evaluate and determine water infiltration into soil based on Richard's equation (Appendix B). Table 4.3 provides a list of features of major DU transport and groundwater flow codes: SWIFT III®, Geoflow®, SWENT®, PTC®, and MODFLOW® which we will later use, along with the objective criteria, to evaluate each of the programs.

4.2.4   Evaluating Alternatives.   Our next step was to provide the framework for evaluation and comparison of the groundwater flow and DU transport modeling alternatives based on the defined objective criteria.

FEATURE	SWIFT III®	Geoflow®	SWENT®	PTC®	MOD-FLOW®
Density Variations	Yes	No	Yes	No	Yes
Confined and Unconfined	Yes	Yes	No	Yes	Yes
Temperature Dependent Viscosity	Yes	No	Yes	No	No
Particle Tracking	Yes	No	No	No	Use MODPATH
Radionuclei Decay Chains	Yes	No	Yes	No	No
Decay of Single Species	Yes	Yes	Yes	Yes	No
Prescribed Fluxes, Heads, Concentrations	Yes	Yes	Yes	Yes	Yes
Waste Leach Model	Yes	No	Yes	No	No
Numerical Solution Method	Finite Difference (FD)	Vertical FD, Horiz. Finite Element (FE)	FD	FD and FE	FD
Problem Size Restriction	Unknown	2000 Element, 30 Layers	1000 grid blocks	2000 Element, 30 Layers	Unknown
Pre and Post Processing Data	Contour Plots	Contour Plots	Simple Plots	Limited Plotting	Contour Plots
Verification	25 Tests	Extensive	Simple Tests	Little	Extensive
User Learning Curve	Large	Large	Large	Large	Little
Code Acquired by AFIT at time of study	No	No	No	No	Yes

Table 4.3 Groundwater Computer Program Features (26).

The evaluation of each DU transport alternative was based on the objective criteria measurables shown in Table 4.4. The table provides a numerical rating system ('points' from 0 to 10) in addition to a descriptive word rating system ('criteria' from barely acceptable to exceptional). Although the two rating scales were roughly equivalent, we used the 'points' system to evaluate alternatives that were being *compared with other alternatives*, and the 'criteria' system for alternatives being rated *independent of other alternatives*.

For obtaining DU concentration in the groundwater, we chose four modeling methods for evaluation, including one analytical and three numerical solutions. We narrowed our alternatives list to those computer models which included numerical solutions based on finite difference or finite element numerical techniques used to solve groundwater flow, radionuclei decay chains, and waste leaching equations. The three computer models were SWIFT III®, SWENT®, and MT3D®.

Our rating of each alternative against the least effort, least money, and best

System Utility Function Chart						
Points	1 2	3 4	5 6	7 8	9 10	
Criteria	Barely Acceptable	Below Average	Average	Above Average	Exceptional	Units
Training Time	> 2 Weeks	2 Weeks	1 Week	1 Day	3 Hr	Hr/Day/Wk
Model Simplicity	1	2	3	4	5	Subjective
Flexibility	1	2	3	4	5	Subjective
Execution Time	> 30 Min	30 Min	5 Min	1 Min	< 10 Sec	Sec/Min
Product Cost	>$1200	$1,200	$800	$400	$0	Dollars
Training Cost	>$1200	$1,200	$800	$400	$0	Dollars
Availability	> Month	Month	2 Weeks	Week	Now	Time

Table 4.4 DU Transport Alternatives System Utility Function

availability objective criteria is shown in Table 4.5. Again, note accuracy was a constraint.

    4.2.5   Selecting an Alternative. To help with selecting an alternative, we used a preference chart and a confidence level chart which we developed below.

Objective Criteria	Analytical	SWIFT III®	SWENT®	MT3D®
Least Effort:				
Training Time	9	2	3	4
Model Simplicity	9	2	4	6
Flexibility	7	10	3	7
Execution Time	4	7	7	6
Least Money:				
Product Cost	10	6	6	6
Training Cost	10	6	6	6
Best Availability:	10	4	4	10

Table 4.5 DU Transport Alternatives Rating using Objective Criteria

    We used the preference chart to establish weighting factors for each of the objective criteria as shown in Table 4.6. These weighting factors were used to calculate a total utility of an alternative as a linear combination of the weighted objectives. The seven objective sub-criteria are spelled out down the first column and represented in abbreviated numerical form along the first row of the chart. Each entry in the chart then represents a rating of the 'column' sub-criteria with respect to the associated 'row' sub-criteria; definition of the rating scale from zero to four is given at the bottom of the chart. For example, if the row representing the 'training time' sub-criteria is selected, we can

Criteria	1	2	3	4	5	6	7	Importance	Total	Weight
1. Training Time	-	0	1	1	0	1	0	Minor Imp.	3	1
2. Model Simplicity	4	-	2	3	2	3	2	Important	16	5 1/3
3. Flexibility	3	2	-	3	2	2	1	Moderate Imp.	13	4 1/3
4. Execution Time	3	1	1	-	1	1	0	Minor Imp.	7	2 1/3
5. Product Cost	4	2	2	3	-	3	2	Important	16	5 1/3
6. Training Cost	3	1	2	3	1	-	1	Moderate Imp.	11	3 2/3
7. Availability	4	2	3	4	2	3	-	Very Important	18	6

Where: 4 means the criteria is much more important
3 means the criteria is more important
2 means both criteria have equal importance
1 means the criteria has less importance
0 means the criteria has much less importance

Table 4.6 DU Transport Alternatives Objective Criteria Preference Chart

read across the row and see this sub-criteria is much less important than model simplicity

(rating of '0'), less important than flexibility (rating of '1'), and so on. The weighting of

each criteria is then determined by selecting the lowest total rating and normalizing by

dividing all total scores by that lowest value (in this case, the lowest was training time

with a total rating of 3). The importance column shows the relative importance in words

of the sub-criteria with regard to the overall objective given in Section 4.2.2.

We also developed confidence levels for the data based on the source for each

alternative which helped with selecting an alternative. These confidence levels are shown

in Table 4.7. The expected outcome of an alternative for a given sub-criteria is the value

expected to be achieved by that alternative based on the utility ratings shown in Table 4.4.

For each model and each sub-criteria we calculated a system utility value using

Equation (4.27):

$$U_i = R_i \cdot WF \qquad (4.27)$$

where R is the rating found in Table 4.5 and WF is the weighting factor.

The weighting factors were assigned using the mapping of importance to weight

factor shown in Table 4.8. We also calculated a discounted system utility value which

Objective Sub-criteria	Alternative	Confidence Level	Support
Training Time	Analytical	VC (0.9)	Data Available
	SWIFT III®	C (0.6)	Estimation
	SWENT®	C (0.6)	Estimation
	MT3D®	VC (0.9)	Data Available
Model Simplicity	Analytical	VC (0.9)	Data Available
	SWIFT III®	C (0.6)	Estimation
	SWENT®	C (0.6)	Estimation
	MT3D®	VC (0.9)	Data Available
Flexibility	Analytical	C (0.6)	Estimation
	SWIFT III®	C (0.6)	Estimation
	SWENT®	C (0.6)	Estimation
	MT3D®	VC (0.9)	Data Available
Execution Time	Analytical	C (0.6)	Estimation
	Swift III®	LC (0.3)	Estimation
	SWENT®	LC (0.3)	Estimation
	MT3D®	VC (0.9)	Data Available
Product Cost	Analytical	VC (0.9)	Data Available
	SWIFT III®	VC (0.9)	Data Available
	SWENT®	LC (0.3)	Estimation
	MT3D®	VC (0.9)	Data Available
Training Cost	Analytical	VC (0.9)	Data Available
	SWIFT III®	LC (0.3)	Estimation
	SWENT®	LC (0.3)	Estimation
	MT3D®	C (0.6)	Estimation
Availability	Analytical	VC (0.9)	Data Available
	SWIFT III®	C (0.6)	Estimation
	SWENT®	C (0.6)	Estimation
	MT3D®	VC (0.9)	Data Available
Abbreviations: LC - low confidence C - confident VC - very confident			

Table 4.7 DU Transport Alternatives Confidence Levels

included a factor to account for uncertainty as shown in Equation (4.28).

$$D_i = U_i \cdot C_i \qquad\qquad (4.28)$$

where C represents an uncertainty factor as assigned in Table 4.7.

Importance	Weight Factor
Very	5
Moderate	3
Average	1.5
Minor	1

Table 4.8 Mapping of
Importance to Weight Factor

We then summarized and combined the results of the preference chart and the

confidence level chart into an evaluation matrix chart for use as a decision making tool as

shown in Table 4.9.

Based on the evaluation matrix, we chose the analytical model as the best

alternative for modeling the DU transport to the groundwater. It had the highest total

value, discounted value, and confidence as compared to the other completing alternatives.

Simply stated, the data available from TA C-64 and TA C-64C was very limited and an

analytical solution for DU concentration was adequate for the information available.

4.2.6 Planning for Implementation. To analytically estimate DU

concentrations in the sand-and-gravel aquifer directly under the kriged 360 ft by 360 ft

(110 m by 110 m) area around TA C-64, information from TA C-64C concerning the soil

and sand-and-gravel aquifer groundwater was used. TA C-64C is located approximately 1

mile from TA C-64 and we assumed that the geological features and the preoperation DU

concentrations in the soil and water were similar between the two sites since, no major

Criteria	Analytical				SWIFT III®				SWENT®				MT3D®			
	R	C	U	D	R	C	U	D	R	C	U	D	R	C	U	D
Very Important (WF=5)																
Availability	10	VC	50	45	4	C	20	12	4	C	20	12	10	VC	50	45
Important (WF=3)																
Model Simplicity	9	VC	27	24	2	C	6	3.6	4	C	12	7.2	6	VC	18	16
Product Cost	10	VC	30	27	6	VC	18	16	6	LC	18	5.4	6	VC	18	16
Moderate Importance (WF=1.5)																
Flexibility	7	C	11	6.3	10	C	15	9	3	C	4.5	2.7	7	VC	11	9.5
Training cost	10	VC	15	14	6	LC	9	2.7	6	LC	9	2.7	6	C	9	5.4
Minor Importance (WF=1)																
Training Time	9	VC	9	8.1	2	C	2	1.2	3	C	3	1.8	4	C	4	2.4
Execution Time	4	C	4	2.4	7	LC	7	2.1	7	LC	7	2.1	6	VC	6	5.4
Total Value			146				77				74				116	
Discounted Value				127				47				34				100
Confidence		0.87				0.61				0.46				0.87		

VC: 0.9
C: 0.6
LC: 0.3
NC: 0.1

R=Relative Rating
C=Confidence
U=System Utility
D=Discounted Utility

Table 4.9 Evaluation Matrix For DU Concentrations

geological discontinuity exits between them. In addition, since site specific information was not available for TA C-64, we chose conservative assumptions for all of our calculations. The DU concentration under the RCA in the sand-and-gravel aquifer was found analytically by estimating the total amount of DU in the soil around the RCA (under the kriged area, excluding the RCA). A confining layer of clay under the RCA effectively isolates the DU in the RCA from the surrounding area. We placed a percentage of that DU into the groundwater, and calculated the resulting groundwater DU concentration.

First, we calculated the volume of water under the kriged area. We found this volume by multiplying the surface area by the saturated thickness of the sand-and-gravel aquifer and the porosity of the aquifer. We used a value for the kriged area of 360 ft by 360 ft (110 m by 110 m) giving an area of 129,600 ft^2 (12,100 m^2). For the thickness, we assumed a water table depth of 89 ft (27.07 m) (excluding the known gully well) and a bottom depth of 120 ft (36.58 m) based on averaged TA C-64C well data (12:34). Using the average porosity value for coarse sand as 0.30 (68:4-22), we calculated a volume of 1,212,282 ft^3 (34,328 m^3) or 9.43E7 liters for the water directly under the kriged area of TA C-64 in the sand-and-gravel aquifer.

To calculate the total mass of DU on the surface of the kriged area (excluding the RCA), we assumed a linear depth distribution of DU in the soil. We used an average concentration of DU in the soil at the surface of 3.68 pCi/g (obtained by averaging the mean point estimates at every kriged block from the soil characterization analysis). The linear depth approximation used, assumed the surface concentration of DU to be 3.68

pCi/g at zero depth which decreased linearly to background concentration levels (less than 1 pCi/g, or the minimum level of detection (12:17)) at a depth of 1.6 ft (0.5 m). This depth was obtained from a one time column soil sediment study of TA C-64 performed by the Los Alamos National Laboratories in 1991. It showed that total uranium concentration levels composed mainly of DU diminished to total background uranium levels composed mainly of natural uranium at approximately 15 to 20 inches of soil depth (11). A linear function fit the data well. So, the resulting relationship for DU concentration as a function of depth is given in Equation (4.29):

$$c = -5.36 \frac{pCi}{g \cdot m} x + 3.68 \frac{pCi}{g} \qquad (4.29)$$

where c is the estimated DU concentration at location x, and x is the location of interest below the surface (positive downward). Integrating the above equation from the soil surface to a depth of 1.6 ft (0.5 m), gave an average concentration, c, of 1.17 pCi/g.

To calculate the total mass of DU, we next found the mass of the soil. Using a soil density of 1 g/cm^3, a soil area of 129,600 ft^2, and a soil depth of 1.6 ft, we estimated the mass of soil containing DU to be 6.0E9 g. This results in total DU mass in the kriged area, outside the RCA, of 19560 g. Please note, again in the above analysis, the RCA's contribution to the DU in the surface soil was not part of the kriged data and was not factored into this total DU mass.

To determine the percentage of the estimated total DU mass that reaches the sand-and-gravel aquifer, we used TA C-64C's sand-and-gravel aquifer groundwater and soil DU concentration data. The TA C-64C average background DU concentration was found

to be 0.82 parts per million (ppm) in the soil (12:26) and less than 0.1 µg/L (or parts per billion (ppb)) in the groundwater (13). We used a value of 0.1 µg/L (or 0.036 pCi/L) as a conservative estimate of the groundwater DU concentration, since the current level of detection is no lower than 0.1 µg/L. Based on these values, we calculated that 0.012 % of the soil DU concentration to be present in the groundwater. Assuming that this percentage of the total DU mass was present in the volume of groundwater under the kriged area resulted in a DU concentration in the groundwater of 0.025 pCi/L. Further, assuming that a conservative 0.036 pCi/L background concentration of uranium also exists in the groundwater volume, we found a total sand-and-gravel aquifer groundwater uranium concentration of 0.06 pCi/L.

For the DU groundwater concentration, we assumed that DU concentrations around TA C-64C were representative of the ratio of soil concentrations to groundwater concentrations around TA C-64 and that the groundwater in the volume of interest did not flow out of the volume to be replaced by additional groundwater.

So, the groundwater uranium concentration to be used for the health risk assessment was a uniformly distributed function with a high of 0.06 pCi/L and a low of 0 pCi/L.

4.3   Air

In this section, the sub-problem of characterizing the DU concentration in the air over TA C-64 is addressed. Specifically, we choose the method that best met our

objectives for conducting this analysis and then used it to describe the airborne DU concentration.

4.3.1 Defining the Problem. Of the twelve products developed in Chapter 3, we further detailed the descriptive scenario and the *need* steps for this section.

Product 2. Descriptive Scenario. Particle entrainment, or the general pickup and movement of particles by the wind, mechanical or other sources of disturbance, occurs as a) suspension, b) resuspension, or c) saltation. Suspension describes particles that remain airborne for long distances by force of the wind, such as those potentially generated during the TA C- 64 sand sifting operations. Resuspension describes particles that were previously suspended, were deposited, and then resuspended. Saltation describes leaping or bounding of particles lifted by the wind that are too heavy to remain airborne.

We postulated several possible mechanisms for the initial atmospheric transport of DU contaminated particles into the environment: gun firing operations, target butt cleaning operations, and wind events when the wind circulates through the opening of the larger target butt. We did not attempt to model this initial particle suspension since no data were available describing airborne particle concentrations at the TA. Saltation was also not modeled because the large size of the particles affected by saltation prevented either sustained suspension or respiration by humans. Resuspension was therefore the primary mechanism of concern for this analysis.

Soil particles contaminated with DU can be resuspended in the air by natural and anthropogenic activities. Natural factors affecting resuspension include meteorological conditions such as wind speed, wind direction, gust intensity, vertical turbulence

exchange, air density, precipitation and can also include surface conditions such as soil type, moisture content, density, texture, particle shape, particle size distribution, particle cohesiveness, surface roughness, amount of vegetation, and topography. Anthropogenic factors can include soil disturbance activities, such as plowing and driving vehicles. These and other typical factors are listed in EPA Report 520/1-90-015 (17:5-4 to 5-5).

These factors can affect particle resuspension in several ways. In general, smaller particles stay airborne longer and travel longer distances, including from off-site locations into the test site. Increased mechanical action such as plowing or vehicular movement increases resuspension of particles. Conversely, increased surface coverage such as by vegetation will tend to decrease resuspension. Increased wind speed will tend to increase resuspension of particles; increased rain will tend to decrease resuspension of particles. Finally, older deposits tend to have less resuspension due to weathering, leaching, and binding of contaminant to soil.

Product 7. Needs. The airborne DU concentration estimate must be in a probabilistic format compatible with the health risk assessment calculations.

4.3.2 Setting Objectives. Our purpose for this step was to define the criteria for determining how best to determine airborne DU concentrations. We considered cost, schedule, and performance to be important factors in the selection process. Specifically, we chose the following objectives to measure potential alternatives against:

1) least cost to acquire and operate the model,

2) least time to acquire the model,

3) least time to set-up and run the model,

4) most applicable model to our case, and

5) most acceptable model in the scientific or public community.

4.3.3 Developing and Modeling Alternatives. Because measured airborne DU concentrations at TA C- 64 were unavailable, we chose a modeling approach for this analysis. Typical model parameters are listed in Table 4.10 (58).

We identified three resuspension model alternatives which are described below. These models occur several places in the literature; the descriptions below are provided by Healy (36).

Parameter	Description	Units
Airborne particulate concentration	activity of DU divided by volume of air	pCi/m^3
Respirable fraction of particles	mass of respirable particles divided by mass of all particles	%
Concentration of DU on particles	mass of DU divided by mass of soil	g/g

Table 4.10 Resuspension Model Parameters

The first model, *mass loading*, is the simplest one and was originally developed to find resuspension of fallout particles after nuclear weapons testing. Equation (4.30) describes this model mathematically.

$$\chi = C_m C_p \tag{4.30}$$

where χ is the air concentration of the material of interest (pCi/m^3), C_m is the concentration of the material of interest in soil $(pCi/\mu g)$, and C_p is the concentration of all particulate matter in the air $(\mu g/m^3)$.

The second model, *resuspension factor*, was developed to relate airborne radioactivity concentrations above a contaminated site soon after the radioactive material had been deposited. Equation (4.31) describes this model.

$$C_a = Sf\ C_s \qquad\qquad (4.31)$$

where C_a is the air concentration of the material of interest (pCi/m^3), Sf is the resuspension factor (a factor empirically derived from C_a/C_s for a site with known air concentrations) $(1/m)$, and C_s is the surface radioactivity soon after deposit (pCi/m^2).

Finally, the *resuspension rate model* was developed to estimate radioactivity concentrations in air over an area of deposited radioactive particles and is given in Equation (4.32).

$$F_v = R\ C_s \qquad\qquad (4.32)$$

where F_v is the radioactivity flux $(pCi/m^2\ days)$, R is the resuspension rate (based on Sf , average wind velocity, and site specific constants), and C_s is the surface radioactivity soon after deposit (pCi/m^2).

4.3.4 Evaluating Alternatives. In this step, we defined specific cost, schedule, and performance criteria to evaluate the three DU particle resuspension models; these criteria are shown in Figure 4.19. Each of the models were evaluated against the objective criteria; results are presented in Table 4.11.

4.3.5 Selecting an Alternative. We chose the mass loading model as the dominant solution. All other criteria being equal, the mass loading model was the most applicable to our case and required the least data. The other models required more detailed information with respect to site characteristics which was unavailable.

We considered several adjustments to the mass loading model to account for inconsistencies between our case study and the mass loading model assumptions. However, for each assumption, we chose the conservative approach of not adjusting the model, due to lack of data to direct specific adjustments. We discuss these possible adjustments below.

Steady state soil particle mass loading. The model assumes that the contaminant is spread over a large enough area that the mass loading over any one location is not affected by differing mass loadings 'blowing' in from adjacent locations. In our case, the contaminated area was relatively small, so that the soil loading was potentially not in equilibrium; no adjustment factors are provided in the literature. Because the larger
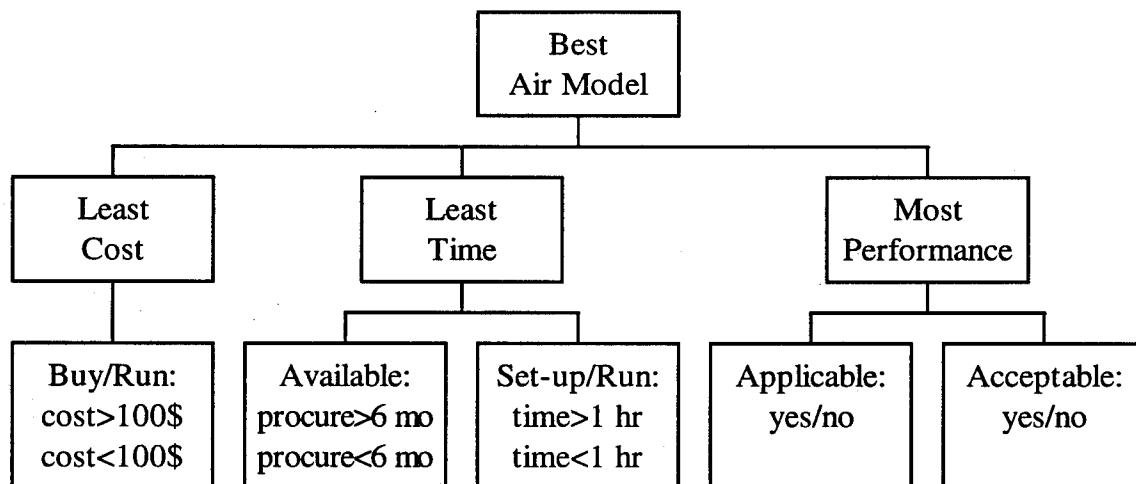
Figure 4.19 Objective Criteria Measurables

4-54

Objective	Mass Loading	Resuspension Factor	Resuspension Rate
Cost	Inexpensive	Inexpensive	Inexpensive
Available	Immediate	Immediate	Immediate
Set-up/run	Short	Short	Short
Applicability	**Applicable**	Not Applicable[1]	Not Applicable[1]
Acceptability	Accepted	Accepted	Accepted
[1] Note: Due to lack of site specific data, complicated models were unwarranted			

Table 4.11 Resuspension Model Evaluation Against Objective Criteria

surrounding area was uncontaminated above background levels and would tend to dilute the mass loading over our site, we chose to be conservative and not adjust for this factor.

Weathering effects. As mentioned in the background section above, older deposits such as TA C-64's typically have a lower mass loading because contaminants tend to dilute, leach, and bind to the soil with time. This tends to reduce the contaminant available for resuspension and make the deposit more homogeneous in the environment. Site specific information is required to appropriately apply an adjustment factor for this effect. Again, in the absence of site specific data, we chose to be conservative and not adjust for this factor.

Distribution of DU with respect to soil particle size. There is some evidence to suggest that radionuclides in soil tend to associate preferentially (up to three times the total activity) with the smaller (less than 20 μm) soil particles (36:228). However, only about 30% of soil is typically in the respirable size range (less than 10 μm) (17:5-23). Without specific information about the distribution of DU with respect to soil particle size, we chose to assume these factors would tend to cancel each other out since the DU concentration in soil which we used in our model was inclusive of all particle sizes.

4.3.6   Planning for Implementation.   In this section, we apply the mass loading

model to characterize the air concentration of resuspended DU-contaminated particles.

Recall Equation (4.33) for the mass loading model:

$$\chi = C_m\, C_p \qquad\qquad (4.33)$$

where χ is the air concentration of DU in the air (pCi/m^3).

To estimate a value for the airborne particulate concentration, C_p, we looked to

the literature to provide examples for similar cases. Anspaugh (4) suggests a "reasonable

mass loading for predictive purposes" of 100 μg/m^3. The National Air Sampling

Network provides a measured value of 33 μg/m^3 for the non-urban Southeastern United

States (17:5-16). Healy suggests an average value of 120 μg/m^3 (35) or a conservative

value of 200 μg/m^3 (36) if mechanical disturbance resuspension effects are included.

Since mechanical disturbance in the area is limited, we chose to use an estimated value in

the range from 33 and 120 μg/m^3 with a uniform distribution. This range covers the

majority of reported values; in the absence of any specific site information, we assumed a

uniform distribution.

The final airborne DU concentration is then found by applying Equation (4.3.1) to

the concentration of the DU-contaminant in the soil, C_m, modeled in Section 4.1. and the

concentration of particulate matter in the air, C_p, estimated by a uniform distribution from

33 to 120 μg/m^3.

4.4   *Overall summary*

In this chapter we used the systems engineering process to select the most appropriate models for characterizing the DU contamination in the soil, groundwater, and air. For soil analysis we used kriging. To obtain the DU concentration in the groundwater we developed an analytical model. To obtain the DU concentration in the air we used an analytical mass loading model   We implemented these models to obtain results in terms of probability density functions as input to the stochastic health risk assessment analysis presented in chapter five.

The soil characterization analysis not only fed into risk assessment, but also fed into groundwater and air analysis. Thus, proper soil characterization was paramount for a sound site characterization. This chapter can be summed up in the following diagram (Figure 4.20).

In the next chapter we develop and implement an appropriate risk assessment model to determine health risk to humans.
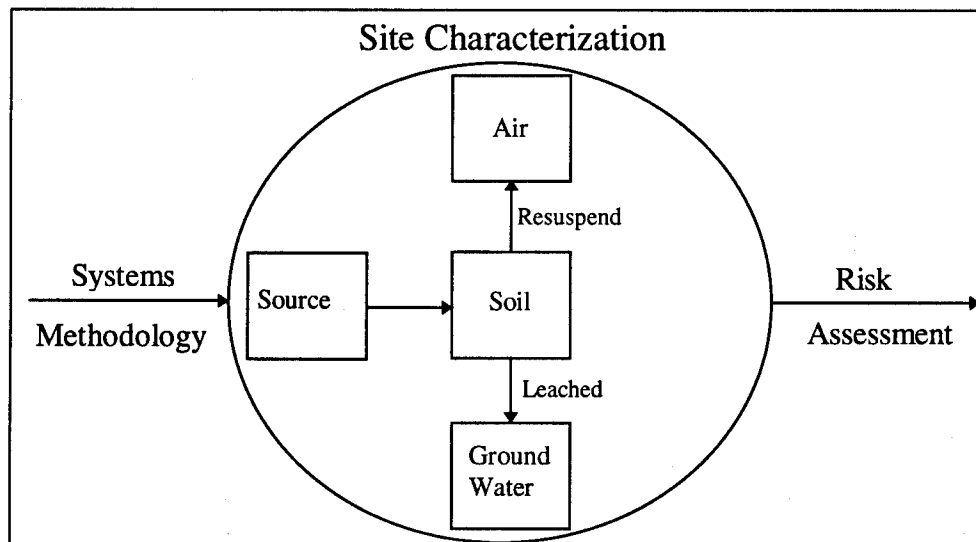
Figure 4.20 Chapter Four Summary Diagram

V. Risk assessment

5.1   Defining the Problem.

We used several tools to define the risk assessment problem adequately. First, we developed a concise statement of the problem to be solved and defined the goal of the risk assessment. Then, for the descriptive scenario, we described the data which would be useful in our analysis. Finally, we further developed the scope portion of the twelve products for the risk assessment. Our results of this step are discussed below.

Well Conceived Title. Our overall goal was *to utilize existing information to develop a quantitative and qualitative description of potential health risks resulting from the DU contamination on which to base risk management decisions.* This main goal was broken down into three sub-problems. First, we needed to decide what types of human health risk to measure (carcinogenic, genetic, etc.). Second, we needed to define the best method by which to calculate risk (empirical models, EPA risk methods, etc.). Finally, we needed to determine how to model these risk measures (probabilistic or deterministic methods).

Descriptive Scenario. The following is a summary of the data we obtained prior to this stage of the assessment. We had characterized the soil activity. From this information, we estimated the radionuclide concentration in the soil, groundwater, and air (Chapter 4). We also had a good understanding of the geology and geography of the area, as well as average weather conditions.

Scope. Next, we addressed the boundaries of the risk assessment. We considered risks for both future and current land use scenarios. We assumed that the future land use of TA C-64 will be as a residential area. The current land use is as a test area for DU-containing munitions.

Our next step was to decide which risks we thought were relevant. The applicable risks for radionuclide exposure are carcinogenic, non-carcinogenic, genetic, and teratological (52). For this study, we decided to consider carcinogenic and non-carcinogenic risks. These two risks allowed us to demonstrate the systems methodology; genetic and teratological risks would be handled similarly.

We simplified the analysis by assuming that all the radionuclide activity estimated in the environment was from DU and that the DU was made up of 99.8% U-238 and 0.2% U-235. For the future land use, we assumed that the DU in the RCA would be cleaned to levels less than or equal to that of the area surrounding the RCA currently. Finally, to simplify our analysis, we looked at health risks due to the current estimates of environmental activity and did not try to estimate how that concentration will change over time. In other words, we did our health risk analysis for a snapshot in time with the estimated concentrations from the environmental models.

5.2   *Setting Objectives*

In this step, we defined what objectives were valuable to us in developing a quantitative and qualitative description of potential risks. These objectives were specific and measurable so that we could determine which risk calculation method was best for

our application. We developed the following objectives: maximize applicability, usability, and acceptability; and minimize use of resources (Figure 5.1).

```
                    ┌─────────────────────┐
                    │ Best Risk Assessment│
                    └─────────────────────┘
        ┌──────────────┬──────────┴──────┬──────────────┐
   ┌─────────┐   ┌─────────┐   ┌─────────┐   ┌─────────┐
   │  Most   │   │  Most   │   │  Most   │   │  Least  │
   │Applicable│  │ Usable  │   │Acceptable│  │Resources│
   └─────────┘   └─────────┘   └─────────┘   └─────────┘
                         ┌──────────┼──────────┐
                    ┌─────────┐ ┌──────────┐ ┌──────────┐
                    │ Public  │ │Regulations│ │Scientists│
                    └─────────┘ └──────────┘ └──────────┘
```
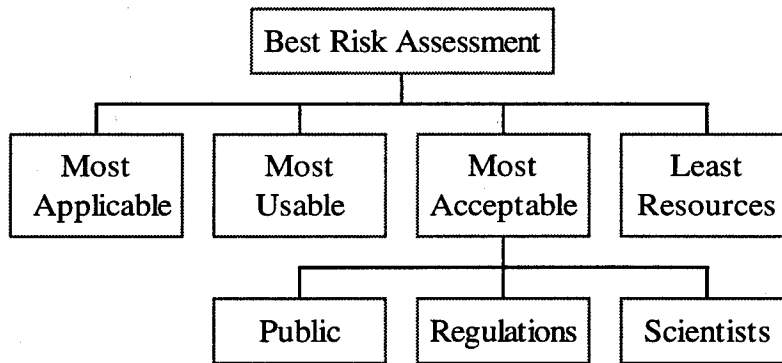
Figure 5.1 Objective Criteria

Applicability. In the area of applicability, the risk assessment method should be compatible with the scenario experienced at TA C-64. In other words, the method used in the risk assessment should be consistent with the type of contamination found at the TA C-64, the environmental conditions, the population type, etc.

Usability. For usability, the amount of data available must be adequate to support the risk method without making unreasonable assumptions. Also, we must have the tools necessary to analyze for risk. The risk method should be documented well enough to follow and understand the underlying assumptions and limitations. The method should also provide a maximum amount of useful information to increase the risk manager's options.

Acceptability. To measure acceptability, we wanted to determine how well the risk method was accepted by the applicable regulators, the scientific community, and the

general public. To measure this, we considered how often each method was used and the degree of opposition associated with it. We also wanted to evaluate the physical grounding or validity of the risk method. A final measure for acceptability was the ease with which regulators could check the quality of the risk assessments using a particular risk method (Quality Assurance).

Resources. Finally, we measured the use of resources by the amount of time and difficulty of analysis necessary to achieve an estimate of risk.

5.3   Developing Alternatives

Now that we had identified the problem and a way to evaluate solutions, we wanted to consider the possible methods of calculating risk.

For our first attempt to generate a list of risk calculation methods, we used different scientific studies on the effects of radiation on human populations, such as Committee on the Biological Effects of Ionizing Radiation (BEIR) reports, United Nations Scientific Committee on the Effects of Atomic Radiation (UNSCEAR) reports, National Council on Radiation Protection and Measurement (NCRP) reports, etc. We found that these studies were the basis for all risk assessments in the literature (59). However, we quickly learned that considerable work was involved to use the information in these reports to derive radionuclide-specific risk factors. Instead of using these studies directly, we decided to use the EPA-generated risk factors for our radionuclides (56). The EPA uses a clear and technically acceptable approach using the studies above to generate reasonable risk factors.

We decided to consider the following three alternatives to calculate risk. The first alternative compared radionuclide intake dose to *federal occupational standards*. The second alternative was the *point estimate*. The third alternative was a *probabilistic risk assessment* using random variables to represent each factor in the risk calculations.

Before moving on to the modeling stage, we examined each of our possible methods for calculating risk to see if any were not feasible or were impossible to model, so that we could reduce the amount of modeling required. The federal occupation standards only indicated passage or failure with respect to established standards and as such yielded little information concerning the magnitude of risk. This violated one of the tenants in the usability criteria, so the federal occupational standards were eliminated. The rest of the alternatives were candidates and were therefore modeled.

5.4   Modeling Alternatives

Before describing the different alternatives, we discuss the appropriate risk models and pathways we considered with these alternatives.

Risk Model Development. Before deciding which method we would use to calculate risk, we had to develop the risk models (equations). We decided to use equations recommended by the EPA Superfund guidance (57) as a starting point and modified them for our particular application. These equations have been used for a wide range of environmental contamination scenarios. Also, they did not require an extensive amount of site specific data, other than contaminant concentrations in the respective media. A description of the risk equations is presented in Appendix C.

For carcinogenic risk, we used equations for the probability of contracting fatal or non-fatal cancer due to DU exposure. For non-carcinogenic risk, we used equations for the hazard index. The hazard index used a reference dose (RfD) which was the maximum level of DU a person could intake without adverse effects. A hazard index calculation equal to unity was the hazard threshold. In other words, a hazard index of less than one was safe; a hazard index of greater than one was harmful. The RfD we used was for uranium-based soluble salts from a rabbit bioassay (56). The RfD was based on the Lowest Observable Adverse Effect Level (LOAEL) with medium confidence and an uncertainty factor and modifying factor of 1000 and 1 respectively. The critical effects from the bioassay were initial body weight loss and moderate nephrotoxicity.

Pathway Model Development. Next we determined which pathways to model. In reality, the number of exposure pathways was almost infinite. In our assessment, we only modeled primary pathways which contributed significantly to risk. To determine which pathways were significant, we considered the following: inadvertent soil ingestion, external irradiation, inhalation of suspended particulate, water ingestion, dermal contact, air immersion, water immersion, meat ingestion (cattle, deer, fish, birds), fruits/vegetables ingestion, and milk ingestion. We believed that inadvertent soil ingestion, external irradiation, and inhalation of suspended particulate were applicable for both land use scenarios. We also thought tap water ingestion was applicable for the future land use because a house might use a residential well. However, no potable wells currently exist at TA C-64, so the water ingestion pathway was not considered for the current occupational land use. Dermal contact was ruled out because skin absorption factors of uranium were

very low and excessively high amounts of uranium were needed to have effects on even small animals (1). Air immersion was not considered because this phenomena was generally applicable for fallout from a nuclear accident. Since the rain run-off did not concentrate in a non-flowing body of water (e.g. a lake), water immersion was ignored. We considered exposure from contaminated meats, fruits/vegetables, and milk as secondary exposure pathways for our scenarios, so they were ignored. We used the same pathways for non-carcinogenic risk, except the irradiation pathway did not have a non-carcinogenic effect and was, therefore, not included (Figure 5.2)

Now that we have determined the equations to use and the pathways to consider, we discuss some relevant theory of risk, in the environmental sense.

Theory. In estimating risk, several scenario dependent variables must be considered. In most environmental risk assessments these variables attempt to characterize the quantity/concentration of harmful substances released into the environment by an event, exposure of individuals/populations to the harmful substances, and the adverse health effects resulting from this exposure. These variables can be represented as a vector as shown in Equation (5.1).

$$\mathbf{U} = (U_1, U_2, ..., U_n). \tag{5.1}$$

The risk can be expressed as some function of these variables, $G(\mathbf{U})$. Inherent to $G(\mathbf{U})$ is the inability to accurately predict what level of each U_i will be observed. The inability to accurately predict $G(\mathbf{U})$ is due to both variability and uncertainty.
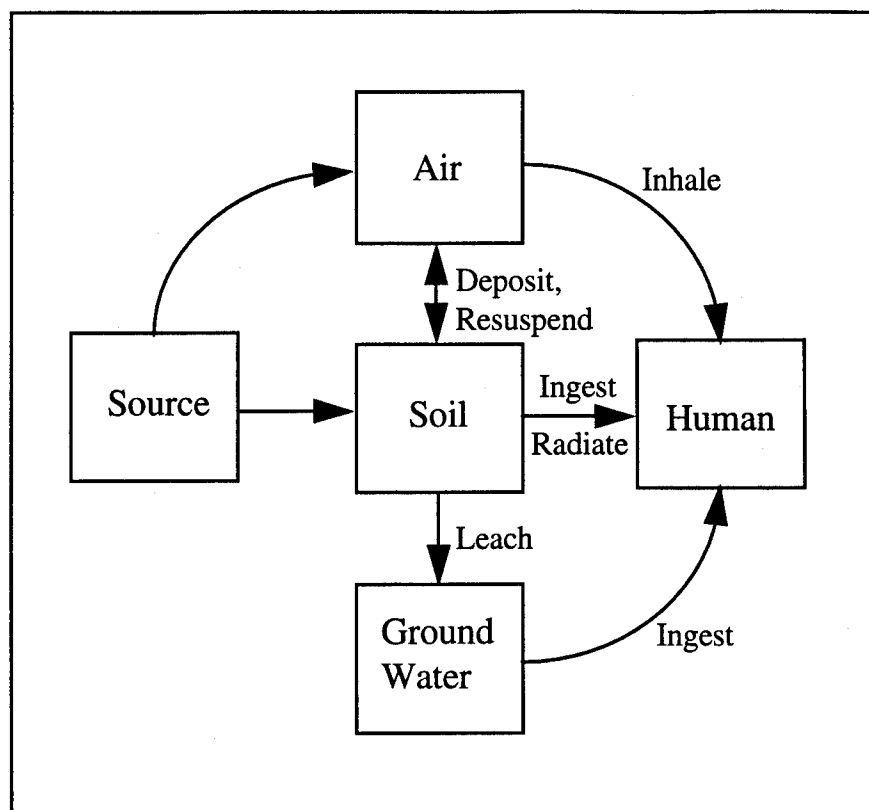
Figure 5.2 Exposure Pathways of Humans to DU

Variability is the imprecision that occurs due to natural differences among

members in the population of interest. For example, if the population of interest is a

contaminated plot of land, the concentration of the contaminant will vary spatially. If the

population of interest is a group of people, then breathing rates will vary from one

individual to another. Again, variability is inherent in each U_i and can not be reduced.

Uncertainty is the imprecision due to a limited understanding of the

phenomena being modeled and/or simplification of the physics of the phenomena. For

example, if you measure contaminant levels at several locations, you can estimate the

spatial variability. Since every location is not sampled, this estimate is uncertain because

of your limited understanding of spatial concentration. Or, if you chose to model the dose response of some contaminant as a linear relationship, when in fact the relationship is non-linear, your model will be imprecise. Generally, uncertainty can be reduced by gathering additional data or by increasing the complexity of the model.

Alternative Models. Having developed the theory, we now present our alternative models.

Deterministic methods (point estimates) use a single value for each U_i to produce a single risk estimate. This type of method ignores the effects of imprecise parameter estimation. In reality these parameters have a range, or distribution, of possible values due to variability and uncertainty. Failure to account for this range means that estimates from deterministic models will be difficult to interpret. Therefore, such estimates provide decision makers limited information to base risk management decisions. If the intent is to explicitly account for the range of possible parameter values, modeling approaches which are stochastic rather than deterministic, should be considered.

Probabilistic methods treat the U_i's as random variables. Therefore, a pdf can model the variability and uncertainty of the U_i's. Since $G(U)$ is a function of random variables, it will also be a random variable. Then the risk of the hazard occurring is the probability that event $G(U)$ occurs. Unfortunately, solving for this probability can be very difficult, if not impossible, in closed form for many real world problems. Typically semi-analytic (first order reliability method (34)) or simulation methods (Monte Carlo (60)) are used to estimate the solution.

An exact, closed form solution can be determined using First Order Reliability Methods (FORM) for a function of Gaussian distributed, independent random variables. However, the FORM algorithm will yield reasonable probability estimates for non-linear functions of non-Gaussian independent random variables. Non-linearity is accounted for by iterating about a first order Taylor series expansion of G(U) until the solution converges. Non-Gaussian random variables are accounted for by determining the first two central moments of the equivalent Gaussian random variables. The resulting equivalent Gaussian pdf has the same slope at the expansion point and same area under the curve as the underlying pdf on either side of the expansion point. A useful output of FORM is the importance factors. The importance factors determine the sensitivities of each random variable relative to the overall variability and uncertainty of the solution.

Another common method used to estimate complicated probability functions is the Monte Carlo simulation. Monte Carlo attempts to simulate all possible outcomes of G(U) through random number generation. A Monte Carlo iteration is performed by randomly selecting a value from each U_i pdf and calculating G(U). Many iterations are required to obtain solution convergence. However, the number of iterations can be significantly reduced by using sampling algorithms that maximize the coverage of pdf sampling (e.g. Latin Hypercube Sampling (LHS)). Parameter importance can be determined by correlating the randomly selected parameter values with the resultant model estimates. The relationship between each parameter variability and uncertainty and the resulting risk variability and uncertainty can be measured by the magnitude of this correlation.

5.5   Evaluating and Selecting Alternatives

In this step, we decided which risk alternative to use. As mentioned earlier, the point estimate did not account for variability and uncertainty. According to our applicability criteria, the risk assessment method needed to be consistent with the actual environmental conditions. The environmental conditions at TA C-64 involved variability and uncertainty with respect to the DU contamination distribution. Therefore, we chose not to use the point estimate as our primary model; however, we used it as a screening tool. By using conservative values for the parameters, we obtained a point estimate which bounded the problem. In other words, if we found that any of the pathways turned out to be insignificant using a conservative point estimate, we ignored them in the detailed analysis. Our criterion for 'significant' was a risk of 1.0E-7, which was an order of magnitude lower than the 1.0E-6 risk goal commonly used as a cut-off for acceptable environmental contamination risk (57). The resulting point estimate for each pathway considered was above the 1.0E-7 risk criterion using conservative parameter values. Therefore, all pathways were analyzed.

At this point, two of the alternatives for evaluating risk remained: FORM and Monte Carlo. Both of these alternatives were probabilistic and required that the independent variables be random. The description and derivation of all random variables is given in Appendix C. To determine which method was best for our application, we ran a test case using each method and compared them using our objective criteria. For our test case, we chose to develop the cumulative density function (cdf) for the irradiation pathway due to its simplicity (i.e. it was only a function of two random variables).

We programmed FORM using MathCad 5.0 Plus ® (47) and used Crystal Ball 3.0®

(22) for the Monte Carlo analysis. The FORM solution converged after 15 iterations. We

performed 15,000 Monte Carlo iterations using LHS. The solution converged after 10,000

iterations. The cdf from both methods compared well with one another for the test case.

The objective criteria are given in Table 5.1 with an evaluation of each method with respect

to each criterion. Based on our objective criteria, we chose to use Monte Carlo via Crystal

Ball 3.0®.

Criteria	Evaluation
Applicability	No difference, both models were equally applicable
Usability	Crystal Ball 3.0® conveniently provided summary percentiles, useful run statistics, a cdf plot, and a pdf plot. However, these 'extras' were not inherent in the Monte Carlo method; rather, they were features of the Crystal Ball 3.0® software package. These same 'extras' could be programmed in MathCad 5.0 Plus ®.
Acceptability	Monte Carlo was commonly used by analysts in environmental risk assessments (67; 18; 21), even though regulators still relied on the point estimates to make remediation decisions. To our knowledge, FORM has not been used in environmental risk assessments; however, reliability engineers have used FORM for many years (34). Independent validation of the analysis results using Monte Carlo was easier to perform because of its simplicity relative to FORM.
Resources	Using Crystal Ball 3.0®, the Monte Carlo method was easier to use. As mentioned earlier, many of the 'extras' found in Crystal Ball 3.0® could be programmed with a good deal of up-front time, making each equally as user friendly.

Table 5.1 Monte Carlo versus FORM Evaluation

5.6   Planning for Implementation

The final step of this section was to develop our risk assessment information for use (or implementation) in the risk management process. We developed risk assessments and hazard indices for both the future residential case and the current occupational case.

Residential Case. In the residential case, we used Crystal Ball 3.0® to run three different probabilistic assessments for clearer information about the risk of cancer at TA C-64: one for background radiation levels, one for average site radiation levels, and one for the high radiation levels at the site. The background pdf was generated using sampling data around the Eglin AFB land range (12) and the average and high pdfs were obtained from the kriging analysis. We found the risk histograms converged after about 10,000 iterations using LHS so we used 15,000 iterations for our assessment to ensure convergence.

The risk histograms shown in Appendix C are empirical cdfs of the risk. The cdfs show the probability that the estimated risk is less than or equal to some arbitrary risk of interest. Table 5.2 is a summary of the residential carcinogenic risk histogram and can be interpreted in the following manner. The tenth row indicates that there is a 90% probability that the estimated risk is less than or equal to 3.49E-7, 6.64E-7, and 8.31E-6 for the background, average, and high soil concentrations, respectively.

We used Crystal Ball 3.0® to create a sensitivity analysis to help us determine how much each random variable contributed to the overall variance. The sensitivity analysis showed us that the exposure duration was by far the biggest cause of uncertainty and variability. We expected this to be the case because of the high variability in moving

Percentiles	Background	Average	High
0	5.66E-12	1.11E-10	1.31E-09
10	6.46E-09	2.21E-08	2.81E-07
20	1.51E-08	4.42E-08	5.85E-07
30	2.66E-08	7.10E-08	9.68E-07
40	4.26E-08	1.03E-07	1.41E-06
50	6.40E-08	1.47E-07	1.96E-06
60	9.36E-08	2.05E-07	2.70E-06
70	1.38E-07	2.81E-07	3.70E-06
80	2.07E-07	4.13E-07	5.25E-06
90	3.49E-07	6.64E-07	8.31E-06
100	2.66E-06	1.68E-05	8.65E-05

Table 5.2 Percentile Probability for Residential Risk of Cancer

characteristics of people in the United States. The next highest contribution to uncertainty and variability in the histograms for average and high concentrations was the soil concentration. Other pdfs contributed little to the uncertainty or variability to the overall risk. We examined the individual risk pathways involved and found, for residential land use, the inhalation risk caused the highest risk, with water ingestion causing the next highest risk. To determine the sensitivity of the water portion of the analysis, we increased the DU concentration in the water by two orders of magnitude. This large change in concentration only doubled the overall risk, indicating the analysis was insensitive to large errors in the water concentration of DU.

For the residential hazard index of TA C-64, we used Crystal Ball 3.0® to develop probabilistic assessments for inhalation, soil ingestion, and water ingestion pathways for the higher soil concentration only. The ingestion pathway results are shown in Table 5.3. For the soil case, the ingestion rate of children caused over 90 percent of the variability

Percentiles	Soil Ingestion	Water Ingestion
0	0.001	0.0000
10	0.007	0.0002
20	0.009	0.0003
30	0.010	0.0005
40	0.012	0.0006
50	0.013	0.0008
60	0.015	0.0009
70	0.018	0.0011
80	0.021	0.0012
90	0.028	0.0015
100	0.104	0.0029

Table 5.3 Percent Probability for
Residential Hazard Index

and uncertainty in the hazard index calculation. For the water case, over 90 percent of the

variability and uncertainty was caused by the concentration of DU in the groundwater.

Occupational Case: In the occupational case, we also used the background,

average, and high radiation levels in the cancer risk calculations. We found that the

histograms also converged after about 10,000 iterations using LHS. The histograms

provided the percentiles of risk for the occupational case shown in Table 5.4.

The sensitivity analysis showed us that occupational variable duration caused the

most uncertainty and variability. We determined that the inhalation pathway contributed

almost all of the risk for the occupational land use (90%).

For the occupational hazard index, we did a probabilistic assessment for the

inhalation and soil ingestion pathways for the high soil concentration only. Inhalation

numbers were too low to be of any concern. The soil ingestion hazard indices are

Percentiles	Background	Average	High
0	3.42E-12	6.23E-10	1.56E-08
10	6.39E-09	1.22E-08	7.12E-08
20	1.28E-08	2.37E-08	1.27E-07
30	1.92E-08	3.53E-08	1.83E-07
40	2.76E-08	4.68E-08	2.73E-07
50	4.05E-08	5.84E-08	3.71E-07
60	5.90E-08	6.99E-08	5.44E-07
70	8.98E-08	8.94E-08	8.25E-07
80	1.49E-07	1.50E-07	1.31E-06
90	2.91E-07	3.01E-07	2.43E-06
100	7.08E-06	2.37E-05	5.18E-05

Table 5.4 Percentile Probability for Occupational Risk of Cancer

provided in Table 5.5. Note that the sensitivities were not calculated for this case since the risk values were so low.

5.7   Conclusion

In this phase of the study, we used the DU concentrations derived in the site characterization (Chapter 4) to assess the risk for both the occupational and residential land use scenarios. We used the systems engineering process to decide the types of risk,

Percentiles	Soil Ingestion
0	0.0000
10	0.0002
20	0.0005
30	0.0007
40	0.0009
50	0.0011
60	0.0014
70	0.0016
80	0.0019
90	0.0022
100	0.0038

Table 5.5 Percent Probability for Occupation Hazard Index

the pathways, and the methods of calculating risk for these scenarios. We analyzed the carcinogenic and non-carcinogenic risks due to irradiation, water ingestion, soil ingestion, and inhalation of DU. These risks were calculated using EPA recommended equations (probability of risk for carcinogenic risks; hazard indices for non-carcinogenic risks) with random variable values for the variables in the equations. This resulted in risk histograms of the probability of encountering a certain level of risk, as presented in Section 5.6 and Appendix C. We found that there was no risk of non-carcinogenic hazard. The interpretation of the carcinogenic risk was left for the risk management phase of this study which is presented in the next chapter.

VI.   Risk Management

At this point, we have estimated pdfs for DU concentration in the soil, groundwater, and air (Chapter 4). From these pdfs, we have estimated health risks for these different media for both occupational and residential land use scenarios (Chapter 5). Based on these health risks, we concluded for both land use scenarios that non-carcinogenic hazards were not of concern; all of the non-carcinogenic hazard indices were below unity. Interpreting the results for the carcinogenic hazards was not as straight forward for two reasons as discussed below.

First, in the derivation of the carcinogenic slope factors, we used the commonly accepted assumption that there was no 'safe' threshold dose below which there was not a chance of contracting cancer. Without a reference dose with which to compare our results, we needed to address the question of how to determine what was an 'acceptable risk.' The answer would differ depending on whether we were asking an individual who tended to be risk-seeking or risk-averse.

Secondly, because of the probabilistic nature of our analyses, the results were characterized by a range of risks with associated probabilities. This further complicated our determination of what was an 'acceptable risk' by adding the question of 'how certain' did we want to be about those ranges of risk. This was even further complicated by social, political, and economic considerations

Guidance for accomplishing risk management objectives can be found in the Code of Federal Regulations (CFR). Specifically, 40 CFR provides guidelines for choosing and

evaluating remedial alternatives by developing alternatives, establishing objectives and criteria, and choosing the best alternative by a trade-off study using the selection criteria (51:Sections (e)-(f)). However, 40 CFR gives no specific guidance on how to do a trade-off study analysis or how to generate a list of alternatives (although innovative technologies are encouraged).

Our objective in this section was to see how the systems engineering process could improve or add to the CFR's effectiveness as a general systematic framework for making risk management decisions. We also present methods to evaluate the questions of 'what is acceptable risk' and 'how certain do we want to be of the risk.' For this study, we decided to develop risk management options for scenarios which exceeded 1.0E-6 risk at some certainty level. Occupational and residential land use scenarios exceeded this risk for background, average and maximum soil pdfs at some certainty level (Chapter 5), so we studied risk management options for both land use scenarios.

6.1   Defining the Problem

In this section, we developed a risk management problem definition using some of the 'twelve products' developed in Chapter 3. Our results from this step are discussed below.

Problem Statement. We developed the following problem statement for risk management: *given the characterization of the site and the risk assessment, determine the best way to reduce the risk to an acceptable level at site TA C-64.*

Needs, Alterables, and Constraints. We defined the needs for this section as follows: reduce estimated health risk to acceptable levels for the occupational and residential land use scenarios. This need was constrained by several items:

1) current laws regarding DU exposure,

2) available technical capabilities,

3) maintenance of current operations at TA C-64 (occupational scenario), and

4) area must be open to all types of public use (residential scenario).

We defined possible alterables as follows:

1) health risk analysis variables,

2) level of acceptable risk and confidence,

3) physical characteristics of the landscape,

4) resources available for remediation,

5) additional sampling data,

6) operational procedures used to operate the area, and

7) remediation options.

6.2   Setting Objectives

We developed objective criteria and measures of effectiveness (MOEs) to support the synthesis of our alternatives (see Figure 6.1). These objectives and MOEs were developed with complete agreement from the CDM. For this case study, the systems engineering students and advisors acted as the CDM. In the following paragraphs, a brief description

The Best Way To Reduce The Estimated Health Risk Exposures
To Acceptable Levels

Minimize Resources

Cost
- Remedation Cost — $
- Control Mech Cost — $
- Sampling Cost — $

Time
- Months

Maximize Performance

Acceptability

Final Risk Level
- Public — Yes/No Subj
- Regulator — Yes/No Subj
- Commander — Yes/No Subj
- Scientists — Yes/No Subj

Method of Solution
- Cancer Risk Uncertainty Level — Subj
- Impacts on Other Environments
  - Physical Environment
    - Short Term — Subj
    - Long Term — Subj
  - Social Environment — Subj
  - Esthetic Environment — Subj
  - Economic Environment
    - Short Term — Subj
    - Long Term — Subj
- Impacts on Ecology — Subj

Effectiveness
- Short Term Effectiveness — Subj
- Long Term Effectiveness — Years

Figure 6.1 Risk Management Objective Criteria

of each objective and the factors considered in assigning an MOE rating are discussed.

Many of the factors were adapted and tailored from a list presented in the *Environmental
Impact Analysis Handbook* (61).

Objective 1. Minimize Resources. The MOEs for costs and time were defined in terms of dollar amounts and months taken, respectively, for implementing a particular alternative.

a) *Cost*

1) *Remediation Cost.* This category included all of the cost related to the actual clean-up operation, including personnel, materials, shipping, storage, paperwork, and other logistics components.

2) *Control Mechanism Cost.* This cost related to limiting exposure to people, and/or implementing physical devices to prevent further transport of contaminants from inside the RCA to outside the RCA.

3) *Sampling Cost.* This was the total cost incurred from characterization studies, transport mechanism studies, or other specialized studies.

b) *Time.* The rating for this category included estimates for contractual lead time, studies, remediation time, and control implementation time required for each alternative.

Objective 2: Maximize Performance

a) *Acceptability:* Most of the MOE's for this objective were based on subjective judgment, except where noted.

1) *Final Risk Level.* This represented our estimate of the acceptability by the public, regulators, scientists, and the commander of the final risk level that would result from implementing the alternative. The estimate was independent of the method used to obtain that risk level.

2) Method of Solution

(a) *Cancer Risk Certainty Level:* We based the rating for this category on the confidence level chosen from the cancer risk cdf for use in determining remediation requirements.

3) Impacts on Other Environments

(b) *Physical Environment.* For both the short term and long term MOE's, we considered whether the alternative would produce any of the following effects: emissions into the atmosphere of toxic or hazardous substances; significant depletion or degradation of the groundwater; significant changes to the land forms and natural soil erosion patterns; excessive noise effecting humans or wildlife; and type of solid waste generated by the alternative.

(b) *Social Environment:* This was a subjective evaluation and considered whether the alternative would cause or impact any of the following factors: changes in the activity patterns of the local population; changes in any institutions or services; attitude of the community towards this alternative; effect on areas with a recognized archaeological value; and effect on public parks or recreational areas.

(c) *Esthetic Environment.* This was a subjective evaluation of whether the alternative would alter the esthetic qualities of the area.

(d) *Economic Environment.* We also broke this sub-objective into two MOEs: short term impacts and long term impacts. The following factors were considered: creation of employment opportunities; effect on land values in the area; and disruption of existing land uses.

4) Impact on Ecology: This rating was subjective and we considered whether the alternative would produce any of the following effects: impact on breeding, nesting, and feeding grounds for birds; substantial alteration of the behavior patterns of fish, mammals, amphibians, reptiles, and insects; significant destruction of vegetation; and impact on endangered species.

b) Effectiveness

1) Short Term. The short term effectiveness MOE was a subjective measure of how much risk the workers would be exposed to during the implementation of the alternative. We considered the following factors in assigning this rating: the risks to workers during remediation and the type of worker protective measures used.

2) Long Term. This represented our estimate of the expected number of years before remediation would be required again.

6.3 *Developing Alternatives*

For the occupational land use scenario, we concluded that the RCA contained high levels of DU but that appropriate precautions were in place. Therefore, we only considered the transport of DU and the DU that already existed outside the RCA for risk management. In contrast, for the residential land use scenario, we considered all of the DU inside and outside the RCA for risk management.

In developing alternatives to reduce risk, we examined the risk equations in Appendix C. Each risk equation was a function of environmental and site specific factors that we modeled as pdfs. We placed each of the pdfs into one of four general categories:

(1) media concentration pdfs (Cs and Cw),

(2) exposure duration pdfs (ED and OD),

(3) exposure frequency pdfs (EF and Efi), and

(4) ingestion pdfs (IRs, IRw, and IRi).

We only focused on the categories that we could control as risk managers, Categories (1) and (3). Categories (2) and (4) were general population characteristics and could not be controlled.

We then developed general risk management options to address Categories (1) and (3). The following paragraphs outline these risk management options.

Option 1. Do nothing. This option should be included in any systems engineering analysis to insure that change was necessary and beneficial, based on the stated objective criteria.

Option 2. Remediate the contaminated areas. We identified three basic methods of remediation. First, the contaminant could be removed and transported off-site or stored on-site. Second, the contaminant could be spread or diluted to acceptable levels. Finally, the contaminant could be remediated on-site.

Option 3. Control exposure to the contaminated areas. For the occupational land use scenario where unlimited access was not a need, methods of controlling exposure could be used. These consist of physical changes in the environment to control further

DU transport or operational changes in terms of procedures. Examples of possible physical changes included increasing the size of the RCA to include outside contaminated regions, building a larger berm for containment of contaminant, planting/erecting a wind barrier to decrease wind velocity around the RCA, enclosing the RCA, and other methods. Examples of possible operational changes designed to decrease exposure would be to move personnel offsite and/or decrease their access frequency; enact tighter weather restrictions for target butt cleaning; or implementing sifting machine enhancements and procedural changes, and other methods.

Option 4. Study the extent of current contamination. Increased sampling, testing, and studying of the soil, groundwater, and air could be completed to further characterize the environment. Although the additional sampling could be used to reduce the uncertainty of the risk analysis, this may or may not reduce the overall estimated health risk to humans. It could also lead to a more precise understanding of the DU contamination distribution and therefore require less area to be remediated. For this reason, we included this in with the risk management options.

Option 5. Study the contaminant transport mechanisms. In addition to studying the extent of current contamination, studying possible transport mechanisms can lead to a better understanding of how the DU traveled outside the RCA. By itself, studying DU transport mechanisms would not manage or reduce risk, but would provide valuable information toward identifying the risk management areas where taking action could reduce further contamination.

It is important to understand that any one of the five risk management options outlined above was not meant to be the exclusive answer to the problem; rather, a mix of management options may be required to provide the 'best' solution. For that reason, a combination of these general management options were put together as 'concepts' to be evaluated for each land use scenario. Table 6.1 summarizes the five general management options discussed in the last few paragraphs.

Option 1: No Action	Option 2: Remediate	Option 3: Limit Exposure	Option 4: Study Current Contamination	Option 5: Study Transport
	Remove Dilute Treat	Physical Changes Operational Changes	Soil Groundwater Air	Soil Groundwater Air

Table 6.1 Risk Management Options

We now separate our analysis into two sections based on the two land use scenarios. In the next section, we develop, model, and evaluate alternatives for the residential land use scenario. Based on the results of this process, we select and plan for implementation of the selected alternative. We then repeat these last five steps of the seven-step systems engineering process for the occupational land use scenario.

6.4   Residential Land Use Scenario

6.4.1   Developing/Modeling Alternatives. We assumed for the residential land use scenario that the RCA required remediation and that the area surrounding the RCA

may or may not require remediation. To address this problem, we developed the management options from the previous section as applied to the residential land use scenario.

Without further analysis, we eliminated no change (Option 1) and control access to exposure (Option 3) as unacceptable options. We discarded Option 1 since we considered it not publicly acceptable for the government to turn over a contaminated Federal site for public use. Option 3 clearly violated our unlimited public land use constraint. We also eliminated further study (Options 4 and 5) as we believed the site to already be adequately characterized for this 'hypothetical' residential land use scenario. Therefore, we focused our attention exclusively on the remediation option (Option 2).

It was not our intent for this study to do an exhaustive analysis of radionuclide contamination remediation, but to instead provide a basis for evaluation of the systems engineering process as applied to environmental risk management. For this reason, only two remediation methods were analyzed to illustrate the value of the process in selecting the best alternative. The first method (Method 1) involved filling 55 gallon drums with all the DU contaminated soil and shipping the drums to a low level radiation disposal site. The second method (Method 2) involved a volume reduction technique (14) which separates the contaminated soil from the clean soil. The contaminated soil is then packed in 55 gallon drums and shipped off to a low level radiation disposal site.

Before proceeding to the evaluation of the alternatives, a few modifications to the MOEs were necessary to accommodate this scenario. Since this scenario involved no sampling or control mechanisms, the cost that was calculated for each alternative was

used as the MOE for the entire cost sub-objective. Additionally, since the actual risk level was known for each alternative, and it was our assessment that risk level acceptability of the alternatives was proportional to this value, we used the risk level as the MOE for this scenario. The subjective criteria were measured using a zero to ten scale, where ten represented an exceptional rating and zero represented barely acceptable. It was unnecessary to include unacceptable as a possible rating. Methods which were unacceptable in any category were not valid alternatives and did not require any further evaluation.

6.4.2 Evaluating Alternatives/Selecting an Alternative. In this section, we developed a method to compare the different alternatives. This comparison was based on the utility that each alternative provided to the CDM. The utility rating for each alternative was a function of all the MOEs discussed in Section 6.2. Next, we explain how utility was calculated. After this explanation, we apply the method to our case study.

We used a four step process to develop the utility for each alternative. In Step A, we determined the relative importance of each MOE with respect to all the other MOEs. This produced a 'weighting factor' for each MOE which reflected how important that MOE was to the CDM. The weighting factors were normalized to have a magnitude of one to avoid biasing.

Our purpose in Step B was to estimate an MOE value for each alternative. For example, if the MOE was the cost of an alternative, then the cost of each alternative was estimated. For MOEs which were subjective in nature, an exact number was not available. For example, we were not able to estimate a specific value for the esthetics

MOE. However, we were able to assign an MOE value by comparing the relative esthetic value of each alternative on a scale of zero to ten.

Since the measures of each MOE were not necessarily on the same scale (e.g. dollars, risk, opinion), we mapped all of the MOE values to a zero to ten scale in Step C. This mapping provided the *utility* of each MOE.

In Step D, we calculated each alternative's utility by summing the MOE utilities each multiplied by its weighting factor as shown in Equation (6.1):

$$Utility_i = \sum_{j=1}^{n} w_j u_{ij} \qquad (6.1)$$

where the summation index 'i' refers to the i-th alternative, the j-th index refers to the MOE, and w represents weighting factors.

We incorporated the uncertainty involved in estimating each MOE in the evaluation using confidence levels of very confident (VC), confident (C), low confidence (LC), and no confidence (NC). The confidence levels were converted to numerical values for the evaluation as follows: 0.9 for VC, 0.6 for C, 0.3 for LC, and 0.1 for NC. We revised Equation (6.1) accordingly to get the discounted utility as shown in Equation (6.2):

$$Discounted\ Utility_i = \sum_{j=1}^{n} c_{ij} w_j u_{ij} \qquad (6.2)$$

where c is the confidence level.

At this part of the systems engineering process, the CDM should be interviewed to provide an understanding of how the weighting of sub-objectives should be assigned

relative to the overall objective. Again, for the purposes of this section, the we acted as the CDM. The remainder of this section applies this four step process to the TA C-64 occupational land use scenario.

Step A: Develop MOE weighting factors. For the 'first' level of sub-objectives, recall we identified *minimize resources* and *maximize performance* as sub-objectives. When only two objectives were to be evaluated at a time, it was adequate to just compare the two. For our two objectives, we decided that performance of an alternative was more important than the resources required to implement it. We therefore defined weighting factors of [1/3; 2/3] for resources and performance, respectively.

For the 'second' level of sub-objectives under resources, we defined the weighting factors to be [4/5; 1/5] for cost and time, respectively. For the 'second' level performance sub-objectives of acceptability and effectiveness, we assigned weighting factors of [3/4; 1/4] meaning acceptability was three times as important as effectiveness.

Next, we defined the 'third' level sub-objectives' weighting factors under cost, acceptability, and effectiveness, respectively, as follows:

1) all costs can be directly compared; no weighting factors were warranted,

2) [1/2; 1/2] for final risk level and method of solution, respectively, and

3) [1/3; 2/3] for short and long term effectiveness, respectively.

For the 'fourth' level sub-objective, method of solution, we used a judgment matrix approach since there were more than two objectives for evaluation (63). Each element, a_{ij} of judgment matrix **A** represented a pair-wise comparison between two sub-objectives. Odd integers from one through nine were used for the upper triangle of the

6-14

matrix. The lower triangle was filled with the reciprocals of the upper portion of the matrix, making **A** reciprocal symmetric. A pair-wise comparisons of a score of one meant that no difference existed between the compared objectives, a score of three meant that objective 'i' was mildly more important than 'j', a score of one third meant that 'j' was mildly more important than 'i', etc. Even numbers were used for compromises and intermediate judgments.

After the matrix was completed, w considered several methods to manipulate the matrix and obtain normalized weighting factors for the MOE's: using normalized eigenvectors corresponding to the largest eigenvalue (63) or using a normalized geometric mean (70). An equation for calculating the normalized geometric mean is shown in Equation (6.3):

$$v_i = \prod_j a_{ij}^{(1/n)} \tag{6.3}$$

Both methods were applicable; however, we believe that the Crawford and Williams method was more straight forward.

Table 6.3 and Table 6.2 show the judgment matrices, the geometric means, and the normalized weighting factors for the 'fourth' level sub-objective *method of solution* and for the 'fifth' level sub-objective, *impacts on other environments*. To read this matrix, select an objective or MOE in the left-hand column of Table 6.2 and read across. For example, *cancer risk* is less important than *impact to environment* and *impact to ecology*.

	Cancer Risk	Impact to Environment	Impact to Ecology	Geometric Mean	Normalized Weighting Factor
Cancer Risk	1.000	0.333	0.333	0.577	0.174
Impact to Environment	3.000	1.000	3.000	1.732	0.523
Impact to Ecology	3.000	0.333	1.000	1.000	0.302
			Totals:	**3.309**	**1.000**

Table 6.3 *Method of Solution* Sub-Objectives Judgment Matrix

Finally, we defined weighting factors for the 'sixth' level sub-objectives of

physical and economic environment, respectively, as follows:

1) [1/3; 2/3] for physical environment, short and long term, respectively

2) [1/3; 2/3] for economic environment, short and long term, respectively

Now that we had defined weighting factors for all of the sub-objectives critical to

the residential land use scenario, we normalized the individual weight factors as shown in

Table 6.4.

Step B: Estimate each MOE. In this step, we first estimated the cost of each

	Physical	Social	Esthetic	Economic	Geometric Mean	Normalized Weighting Factor
Physical	1.000	5.000	5.000	3.000	2.943	0.565
Social	0.200	1.000	3.000	1.000	0.880	0.169
Esthetic	0.200	0.333	1.000	0.333	0.386	0.074
Economic	0.333	1.000	3.000	1.000	1.000	0.192
				Totals:	**5.209**	**1.000**

Table 6.2 *Impact on Other Environments* Sub-Objectives Judgment Matrix

Criteria	Weighting Factor
Cost:	w1 = 0.267
Completion Time:	w2 = 0.067
Risk Acceptance:	w3 = 0.250
Cancer Risk Uncertainty Level:	w4 = 0.044
Physical Environment Impacts, Short Term:	w5 = 0.025
Physical Environment Impacts, Long Term:	w6 = 0.049
Social Environment Impacts:	w7 = 0.022
Esthetic Environment Impacts:	w8 = 0.010
Economic Environment Impacts, Short Term:	w9 = 0.008
Economic Environment Impacts, Long Term:	w10 = 0.017
Impacts on Ecology:	w11 = 0.076
Effectiveness, Short Term:	w12 = 0.056
Effectiveness, Long Term:	w13 = 0.111
	Total = 1.000

Table 6.4 Residential Land Use Weighting Factors

alternative to attain different risk levels. Then we estimated the other MOEs and rated

each concept in each of the criteria. In addition to assigning MOE values, confidence

levels were assigned to each measure. A tabular summary of the MOEs is presented in

Table 6.5.

To estimate cost as a function of risk, we chose certainty levels for the risk level

and soil concentration; this was required since the risk assessment and the soil

characterization were probabilistic. We defined the risk certainty level as a statistical

statement which indicated that, for a given percent of the time (say 95%), a particular risk

would not be exceeded (say 1.0E-6). We also defined the soil concentration certainty

level as a statistical statement meaning that, for a given percent of the time (say 95%), the

soil concentration would not exceed some value (say 35 pCi/g). Several certainty levels

were included in our analysis to provide the CDM with information on the effect of

variations, for instance, of remediation costs with certainty level. Therefore, we treated the risk, cost, and certainty as variables.

The following is a step-wise description of the elements of Step B, as applied to TA C-64, of the process we used to estimate the risk, cost, and certainty of each alternative at different decision points.

Element 1) Determine the range of risks of interest.

TA C-64 Application: The risk range we originally settled on was from 1.0E-6 to 1.0E-5. Most Superfund sites target a remediated risk level of between 1.0E-6

Alternatives	Drum Disposal		Volume Reduction and Drum Disposal	
	90% Level	95% Level	90% Level	95% Level
Resource Cost	(Table 6.9) (C)	(Table 6.9) (C)	(Table 6.10) (C)	(Table 6.10) (C)
Resource Time	24 months (LC)	24 months (LC)	24 months (LC)	24 months (LC)
Physical Env. Imp. Short Term	6 (C)	5 (C)	7 (C)	6 (C)
Physical Env. Imp. Long Term	6 (C)	7 (C)	6 (C)	7 (C)
Social Env.Impacts	5 (C)	5 (C)	5 (C)	5 (C)
Esthetic Env. Impacts	5 (C)	6 (C)	5 (C)	6 (C)
Economic Env. Imp. Short Term	6 (C)	7 (C)	5 (C)	5 (C)
Economic Env. Imp. Long Term	5 (C)	6 (C)	5 (C)	6 (C)
Impacts on Ecology	5 (C)	5 (C)	5 (C)	5 (C)
Effectiveness Short Term	5 (LC)	5 (LC)	5 (LC)	5 (LC)
Effectiveness Long Term	100+ years (VC)	100+ years (VC)	100+ years (VC)	100+ years (VC)

Table 6.5 Characteristics For Residential Land Use Alternatives

and 1.0E-4, depending on site and scenario specific conditions. As a goal, we wanted to investigate the lower half of that range. However, after iterating through the process once, we found we needed to extend the range to 1.9E-5 to simulate the full range of possibilities.

Element 2) Divide the risk range into intervals. As the number of intervals increases, so does the resolution of the final answer and the effort required to perform the analysis.

TA C-64 Application: We chose the following risk intervals because they spanned the range of interest and were the least number of intervals for our desired resolution: 1.0E-6, 3.0E-6, 5.0E-6, 7.0E-6, 1.0E-5, 1.3E-5, and 1.9E-5.

Element 3) Determine the risk certainty levels to evaluate

TA C-64 Application: We picked our risk certainties at 90% and 95% because we only wanted a 10% and 5% chance, respectively, of under-predicting the risk.

Element 4) Run a Monte Carlo risk analysis using a risk certainty level and a deterministic soil concentration value. In Chapter 5, we discussed risk as a function of several environmental and site specific variables, U, as shown in Equation (6.4):

$$Risk = f(U_1, U_2, ..., U_n) \tag{6.4}$$

where U_i's are random variables. In this step, we let U_i be the soil concentration and treat it as an unknown deterministic value, X_i. The problem is shown in equation form as Equation (6.5).

$$[Risk]_{90\%} = \begin{bmatrix} 1.0E-6 \\ \cdot \\ \cdot \\ \cdot \\ 1.9E-5 \end{bmatrix} \qquad (6.5)$$

where the left hand side of the Equation (6.5) is the risk intervals from Step B. Therefore, Equation (6.4) can be written as follows.

$$[Risk]_{90\%} = \begin{bmatrix} f(X_1,U_2,U_3...,U_n) \\ \cdot \\ \cdot \\ \cdot \\ f(X_n,U_2,U_3...,U_n) \end{bmatrix} \qquad (6.6)$$

Solve Equation (6.6) for $[X_1, X_2, ..., X_n]^T$ such that it satisfies Equation (6.5). Repeat for the 90% risk certainty level. Iterate process until you have a soil concentration for each risk interval in Element 2. Perform the whole process for each certainty level in Element 3.

TA C-64 Application: Using the Monte Carlo analysis, we determined the soil concentrations at our risk intervals as shown in Table 6.6.

| | DU Concentration (pCi/g) | |
Risk	90% Level	95% Level
1.0E-6	5	4
3.0E-6	14	10
5.0E-6	24	17
7.0E-6	33	24
1.0E-5	50	36
1.3E-5	62	45
1.9E-5	62	62

Table 6.6 Risk vs. Soil Concentration

Element 5) Determine the soil concentration certainty levels to evaluate.

TA C-64 Application: We picked our soil concentration certainty at 95% because we only wanted a 5% chance of under predicting the soil concentration. We then generated the results in the form of a soil concentration contour map using the kriging analysis for the given soil concentration certainty level from Chapter 4.

Element 6) Determine the area that exceeds the soil concentration for each risk interval found in Element 4. Repeat this step for each soil concentration certainty level.

TA C-64 Application: Using our kriging analysis contour plots, we determined the areas that exceed the soil concentrations found in Element 4. The soil areas for the 90% and 95% risk levels are presented in Table 6.7.

Risk	Soil Area (ft^2)	
	90% Level	95% Level
1.0E-6	74,600	78,600
3.0E-6	45,300	60,200
5.0E-6	39,000	43,300
7.0E-6	36,200	39,000
1.0E-5	31,200	35,000
1.3E-5	30,000	31,865
1.9E-5	30,000	30,000

Table 6.7 Risk vs. Soil Area

Element 7) Determine to what depth the soil needs to be remediated.

TA C-64 Application: Based on the data presented in the groundwater section (4.2.6), we decided to remediate to a depth of 1.5 ft.

6-21

Element 8) Calculate the volume of soil to be cleaned for each risk interval at each risk and soil certainty level .

TA C-64 Application: Using the information in Elements 6 and 7, we calculated the soil volumes that required remediation at both risk certainty levels as shown in Table 6.8.

Risk	Soil Volume (ft^3)	
	90% Level	95% Level
1.0E-6	111,900	117,900
3.0E-6	67,950	90,300
5.0E-6	58,500	64,950
7.0E-6	54,300	58,500
1.0E-5	46,800	52,500
1.3E-5	45,000	47,800
1.9E-5	45,000	45,000

Table 6.8 Risk vs. Soil Volume

Element 9) Estimate the cost to remediate each volume of soil in Element 8 for each alternative remediation technique being considered. To evaluate the sensitivities of the cost assumptions, run this analysis for the best, worst, and most probable cost to see if the final answer changes under different cost assumptions.

TA C-64 Application: Most low level radiation disposal sites do not accept waste that is pyrophoric, such as DU. Therefore, we included in our estimates for both methods the cost of processing the contaminated soil to render the waste portion non-pyrophoric using a rotary dryer (46). Also, we did not estimate the cost of soil excavation because we believed it would be minor compared to the overall project cost.

Also, the cost would be the same for each remediation method, and therefore would not have an impact on discriminating between the two remediation methods.

For Method 1, the overall cost of processing the contaminated soil, packing it in drums, shipping, and disposal was estimated at $447 per drum in 1994 dollars (46).

For Method 2, the contractor who was consulted for the volume reduction method, Thermo Analytical Inc., reported that they had attained better than 90% volume reduction at Johnston Atoll Island. However, the actual volume reduction was dependent on the soil burden at a specific site. TA C-64 has a similar soil activity level as Johnston Atoll Island, so a similar volume reduction might be expected. For a conservative cost estimate we assumed an 80% and 20% volume reduction for the area outside and inside the RCA, respectively. The cost involved in the volume reduction process involves shipping the equipment to the site and $25,000 per 40 hour week for labor and equipment depreciation. We estimated the shipment and set-up of the equipment would cost $10,000. Thermo Analytical Inc. said that, at Johnston Atoll, they were able to process 10 yd^3/hr of sand (43). We estimated a 5 yd^3/hr rate for TA C-64 since the process may have to be slowed down to detect DU at the same activity levels as they did plutonium at Johnston Atoll.

Table 6.9 and Table 6.10 provide estimates of the number of drums that would require disposal for each remediation method and the total cost of the clean-up effort for 90% and 95% risk interval certainty:

	Drums for Disposal (No.)		Total Cost ($)	
Risk	90% Level	95% Level	90% Level	95% Level
1.0E-6	15,329	16,151	$6,851,959	$7,219,356
3.0E-6	9,308	12,370	$4,160,774	$5,529,329
5.0E-6	8,014	8,897	$3,582,123	$3,977,075
7.0E-6	7,438	8,014	$3,324,945	$3,582,123
1.0E-5	6,411	7,192	$2,865,699	$3,214,726
1.3E-5	6,164	6,548	$2,755,479	$2,926,778
1.9E-5	6,164	6,164	$2,755,479	$2,755,479

Table 6.9 Drum Disposal (Method 1): Risk vs. Number of Drums and Cost

Element 10) Graph risk versus cost for each remediation alternative for each risk and soil certainty. Ideally, all the curves should be on the same plot for easy comparison. However, this may not be practical depending on the number of alternatives and risk/soil certainties under consideration. If this is the case, determine the most attractive options and plot them against each other.

TA C-64 Application: Figure 6.2 shows the risk versus cost at the different risk certainty intervals. Each of the data points on this figure represents a

	Drums for Disposal (No.)		Total Cost ($)	
Risk	90% Level	95% Level	90% Level	95% Level
1.0E-6	6,764	6,926	$3,551,632	$3,652,889
3.0E-6	5,560	6,172	$2,809,923	$3,187,106
5.0E-6	5,301	5,478	$2,650,443	$2,759,294
7.0E-6	5,186	5,301	$2,579,563	$2,650,443
1.0E-5	4,981	5,137	$2,452,991	$2,549,186
1.3E-5	4,931	5,008	$2,422,614	$2,469,825
1.9E-5	4,931	4,931	$2,422,614	$2,422,614

Table 6.10 Volume Reduction, Drum Disposal (Method 2): Risk vs. Number of
Drums and Cost
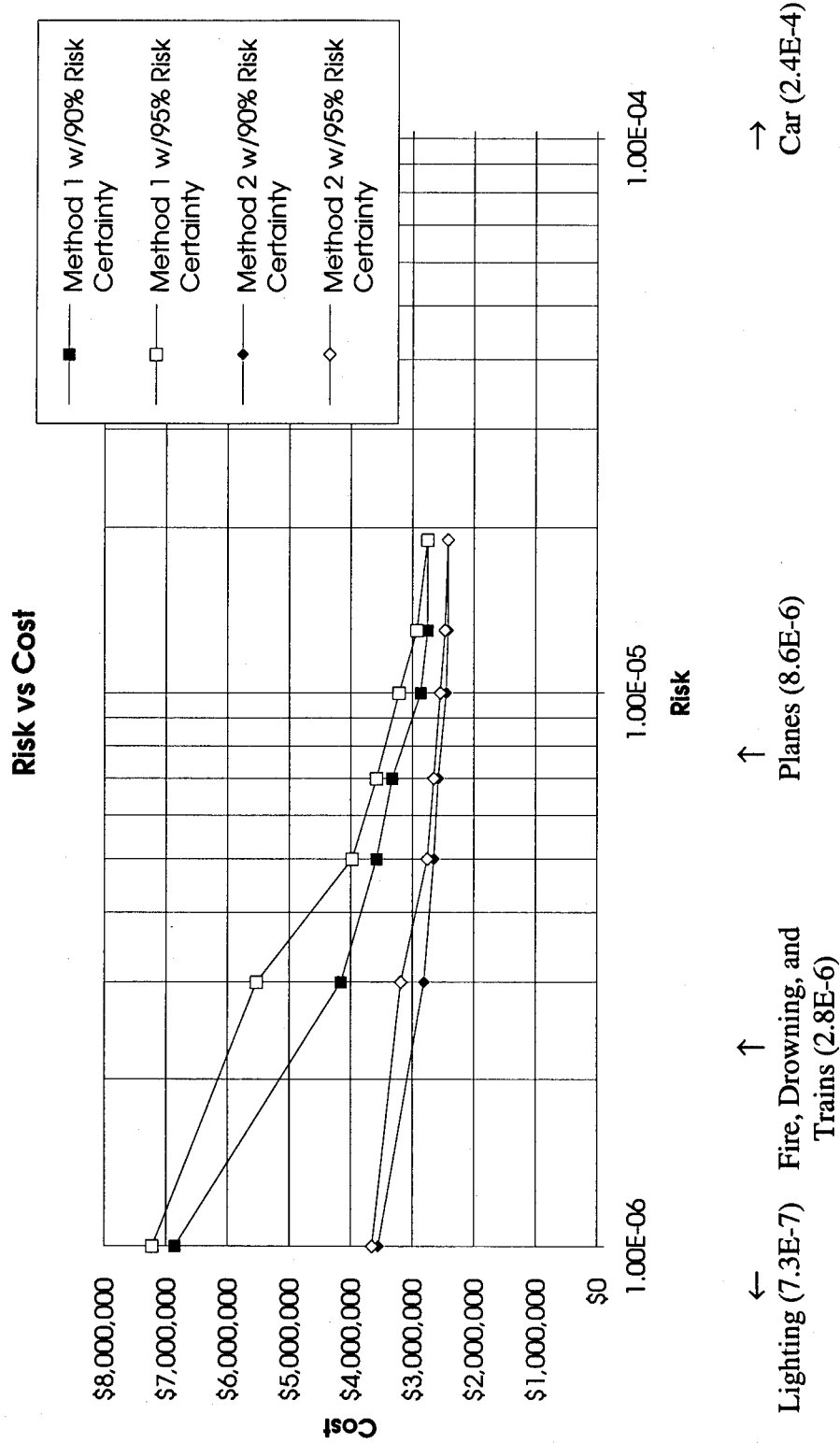
Figure 6.2 Risk vs. Cost For Remediation Method 1 and 2 at 90% and 95% Risk Certainty

possible remediation alternative. Risks of fatalities associated with other activities are included for reference (57).

Step C: Map MOE Utility. In this step, we construct the System Utility Function Chart (7) shown in Table 6.11. This chart is used to map each MOE onto a 0 to 10 scale (note: the scale does not have to be linear). The chart is used as a yardstick to determine what scores in each criterion are considered exceptional, above average, average, below average, and barely acceptable. In this chart, a 10 represents the most favorable rating. For example, a raw score of 0 for remediation cost, which means no cost at all, becomes a 10 with this chart. Having all criteria on the same scale, will allow us to evaluate alternatives using numerical techniques.

For the acceptability sub-objectives of cost and risk level, we created functions to map the alternatives onto a 0 to 10 scale. For cost, the mapping was linear with cost as the independent variable and cost utility as the dependent variable. Equation (6.7) was found by mapping a cost of $10 million to a utility value of zero and mapping a cost of $0 to a value of 10 :

$$Utility_{cost} = -\frac{1}{Million}Cost + 10 \qquad (6.7)$$

For risk level acceptability, the mapping was exponential with risk level as the independent variable and risk level utility as the dependent variable. Equation (6.8) was obtained by mapping a range of risk from 1.0E-4 to 1.0E-6 to a utility value of 0 to 10, respectively.

$$Utility_{risk} = -5\log(RiskLevel) - 20 \qquad (6.8)$$

Points	1	3	5	7	9
Criteria	Barely Acceptable	Below Average	Average	Above Average	Exceptional
Resource Sampling Cost	$10 Million	$7.5 Million	$5 Million	$2.5 Million	0
Resource Time	40 months	32 months	24 months	16 months	8 months
Acceptability Final Risk Level	1.0E-4	5.0E-5	1.0E-5	5.0E-6	1.0E-6
Cancer Risk Uncertainty Level	Barely Acceptable	Below Average	Average	Above Average	Exceptional
Physical Env. Imp. Short Term	1	3	5	7	9
Physical Env. Imp. Long Term	1	3	5	7	9
Social Env. Impacts	1	3	5	7	9
Esthetic Env. Impacts	1	3	5	7	9
Economic Env. Short Term	1	3	5	7	9
Economic Env. Long Term	1	3	5	7	9
Impacts on Ecology	1	3	5	7	9
Effectiveness Short Term	1	3	5	7	9
Effectiveness Long Term	0	10	25	50	100

Table 6.11 System Utility Function Chart

Step D: Calculate Utility and Discount Utility. For each of the remediation methods, only the cost and the final risk level MOEs actually changed with changing risk levels; the other MOEs remained constant. Therefore, shortened versions of Equations 6.1 and 6.2 were derived for each method. These equations are shown as Equations 6.9 through 6.16.

<u>Method 1</u>: Drum Disposal (90% Risk Level):

$$Utility = -0.26\overline{6}Cost - 1.25Log(Risk) + 0.61 \tag{6.9}$$

$$DiscountUtility = -0.16Cost - 0.75Log(Risk) + 0.48 \tag{6.10}$$

<u>Method 1</u>: Drum Disposal (95% Risk Level):

$$Utility = -0.26\overline{6}Cost - 1.25Log(Risk) + 0.76 \tag{6.11}$$

$$DiscountUtility = -0.16Cost - 0.75Log(Risk) + 0.57 \tag{6.12}$$

<u>Method 2</u>: Volume Reduction, Drum Disposal (90% Risk Level):

$$Utility = -0.26\overline{6}Cost - 1.25Log(Risk) + 0.63 \tag{6.13}$$

$$DiscountUtility = -0.16Cost - 0.75Log(Risk) + 0.49 \tag{6.14}$$

<u>Method 2</u>: Volume Reduction, Drum Disposal (90% Risk Level):

$$Utility = -0.26\overline{6}Cost - 1.25Log(Risk) + 0.76 \tag{6.15}$$

$$DiscountUtility = -0.16Cost - 0.75Log(Risk) + 0.58 \tag{6.16}$$

The results of these equations are tabulated in Table 6.12 and Table 6.13 and plotted in Figure 6.3 and Figure 6.4.

6.4.3   Conclusions and Recommendations for Residential Land Use

The utility values we determined for each alternative represent the overall worth of each alternative with respect to our objective criteria system. Based on the results presented in Table 6.12 and Table 6.13, our recommendation for the residential land use scenario would be to remediate to the 1E-6 risk level using Method 2, volume reduction, at the 95% certainty level. Of the two alternatives, this alternative was rated the highest in both utility and discounted utility.

	Drum Disposal					
	90% Level			95% Level		
Risk	Cost ($)	Utility	Discount Utility	Cost ($)	Utility	Discount Utility
1.00E-06	$6,851,959	6.28	3.89	$7,219,356	6.33	3.92
3.00E-06	$4,160,774	6.40	3.96	$5,529,329	6.19	3.83
5.00E-06	$3,582,123	6.28	3.89	$3,977,075	6.32	3.91
7.00E-06	$3,324,945	6.17	3.82	$3,582,123	6.25	3.86
1.00E-05	$2,865,699	6.10	3.77	$3,214,726	6.15	3.81
1.30E-05	$2,755,479	5.98	3.71	$2,926,778	6.08	3.77
1.90E-05	$2,755,479	5.78	3.58	$2,755,479	5.92	3.67

Table 6.12 Drum Disposal (Method 1) Cost, Utility, and Discount Utility Data

	Volume Reduction and Drum Disposal					
	90% Level			95% Level		
Risk	Cost ($)	Utility	Discount Utility	Cost ($)	Utility	Discount Utility
1.00E-06	$3,551,632	7.18	4.42	$3,652,889	7.29	4.49
3.00E-06	$2,809,923	6.78	4.19	$3,187,106	6.82	4.20
5.00E-06	$2,650,443	6.55	4.04	$2,759,294	6.66	4.11
7.00E-06	$2,579,563	6.38	3.95	$2,650,443	6.50	4.01
1.00E-05	$2,452,991	6.22	3.85	$2,549,186	6.33	3.91
1.30E-05	$2,422,614	6.09	3.77	$2,469,825	6.21	3.84
1.90E-05	$2,422,614	5.88	3.65	$2,422,614	6.02	3.72

Table 6.13 Volume Reduction/Drum Disposal (Method 2): Cost, Utility, and Discount Utility Data

Method 1, which involves placing all of the contaminated soil in drums without volume reduction, was approximately equal to Method 2 when the final risk level is greater than 1E-5. However, when cleaning to a lower final risk level, the utility of the this method decreases sharply because of the high cost involved in comparison to Method 2. Method 1 also showed diminishing returns at lower risk levels.
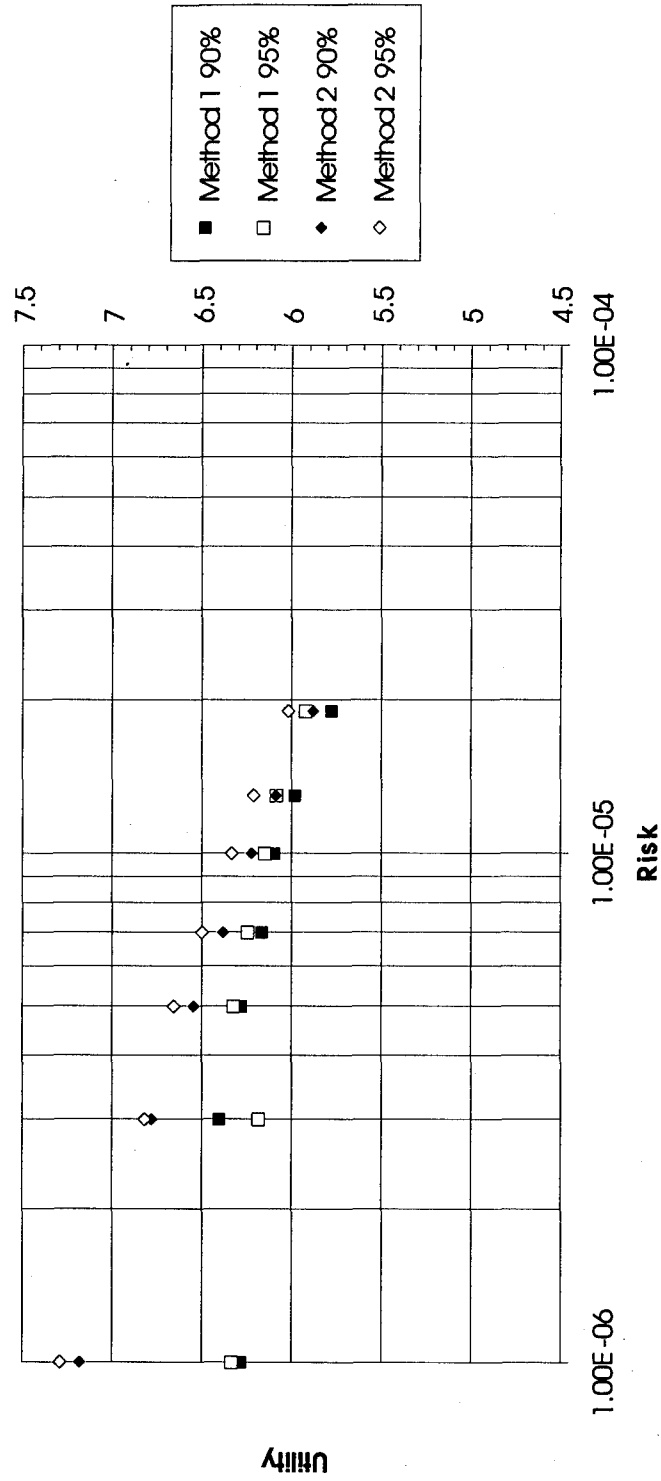
Figure 6.3 Utility vs Risk

Figure 6.4 Discount Utility vs Risk

6.5   Occupational Land Use Scenario

6.5.1   Developing Alternatives.   In the risk assessment section, we showed that the inhalation pathway dominated the estimated risk to humans. However, we believe the inhalation risk was over estimated due to the crude characterization of the mass loading factor, i.e. the air concentration was only a fraction of what was estimated. Lacking air sampling data, we had no basis from which to refine the mass loading estimate. Realistically, the best approach would be to obtain air sampling data to properly characterize the air DU concentration before proceeding. For the purposes of this thesis, we assumed that the current mass loading factor accurately represented the condition at TA C-64 and that the inhalation pathway represented a health concern. Please note, this was an assumption for the purposes of this study and did not necessarily reflect the actual situation. Having said this, we developed five general concepts toward reducing the estimated health risk from the mix of the five general risk management options described in Section 6.3.

Concept 0. Do nothing.

Concept 1. Study the air transport mechanisms and implement appropriate controls. In addition, air DU concentration measurements should be made after control implementation and input into the risk analysis to insure control mechanisms are effective.

Concept 2. Remediate area outside the RCA and measure the air DU concentration to measure effectiveness.

Concept 3. Remediate the area inside and outside the RCA and measure the air

DU concentration to measure effectiveness.

Concept 4. Limit access and/or provide breathing protection for workers.

6.5.2 Modeling Alternatives. In this section we will establish the specific

methods for evaluating the overall concepts for the occupational land use scenario. This

is the same process used in section 6.4. All of the MOE's are identical except the cost

and final risk level MOEs.

Step A: Develop MOE Weighting Factors. The *cost* and *final risk level* sub-

objectives' judgment matrices are shown below in Table 6.14 and Table 6.15.

Now that we defined weighting factors for all of the sub-objectives critical to the

residential land use scenario, we combined the vectors into an overall, normalized MOE

worth vector shown in Table 6.16.

Step B: Estimate each MOE. Table 6.17 shows the MOE estimates with the

associated confidence ratings.

Cost:		Control		Geometric Mean	Normalized Weighting Factor
	Remediation	Mechanism	Sampling		
Remediation	1.000	5.000	5.000	2.924	0.714
Control Mech.	0.200	1.000	1.000	0.585	0.143
Sampling	0.200	1.000	1.000	0.585	0.143
			Totals:	4.094	1.000

Table 6.14 Cost Sub-Objective Judgment Matrix

	Public	Regu-lator	Com-mander	Scientists	Geometric Mean	Normalized Weighting Factor
Public	1.000	0.333	0.333	1.000	0.577	0.125
Regulator	3.000	1.000	1.000	3.000	1.732	0.375
Commander	3.000	1.000	1.000	3.000	1.732	0.375
Scientists	1.000	0.333	0.333	1.000	0.577	0.125
				Totals:	**4.619**	**1.000**

Table 6.15 Final Risk Level Sub-Objective Judgment Matrix

Step C: Map MOE utility. The mapping of raw scores to a zero to ten scale for this scenario is shown in Table 6.18.

Step D: Calculate Utility and Discounted Utility. Using Equations (6.1) and (6.2), Table 6.19 and Table 6.20 were generated.

6.5.3   Conclusions and Recommendations for Occupational Land Use

The evaluation summary shown in Table 6.21 shows the utility, discounted utility, and confidence level for each alternative. The result of the occupational land use scenario evaluation were somewhat more difficult to interpret than the results for the residential land use. For this case, the alternative received the lowest utility received the highest discounted utility rating.

First, we looked at the utility values. Concepts 1 and 3 which received utility ratings of 5.59 and 5.67, respectively, scored the highest. Based on the subjective nature of the evaluation, the difference in utility rating was not significant enough to conclude

MOE	Weighting Factor	
Remediation Cost	$w1 =$	0.190
Control Mechanism Cost	$w2 =$	0.038
Sampling Cost	$w3 =$	0.038
Completion Time	$w4 =$	0.067
Risk Acceptance, Public	$w5 =$	0.031
Risk Acceptance, Regulator	$w6 =$	0.094
Risk Acceptance, Commander	$w7 =$	0.094
Risk Acceptance, Scientists	$w8 =$	0.031
Cancer Risk Uncertainty Level	$w9 =$	0.044
Physical Environment Impacts, Short Term	$w10 =$	0.025
Physical Environment Impacts, Long Term	$w11 =$	0.049
Social Environment Impacts	$w12 =$	0.022
Esthetic Environment Impacts	$w13 =$	0.010
Economic Environment Impacts, Short Term	$w14 =$	0.008
Economic Environment Impacts, Long Term	$w15 =$	0.017
Impacts on Ecology	$w16 =$	0.076
Effectiveness, Short Term	$w17 =$	0.056
Effectiveness, Long Term	$w18 =$	0.111
	Total =	**1.000**

Table 6.16 Occupational Land Use Weighting Factors

Alternatives	Concept 0 No action	Concept 1 Study	Concept 2 Remediate (partial)	Concept 3 Remediate (all)	Concept 4 Control
Resource Sampling Cost	0 (VC)	8 (LC)	5 (C)	5 (C)	0 (LC)
Resource Remed. Cost	0 (VC)	0 (VC)	7 (C)	9 (C)	0 (VC)
Resource Control Cost	0 (VC)	7 (C)	0 (VC)	0 (VC)	3 (LC)
Resource Time to Compl.	0 (VC)	12 (C)	6 (C)	9 (C)	1 (LC)
Final Risk Level Public	Barely Acc. (LC)	Accept (C)	Above Avg (C)	Exceptional (C)	Barely Acc. (LC)
Final Risk Level Regulator	Barely Acc. (C)	Accept (C)	Above Avg (C)	Exceptional (C)	Barely Acc. (LC)
Final Risk Level Commander	Barely Acc. (C)	Accept (C)	Above Avg (C)	Exceptional (C)	Barely Acc. (LC)
Final Risk Level Scientific	Barely Acc. (C)	Accept (C)	Above Avg (C)	Exceptional (C)	Barely Acc. (LC)
Cancer Risk Uncertainty Level	Barely Acc. (C)	Accept (C)	Above Avg (C)	Exceptional (C)	Barely Acc. (LC)
Physical Env. Imp. Short Term	7 (VC)	7 (C)	6 (C)	6 (C)	7 (VC)
Physical Env. Imp. Long Term	1 (LC)	5 (C)	7 (C)	8 (C)	1 (LC)
Social Environment	3 (LC)	5 (LC)	6 (LC)	7 (LC)	5 (LC)
Esthetic Environment	5 (C)	5 (C)	5 (C)	5 (C)	5 (C)
Economic Env. Short Term	3 (LC)	5 (LC)	6 (LC)	7 (LC)	5 (LC)
Economic Env. Long Term	5 (LC)	5 (LC)	6 (LC)	7 (LC)	5 (LC)
Impacts on Ecology	3 (LC)	5 (LC)	6 (LC)	7 (LC)	3 (LC)
Effectiveness Short Term	3 (C)	3 (C)	1 (LC)	1 (LC)	7 (C)
Effectiveness Long Term	0 (VC)	20 (NC)	20 (LC)	20 (LC)	20 (LC)

Table 6.17 Characteristics for Occupational Land Use Alternatives

Rating	1	3	5	7	9
Criteria	Barely Accept.	Below Average	Average	Above Average	Exceptional
Resource Sampling Cost	9	7	5	3	1
Resource Remed. Cost	9	7	5	3	1
Resouce Control Cost	9	7	5	3	1
Resouce Time to Compl.	above 18	18	12	6	3
Final Risk Level Public	Barely Accept.	Below Average	Average	Above Average	Exceptional
Final Risk Level Regulator	Barely Accept.	Below Average	Average	Above Average	Exceptional
Final Risk Level Commander	Barely Accept.	Below Average	Average	Above Average	Exceptional
Final Risk Level Scientific	Barely Accept.	Below Average	Average	Above Average	Exceptional
Cancer Risk Uncertainty Level	Barely Accept.	Below Average	Average	Above Average	Exceptional
Physical Env. Imp. Short Term	1	3	5	7	9
Physical Env. Imp. Long Term	1	3	5	7	9
Social Environment	1	3	5	7	9
Esthetic Environment	1	3	5	7	9
Economic Env. Short Term	1	3	5	7	9
Economic Env. Long Term	1	3	5	7	9
Impacts on Ecology	1	3	5	7	9
Effectiveness Short Term	1	3	5	7	9
Effectiveness Long Term	0	10	25	50	100

Table 6.18 Occupational Land Use System Utility Function Chart

Criteria	Utility	Concept 0				Concept 1				Concept 2			
		R	C	U	D	R	C	U	D	R	C	U	D
Sampling Cost	0.038	10	VC	0.381	0.343	2	LC	0.076	0.023	5	C	0.190	0.114
Remediation Cost	0.190	10	VC	1.905	1.714	10	VC	1.905	1.714	3	C	0.571	0.343
Control Mechanism Cost	0.038	10	VC	0.381	0.343	3	C	0.114	0.069	10	VC	0.381	0.343
Completion Time	0.067	10	VC	0.667	0.600	5	C	0.333	0.200	7	C	0.467	0.280
Risk Acceptance Public	0.031	1	LC	0.031	0.009	5	C	0.156	0.094	7	C	0.219	0.131
Risk Acceptance Regulator	0.094	1	C	0.094	0.056	5	C	0.469	0.281	7	C	0.656	0.394
Risk Acceptance Commander	0.094	1	C	0.094	0.056	5	C	0.469	0.281	7	C	0.656	0.394
Risk Acceptance Scientists	0.031	1	C	0.031	0.019	5	C	0.156	0.094	7	C	0.219	0.131
Cancer Risk Uncertainty Level	0.044	1	C	0.044	0.026	5	C	0.218	0.131	7	C	0.305	0.183
Physical Environment, Short Term	0.025	7	VC	0.172	0.155	7	C	0.172	0.103	6	C	0.148	0.089
Physical Environment, Long Term	0.049	1	LC	0.049	0.015	5	C	0.246	0.148	7	C	0.345	0.207
Social Environment	0.022	3	LC	0.066	0.020	5	LC	0.111	0.033	6	LC	0.133	0.040
Esthetic Environment	0.010	5	C	0.048	0.029	5	C	0.048	0.029	5	C	0.048	0.029
Economic Environment, Short Term	0.008	3	LC	0.025	0.008	5	LC	0.042	0.013	6	LC	0.050	0.015
Economic Environment, Long Term	0.017	5	LC	0.084	0.025	5	LC	0.084	0.025	6	LC	0.100	0.030
Impacts on Ecology	0.076	3	LC	0.227	0.068	5	LC	0.378	0.113	6	LC	0.453	0.136
Effectiveness, Short Term	0.056	3	C	0.167	0.100	3	C	0.167	0.100	1	LC	0.056	0.017
Effectivness, Long Term	0.111	1	VC	0.111	0.100	4	NC	0.444	0.044	4	LC	0.444	0.133
Total Value	1.000			4.577				5.589				5.443	
Discounted Value					3.686				3.496				3.009
Confidence			0.805				0.625				0.553		

R=Relative Rating

C=Confidence

U=System Utility

D=Discounted Utility

VC: 0.9

C: 0.6

LC: 0.3

NC: 0.1

Table 6.19 Evaluation Matrix for Concept 0, Concept 1 and Concept 2

Criteria	Utility	Concept 3				Concept 4			
		R	C	U	D	R	C	U	D
Sampling Cost	0.038	5	C	0.190	0.114	10	VC	0.381	0.343
Remediation Cost	0.190	1	C	0.190	0.114	10	VC	1.905	1.714
Control Mechanism Cost	0.038	10	VC	0.381	0.343	7	LC	0.267	0.080
Completion Time	0.067	6	C	0.400	0.240	9	LC	0.600	0.180
Risk Acceptance Public	0.031	9	C	0.281	0.169	1	LC	0.031	0.009
Risk Acceptance Regulator	0.094	9	C	0.844	0.506	1	LC	0.094	0.028
Risk Acceptance Commander	0.094	9	C	0.844	0.506	1	LC	0.094	0.028
Risk Acceptance Scientists	0.031	9	C	0.281	0.169	1	LC	0.031	0.009
Cancer Risk Uncertainty Level	0.044	7	C	0.305	0.183	1	C	0.044	0.026
Physical Environment, Short Term	0.025	6	C	0.148	0.089	7	VC	0.172	0.155
Physical Environment, Long Term	0.049	8	C	0.394	0.237	1	LC	0.049	0.015
Social Environment	0.022	7	C	0.155	0.093	5	LC	0.111	0.033
Esthetic Environment	0.010	5	C	0.048	0.029	5	C	0.048	0.029
Economic Environment, Short Ter	0.008	7	LC	0.059	0.018	5	LC	0.042	0.013
Economic Environment, Long Ter	0.017	7	LC	0.117	0.035	5	LC	0.084	0.025
Impacts on Ecology	0.076	7	LC	0.529	0.159	3	LC	0.227	0.068
Effectiveness, Short Term	0.056	1	LC	0.056	0.017	7	C	0.389	0.233
Effectivness, Long Term	0.111	4	LC	0.444	0.133	4	VC	0.444	0.400
Total Value	1.000			5.667				5.012	
Discounted Value					3.153					3.390
Confidence			0.556				0.676		

Table 6.20 Evaluation Matrix for Concept 3 and Concept 4

that one was superior to the other. Concept 0, however, scored more than one full point below these concepts in utility.

The discounted utility measure was designed to incorporate the confidence associated with the estimates used in the evaluation. It represented the worst case utility of an alternative. Because Concept 0, which involved leaving the site in its current state, involved very little estimation, its utility was not discounted as much as the other concepts and had the highest of all the options at 3.69. Concept 1, which had one of the highest utility ratings, also has a reasonably high discounted utility rating of 3.50.

Although discounted utility of Concept 1 was less than that of Concept 0, its weighting factors were higher. Depending on how conservative the CDM was, either concept may be acceptable. Our recommendation was Concept 1, studying air transport mechanisms and implementing controls, if required. The worst case utility of the concept was close to Concept 0 but the potential benefit was much higher.

One other option was available to the CDM. The large change from utility value

Concept	Value	Discounted Value	Confidence
Concept 0 (No change)	4.56	3.69	0.81
Concept 1 (Study)	5.59	3.50	0.63
Concept 2 (Remediate-partial)	5.44	3.01	0.55
Concept 3 (Remediate-all)	5.67	3.15	0.56
Concept 4 (Control)	5.01	3.39	0.68

Table 6.21 Evaluation Matrices Summary

to discounted utility value for some of the concepts was due to the low confidence rating

assigned to the estimates used in calculations. Further research into refining specific

MOEs could result in more accurate discounted utility values. Ideally, the specific

MOE's could be treated as random variables, i.e. the MOE's could be expressed as pdfs

rather than as point estimates. This would eliminate the need for the discounted utility

function because the uncertainty information would be incorporated explicitly into the

MOE pdfs. Evaluating Equation (6.3) using Monte Carlo simulation for each alternative

would provide additional information to the CDM upon which to base a decision. Of

course, the potential gain from performing such an analysis should outweigh the cost of

the additional research required in developing the MOE pdfs.

VII.   Conclusions and Recommendations

In this chapter, we present the conclusions and recommendations from both our case study of DU contamination at TA C-64 and our systems engineering application to environmental risk management. We begin with a discussion of the case study, including what we have learned about the site and further actions that we recommend. We conclude with a discussion of the systems engineering process, including its strengths and weaknesses in the area of environmental risk management and how it compares with other methodologies available today.

7.1   Case Study

We begin this section with a discussion of each phase of the case study and conclude with some overall comments.

7.1.1   Site Characterization.   For the soil, groundwater, and air media, we used the systems engineering process to develop estimates of the concentration of DU activity. These estimates were statistical distributions which we determined to be necessary for the risk assessment and risk management phases.

Soil.   Since the soil model was constrained by the requirement that no further data would be gathered and by our requirement to use a statistical distribution, the kriging model dominated all other alternatives. Kriging provided an excellent characterization for the purposes of our study.

Groundwater.   Due to the lack of site specific data, we used a first order model to estimate the distribution of DU in the groundwater. During the risk assessment, we

determined that this model was good enough to show that no significant risk resulted from the groundwater so that no further sampling or modeling was necessary.

Air. Due to the lack of any site specific data, the DU airborne concentration model was also quite simple. During the risk assessment, we determined that the simplistic, mass-loading approach introduced enough uncertainty into our analysis that the airborne concentration of DU could not be ruled out as a health risk for the occupational land use scenario. For this medium, we concluded that on-site air sampling would better characterize the airborne DU concentration and refine the determination of the risk due to inhalation of contaminated particles. Because many factors affect soil particle resuspension rates, sampling would have to be done under a variety of conditions to include the effects of meteorological and anthropogenic influences.

7.1.2 Risk Assessment. In order to describe the risk, the systems engineering process led us to develop a probabilistic risk assessment for both the current occupational land use and a hypothetical future residential land use. We evaluated the following exposure pathways: soil and water ingestion, irradiation, and inhalation for carcinogenic risk; and soil and water ingestion for non-carcinogenic risk. We determined that the carcinogenic risks ranged from approximately 10E-5 to 10E-10; the non-carcinogenic risks were statistically insignificant. As referred to above, the main pathway of concern was the inhalation pathway for current occupational land use. Again, we recommend sampling in the air to reduce this uncertainty, which we suspect will lower the uncertainty and probably the calculated risk associated with inhalation.

We found that a probabilistic approach provided a much more useful assessment of the risk than the prevalent deterministic approach. This was especially true since the risk was in the range where it was unclear whether further management was necessary. A deterministic approach which provided potentially misleading point estimates (implying the risk is precisely known) was not helpful to us since we wanted to manage risk to a specific confidence level. Also, the probabilistic approach provided us with an understanding of which variables in the risk calculation caused the most uncertainty. Using this information, we were able to focus on certain variables to reduce the range of risk. However, the deterministic method did provide some benefit to our analysis: we used this method, along with conservative estimates of the risk variables, in order to efficiently screen some pathways of risk that might have been too low to warrant further evaluation.

7.1.3 Risk Management. The risk management approach developed for this case study included explicit recognition of desired management objectives and analytical decision tools designed to help weight the different objectives, account for confidence in the alternative models, and distinguish between the relative worth of the alternatives. These tools and approaches were very helpful in providing a clear, precise way to choose the best solution. In particular, we found that the ability to iterate in the process was very valuable in allowing us to improve our risk management objectives and further improve the site characterization and risk assessment phases.

To manage the risk, we developed a strong, systematic approach to choose among management alternatives, and ran some sample alternatives against this approach. We

found that for the current occupational land use, further study (air sampling to reduce uncertainty) was the best among our alternatives. For future residential land use, remediation by soil volume reduction and shipment off-site was the best alternative of the two we evaluated.

One weakness in our approach was the overpowering effect that confidence ratings had on lowering the utility of a management alternative. To remedy this, we recommend developing probability density functions (perhaps triangular for simplicity) for each MOE rather than point values and confidence ratings.

We chose to use ourselves as the decision makers in this study. We recommend that the objectives of the decision maker for this site be well-defined so these tools can be used more effectively. Also, the objectives concerning the acceptance of the method of solution should be tailored to the concerns of the public, technical, regulatory, and military communities in the Eglin AFB area.

7.1.4   Overall Case Study. This thesis provided the following benefits for the TA C-64 site manager: a snapshot of the current state of contamination at TA C-64 including information on the areas of greatest uncertainty with regard to site characterization; information on present levels of risk and on the predominant factors that contribute to the risk; a method for accomplishing future site characterization and risk assessment; and the framework for making risk management decisions in the future.

The most significant area of uncertainty in site characterization was airborne DU contamination. A lack of recent soil surface DU concentration data inside the RCA and a lack of airborne particulate data made risk estimation for the occupational land use

scenario difficult. In addition, the risk assessment model indicated that the inhalation pathway was the primary source of risk for this scenario. If the site manager desires to reduce uncertainty in the risk, we recommend the following:

   a. air sampling to refine the airborne DU distribution, and

   b. soil sampling inside the RCA to refine the soil DU distribution.

We also strongly recommend the probabilistic approach to risk assessment for this type of study. It provided a good analysis of risk and gave greater flexibility to the risk management phase. Additionally, the probabilistic analysis provided information on which specific input information most effected the final risk. This information was used to determine what level of detail was required for site characterization.

Finally, the tools we used for risk management were very helpful and we recommend using them for comparison of different alternatives in the future. Specifically, the utility function and weighting factor analysis tools aided us in isolating the best solution out of several alternatives.

7.1.5 Recommendations for Further Research. There are several topics related to this thesis that warrant further study. We suggest that the following be considered as future thesis topics:

a) *Determine depleted uranium leaching rates through samples of test site soil.* Very little is currently known about the leaching of DU into the soil at the Eglin AFB test sites. One limited study indicated contamination down to 33" below the surface inside the RCA. It is unknown whether the DU reached this depth due to leaching or due to a tilling effect from heavy machinery operating within the RCA.

b) *Design a method to locate all of the potential installation restoration program sites at Eglin AFB.* Because the Eglin AFB range is so large and testing has been ongoing for many years, it is difficult to determine whether all environmentally contaminated sites have been identified. Interviews with retiring 'old timers' and aerial photography are among the methods used to date.

c) *Evaluate ecological risk to DU testing at test sites C-64 and C-74.* The scope of this thesis was to evaluate the risk to humans from the DU. The Environmental Assessment Branch at Eglin AFB is currently studying the effects of DU on wildlife and vegetation.

d) *Design a remediation plan for test site C-74.* Although TA C-74 is currently permitted for DU use, depleted uranium munitions testing is not conducted on the site anymore. Site remediation is being considered in order to eliminate the need for a permit.

e) *Evaluate the transport mechanisms involved in the spread of DU at TA C-64.* In this study, no attempt was made to explain how the DU reached the non-RCA areas. Perhaps with this knowledge, better control mechanisms could be implemented to contain the DU.

7.2   Method Comparison

Application of systems engineering to environmental risk management produced a process similar to that of CERCLA and SAFER. All three methods used similar site characterization, risk assessment, and risk management phases. However, we found that the more iterative, flexible, and universal nature of the systems engineering process tools

and precepts allowed us to refine and optimize the problem definition, objectives, and alternatives throughout the project.

Iterative. We iterated both within and between steps to optimize the process. For example, the objective setting step strongly emphasized refinement through iteration as alternatives developed. In our case study, we iterated several times within this step before we felt we had identified the correct objectives. We also iterated between steps to optimize the characterization of DU contamination in the soil. Initially, we used a point estimate for this characterization. However, as we optimized our approach to the risk assessment and risk management portions of the analysis, we determined that a probabilistic approach better represented the uncertainty in our knowledge about the contaminant distribution. The iterative nature of the analysis allowed us to step back and recharacterize the soil DU concentration using a kriging technique which explicitly included these uncertainties.

Flexible. We also had the flexibility to select the objective criteria, alternative solutions, and analysis tools best tailored to our site. We found that the EPA's nine criteria mentioned in Literature Review (Chapter 2), as implemented, placed secondary importance on the cost effectiveness criteria. We chose to weight this criteria on a par with the performance criteria to better reflect our concern with limiting expenditure of resources. The EPA's nine criteria also included clear preference for volume and toxicity reduction when rating remediation alternatives. However, for the occupation land use scenario, the results of our weighting of objective criteria suggested that control and further study of the situation was the better alternative. It should be noted here that the

flexible application of the systems engineering process might not be appropriate where the perception of environmental equity dictates that similar solutions be used at similar sites.

Universal. Systems engineering was applicable to our site independent of legal or other requirements for environmental risk management at TA C-64. With liability for clean-up being legally interpreted as retroactive, system engineering provided us a method for addressing environmental risk management before outside agencies became involved. Although the data available to conduct the case study analysis were limited, the process provided us a method to evaluate the situation to the extent possible with the existing data.

Tools and Precepts. Finally, the tools and precepts of systems engineering proved very useful in our analysis. We found the twelve products of problem definition very useful in helping to define the problem fully. Not every product was required for each sub-problem, but we found the list of products helpful in ensuring complete coverage of the subject. Weighting of objectives, preference charts, and confidence discounting were all helpful tools in choosing between competitive alternatives. Systems engineering did not provide us with an 'answer' --- it provided us a tool to assist with decision making.

Overall, we found that the seven-step process used for the case study of DU contamination at TA C-64 provided a good framework and should be available as a tool for environmental risk management. However, in cases where the problem is already well understood and a known solution exists, the full systems engineering process could

be unnecessarily burdensome, but the tools of systems engineering could significantly improve current methods.

Assessing and managing risk will continue to be a complicated field of study, but we believe insights from the discipline of systems engineering can provide powerful resources to help work through this complicated process.

Appendix A.   Soil Analysis

A.1   TA C-64 Soil Sample Data

Presented on the following pages is the raw DU concentration data used for the soil kriging analysis. The tables (Tables A.1, A.2 and A.3) contain soil data for all points since sampling began in 1979. Only the month and the year was recorded for samples prior to August 1988. These early samples were calculated in µg/g and converted to pCi/g for consistency with current data. Values listed as 1 pCi/g indicates background level readings, values listed as 1.01 were actually measured at 1.

Prior to April of 1989 samples were not taken beyond 180 ft from the target butt. Sample location is given by *distance-direction* coordinates as explained in chapter four section one.

	1-7	1-9	1-11	1-13	2-4	2-6	2-8	2-10	2-12	2-14
31-Mar-94	42.32	1.00	1.00	1.00	3.26	3.56	1.00	1.00	1.00	1.00
21-Jan-94	22.46	1.68			22.27	4.65				
22-Sep-93	46.20	12.11			25.80	3.01				
15-Jun-93	22.95	1.00	3.64	4.50	29.59	6.92	1.00	1.62	1.00	1.00
29-Mar-93	63.87	15.00	1.00	3.22	11.05	16.64	1.00	1.00	1.00	1.00
19-Jan-93	20.03	6.15	1.00	3.21	7.04	7.89	1.00	1.00	1.00	1.00
29-Sep-92	29.11	2.21	1.00	5.80	9.52	5.50	1.00	1.00	1.00	1.00
22-Apr-92	10.29	1.00	1.00	1.00	6.89	1.66	1.00	1.00	1.00	1.00
15-Jan-92	74.62	4.83	1.00	2.15	23.67	11.61	1.00	1.00	2.68	1.00
23-Oct-91	12.98	17.97	6.48	1.56	19.65	9.29	1.00	1.00	1.00	1.00
3-Oct-91	86.71	9.88	9.57	2.61	40.89	9.64	1.00	1.00	1.00	1.00
24-Jun-91	25.55	10.82	2.17	1.98	51.53	5.81	1.00	1.00	1.00	1.00
26-Mar-91	52.10	18.74	3.86	1.00	36.46	2.94	1.00	1.00	1.00	
5-Dec-90	12.21	5.13	1.20	1.00	2.75	1.72	1.00	1.00	1.00	1.00
13-Sep-90	11.87	1.00	1.00	1.00	6.95	2.37	1.00	1.00	1.00	1.00
9-May-90	4.23	1.00	1.00	1.00	5.12	1.29	1.00	1.00	1.00	1.00
12-Jan-90	6.73	4.55	1.00	1.00	1.00	1.00	1.00	1.00		1.00
11-Oct-89	3.03	1.00	1.00	1.00	1.67	1.62	1.00	1.00	1.22	1.00
27-Jul-89	2.79	1.03	1.00	1.00	1.00	1.00	1.00	1.00	1.00	1.00
13-Apr-89	18.15	1.09	3.74	2.05	11.85	2.18	1.00	1.00	1.00	1.00
10-Jan-89	13.48	9.12	3.80	1.49	4.34	3.04	2.40	1.00	1.74	1.00
11-Oct-88	39.66	11.81	9.07	4.10	1.00	1.00	1.00	1.00	1.00	1.00
30-Aug-88	7.44	1.00	1.00	1.00	10.11	3.05	1.00	1.00	1.00	1.00
Apr-88	8	23	3	1.01	2	3	1	2	1	1
Feb-88	8	1	2	1		1	1	1	1	1
Oct-87	6	17	1.01	1	1	1	1	1	1	1
Jul-87	2	16	2	2	5	1	1	1	1	1
May-87	27	2	5	7	10	1	1	1	1.01	1
Feb-87	9	11	1	2	4	1	1	1		1
Dec-86	12	26	4	4	10	1	1	1		
Sep-86	5	13	1	1	5	12	1	1	1	1
Jun-86	8	13	1	1	5	6	1	1	1	1
Feb-86	6	9	1	2	4	4	1	1	1	1
Dec-85	9	7	9	7	1	1	1	1	1	1
Jul-85	27	32	17	10		1	1	1	1	1
May-85	23	26	20	10	2	1	10	1	1	1
Jan-85	1	1	1	1		1	1	1	1	1
Nov-84	68	1	1	1		1	1	1	1	1
Aug-84	1	1	1	1		1	1	1	1	1
Jan-84	1	1	1	1		1	1	1	1	1
Oct-83	22	1	1	1		1	18	1	1	1
Apr-82	15	6	1	1	22	1	1	1	1	1
Apr-81	1	1	1	1	1	1	1	1	1	1
May-80	1	1	1	1	5	1	1	1	1	1
Oct-79	1	1	1	1	1	1	1	1	1	1

Table A.1 TA C-64 Soil Sample Data (All values in pCi/g)

	3-3	3-5	3-7	3-9	3-11	3-13	3-15	4-0	4-6	4-8	4-10	4-12	4-14
31-Mar-94	1.11	1.00	1.00	1.00	1.00	1.00	1.56	1.00	1.00	1.00	1.00	1.00	1.00
21-Jan-94	3.16	9.15			1.00	1.00			1.00	1.00	1.00	1.00	1.00
22-Sep-93	1.00	1.00			1.00	1.00			1.00	4.84	1.00	1.00	1.00
15-Jun-93	4.48	7.65	1.00	1.00	1.00	1.00	3.54	1.00	1.00	1.00	1.00	1.00	1.00
29-Mar-93	1.00	3.87		1.00	1.00	1.00	1.00	1.00	1.00	1.00	1.00	1.00	1.00
19-Jan-93	1.00	1.00	1.00	1.00	1.00	1.00	1.00	1.00	1.00	1.00	1.00	1.00	1.00
29-Sep-92	2.26	7.55	1.00	1.00	1.00	1.00	1.00	1.00	1.00	1.00	1.00	1.00	1.00
22-Apr-92	1.00	1.00	1.00	1.00	1.00	1.00	1.00	1.00	1.00	1.00	1.00	1.00	1.00
15-Jan-92	3.63	5.66	2.55	1.00	2.80	2.63	1.00	1.00	2.47	1.00	1.00	1.00	1.00
23-Oct-91	1.78	3.56	1.00	1.00	1.00	1.00	1.00	1.00	1.68	1.00	1.00	1.00	1.00
3-Oct-91	2.96	7.79	1.00	1.00	1.00	2.00	1.00	1.00	1.00	1.00	1.13	1.00	1.00
24-Jun-91	1.00	5.06	1.00	1.00	1.00	1.00	1.00	1.00	1.00	1.00	1.00	1.00	1.00
26-Mar-91	1.00	14.44	1.90	1.00	1.00	1.00	1.00	1.00	1.00	1.00	1.00	1.00	1.00
5-Dec-90	1.00	1.00	1.00	1.00	1.00	1.00	1.00	1.00	1.00	1.00	1.00	1.00	1.00
13-Sep-90	1.00	1.64	1.00	1.00	1.00	1.00	1.00	1.00	1.00	1.00	1.00	1.00	1.00
9-May-90	1.00	1.66	1.00	1.00	1.00	1.00	1.00	1.00	1.00	1.00	1.00	1.00	1.00
12-Jan-90	1.00	1.00	1.00	1.00	1.00	1.00	1.00	1.00	1.00	1.00	1.00	1.00	1.00
11-Oct-89	1.00	5.79	2.42	1.00	1.00	1.62	1.00	1.00	1.00	1.00	1.00	2.09	1.00
27-Jul-89	1.00	1.00	1.00	1.00	1.00	1.00	1.00	1.00	1.00	1.00	1.00	1.00	1.00
13-Apr-89	1.20	3.50	1.00	1.00	1.00	2.05	1.00	1.00	1.00	1.00	1.00	1.00	1.00
10-Jan-89	1.00	1.00	1.00	2.18	1.00	2.94							
11-Oct-88	1.00	1.00	1.00	1.00	1.00	1.00	1.00						
30-Aug-88	1.00	3.12	1.00	1.00	1.00	1.00	1.00						
Apr-88	1	2	1	1		1.01	1						
Feb-88	1	1	1	1		1	1						
Oct-87	1	1	1	1		1	1						
Jul-87	1	1	1	1	1	1	1						
May-87	1	1	1	1	1	1	1						
Feb-87	3	1.01		1	1	1	1						
Dec-86	2	2	2	1	1	3							
Sep-86	1	1	1	1	1	1	1						
Jun-86	1	1	1	1	1	3	1						
Feb-86	1	1	1	1	1	2							
Dec-85	1	1	1	1	1	1	1						
Jul-85	1	1	1	1	1	1	1						
May-85	1	1	1	1	1	1	1						
Jan-85	1	1	1	1	1	1	1						
Nov-84	1	1	1	1	1	1	1						
Aug-84	1	1	1	1	1	1	1						
Jan-84	1	1	1	1	1	1	1						
Oct-83	1	1	1	1	1	1	1						
Apr-82	1	1	1	1	1	1	1						
Apr-81	1	1	1	1	1	1	1						
May-80	1	1	1	1	1	1	1						
Oct-79	1	1	1	1	1	1	1						

Table A.2 TA C-64 Soil Sample Data Continued (All values in pCi/g)

	5-3	5-7	5-9	5-11	5-13	5-15	6-10	6-12	6-14
31-Mar-94	1.00	1.00	1.00	1.00	1.00	1.00	1.00	1.00	1.00
21-Jan-94	1.00	1.00	1.00	1.00	1.00	1.00	1.00	1.00	
22-Sep-93	1.00	1.00	1.00	1.00	1.00	1.00	1.00	1.00	
15-Jun-93	1.00	1.00	1.00	1.00	1.00	1.00	1.00	1.00	
29-Mar-93	1.00	1.00	1.00	1.00	1.00	1.00		1.00	
19-Jan-93	1.00	1.00	1.00	1.00	1.00	1.00	1.00	1.00	
29-Sep-92	1.00	1.00	1.00	1.00	1.00	1.00	1.00	1.00	
22-Apr-92	1.00	1.00	1.00	1.00	1.00	1.00	1.00	1.00	
15-Jan-92	1.00	1.00	1.00	1.00	1.00	1.00	1.00	1.00	
23-Oct-91									
3-Oct-91	1.00	1.00	1.00	1.00	1.00	1.00	1.00	1.00	
24-Jun-91	1.00	1.00	1.00	1.00	1.00	1.00	1.00	1.00	
26-Mar-91	1.00	1.00	1.00	1.00	1.00	1.00	1.00	1.00	
5-Dec-90	1.00	1.00	1.00	1.00		1.00	1.00	1.00	
13-Sep-90	1.00	1.00	1.00	1.00	1.00	1.00	1.00	1.00	
9-May-90	1.00	1.00	1.00	1.00	1.00	1.00	1.00	1.00	
12-Jan-90	1.00	1.00	1.00	1.00	1.00	1.00	1.00	1.00	1.00
11-Oct-89	1.00	1.00	1.00	1.00	1.00	1.00	1.00	1.00	1.00
27-Jul-89									
13-Apr-89	1.00	1.00	1.00	1.00	1.00	1.00	1.00	1.00	1.00
10-Jan-89									
11-Oct-88									
30-Aug-88									
Apr-88									
Feb-88									
Oct-87									
Jul-87									
May-87									
Feb-87									
Dec-86									
Sep-86									
Jun-86									
Feb-86									
Dec-85									
Jul-85									
May-85									
Jan-85									
Nov-84									
Aug-84									
Jan-84									
Oct-83									
Apr-82									
Apr-81									
May-80									
Oct-79									

Table A.3 TA C-64 Soil Sample Data Continued (All values in pCi/g)

A.2   MathCad 5.0® Plus Kriging Program

The MathCad 5.0® Plus program used for the kriging analysis is presented in the following pages. It includes charts and tables referred to in Section 4.1.

**   Authors: C. Carter, E. Masterson   Last Update: Sept. 5, 1994   2039
**

**   This program analyzes sample data from Eglin AFB Site C-64.   The data is used to develop a
**   semi-variogram, perform a kriging analysis, and display the results.
**

The data on this page represents the average value obtained at each sampling location, within 300 feet of the target butt, since the last cleaning/sifting operation occurred in 1990. Samples were taken quarterly. The complete data set is in an Excel database

ORIGIN := 1   N := 20   CnfdncFactor := 1.645

                       N=the number of samples taken

$i := 1 .. N$ $distnum_i$ = distance number (first number of sample point)

                       $dirnum_i$ = direction number (second number of sample point)

$sample_i := i$
                       $value_i$ = sample value at location i (pC/g)

$sample_i$	$distnum_i :=$	$dirnum_i :=$	$value_i :=$
1	1	7	37.24
2	1	9	7.68
3	1	11	2.74
4	1	13	2.42
5	2	4	20.74
6	2	6	6.49
7	2	8	1
8	2	10	1.05
9	2	12	1.14
10	2	14	1
11	3	3	1.88
12	3	5	4.98
13	3	7	1.22
14	3	9	1
15	3	11	1.13
16	3	13	1.19
17	3	15	1.26
18	4	6	1.15
19	4	10	1.01
20	4	14	1.00

This converts the distance number to actual distance: $dist_i := distnum_i \cdot 60$
This will convert the direction number to an angle θ. θ is defined such that θ = 0 is east, and positive θ is counterclockwise:

$$\theta_i := \frac{\pi}{2} - \frac{dirnum_i \cdot \pi}{8}$$

A-6

This will determine the cartesian coordinates of each sample point. (0,0) is the target butt inside the RCA, and the positive x direction is east.

$$x_i := dist_i \cdot \cos(\theta_i) \qquad y_i := dist_i \cdot \sin(\theta_i)$$

$sample_i$	$distnum_i$	$dirnum_i$	x_i	y_i	$value_i$
1	1	7	22.9610059	-55.432772	37.24
2	1	9	-22.9610059	-55.432772	7.68
3	1	11	-55.432772	-22.9610059	2.74
4	1	13	-55.432772	22.9610059	2.42
5	2	4	120	0	20.74
6	2	6	84.8528137	-84.8528137	6.49
7	2	8	$7.3476381 \cdot 10^{-15}$	-120	1
8	2	10	-84.8528137	-84.8528137	1.05
9	2	12	-120	$-1.4695276 \cdot 10^{-14}$	1.14
10	2	14	-84.8528137	84.8528137	1
11	3	3	166.2983159	68.8830178	1.88
12	3	5	166.2983159	-68.8830178	4.98
13	3	7	68.8830178	-166.2983159	1.22
14	3	9	-68.8830178	-166.2983159	1
15	3	11	-166.2983159	-68.8830178	1.13
16	3	13	-166.2983159	68.8830178	1.19
17	3	15	-68.8830178	166.2983159	1.26
18	4	6	169.7056275	-169.7056275	1.15
19	4	10	-169.7056275	-169.7056275	1.01
20	4	14	-169.7056275	169.7056275	1

mean(value) = 4.866

median(value) = 1.205

var(value) = 75.036054

A-7

Histogram analysis of the input data

$r := 1 .. 10 \qquad s := 1 .. 9$

$intrvl_r :=$

$histval := hist(intrvl, value)$

intrvl
0
5
10
15
20
25
30
35
40
45

$$histval = \begin{bmatrix} 16 \\ 2 \\ 0 \\ 0 \\ 1 \\ 0 \\ 0 \\ 0 \\ 1 \\ 0 \end{bmatrix}$$

Number of samples
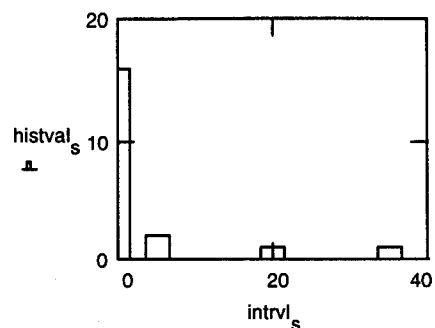
The histogram above shows that the data is skewed to the right

$b_i := \ln\left(value_i\right)$

$logintrvl_r :=$

$histb := hist(logintrvl, b)$

logintrvl
0
.5
1
1.5
2
2.5
3
3.5
4
4.5

$$histb = \begin{bmatrix} 12 \\ 2 \\ 1 \\ 2 \\ 1 \\ 0 \\ 1 \\ 1 \\ 0 \end{bmatrix}$$
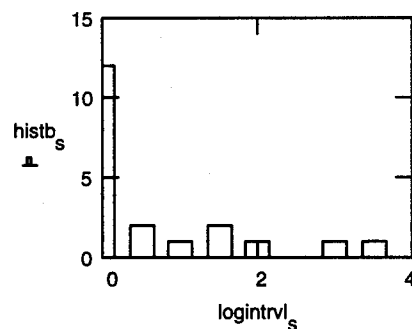
The data does spread out more but there is still a tall column on the left. This is due to the fact that the equipment cannot measure values below 1.0. All samples less than or equal to 1 were considered to be 1. If the actual values were known the column on the left would certainly have been flattened out by a logrithmic transformation.

Calculation of the Semi-variogram $\qquad$ $j := 1 .. N$

$$\text{distance}(a, b) := \sqrt{\left(x_a - x_b\right)^2 + \left(y_a - y_b\right)^2}$$

$$h_{i,j} := \text{distance}(i, j) \qquad\qquad W_{i,j} := \frac{\left(b_i - b_j\right)^2}{2}$$

This is a scatterplot of all possible values of h and the
corresponding value of W
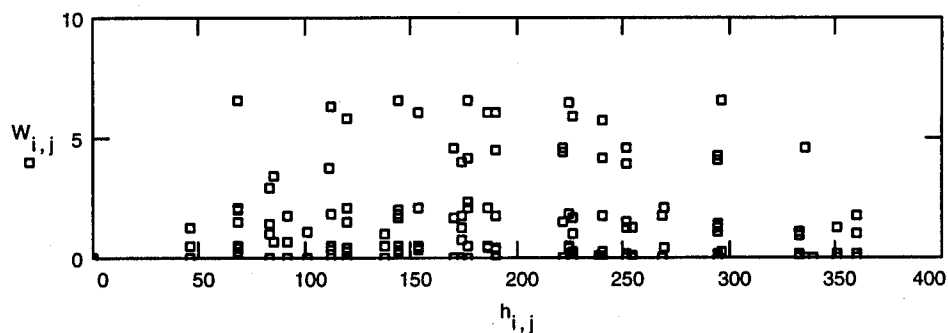
Semi-variogram Subroutine

This subroutine works by creating a matrix with column 1 consisting of the distance between all the possible combinations of sample points, and column 2 the associated value of W for that combination. The matrix is sorted so col1 is in ascending order.   This column is then divided into groups of whatever size is input as the interval

$$z := 1 .. \sum_{i=1}^{N-1} i \qquad\qquad \text{intervalsize} := 30 \qquad\qquad \text{maxdist} := 400$$

The next series of equations are needed to form the vectors "hvector" and "wvector" by listing all the data points below the main diagonal of the matrix h_{ij}

$$\text{rowindex}_1 := 2$$

$$\text{rowindex}_{z+1} := \text{if}\left(\sum_{i=1}^{\text{rowindex}_z - 1} i > z, \text{rowindex}_z, \text{rowindex}_z + 1 \right)$$

A-9

$$\text{colindex}_1 := 1 \qquad\qquad \text{colindex}_{z+1} := \text{if}\left(\text{colindex}_z < \text{rowindex}_z - 1, \text{colindex}_z + 1, 1\right)$$

$$\text{hvector}_z := h_{\text{rowindex}_z, \text{colindex}_z} \qquad\qquad \text{wvector}_z := W_{\text{rowindex}_z, \text{colindex}_z}$$

$$\text{rawdata} := \text{augment}(\text{hvector}, \text{wvector})$$

This sorts the rows of the matrix "rawdata" by ordering the values in column 1 in ascending order.

$$\text{sortdata} := \text{csort}(\text{rawdata}, 1)$$

$$\text{hvector}_z := \text{sortdata}_{z,1} \qquad\qquad \text{wvector}_z := \text{sortdata}_{z,2}$$

This creates a vector defining the intervals for use in the histogram function.
The histogram function must have vectors for inputs

$$i := 1 .. \frac{\text{maxdist}}{\text{intervalsize}} + 1$$

$$\text{interval}_i := \text{intervalsize} \cdot i - \text{intervalsize}$$

The histogram function will output a vector that contains the number a values falling into each
of the intervals specified in the interval vector. It contains 1 less value than the interval vector

$$\text{histdata} := \text{hist}(\text{interval}, \text{hvector})$$

$$i := 1 .. \frac{\text{maxdist}}{\text{intervalsize}}$$

In this section the data from the histogram is used to find the start and stop positions,
within each column vector, corresponding to various intervals

$$\text{startnum}_1 := 0$$

$$\text{startnum}_{i+1} := \sum_{j=1}^{i} \text{histdata}_j + 1 \qquad\qquad \text{stopnum}_i := \left(\text{startnum}_i + \text{histdata}_i\right) - 1$$

In each interval, the data point will be plotted
at the average value of the data points that were
grouped together

$$dist_i := if\left[startnum_i < stopnum_i, \frac{\displaystyle\sum_{j \,=\, startnum_i}^{stopnum_i} hvector_j}{\left(stopnum_i - startnum_i\right) + 1}, 0\right]$$

$$\gamma_i := if\left[startnum_i < stopnum_i, \frac{\displaystyle\sum_{j \,=\, startnum_i}^{stopnum_i} wvector_j}{\left(stopnum_i - startnum_i\right) + 1}, 0\right]$$

$$\gamma 2_i := var(b)$$

$$dist_1 = 0 \qquad dist_2 = 45.9220119$$
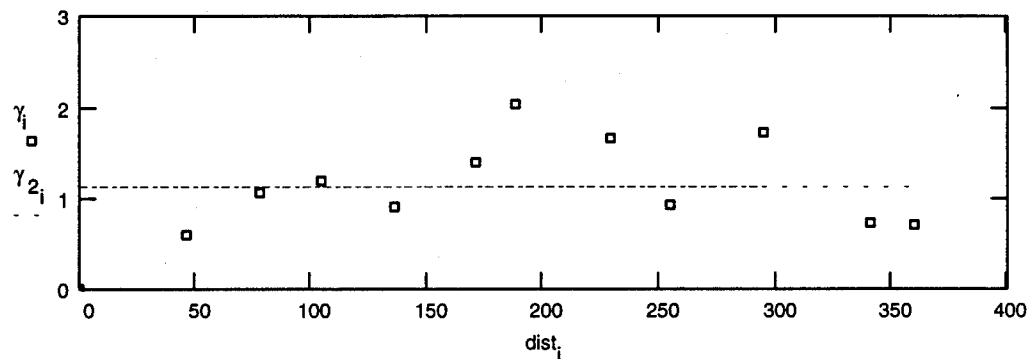
Classical semi-variogram models

Spherical Semi-Variogram Model

Using the graphical approach,

C=sill value $C := var(b)$ $C = 1.1245901$

the parameter a=3/2 * tandist   where tandist is defined as the the distance when a line tangent to the experimental semi-variogram at h=0 reaches the sill

$$tandist := \frac{C \cdot dist_2}{\gamma_2} \qquad tandist = 86.7912732$$

a=range of influence parameter $a := \frac{3}{2} \cdot tandist$ $a = 130.1869098$

A-11

$$\gamma_{sph}(r) := if\left[r < a, C \cdot \left(\frac{3 \cdot r}{2 \cdot a} - \frac{1 \cdot r^3}{2 \cdot a^3}\right), C\right] \qquad r := 0, 10 .. 600$$

Exponential Model

For this model, the distance when the semi-variogram reaches 95% of the sill is defined to be 3a

$$C = 1.1245901 \qquad range := \frac{.95 \cdot C \cdot dist_2}{\gamma_2} \qquad a_2 := \frac{1}{3} \cdot range \qquad a_2 = 27.4839032$$

$$\gamma_{exp}(t) := C \cdot \left(1 - exp\left(-\frac{t}{a_2}\right)\right) \qquad t := 0, 10 .. 600$$

Guassian model

For this model, a = 1/sqrt(3) of the distance to 95% of the sill

$$a_3 := \frac{1}{\sqrt{3}} \cdot range \qquad \gamma_{gau}(t) := C \cdot \left(1 - exp\left(-\frac{t^2}{a_3^2}\right)\right) \qquad a_3 = 47.6035167$$

Summary of Semi-variogram models
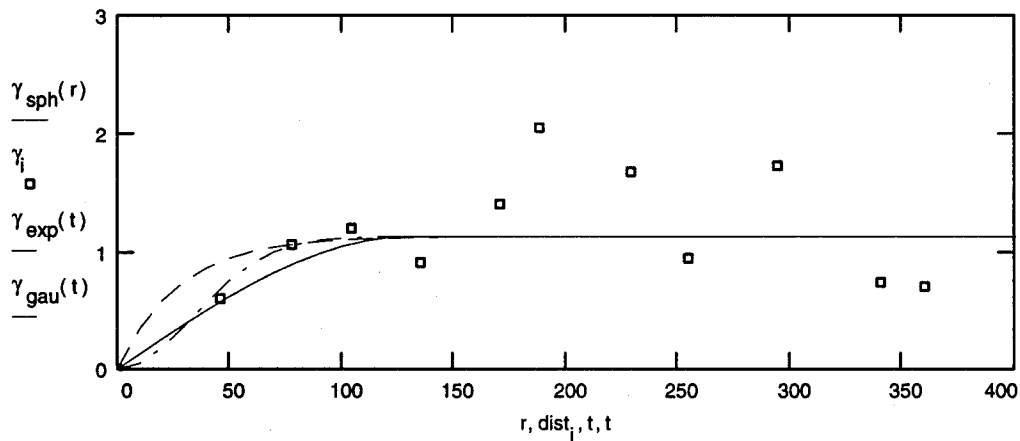
Conclusion: Best fit is gaussian model

$$\gamma(r) := \gamma_{gau}(r)$$

A-12

The kriging equation which must be solved for each point where a prediction is needed is:

$$\Gamma \cdot wf \cong sv \qquad \text{or} \qquad \Gamma^{-1} \cdot sv \cong wf$$

where　Γ = known covariance matrix
　　　　wf = weighting factors
　　　　γsa = semi-varigram values between sample points and kriging point

$i := 1 .. N$

Γ is an 21 x 21 matrix but I can build it by creating most of it with the equation below

$$\Gamma = \begin{matrix} \gamma(S1,S1) & \gamma(S1,S2) & \dots & \gamma(S1,S20) \\ \gamma(S2,S1) & \gamma(S2,S2) & \dots\dots \\ \cdot \\ \cdot \\ \gamma(S20,S1) & \gamma(S20,S2) & \dots\dots & \gamma(S20,S20) \end{matrix}$$

$$\Gamma_{i,j} := \gamma(h_{i,j})$$

These steps complete the main matrix. This matrix stays the same in all calculations.

$lastrow_i := 1$　　　　　　　　　$\Gamma := stack\left(\Gamma, lastrow^T\right)$

$lastcol_i := 1$　　$lastcol_{N+1} := 0$　　$\Gamma := augment(\Gamma, lastcol)$

***** The equation below are necessary to free up memory. The variables are no longer needed. ******

$h := 0$　　　$W := 0$　　$dirnum := 0$　　$distnum := 0$　　$\theta := 0$　　$i := 0$　　$rawdata := 0$

****

$$G := \Gamma^{-1}$$

A-13

Kriging/Displaying Subroutine

Input: kriging area   distance between kriging points

$xmin := -180$ $xmax := 180$

$ymin := -180$ $ymax := 180$

$xintrvl := 30$
$yintrvl := 30$

Number of points

$$xnum := \frac{xmax - xmin}{xintrvl} + 1 \qquad\qquad ynum := \frac{ymax - ymin}{yintrvl} + 1$$

$pts := xnum \cdot ynum$ $pts = 169$ $xnum = 13$ $ynum = 13$

This is the x and y position of the points to be kriged $z := 1 .. pts$

$$xpos_z := (xmin - xintrvl) + \left[z - \left(ceil\left(\frac{z}{xnum}\right) - 1 \right) \cdot xnum \right] \cdot xintrvl$$

$$ypos_z := (ymax + yintrvl) - ceil\left(\frac{z}{xnum}\right) \cdot yintrvl$$

building the $\gamma(S,A)$ vector $n := 1 .. N$

dist between sample points
and kriging point

$$sampdist_{n,z} := \sqrt{\left(x_n - xpos_z\right)^2 + \left(y_n - ypos_z\right)^2}$$

$$\gamma sa_{n,z} := \gamma\left(sampdist_{n,z}\right) \qquad\qquad \gamma sa_{N+1,z} := 1$$

determine weighting factors $wf := G \cdot \gamma sa$

predicted values at the kriging point

The variance at the kriging point is

$$\mu_z := \sum_{i=1}^{N} wf_{i,z} \cdot b_i$$

$$\sigma 2_z := max\left[\left[\begin{matrix} 0 \\ \sum_{i=1}^{N} wf_{i,z} \cdot \gamma sa_{i,z} + wf_{N+1,z} \end{matrix} \right] \right]$$

**Note: Because of numerical error, in some instances where the
variance is zero (at sample points) the equations yield a value which
is slightly below zero. The above equation prevents σ^2 from being negative.

****

$sampdist := 0$

****

$$E(X) \qquad\qquad V(X)$$

$$\text{pred}_z := \exp\!\left(\mu_z + \frac{\sigma 2_z}{2}\right) \qquad\qquad \text{Var}_z := \exp\!\left(2\cdot\mu_z + \sigma 2_z\right)\cdot\left(\exp\!\left(\sigma 2_z\right) - 1\right)$$

95 % upper bound surface
   Note: pred + 1.645 σ gives the 95% upper bound value

$$\sigma_z := \sqrt{\sigma 2_z}$$

$$\text{ube}_z := \mu_z + \text{CnfdncFactor}\cdot\sigma_z \qquad\qquad \text{ub}_z := \exp\!\left(\text{ube}_z\right)$$

Display Subroutine

$$r := 1\,..\,\text{ynum} \qquad\qquad s := 1\,..\,\text{xnum}$$

Note: A value of 99 is used in the tables in all position that correspond to the RCA

Tables:

$$\text{RCAx}_{(r-1)\cdot\text{xnum}+s} := \text{if}\!\left[-40 < \text{xpos}_{(r-1)\cdot\text{xnum}+s}, 0, 1\right] + \text{if}\!\left[\text{xpos}_{(r-1)\cdot\text{xnum}+s} < 110, 0, 1\right]$$

$$\text{RCAy}_{(r-1)\cdot\text{xnum}+s} := \text{if}\!\left[-40 < \text{ypos}_{(r-1)\cdot\text{xnum}+s}, 0, 1\right] + \text{if}\!\left[\text{ypos}_{(r-1)\cdot\text{xnum}+s} < 160, 0, 1\right]$$

$$\text{Vtable}_{r,s} := \text{if}\!\left[\text{RCAx}_{(r-1)\cdot\text{xnum}+s} + \text{RCAy}_{(r-1)\cdot\text{xnum}+s} \equiv 0, 99, \text{pred}_{(r-1)\cdot\text{xnum}+s}\right]$$

$$\mu\text{table}_{r,s} := \text{if}\!\left[\text{RCAx}_{(r-1)\cdot\text{xnum}+s} + \text{RCAy}_{(r-1)\cdot\text{xnum}+s} \equiv 0, 99, \mu_{(r-1)\cdot\text{xnum}+s}\right]$$

$$\sigma\text{table}_{r,s} := \text{if}\!\left[\text{RCAx}_{(r-1)\cdot\text{xnum}+s} + \text{RCAy}_{(r-1)\cdot\text{xnum}+s} \equiv 0, 99, \sigma_{(r-1)\cdot\text{xnum}+s}\right]$$

$$\text{UBtable}_{r,s} := \text{if}\!\left[\text{RCAx}_{(r-1)\cdot\text{xnum}+s} + \text{RCAy}_{(r-1)\cdot\text{xnum}+s} \equiv 0, 99, \text{ub}_{(r-1)\cdot\text{xnum}+s}\right]$$

Surface Contour Plots:

$$\text{Vcontour}_{s,r} := \text{pred}_{(\text{ynum}-r)\cdot\text{xnum}+s} \qquad\qquad \text{UBcontour}_{s,r} := \text{ub}_{(\text{ynum}-r)\cdot\text{xnum}+s}$$

Note 1:   The equations above, which create matrices for use in presenting tables and creating surfaces plots, are set up so the output will be oriented with North up and East to the right.

Note 2: The surface plots are for visual interpretation of the data only. MathCad's built in countour plot function draws the contour lines. The data presented in the tables represents the actual results of the kriging analysis.

Note3: When creating surface plots, insure the xmin, xmax, ymin, and ymax points are entered into the surface plot dialog box for each plot.

predicted value of DU concentration
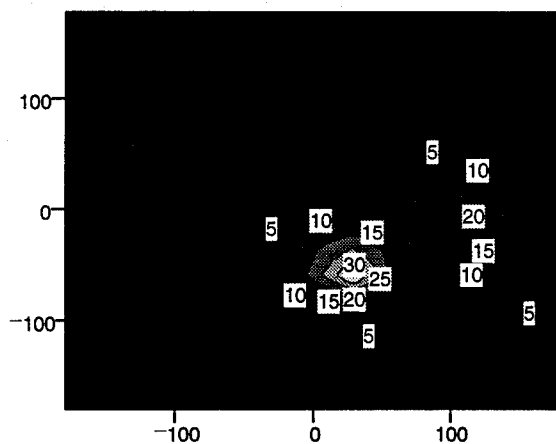
Vcontour
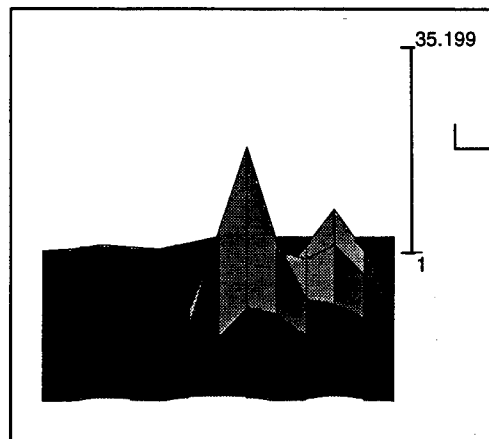
Vcontour

95% Upper Bound Surface
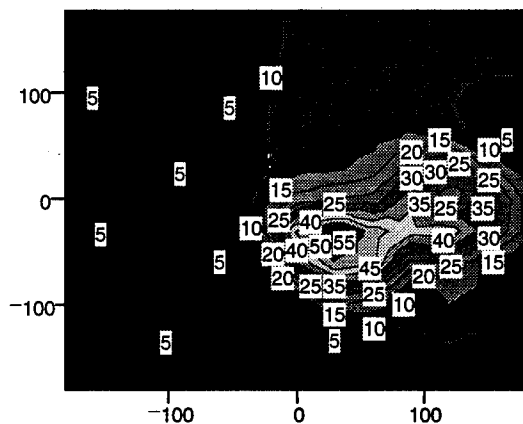
UBcontour

UBcontour

A-16
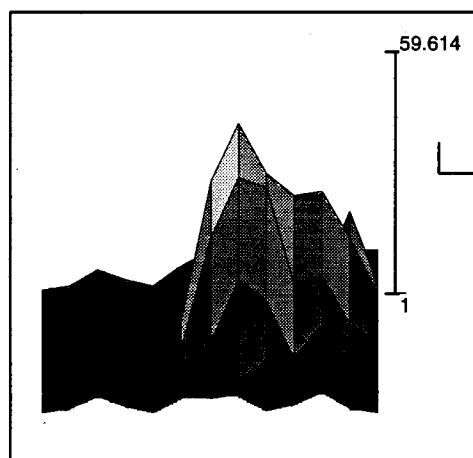
μtable =

	1	2	3	4	5	6	7	8	9	10	11	12	13
1	0.07	0.12	0.34	0.32	0.3	0.49	0.64	0.69	0.69	0.69	0.69	0.69	0.69
2	0.12	0.15	0.31	0.25	0.25	99	99	99	99	99	0.69	0.68	0.68
3	0.33	0.3	0.28	0.15	0.24	99	99	99	99	99	0.67	0.65	0.64
4	0.29	0.21	0.13	-0.01	0.19	99	99	99	99	99	0.7	0.61	0.58
5	0.25	0.15	0.14	0.17	0.43	99	99	99	99	99	1.09	0.86	0.64
6	0.4	0.22	0.19	0.44	0.79	99	99	99	99	99	2.2	1.65	0.93
7	0.47	0.23	0.13	0.46	0.92	99	99	99	99	99	3.03	2.3	1.23
8	0.37	0.19	0.16	0.41	0.91	99	99	99	99	99	2.53	2.11	1.37
9	0.21	0.11	0.13	0.2	0.67	1.66	3.01	3.54	2.72	2.02	1.83	1.76	1.48
10	0.26	0.18	0.13	0.03	0.25	0.76	1.48	2.08	2.03	1.72	1.45	1.39	1.27
11	0.32	0.29	0.27	0.1	0.03	-0.04	$-5.5 \cdot 10^{-15}$	0.46	0.89	1.03	0.94	0.81	0.75
12	0.12	0.15	0.26	0.1	-0.04	-0.07	-0.08	0.08	0.26	0.42	0.49	0.33	0.28
13	0.08	0.12	0.29	0.18	0.1	0.25	0.36	0.32	0.23	0.31	0.38	0.23	0.19

Non-RCA average conc.

$$AverConc := \frac{\displaystyle\sum_{i=1}^{ynum} \sum_{j=1}^{xnum} Vtable_{i,j} - 35 \cdot 99}{ynum \cdot xnum - 35}$$

AverConc = 3.6396256

$\sigma\text{table} =$

	1	2	3	4	5	6	7	8	9	10	11	12	13
1	0.44	0.63	0.96	0.69	0.49	0.95	1.08	1.09	1.09	1.09	1.09	1.09	1.09
2	0.63	0.75	0.97	0.71	0.54	99	99	99	99	99	1.09	1.09	1.09
3	0.96	0.97	0.98	0.81	0.88	99	99	99	99	99	1.08	1.04	1.03
4	0.69	0.71	0.81	0.22	0.7	99	99	99	99	99	1.02	0.73	0.7
5	0.49	0.53	0.85	0.64	0.68	99	99	99	99	99	0.97	0.53	0.49
6	0.93	0.82	0.75	0.73	0.22	99	99	99	99	99	0.77	0.83	0.93
7	1.04	0.77	0		0.6	0.33	99	99	99	99	$1.72 \cdot 10^{-8}$	0.78	1.04
8	0.93	0.83	0.75	0.72	0.22	99	99	99	99	99	0.75	0.83	0.93
9	0.49	0.53	0.85	0.64	0.6	0.22	0.33	0.22	0.68	0.68	0.85	0.53	0.49
10	0.69	0.71	0.81	0.22	0.64	0.72	0.6	0.73	0.64	0.22	0.81	0.71	0.69
11	0.96	0.97	0.98	0.81	0.85	0.75	0	0.75	0.85	0.81	0.98	0.98	0.96
12	0.63	0.75	0.97	0.71	0.53	0.83	0.77	0.82	0.53	0.71	0.97	0.75	0.63
13	0.44	0.63	0.96	0.69	0.49	0.93	1.04	0.93	0.49	0.69	0.96	0.63	0.44

Kriging/Displaying Subroutine

kriging at 10 foot intervals in area of greatest concern

Input: kriging area distance between kriging points

$$xmin := 0 \qquad xmax := 140$$

$$ymin := -90 \qquad ymax := 10$$

$$xintrvl := 10$$
$$yintrvl := 10$$

Number of points

$$xnum := \frac{xmax - xmin}{xintrvl} + 1 \qquad\qquad ynum := \frac{ymax - ymin}{yintrvl} + 1$$

$$pts := xnum \cdot ynum \qquad pts = 165 \qquad xnum = 15 \qquad ynum = 11$$

This is the x and y position of the points to be kriged $\qquad z := 1 .. pts$

$$xpos_z := (xmin - xintrvl) + \left[z - \left(ceil\left(\frac{z}{xnum}\right) - 1 \right) \cdot xnum \right] \cdot xintrvl$$

$$ypos_z := (ymax + yintrvl) - ceil\left(\frac{z}{xnum}\right) \cdot yintrvl$$

building the $\gamma(S,A)$ vector $\qquad n := 1 .. N$

dist between sample points
and kriging point
$$sampdist_{n,z} := \sqrt{\left(x_n - xpos_z\right)^2 + \left(y_n - ypos_z\right)^2}$$

$$\gamma sa_{n,z} := \gamma\left(sampdist_{n,z}\right) \qquad \gamma sa_{N+1,z} := 1$$

determine weighting factors $\qquad wf := G \cdot \gamma sa$

predicted values at the kriging point

The variance at the kriging point is

$$\mu_z := \sum_{i=1}^{N} wf_{i,z} \cdot b_i$$

$$\sigma 2_z := max\left[\left[\begin{matrix} 0 \\ \sum_{i=1}^{N} wf_{i,z} \cdot \gamma sa_{i,z} + wf_{N+1,z} \end{matrix}\right]\right]$$

A-19

$$E(X) \qquad\qquad V(X)$$

$$\text{pred}_z := \exp\left(\mu_z + \frac{\sigma2_z}{2}\right) \qquad \text{Var}_z := \exp\left(2 \cdot \mu_z + \sigma2_z\right) \cdot \left(\exp\left(\sigma2_z\right) - 1\right) \qquad \sigma_z := \sqrt{\sigma2_z}$$

$$\text{ub}\varepsilon_z := \mu_z + \text{CnfdncFactor} \cdot \sigma_z \qquad \text{ub}_z := \exp\left(\text{ub}\varepsilon_z\right)$$

Display $\qquad r := 1 .. \text{ynum} \qquad s := 1 .. \text{xnum}$

Tables:

$$\text{RCAx}_{(r-1) \cdot \text{xnum} + s} := \text{if}\left[-40 < \text{xpos}_{(r-1) \cdot \text{xnum} + s}, 0, 1\right] + \text{if}\left[\text{xpos}_{(r-1) \cdot \text{xnum} + s} < 110, 0, 1\right]$$

$$\text{RCAy}_{(r-1) \cdot \text{xnum} + s} := \text{if}\left[-40 < \text{ypos}_{(r-1) \cdot \text{xnum} + s}, 0, 1\right] + \text{if}\left[\text{ypos}_{(r-1) \cdot \text{xnum} + s} < 160, 0, 1\right]$$

$$\text{Vtable2}_{r,s} := \text{if}\left[\text{RCAx}_{(r-1) \cdot \text{xnum} + s} + \text{RCAy}_{(r-1) \cdot \text{xnum} + s} \equiv 0, 99, \text{pred}_{(r-1) \cdot \text{xnum} + s}\right]$$

$$\mu\text{table2}_{r,s} := \text{if}\left[\text{RCAx}_{(r-1) \cdot \text{xnum} + s} + \text{RCAy}_{(r-1) \cdot \text{xnum} + s} \equiv 0, 99, \mu_{(r-1) \cdot \text{xnum} + s}\right]$$

$$\sigma\text{table2}_{r,s} := \text{if}\left[\text{RCAx}_{(r-1) \cdot \text{xnum} + s} + \text{RCAy}_{(r-1) \cdot \text{xnum} + s} \equiv 0, 99, \sigma_{(r-1) \cdot \text{xnum} + s}\right]$$

$$\text{UBtable2}_{r,s} := \text{if}\left[\text{RCAx}_{(r-1) \cdot \text{xnum} + s} + \text{RCAy}_{(r-1) \cdot \text{xnum} + s} \equiv 0, 99, \text{ub}_{(r-1) \cdot \text{xnum} + s}\right]$$

Surface Contour Plots: $\qquad$ (RCA not shown with true values)

$$\text{Vcontour2}_{s,r} := \text{pred}_{(\text{ynum} - r) \cdot \text{xnum} + s} \qquad\qquad \text{UBcontour2}_{s,r} := \text{ub}_{(\text{ynum} - r) \cdot \text{xnum} + s}$$

Vcontour2

UBcontour2
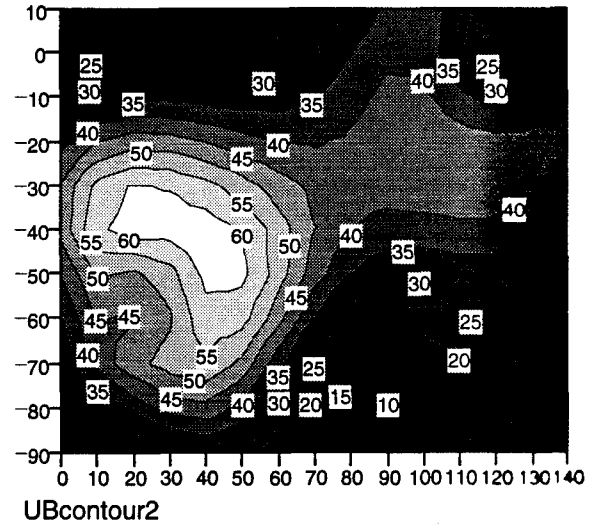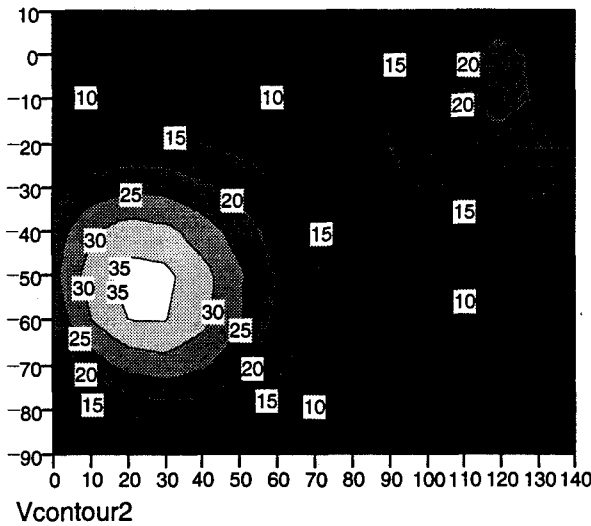
$$\text{ztable}_{r,s} := \text{if}\left[RCAx_{(r-1)\cdot xnum+s} + RCAy_{(r-1)\cdot xnum+s} = 0, 0, (r-1)\cdot xnum+s \right]$$

$\mu\text{table2} =$

	1	2	3	4	5	6	7	8	9	10	11	12	13	14	15
1	99	99	99	99	99	99	99	99	99	99	99	2.8	2.9	2.8	2.5
2	99	99	99	99	99	99	99	99	99	99	99	2.9	3	2.9	2.7
3	99	99	99	99	99	99	99	99	99	99	99	2.9	3	2.9	2.7
4	99	99	99	99	99	99	99	99	99	99	99	2.7	2.8	2.7	2.5
5	99	99	99	99	99	99	99	99	99	99	99	2.5	2.5	2.5	2.3
6	2.9	3.2	3.4	3.3	3.1	2.8	2.5	2.3	2.2	2.2	2.2	2.2	2.3	2.2	2.1
7	3.1	3.4	3.6	3.6	3.4	3	2.7	2.4	2.2	2.1	2	2	2	2	1.9
8	3	3.4	3.5	3.5	3.4	3.1	2.7	2.4	2.2	2	1.9	1.9	1.8	1.8	1.8
9	2.7	3	3.2	3.2	3.1	2.9	2.6	2.4	2.1	2	1.8	1.8	1.7	1.7	1.7
10	2.1	2.4	2.6	2.7	2.7	2.6	2.4	2.2	2	1.9	1.7	1.6	1.6	1.5	1.5
11	1.5	1.7	2	2.1	2.1	2.1	2	1.9	1.8	1.7	1.6	1.5	1.5	1.4	1.4

$\sigma\text{table2} =$

	1	2	3	4	5	6	7	8	9	10	11	12	13	14	15
1	99	99	99	99	99	99	99	99	99	99	99	0.43	0.3	0.42	0.62
2	99	99	99	99	99	99	99	99	99	99	99	0.31	$1.72 \cdot 10^{-8}$	0.31	0.57
3	99	99	99	99	99	99	99	99	99	99	99	0.42	0.3	0.42	0.62
4	99	99	99	99	99	99	99	99	99	99	99	0.62	0.56	0.61	0.72
5	99	99	99	99	99	99	99	99	99	99	99	0.78	0.75	0.76	0.79
6	0.54	0.51	0.46	0.49	0.62	0.76	0.86	0.91	0.92	0.9	0.88	0.87	0.85	0.84	0.81
7	0.36	0.3	0.18	0.25	0.46	0.66	0.77	0.82	0.83	0.83	0.85	0.87	0.88	0.85	0.77
8	0.33	0.28	0.15	0.22	0.43	0.6	0.68	0.69	0.67	0.68	0.74	0.82	0.85	0.82	0.71
9	0.46	0.45	0.41	0.43	0.53	0.61	0.61	0.54	0.45	0.46	0.59	0.73	0.81	0.8	0.68
10	0.58	0.59	0.59	0.62	0.66	0.67	0.59	0.42	0.2	0.22	0.46	0.67	0.79	0.8	0.72
11	0.6	0.63	0.67	0.73	0.77	0.75	0.64	0.45	0.22	0.22	0.46	0.68	0.81	0.85	0.81

$$ztable =$$

	1	2	3	4	5	6	7	8	9	10	11	12	13	14	15
1	0	0	0	0	0	0	0	0	0	0	0	12	13	14	15
2	0	0	0	0	0	0	0	0	0	0	0	27	28	29	30
3	0	0	0	0	0	0	0	0	0	0	0	42	43	44	45
4	0	0	0	0	0	0	0	0	0	0	0	57	58	59	60
5	0	0	0	0	0	0	0	0	0	0	0	72	73	74	75
6	76	77	78	79	80	81	82	83	84	85	86	87	88	89	90
7	91	92	93	94	95	96	97	98	99	100	101	102	103	104	105
8	106	107	108	109	110	111	112	113	114	115	116	117	118	119	120
9	121	122	123	124	125	126	127	128	129	130	131	132	133	134	135
10	136	137	138	139	140	141	142	143	144	145	146	147	148	149	150
11	151	152	153	154	155	156	157	158	159	160	161	162	163	164	165

To find the x and y position of a specific point, enter the row and column of the position:

$$\text{row} := 7 \qquad \text{column} := 4$$

$$\text{xpos}_{(row - 1) \cdot xnum + column} = 30 \qquad \text{ypos}_{(row - 1) \cdot xnum + column} = -50$$

$$\text{zpos} := (row - 1) \cdot xnum + column$$

$$\text{zpos} = 94$$

distribution parameters

Log space $\qquad \mu_{zpos} = 3.5630672 \qquad \sigma_{zpos} = 0.2459442$

Original space

$\qquad$ mean $\qquad \text{pred}_{zpos} = 36.3542628$

$\qquad$ Var(x)= $\qquad \text{Var}_{zpos} = 82.4109449$

$\qquad$ median $\qquad e^{\mu_{zpos}} = 35.2712152$

$$\text{logpdf}(z, x) := \frac{1}{\sigma_z \cdot x \cdot \sqrt{2 \cdot \pi}} \cdot \exp\left[-\frac{1}{2} \cdot \left[\left(\frac{\ln(x) - \mu_z}{\sigma_z}\right)^2\right]\right]$$

$$x := 1 .. 80$$
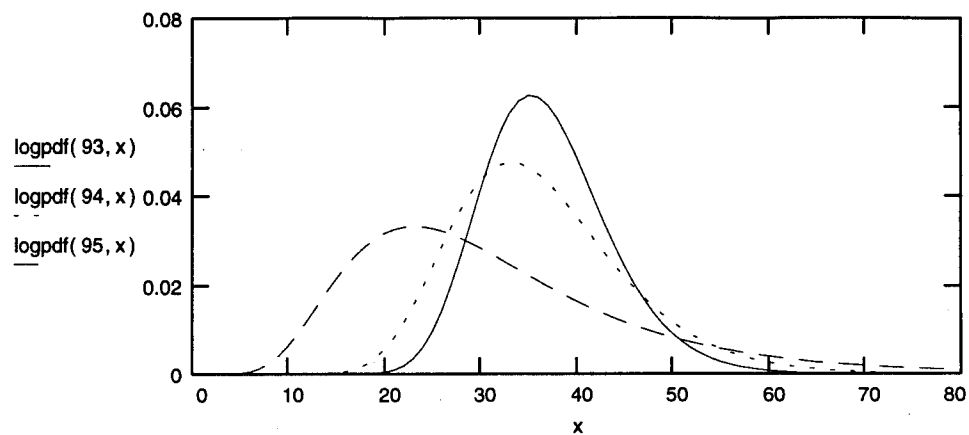
This is a plot of the pdf at the point with the worst case mean and the pdf's of several points near that point.

A.3 Surface Water Runoff

One other possible method for contamination to reach the streams near TA C-64 is by surface water runoff. Outside the asphalt berm that borders the RCA, rainwater run-off will go to one of two places. On the south side of the RCA, the surface slopes down sharply from the berm down to a low point between sample points 2-8 and 3-9. Rain falling on the east, west, and north sides of the RCA will drain toward an area to the northeast of the RCA and then away from the site in a northerly direction. The closest stream, and the one most likely to be affected by rainwater run-off is Titi Creek. At its nearest point, Titi Creek is approximately 1500 feet from the RCA. Based on soil surface concentration samples and the local topography, this scenario appears highly unlikely.

Sample point 1-7, located just south of the RCA, is the site of the most consistently high readings, averaging 37.24 pCi/g since the last cleaning operation. Despite the fact that sample point 2-8 is near the low point and almost directly on a downhill gradient from sample point 1-7, the samples at location 2-8 have consistently been below the level of detection. These two sample points are approximately 114 feet apart.

Sample point 5-15 is located to the north-west of the RCA, directly in the run-off pathway. Quarterly samples at this location have never been observed to be above the level of detection. If deplete uranium was transported in significant amounts by rainwater run-off, one would expect to observe elevated level of DU along this pathway.

Inside the RCA, the concentration of DU in the soil is much higher than it is outside the RCA. In this area, the ground is sloped toward a man made swell, where rainwater collects and eventually evaporates or infiltrates the ground. This has been an effective rainwater collection method with the exception of one instance, in August of 1983, when heavy rain caused excess run-off to spill over the asphalt berm. Six samples were taken at that time, along the drainage ways flowing away from the RCA. Three of the samples indicated elevated levels of DU (from 37.8 to 65.52 pCi/g) and three were below the level of detection (12). Although this isolated incident does indicate that it is possible for some DU to be transported short distances by surface water run-off, the evidence as a whole indicates that contamination of Titi Creek, 1500 feet away, is not a significant concern.

A.4   Wind Data Analysis

Although it was not a goal of this study to determine the transport mechanisms involved in the spread of contamination, it is interesting to speculate.

Precautions are taken to decontaminate clothing and equipment when workers exit the RCA and can be ruled out as a transport mechanism. Some shrapnel may be able to exit the gun butt during firing operations, but no data is available to substantiate this theory. Contaminated sand can be kicked up and tacked by wildlife, as fresh deer tracks were observed crossing the RCA during the site visit, but again can be ruled out as a significant transport mechanism. The most likely transport mechanism is wind.

Duke Field, an auxiliary to Eglin AFB, is located just six miles west of TA C-64. As an active airfield weather data is observed and recorded. This data is available through the Federal Climate Complex (51). Figure A.1 shows the frequency that the surface wind has been recorded from a given direction. This data comes from hourly observations through 1992 without including observations of calm, which account for 11 percent of the time.
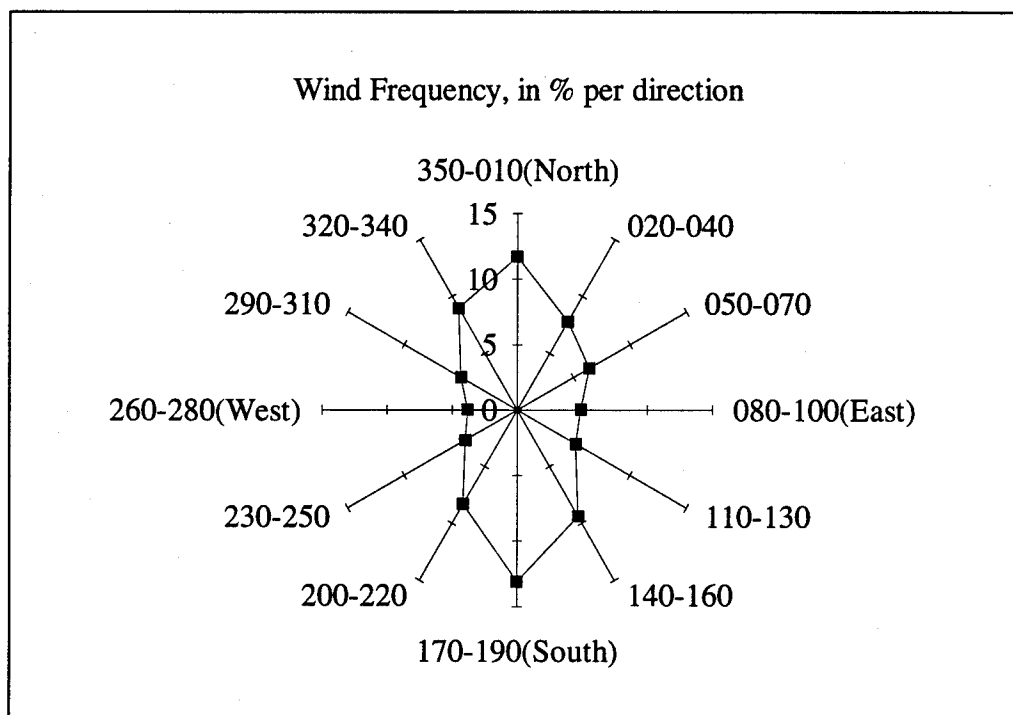
Figure A.1 Wind Frequency (% per direction)

The wind data tends to support a distribution pattern which would be elongated in the north-south direction. The mean wind speed from any given direction ranges from 5.2 to 8.7 knots. In addition to the winds being recorded as calm 11% of the time they were less than 5 knots 45% of the time, less than 10 knots 85%, and less than 15 knots 98.5% of the time (Figure A.2).

Mean Wind Speed (kts)

350-010(North)

320-340   10   020-040

290-310   5   050-070

260-280(West)   0   080-100(East)

230-250   110-130

200-220   140-160

170-190(South)
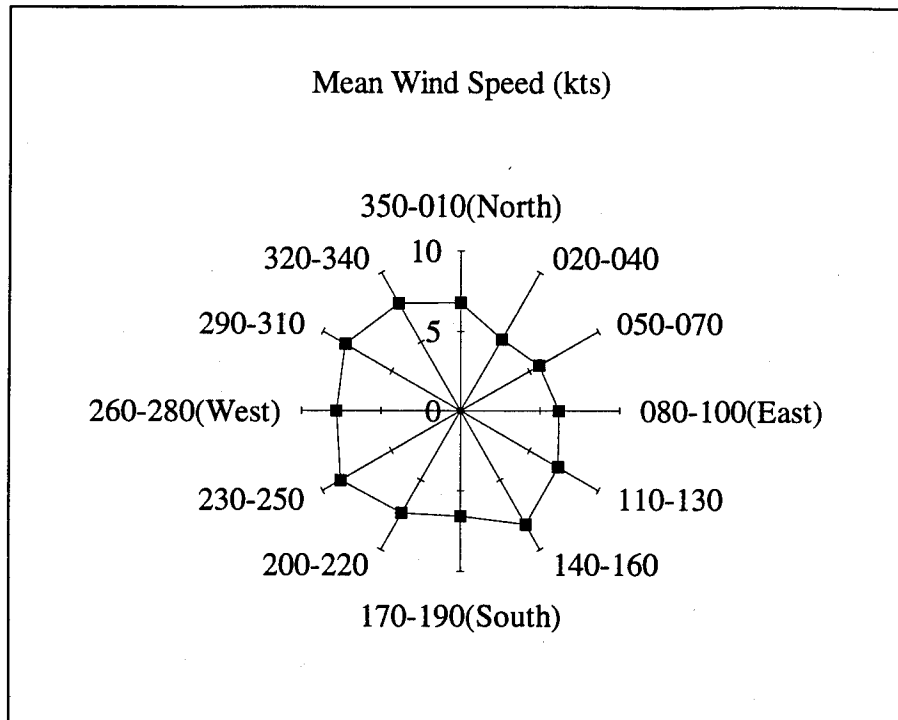
Figure A.2 Mean Wind Speed (kts)

The kriging analysis indicated that most of the contamination outside the RCA is

on the south side of the RCA. The target butt is located in the southwest corner of the

RCA. The wind data does not support the theory that wind is a primary factor in the

spread of contamination , but no firm conclusions can be drawn.

Appendix B.   Groundwater Appendix

B.1   Hydrogeologic Characterization of the Environment at TA C-64

Geology.   The Eglin AFB geologic setting is one of Holocene to Eocene age (present time to 36 million years ago (Ma)) coastal plain sediments (8:5; 12:2). These sediments consist mainly of sand, clay, limestone, and dolomite and range in thickness from 1500 ft in the northeast of Eglin AFB to greater than 2500 ft in the southwest of Eglin AFB. Below the coastal plain sediments is a thick sequence of limestones, dolostones, and shales.

Beneath the topsoil lies the sand-and-gravel aquifer made up of Holocene to Pliocene sands and Citronelle formation. Below the sand-and-gravel aquifer is the Pensacola confining bed made up of Miocene series soils which are Miocene coarse clastics, intracoastal formations, the Alum Bluff Group and Pensacola Clay.

The Pensacola confining bed separates the sand-and-gravel aquifer from the next aquifer, the Upper Floridan aquifer which consists of Chickasawhay and Tampa Limestone, also of the Miocene series. The lowest aquifer, the Lower Floridan aquifer, is made up of Ocala limestone of the Eocene series and is separated from the Upper Floridan aquifer by the Bucatunna Clay confining bed. The Bucatunna confining bed consists of Bucatunna formations of medium brown to dusky yellowish brown calcareous clay of the Oligocene series.

Finally the Lisbon and Tallahatta Formation, also of the Eocene series, forms the lowest confining unit, the Lisbon-Tallahatta confining unit. Table B.1 lists the geologic

units in order of age and provides their thickness, lithologic description, and respective hydrogeologic unit names (9). In addition, Figure B.1 shows the relationship of these hydrogeologic units in a cross section taken from the location shown in Figure B.2 on Eglin AFB.

Soil. From Becker et. al., Figure B.3 shows the distribution of soil associations (similar soil characteristics and spatially related) over the Eglin Air Force Base area. The four soil types or associations are 1) Lakeland, 2) Norfolk-Shubuta, 3) Rutlege-Leon-Chipley-Foxworth, and 4) Kinston-Bibb-Dorovan-Pickney. Of the four soil types Lakeland and Kinston-Bibb-Dorovan-Pickney are found around TA C-64 and are described below (12:2, 7-8).

The lakeland series formed in thick beds of eolian (wind-blown) or marine sands. The soils are deep and very well drained with slopes of up to 30 percent possible, though the slopes range typically from 0 to 12 percent. The surface layer of the lakeland series consists of a 3 in. thick layer of very dark grayish brown sand, followed by yellowish brown sand from a depth of 3 to 64 in.., and then, from 64 in. in depth down to 90 in., a very pale brown sand. Reaction of the soil ranges from very strong acidity, pH 4.5, to medium acidity, pH 6.0.

The Kinston series were formed on the Coastal Plain floodplains, are very poorly drained, and have slopes ranging from 0 to 2 percent. The surface layer is 0 to 5 in. thick of dark gray loam, followed by a 5 to 60 in. of gray loam to gray clay loam, and finally,

Formation or Group	Thickness (ft)	Lithology	Hydrogeologic Unit
Holocene to Pliocene Series			
Unnamed Holocene to Pliocene Sands	50-250	Unconsolidated, white to light gray, fine to medium quartz sand.	Sand and Gravel aquifer
Citronelle Formation		Predominantly nonmarine quartz sands with thin stringers of clay or gravel discontinuous over short distances.	
Miocene Series			
Miocene Coarse Clastics	50-200	Poorly consolidated sand, silt, clay, and shell.	
Intracoastal Formation	0-360	Upper and lower carbonate layers of poorly consolidated, sandy, clayey, microfossiliferous limestone. The layers are separated by a phosphatic sand.	Pensacola confining bed
Alum Bluff Group	0-300	Mix of sand, clay, and shell in relatively well-sorted thin beds, cemented by clay or carbonate.	
Pensacola Clay	0-190	Bluish gray to olive gray, dense, silty clay.	
Bruce Creek Limestone	20-220	Light gray to white, granular clastic limestone	
Tampa Limestone Equivalent and Chickasawhay	30-260	Both primarily a tan, sugary dolomite but can also occur as a cream to buff fossiliferous limestone. The tampa has slightly less dolomite, and silt and clay content increase towards the top.	Upper limestone of the Floridan aquifer
Oligocene Series			
Bucatunna Formation	0-130	Medium brown to dusky yellowish brown calcareous clay.	Bucatunna Clay confining bed
Eocene Series			
Ocala Limestone	165-600	White to light gray, chalky, fossiliferous limestone. May be interlayered with thin streaks of tan dolomite.	Lower limestone of the Floridan aquifer
Lisbon and Tallahatta Formation	345-500, 170-300	Massive shaly to chalky limestones. Color ranges from dark gray to brownish gray to cream. Abundant foraminifera are present.	Lisbon-Tallahatta confining unit

Table B.1 Geologic Units, Lithology, and Hydrogeologic Units in Okaloosa and Walton Counties, Florida (12:4).
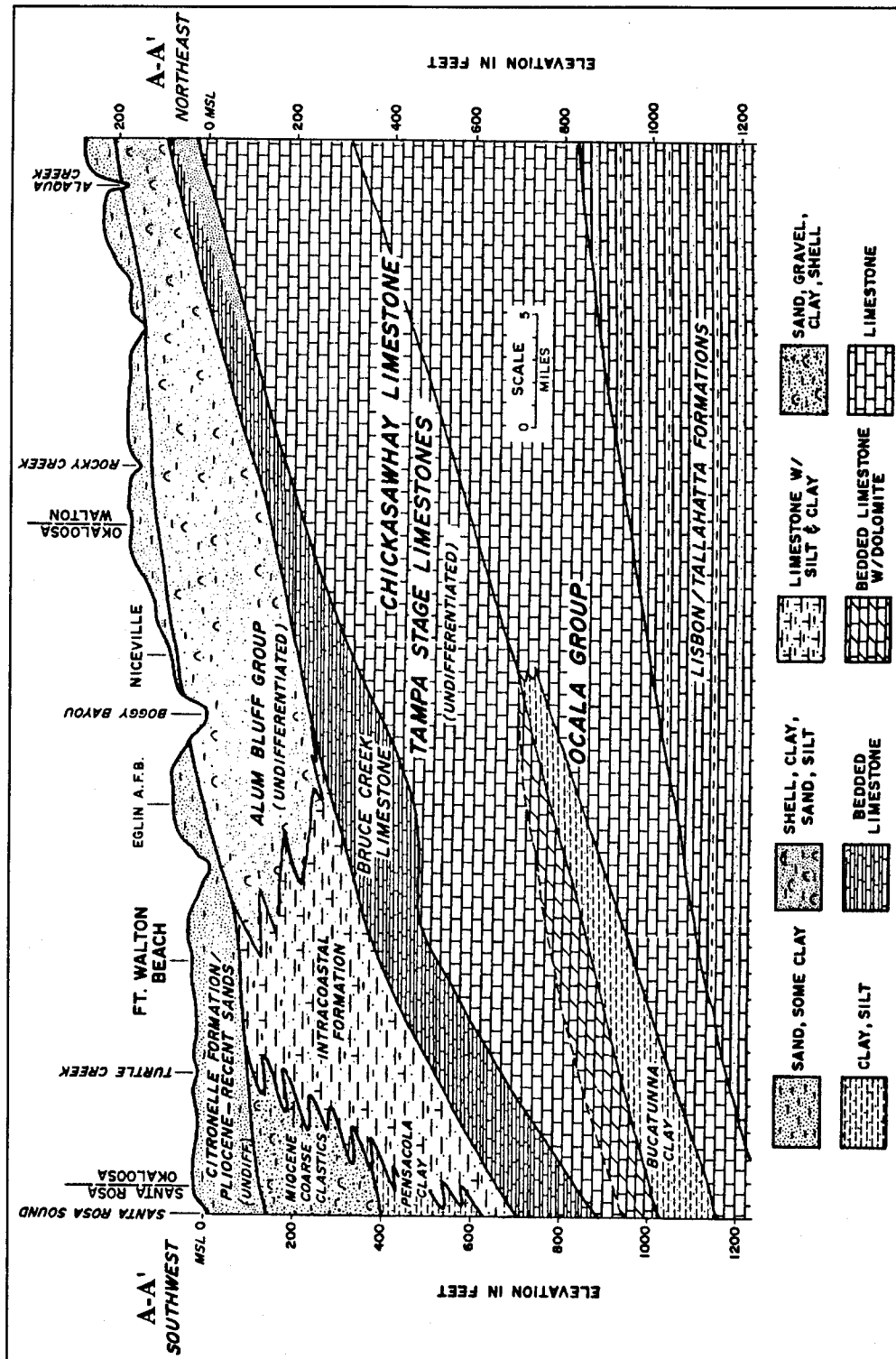
Figure B.1 "Geologic Cross Section" (9)

B-4
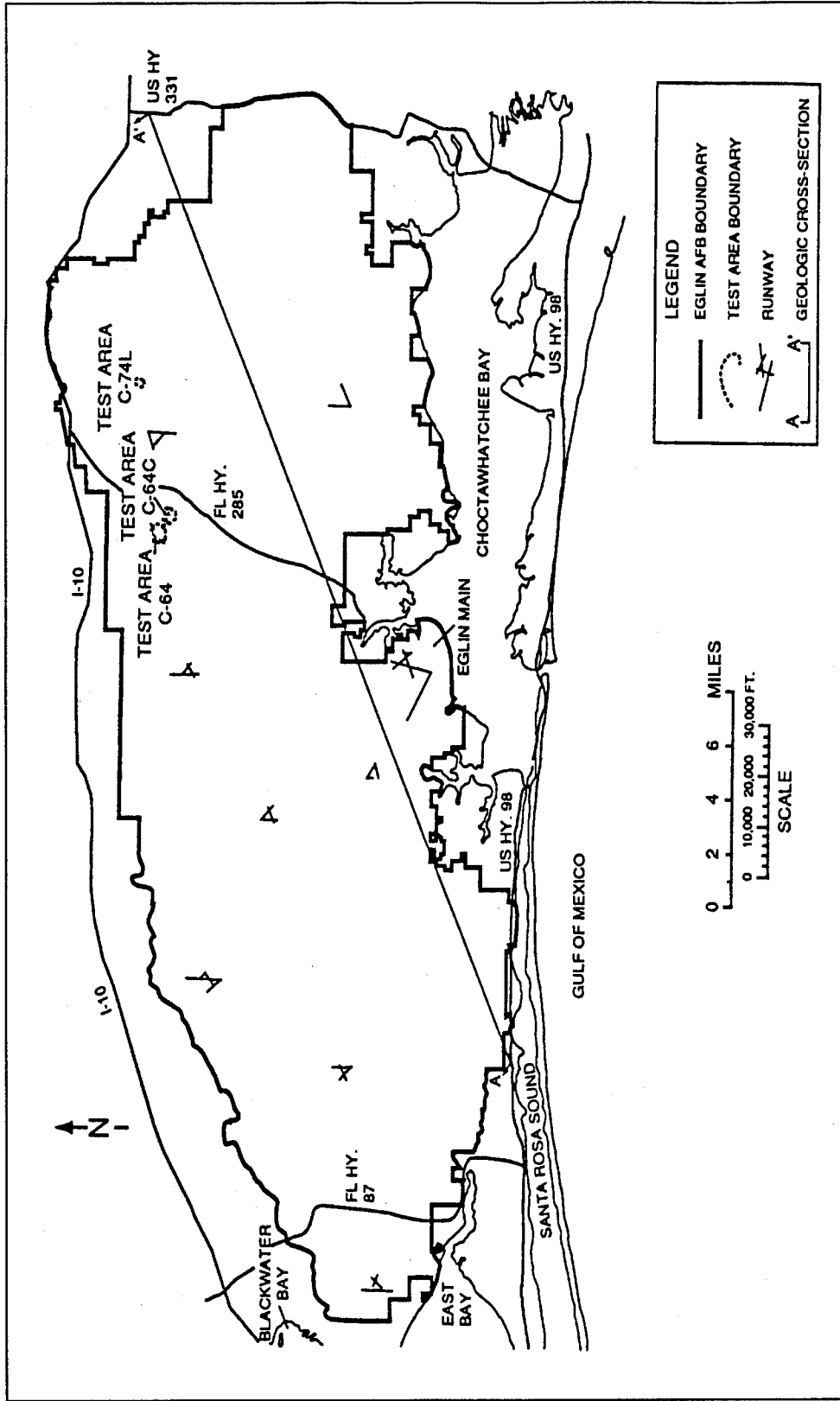
Figure B.2 "General Location Map of Eglin AFB" (9)

60 to 72 in. of gray gravely loamy sand. Reaction of the soils range from strongly acid, pH 4.5, to very strongly acid, pH 5.5.

The Bibb series formed in the Coastal Plain floodplains on alluvial deposits of streams. The series is poorly drained, have slow run off, and are often flooded with slopes ranging from 0 to 2 percent. The surface layer consists of from 0 to 4 in. of brown sandy loam, mottled dark gray and dark grayish brown sandy loam from 4 to 12 in., gray sandy loam with strong brown mottles and thin lines of silt loam to loamy sand from 12 to 37 in., and finally, gray silt loam layered with sandy loam and loamy sand from 37 to 60 in. The soil ranges from very strong acidity, pH 4.5, to strong acidity, pH 5.5.

The Dorovan series is found on hardwood swamps, floodplains, and depressions in the East Gulf Coast flatwoods, Atlantic coast flatwoods, and Southern Coastal Plain areas and was formed in black, highly decomposed acid-organic materials. The soil is very poorly drained and saturated to the surface, with depressions usually ponded with water. Slopes range from 0 to 2 percent. The soil consists of a top layer from 0 to 75 in. of decomposed organic matter, followed by dark grayish brown sand to 80 in. or more. Reaction of the soil ranges from very strong acidity, pH 4.5, to strong acidity, pH 5.5.

The Pickney series is found in depressions and drainageways of the Coastal Plains and is very poorly drained with a water table depth of usually less than 10 in. and slopes less than 2 percent. The surface soil layer consists of black, loamy fine sand from 0 to 34 in., followed by an underlying soil layer from 34 to 80 in. of dark gray fine sand. The soil ranges from extreme to strong acidity in the surface layer, pH less than 4.5 to 5.5, and very strong to medium acidity, pH ranging from 4.5 to 6.0, in the underlying soil layer.

Surface Water.   The Yellow, Shoal, and East Bay Rivers and Live Oak, Turtle, Lightwood Knot, Garnier, Roague, Turkey, Juniper, Tenmile, Tom's Swift, Rocky, Titi, Long Basin, Alaqua and Lafayette Creeks are the major streams on Eglin AFB (19:29; 12:8) (see Figure B.4). The westerly flowing rivers are the Yellow River, Shoal River, and Titi Creek which empty into the Blackwater Bay. The southward flowing streams are Live Oak Creek and Turtle Creek, which flow south into East Bay River, which in turn flows into the East Bay. All other streams flow south into the Choctawhatchee Bay.

Barr and others (8) studied the flow of Turkey Creek, Figure B.5 shows the maximum, minimum, and mean monthly discharge near Niceville, Florida. The location of the gauging station near the government railroad is shown on Figure B.4.

The mean monthly flow varied little throughout the year and was fairly representative of other streams in the study area. Little variation in the mean monthly flow, as indicated by Barr, shows a close interaction between the surface steams and groundwater. During excess rainfall the streams recharged the groundwater system and during droughts the groundwater fed the streams, keeping the stream discharge relatively steady throughout the year. Base flow of sustained runoff of Turtle Creek was also studied by Barr and others (8). During the 1978 and 1979 years, 92 to 98 percent of the total flow of the stream was due to groundwater discharge. This supports Barr's assumption of close surface and groundwater interaction.
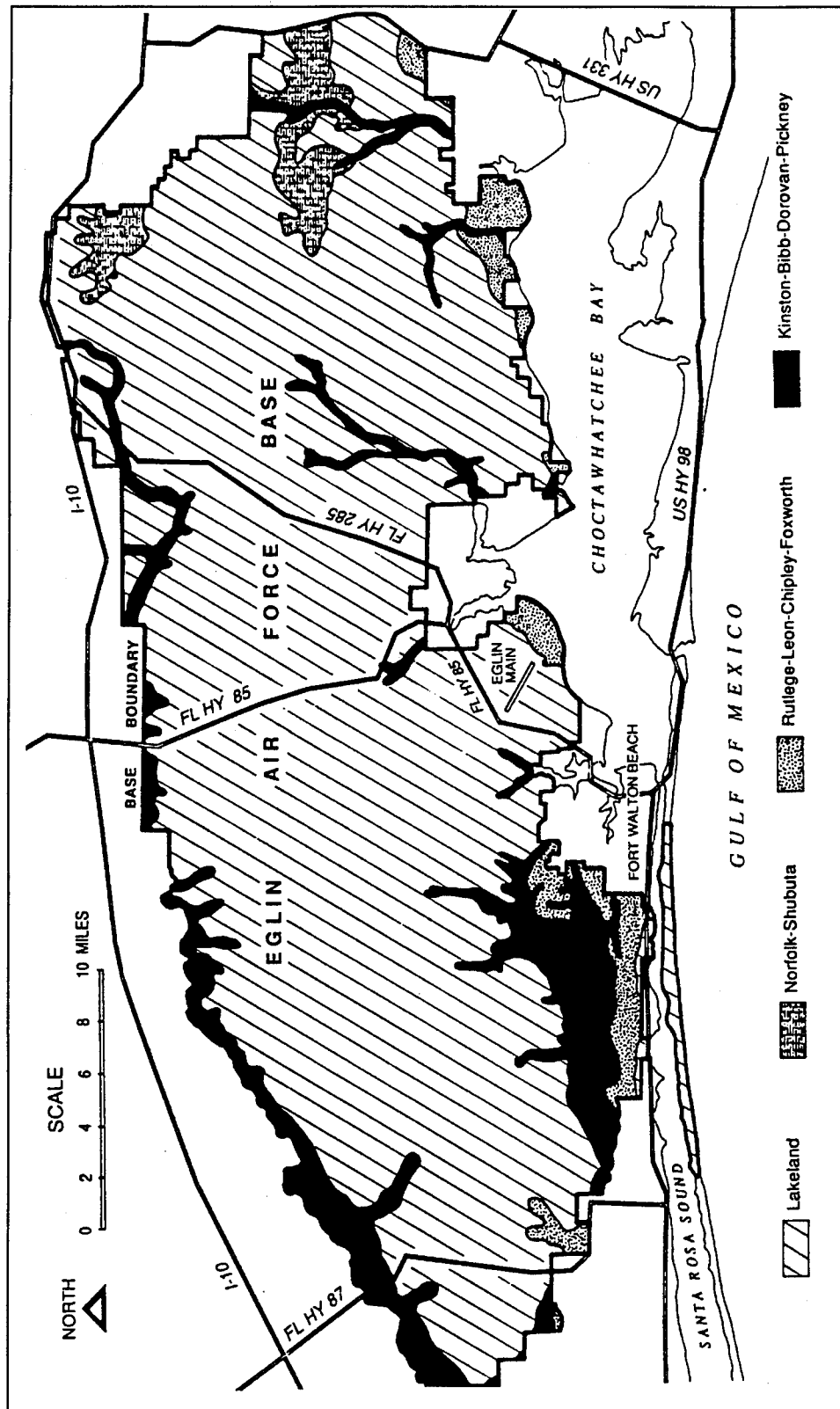
Figure B.3 "Soil Maps of Eglin AFB" (12:6)

Figure B.4 "Location Map of Rivers, Creeks, and Wells" (12:9)

B-9
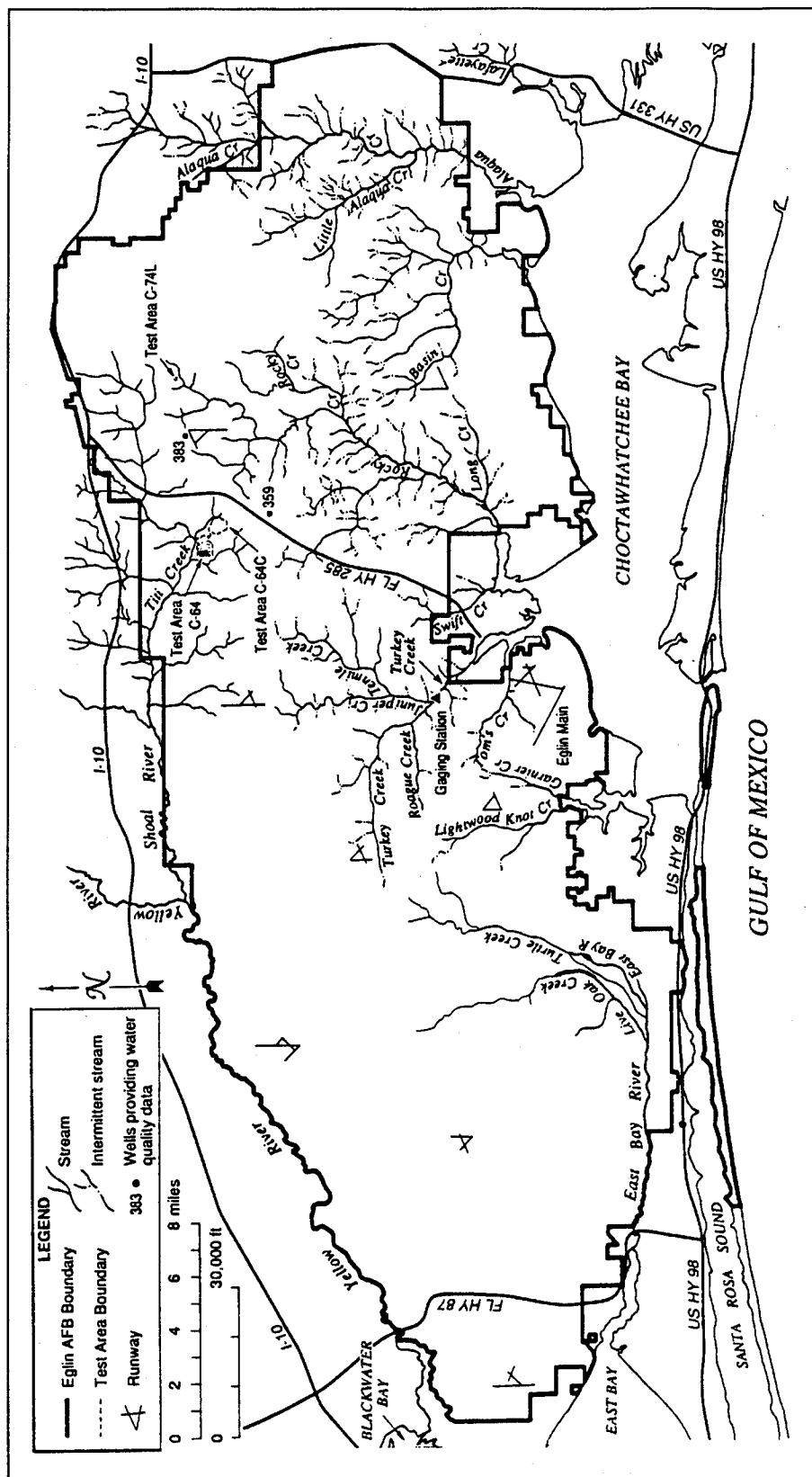
In addition, Barr and others measured the water quality of streams on Eglin AFB. The pH of these streams averaged 5.5 and varied from a low of 4.2 to a high of 7.4. The water was very soft with an average of 0.16 mg/L of iron present. Water temperatures averaged about 67°F with a low of 45°F and a high of 82°F. Trapp and others (69) measured the water quality in the streams around Eglin AFB and Table 3.2 shows a list of selected constituents.

Although surface water at Eglin AFB is not a source of potable water, it is used for lawn irrigation at the golf courses on the reservation.

Rainfall and Temperature. As reported by Barr and others (8) the annual rainfall since 1941 has ranged from a low of 31.01 in. in 1954 to a high of 95.43 in. in 1975 (Figure B.7) with an average annual rainfall at the National Weather Service Station at Niceville, Florida of 64.1 inches. July and August are the wettest months, with 8.70 and 7.26 in., respectively (Figure B.6) with July having a maximum and minimum rainfall of 2.5 to 23.2 inches, respectively. October is the driest month, with an average rainfall of 2.62 inches and a minimum and maximum of 0 and 14.47 inches, respectively. Winter month average temperature is 50°F with a low of 18°F to a high of 74°F possible between December and February. Summer month average temperature for July and August is 82°F with a low of 70°F to a high of 88°F.

Thunderstorms and frontal-type weather systems both provide rainfall over the study area. A thunderstorm (convective storm) is produced when warm, moist air rises high over colder, denser surroundings and then cools, releasing its condensed moisture.

Constituent	Range
Discharge (cfs)	14 - 246
Specific conductance (μmho/cm^2 at 25°C)	10 - 90
pH (pH units)	5.6 - 6.4
Temperature ($^{\circ}$C)	17 - 23
Iron (μg/L)	10 - 50
Alkalinity as $CaCO_3$	0 - 34
Bicarbonate	0 - 41
Calcium	0.1 - 12
Chloride	2.2 -3.8
Fluoride	0 - 0.1
Total hardness	1 - 38
Magnesium	0.2 - 2.0
Nitrate as NO_3	0.1 - 1.3
Phosphate	0.03 - 0.13
Potassium	0.1 - 0.4
Total dissolved solids	8 - 52
Silica	3.6 -5.7
Sodium	1.0 - 2.5
Sulfate	0.0 - 4.8
Dissolved oxygen	6.6 - 8.7

Table B.2 Range in major inorganic chemical constituents in streams and creeks at Eglin AFB (mg/L unless noted) (69).
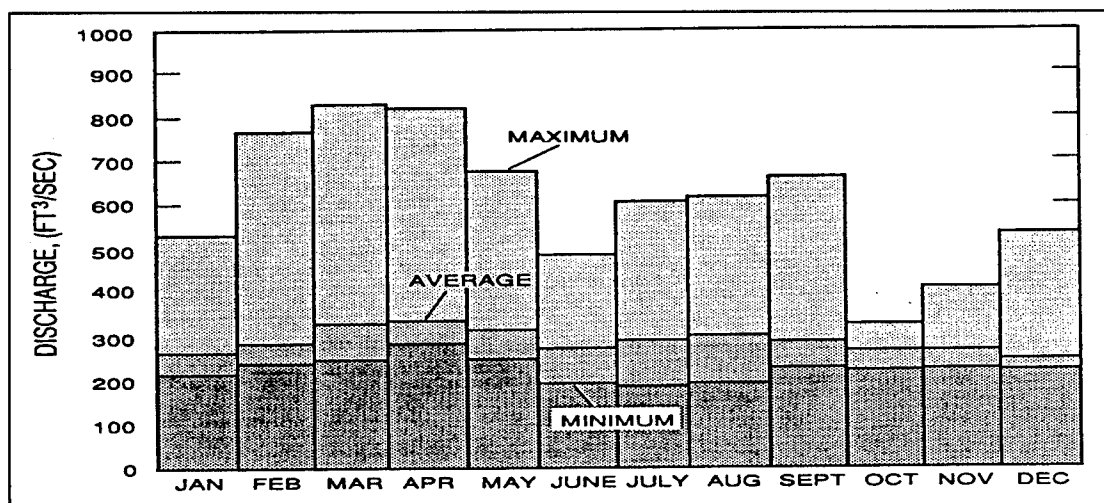
Figure B.5 "Average Monthly Streamflow at Turkey Creek near Niceville, Florida" (12:10)
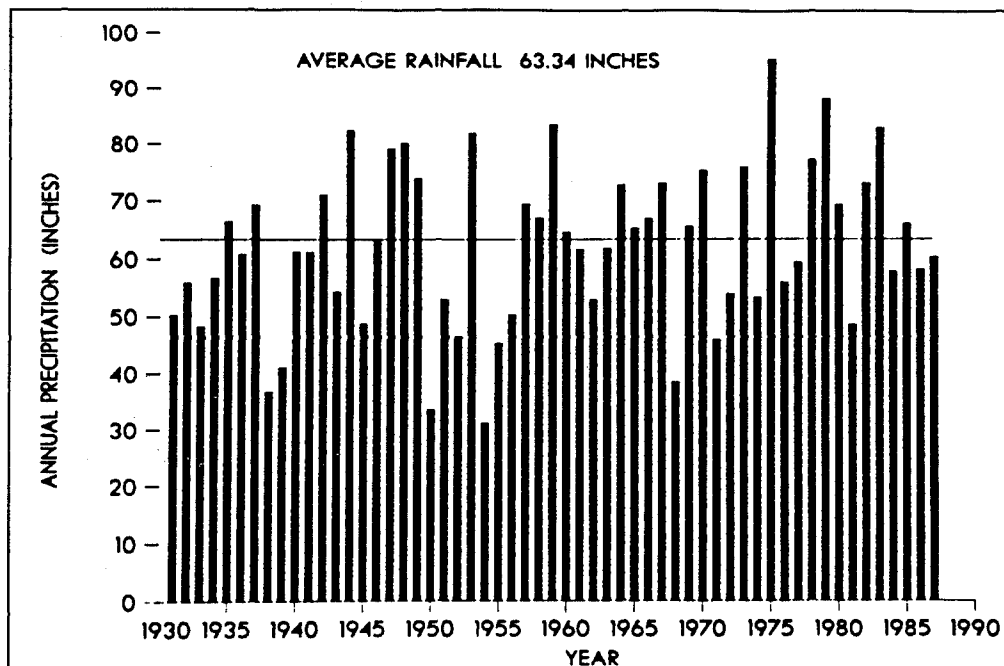
Figure B.7 "Annual Rainfall at Niceville, Florida (records for some years are incomplete)" (12:14)
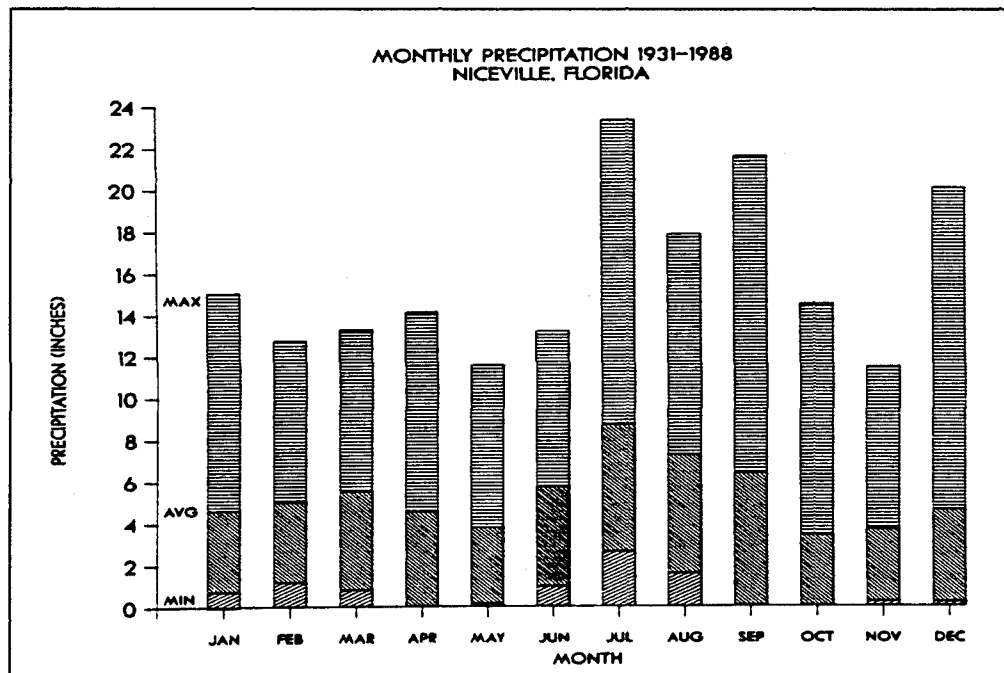
Figure B.6 "Average, Minimum, and Maximum Monthly rainfall at Niceville, Florida" (12:15)

Thunderstorms usually are of short duration and can be quite strong. They occur mainly during the summer months from June through September during late afternoon or early evening.

Frontal storm systems are a result of converging polar and tropical air masses (low and high pressure systems) and usually occur during the winter months. Frontal storms produce showers of lower intensity and longer duration than convective storms and cover a large geographic area.

Tropical storms and hurricanes can drop heavy rain and occur during the months of June through November. During the September (when more then half of the storms occur) hurricanes of 1906, 1950, and 1953, 12 inches of rain fell in the Choctawhatchee Bay area.

B.2   Available Well Data near TA C-64

Well data required for calibration of the groundwater flow analysis presented in Appendix B.4 is obtained from six monitoring wells located in TA C-64C. This TA's well sites are shown in Figure B.8. Table B.3 presents the well (slotting) depth data and the water level below ground surface for the respective wells (12:32, 33-35). The average surface elevation at TA C-64C is 227 ft.

Monitoring Well Number	Slotting Depth From Surface (ft)	Water Level Below Ground Surface (ft)
1	100 - 110	92.3
2	100 - 110	99.5
3	110 - 120	96.2
4	58 - 68.5	56.8
5	90 - 100	75.4
6	90 - 100	80.7

Table B.3 Test Area C-64C monitoring well head data

Table B.3 indicates that the water level is on average 83.5 feet below the ground at TA C-64C. However, from Table B.3, one can notice that well four is located in a gully below the average surface elevation of 227 ft. If we neglect its water level measurement of 56.8 ft below the gully surface, then the water level is on average 88.8 feet below the surface.
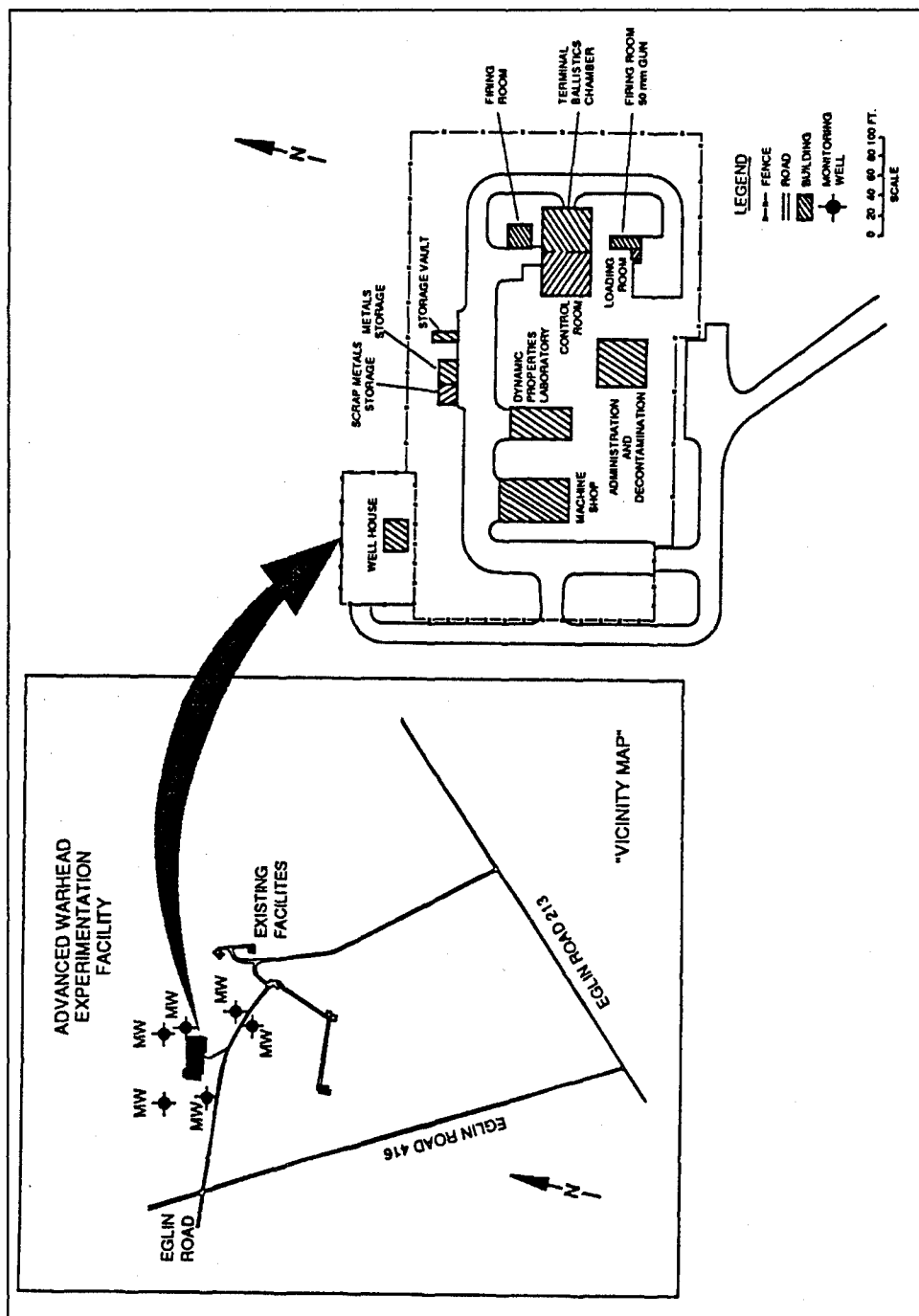
Figure B.8 "Location of Monitoring Wells at test area C-64C-AWEF" (12:32)

B.3 Systems Engineering Process for Groundwater Flow Characterization of TA C-64

The systems engineering process presented in section 4.2 of the main body is continued for the groundwater flow characterization area of concern. These three areas of concern as outlined in section 4.2 are: the leakage between the sand-and-gravel and Upper Floridan aquifers; the horizontal groundwater flow in the sand-and-gravel aquifer beneath TA C-64 and vicinity; and the modeling of the unsaturated region of the sand-and-gravel aquifer. The first four steps of the systems process with respect to the latter three areas of concern are presented in section 4.2. So in this Appendix section, we evaluated alternatives and ended with planning for implementation for these three areas of concern.

Evaluating Alternatives. The presentation in this section is based on the system's utility function Table 4.4. For the first case, leakage between the sand-and-gravel and Upper Floridan aquifers, six possible alternatives were capable of providing information regarding groundwater flow. Of the six alternatives, one is an analytical solution using a coefficient of leakage and the leakage Equation B.1. The other five alternatives are computer models based on finite difference or finite element numerical techniques to solve groundwater flow differential equations. The five models are SWIFT III®, Geoflow®, SWENT®, PTC®, and MODFLOW®.

The rating of each alternative with respect to the value system is shown in Table B.4.

Objective Criteria	Analytical	SWIFT III®	Geoflow®	SWENT®	PTC®	MODFLOW®
Least Effort:						
Training Time	10	2	3	3	3	6
Model Simplicity	10	2	5	4	5	6
Flexibility	7	10	7	3	7	7
Execution Time	10	7	7	7	7	8
Least Money:						
Product Cost	10	6	6	6	6	6
Training Cost	10	6	6	6	6	6
Best Availability:	10	4	4	4	4	10

Table B.4 Leakage Between the Sand-and-Gravel Aquifer: Alternatives Rating using Objective Criteria

For the second case, unconfined sand-and-gravel aquifer horizontal groundwater flow, five alternatives were evaluated. Of the five alternatives, one is an analytical solution and the other four alternatives are computer models based on finite difference or finite element numerical techniques to solve groundwater flow differential equations. The four models are SWIFT III®, Geoflow®, PTC®, and MODFLOW®.

The rating of each alternative with respect to the value system is shown in Table B.5.

Objective Criteria	Analytical	SWIFT III®	Geoflow®	PTC®	MODFLOW®
Least Effort:					
Training Time	10	2	3	3	6
Model Simplicity	4	2	5	5	8
Flexibility	5	10	7	7	7
Execution Time	1	7	7	7	8
Least Money:					
Product Cost	10	6	6	6	6
Training Cost	10	6	6	6	6
Best Availability:	10	4	4	4	10

Table B.5 Unconfined Sand-and-Gravel Aquifer Horizontal Groundwater Flow: Alternatives Rating using Objective Criteria

Finally, for the third case, unsaturated groundwater flow, four alternatives were evaluated. Of the four alternatives, one is an analytical solution and the other three are computer models based on finite difference or finite element numerical techniques to solve unsaturated groundwater flow. The three models are SWIFT III®, SWENT®, and Infil®.

The rating of each alternative with respect to the value system is shown in Table B.6.

Objective Criteria	Analytical	SWIFT III®	SWENT®	Infil®
Least Effort:				
Training Time	7	2	3	7
Model Simplicity	5	2	4	6
Flexibility	7	8	3	7
Execution Time	1	7	7	10
Least Money:				
Product Cost	10	6	6	10
Training Cost	10	6	6	10
Best Availability:	10	4	4	10

Table B.6 Unsaturated Groundwater Flow: Alternatives Rating using Objective Criteria

Selecting an Alternative.   For the first area of concern, groundwater leakage between two aquifers, the value system confidence levels are shown in Table B.7. For the second area of concern, sand-and-gravel aquifer horizontal groundwater flow, the value system confidence levels are shown in Table B.8. For the third area of concern, unsaturated groundwater flow, the value system confidence levels are shown in Table B.9. The confidence levels in these tables are: VC (very confident), C (confident), and LC (low confidence). The numeric value assigned for these confidence levels are: VC (0.9), C (0.6), and LC (0.3).

Objective Sub-criteria	Alternative	Confidence Level	Support
Training Time	Analytical	VC	Data Available
	SWIFT III®	C	Estimation
	Geoflow®	C	Estimation
	SWENT®	C	Estimation
	PTC®	C	Estimation
	MODFLOW®	VC	Data Available
Model Simplicity	Analytical	VC	Data Available
	SWIFT III®	C	Estimation
	Geoflow®	C	Estimation
	SWENT®	C	Estimation
	PTC®	C	Estimation
	MODFLOW®	VC	Data Available
Flexibility	Analytical	VC	Data Available
	SWIFT III®	C	Estimation
	Geoflow®	C	Estimation
	SWENT®	C	Estimation
	PTC®	C	Estimation
	MODFLOW®	VC	Data Available
Execution Time	Analytical	VC	Data Available
	SWIFT III®	LC	Estimation
	Geoflow®	LC	Estimation
	SWENT®	LC	Estimation
	PTC®	LC	Estimation
	MODFLOW®	VC	Data Available
Product Cost	Analytical	VC	Data Available
	SWIFT III®	VC	Estimation
	Geoflow®	LC	Estimation
	SWENT®	LC	Estimation
	PTC®	LC	Estimation
	MODFLOW®	VC	Data Available
Training Cost	Analytical	VC	Data Available
	SWIFT III®	LC	Estimation
	Geoflow®	LC	Estimation
	SWENT®	LC	Estimation
	PTC®	LC	Estimation
	MODFLOW®	VC	Data Available
Availability	Analytical	VC	Data Available
	SWIFT III®	C	Estimation
	Geoflow®	C	Estimation
	SWENT®	C	Estimation
	PTC®	C	Estimation
	MODFLOW®	VC	Data Available

Table B.7 Leakage Between the Sand-and-Gravel Aquifer: Alternatives Confidence Levels

Objective Sub-criteria	Alternative	Confidence Level	Support
Training Time	Analytical	VC	Data Available
	SWIFT III®	C	Estimation
	Geoflow®	C	Estimation
	PTC®	C	Estimation
	MODFLOW®	VC	Data Available
Model Simplicity	Analytical	VC	Data Available
	SWIFT III®	C	Estimation
	Geoflow®	C	Estimation
	PTC®	C	Estimation
	MODFLOW®	VC	Data Available
Flexibility	Analytical	VC	Data Available
	SWIFT III®	C	Estimation
	Geoflow®	C	Estimation
	PTC®	C	Estimation
	MODFLOW®	VC	Data Available
Execution Time	Analytical	C	Estimation
	SWIFT III®	LC	Estimation
	Geoflow®	LC	Estimation
	PTC®	LC	Estimation
	MODFLOW®	VC	Data Available
Product Cost	Analytical	VC	Data Available
	SWIFT III®	VC	Data Available
	Geoflow®	LC	Estimation
	PTC®	LC	Estimation
	MODFLOW®	VC	Data Available
Training Cost	Analytical	VC	Data Available
	SWIFT III®	LC	Estimation
	Geoflow®	LC	Estimation
	PTC®	LC	Estimation
	MODFLOW®	VC	Data Available
Availability	Analytical	VC	Data Available
	SWIFT III®	C	Estimation
	Geoflow®	C	Estimation
	PTC®	C	Estimation
	MODFLOW®	VC	Data Available

Table B.8 Unconfined Sand-and-Gravel Aquifer Horizontal Groundwater
Flow: Alternatives Confidence Levels

Objective Sub-criteria	Alternative	Confidence Level	Support
Training Time	Analytical	VC	Data Available
	SWIFT III®	C	Estimation
	SWENT®	C	Estimation
	Infil®	VC	Data Available
Model Simplicity	Analytical	VC	Data Available
	SWIFT III®	C	Estimation
	SWENT®	C	Estimation
	Infil®	VC	Data Available
Flexibility	Analytical	VC	Data Available
	SWIFT III®	C	Estimation
	SWENT®	C	Estimation
	Infil®	VC	Data Available
Execution Time	Analytical	C	Estimation
	SWIFT III®	LC	Estimation
	SWENT®	LC	Estimation
	Infil®	VC	Data Available
Product Cost	Analytical	VC	Data Available
	SWIFT III®	VC	Data Available
	SWENT®	LC	Estimation
	Infil®	VC	Data Available
Training Cost	Analytical	VC	Data Available
	SWIFT III®	LC	Estimation
	SWENT®	LC	Estimation
	Infil®	C	Data Available
Availability	Analytical	VC	Data Available
	SWIFT III®	C	Estimation
	SWENT®	C	Estimation
	Infil®	VC	Data Available

Table B.9 Unsaturated Groundwater Flow: Alternatives Confidence Levels

The use of a criteria preference chart (section 4.2), system utility function chart
(section 4.2), and confidence levels for each alternative, under each area of concern,
allows the results to be summarized in an evaluation matrix chart for use as a decision
making tool in deciding how to best provide information regarding groundwater flow

around TA C-64. For each area, the evaluation matrices are shown on the following pages (Tables B.10, B.11 and B.12).

Based on the systems engineering process and the evaluation matrices for each of the four areas of concerns, the best means to properly characterize the groundwater flow under TA C-64 are to use the analytical groundwater leakage equation, MODFLOW, and Infil. The following paragraphs will outline the reasons for each alternative selection as the method of choice for the information required.

For the leakage of groundwater between the sand-and-gravel and Upper Floridan aquifers, the analytical method using the leakage Equation B.1 had the highest discounted value, 140, and the highest confidence, 0.90 in the evaluation matrix, Table B.10. In addition, U.S. Geological Survey data provides information on the coefficient of leakage, C. For the level of data available for this problem, the analytical solution provides an appropriate level of information for the overall groundwater system.

To characterize the sand-and-gravel aquifer and understand the general directions and velocities of water flow around TA C-64, the horizontal flow of the sand-and-gravel aquifer needs to be modeled. Based on the evaluation matrix, Table B.11, the analytical solution (Darcy's Law explained in Appendix B.5) and MODFLOW tied in total value but, with a better confidence in MODFLOW, the discounted value was slightly in MODFLOW's favor. MODFLOW also allows easier manipulation of data and visualization tools to provide a better view of the groundwater flow. It is important to note however, that the outputs of MODFLOW (and an analytical solution as well), only reflect the inputs and preconception of the groundwater flow. Using the level of data

currently available at TA C-64 without additional soil test, drawdown tests, etc., the output of MODFLOW will only give us a general idea of the groundwater flow and not necessarily a very accurate model of the flow.

Finally, for unsaturated groundwater flow, Infil had the highest total value, discounted value, and confidence as compared to the other competing alternatives. Infil will be used to get a very general idea of the amount of time it takes surface water to seep down into the sand-and-gravel aquifer and is not expected to provide a very accurate answer based on data available.

It is apparent from the above paragraphs that the selection of models for all areas is driven by a lack of data, as much as, accuracy of output and that the answers provided by these models represent generalities and not necessarily an exact description of the groundwater flow around TA C-64.

Criteria	Analytical R	C	U	D	SWIFT III® R	C	U	D	Geoflow® R	C	U	D	SWENT® R	C	U	D	PTC® R	C	U	D	MODFLOW® R	C	U	D
Very Important (wt=5)																								
Availability	10	VC	50	45	4	C	20	12	4	C	20	12	4	C	20	12	4	C	20	12	10	VC	50	45
Important (wt=3)																								
Model Simplicity	10	VC	30	27	2	C	6	3.6	5	C	15	9	4	C	12	7.2	5	C	15	9	6	VC	18	16
Product Cost	10	VC	30	27	6	VC	18	16	6	LC	18	5.4	6	LC	18	5.4	6	LC	18	5.4	6	VC	18	16
Moderate Importance (wt=1.5)																								
Flexibility	7	VC	11	9.5	10	C	15	9	7	C	11	6.3	3	C	4.5	2.7	7	C	11	6.3	7	VC	11	9.5
Training cost	10	VC	15	14	6	LC	9	2.7	6	LC	9	2.7	6	LC	9	2.7	6	LC	9	2.7	6	VC	9	8.1
Minor Importance (wt=1)																								
Training Time	10	VC	10	9	2	C	2	1.2	3	C	3	1.8	3	C	3	1.8	3	C	3	1.8	6	VC	6	5.4
Execution Time	10	VC	10	9	7	LC	7	2.1	7	LC	7	2.1	7	LC	7	2.1	7	LC	7	2.1	8	VC	8	7.2
Total Value			156				77				83				74				83				120	
Discounted Value				140				47				39				34				39				108
Confidence		0.90				0.61				0.48				0.46				0.48				0.90		

R=Relative Rating
C=Confidence
U=System Utility
D=Discounted Utility

VC: 0.9
C: 0.6
LC: 0.3
NC: 0.1

Table B.10 Evaluation Matrix for Groundwater Leakage Between Aquifers

Criteria	Analytical R	C	U	D	SWIFT III® R	C	U	D	Geoflow® R	C	U	D	PTC® R	C	U	D	MODFLOW® R	C	U	D
Very Important (wt=5)																				
Availability	10	VC	50	45	4	C	20	12	4	C	20	12	4	C	20	12	10	VC	50	45
Important (wt=3)																				
Model Simplicity	4	VC	12	11	2	C	6	3.6	5	C	15	9	5	C	15	9	8	VC	24	22
Product Cost	10	VC	30	27	6	VC	18	16	6	LC	18	5.4	6	LC	18	5.4	6	VC	18	16
Moderate Importance (wt=1.5)																				
Flexibility	5	VC	7.5	6.8	10	C	15	9	7	C	11	6.3	7	C	11	6.3	7	VC	11	9.5
Training cost	10	VC	15	14	6	LC	9	2.7	6	LC	9	2.7	6	LC	9	2.7	6	VC	9	8.1
Minor Importance (wt=1)																				
Training Time	10	VC	10	9	2	C	2	1.2	3	C	3	1.8	3	C	3	1.8	6	VC	6	5.4
Execution Time	1	C	1	0.6	7	LC	7	2.1	7	LC	7	2.1	7	LC	7	2.1	8	VC	8	7.2
Total Value			126				77				83				83				126	
Discounted Value				113				47				39				39				113
Confidence		0.90				0.61				0.48				0.48				0.90		

R=Relative Rating
C=Confidence
U=System Utility
D=Discounted Utility

VC: 0.9
C: 0.6
LC: 0.3
NC: 0.1

Table B.11 Evaluation Matrix for Sand-and-Gravel Aquifer Groundwater Flow

Criteria	Analytical				SWIFT III®				SWENT®				Infil®			
	R	C	U	D	R	C	U	D	R	C	U	D	R	C	U	D
Very Important (wt=5)																
Availability	10	VC	50	45	4	C	20	12	4	C	20	12	10	VC	50	45
Important (wt=3)																
Model Simplicity	5	VC	15	14	2	C	6	3.6	4	C	12	7.2	6	VC	18	16
Product Cost	10	VC	30	27	6	VC	18	16	6	LC	18	5.4	10	VC	30	27
Moderate Importance (wt=1.5)																
Flexibility	7	VC	11	9.5	8	C	12	7.2	3	C	4.5	2.7	7	VC	11	9.5
Training cost	10	VC	15	14	6	LC	9	2.7	6	LC	9	2.7	10	VC	15	14
Minor Importance (wt=1)																
Training Time	7	VC	7	6.3	2	C	2	1.2	3	C	3	1.8	7	VC	7	6.3
Execution Time	1	C	1	0.6	7	LC	7	2.1	7	LC	7	2.1	10	VC	10	9
Total Value			129				74				74				141	
Discounted Value				115				45				34				126
Confidence		0.90				0.61				0.46				0.90		

VC: 0.9
C: 0.6
LC: 0.3
NC: 0.1

R=Relative Rating
C=Confidence
U=System Utility
D=Discounted Utility

Table B.12 Evaluation Matrix for Unsaturated Groundwater Flow

B-26

B.4 Planning for Implementation: Groundwater Characterization

Groundwater Leakage. Groundwater leakage from the sand-and-gravel aquifer to the Upper Floridan aquifer was found by using the leakage equation (Equation B.1)

$$q_v = \frac{1}{C}\Delta h \qquad (B.1)$$

where q_v is the vertical leakage rates, C is the coefficient of leakage, and Δh is the vertical piezometric head difference between aquifers. The vertical velocity of the water flow was found by (Equation B.2)

$$v = \frac{q_v}{n} \qquad (B.2)$$

where n is the porosity of the confining layer (10:28). The coefficient of leakage provided by U.S. Geological Survey data is 1/0.01 (inches (inches/year)/ foot) or less (19:Plate 3). The piezometric head difference has to be inferred from TA C-64C sand-and-gravel well data and Upper Floridan potable well data. This assumes the piezometric head difference below TA C-64C is representative of the head difference around TA C-64. TA C-64C is located approximately one mile away in a 120 degree east, south-east direction. For the level of accuracy expected, and using U.S. Geological Survey charts showing piezometric surfaces of the sand-and-gravel and Floridan aquifers, the latter assumption seemed reasonable.

Using the Upper Floridan potable well head value of 159.8 ft (12:26) below the surface, and a low of 56.8 ft and a high of 99.5 ft below the surface (12:33-35) of the monitoring wells from the sand-and-gravel aquifer, the resulting piezometric head

difference was as high as -130 ft and as low as -60.3 ft. The large difference from the high and low water depth in the sand-and-gravel aquifer is because the low monitoring well is located in a gully (Appendix B.2). The value was still used in the calculations as a means to get the worst case scenario for the aquitard leakage, where the largest head difference gives the largest leakage rate. Using Equation B.1 gave a value of q_v equal to a high of 1.03 inches/year and a low of 0.603 inches/year of vertical leakage from the sand-and-gravel aquifer through the Pensacola confining bed into the Upper Floridan aquifer. Porosity values, n, for sand range from 0.25 to 0.50, and for clay ranges from 0.40 to 0.70 (28:25). Since the retardation factor for uranium was only calculated for sand, the sand porosity values were used to calculate the velocity (worst case) of the groundwater leakage, and the time for the water and DU to leak from the sand-and-gravel aquifer into the Upper Floridan aquifer. Since clay has a higher porosity and acts as an effective boundary to contaminate flow, the assumption of sand DU retardation and porosity represents an error on the side of conservatism and a worst case time frame for water and DU to travel through the confining bed.

Calculating the vertical water velocity using Equation B.2, using n equal to a low of 0.25 and a high of 0.50, gave 4.12 inches/year and 2.06 inches/year, respectively. The thickness of the Pensacola confining bed was found by taking the difference between the bottom of the sand-and-gravel aquifer, 120 ft based on monitoring well data (12:33-35) and the top of the Upper Floridan aquifer, 378 on potable well data (12:27). The thickness of the Pensacola confining bed was calculated to be 258 ft. Using Equation B.3,

$$t = 12\frac{\Delta L}{v} \qquad\qquad (B.3)$$

the amount of time required for water to flow through the confining bed was found to be

751 years based on a porosity of 0.25 and 1503 years using a porosity of 0.50. The

retardation factors for uranium transport through sand are 11.6 and 32.8 times for a

porosity of 0.50 and 0.25, respectively. Using the retardation factor, the time for the

uranium to leak from the sand-and-gravel aquifer to the Upper Floridan aquifer was found

to be a high of 24,650 years to a low of 17,430 years (worst case). Based on this data, the

Pensacola clay confining bed forms an effective barrier between the two aquifers. This

assumption agrees with Bush and Johnston, U.S. Geological Survey Report which states

the Pensacola clay above the Upper Floridan aquifer provides an "effective seal" from the

superficial aquifer and salt-water encroachment (19:C70). For this reason, uranium

transport from TA C-64 into the Upper Floridan aquifer was not considered to be a

problem.

To recap, we have ruled out uranium transport from the TA to the Upper Floridan

aquifer as a problem. However, we still need to characterize uranium transport in the

sand-and-gravel aquifer. To do this we next develop an appropriate groundwater flow

model and use its output for particle tracking analysis.

MODFLOW® groundwater flow model. To characterize the sand-and-gravel aquifer,

four groundwater models were developed. The faults of the first three models, are

outlined and the fourth and final model, which appropriately characterized the

groundwater flow beneath TA C-64 and vicinity, is described completely in this section.

The results of the fourth model are used in particle tracking analysis. Basic groundwater modeling theory is presented in Appendix B.5, and should be read to get an understanding of the terminology. Please note that this section assumes that the reader is familiar with groundwater modeling.

The first groundwater model was grided for the whole of Eglin AFB and vicinity. Due to the lack of hydrogeologic data and the expected macroscopic scale of the resulting output with respect to the TA C-64, this model was only conceptualized and not used.

The second groundwater model was actually entered into MODFLOW®, the 2-D multi-layer groundwater flow modeling program. This two layer groundwater model modeled both the sand-and-gravel and the Upper Floridan aquifer. MODFLOW® results were obtained, but no further analysis was performed with this two layer model since; analytical calculations of the leakage through the Pensacola confining bed indicated that the Upper Floridan aquifer did not pose any threat in terms of contaminant transport. The Pensacola clay confining bed acts like an "effective seal" between the two aquifers due to its thickness (95.7 m) and the extremely low hydraulic conductivity of the clay (approximately 10^{-7} m/s). Fort Walton Beach drinking supply wells pump the Upper Floridan aquifer groundwater heavily (20 Mgal/day or 0.8762 m^3/s), causing a large piezometric level local depression cone very close to the neighboring Choctawhatchee Bay. The lack of salt water intrusion into the drinking water supply after so many years of pumping clearly indicated the relative impermeability of the Pensacola Clay confining bed. (19:C60,C70) Due to these facts, only the sand-and-gravel aquifer needed to be

modeled. A one layer groundwater model accomplished this with a reduction in complexity and a resulting increase in confidence in the model.

The third groundwater MODFLOW® model, modeled only the sand-and-gravel aquifer. The fault of this model was that it was still too detailed for the available data. The interactions between the creeks surrounding the test area and the sand-and-gravel aquifer were modeled using the river package in MODFLOW® (actual creek flow was not modeled). This interaction took into account the dimension of the creek, the hydraulic conductivity of the creek bed, and the head difference amongst the blocks. Creek dimensions in the area of interest were unavailable. The dimensions were hypothesized using regional maps (a very crude approximation). Bull and Ramer creeks were assumed identical in width, length, and thickness (of the river bed) and Titi creek was assumed to be approximately twice as large. These crude approximations brought about doubt and uncertainty in the model results. Calibration of results with actual data was lacking, and a simpler model, which took advantage of available actual data, would provide more confidence.

The fourth and final MODFLOW® model was simpler in nature. It did not simulate the creeks using the river package. Rather, the creeks were modeled as constant head boundaries (i.e., their stages were constant throughout the steady state simulation). All the other head values changed in response to their values. This assumption was based on the fact that "... streamflow remains fairly constant year-round." (12:8). The fourth groundwater model, as well as model two and three, characterized the discretized region shown in Figure B.9. The discretized blocks used in MODFLOW® were 250 meters by

250 meters. The grid was rotated so that the cross section along the horizontal grid line was parallel to the geologic cross section used by the U.S.G.S. to characterize the dimensions and locations of the geologic units beneath the surface (Figure B.1). Furthermore, rotating the grid allows one to conveniently use the surrounding creeks as constant hydraulic head boundaries for the test area and vicinity.

The simulation ran for two years in one month time steps. Steady state condition was specified, theoretically indicating that all time derivative terms in the groundwater flow equation were zero (i.e. storage in a cell was zero). This means that at any location in a flow field the magnitude and direction of the flow velocity are constant with respect to time (28:52). MODFLOW[®] used the specified initial heads as the initial guess in solving the discretized groundwater flow equation through the iterative process used in the strongly implicit procedure (SIP). For the next time step it used the previous time step's solution as the initial guess. This process was continued for the specified number of time steps. After the first few time steps (for steady state condition), MODFLOW[®] arrived at a fairly constant solution for the remaining time steps.

Wells were not modeled, because there were no injection or extraction wells in the grided area. However, there are six monitoring wells in TA C-64C which are used to monitor the chemical constituents in the groundwater of the sand-and-gravel aquifer. Since the sand-and-gravel aquifer is unconfined (water-table aquifer), topography of the test area was used as the initial hydraulic head data for the aquifer. This assumed that the water table was very close to the surface, indicating a thin unsaturated region (Topography $\approx$ h). In actuality, data from the six monitoring wells indicated a unsaturated

Legend:
- Map Grid Block: 1000 m by 1000 m
- Model Grid Block: 250 m by 250 m
- Location: Longitude (between 86 15' and 30') and Latitude (between 30 30' and 45')
- X -- Calibration block (10,8)
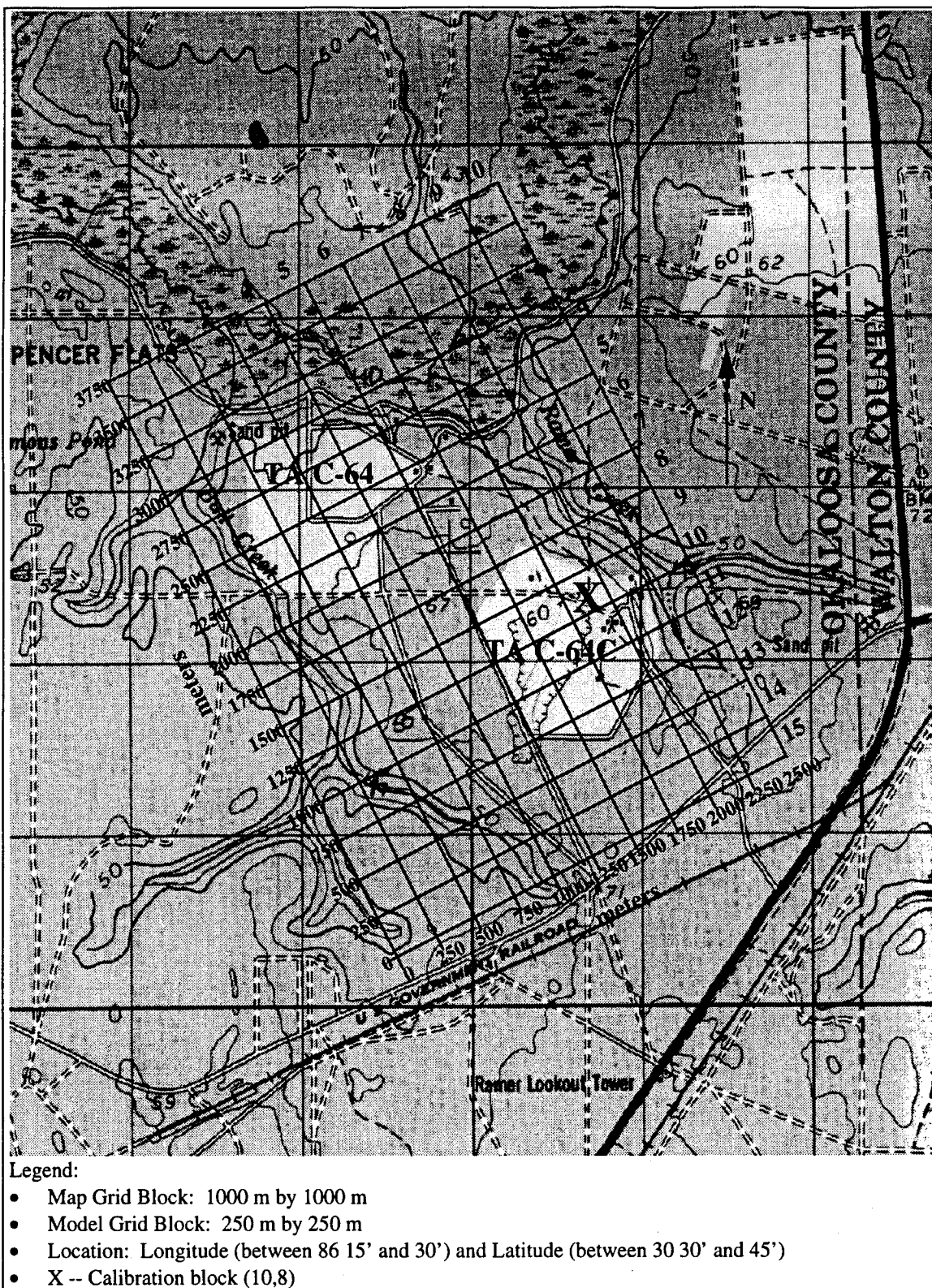
Figure B.9 Discretized Area for MODFLOW® Modeling

region of 25.45 meters thick in TA C-64C (block (row 10, column 8) in Figure B.9) (12). However, for an initial guess (with respect to steady state assumption) the topography was a good approximation since, the water table tends to follow the topography in a unconfined aquifer.

In the groundwater model, isotropy and homogeneity (within each layer) was assumed. Therefore, hydraulic conductivity (unconfined aquifer) and transmissivity (confined aquifer) were the same in all directions. The hydraulic conductivity (K) for the sand-and-gravel aquifer was 0.001 m/s (This value was the median value in the sand and gravel range) (28:29). Evaporation of water was modeled by using the average evapotransporation rate (36 in/year or 2.9×10^{-8} m/s) for the discretized region from regional U.S.G.S. data (19:Plate 9). The evapotransporation surface was assumed to be the topography, and the depth to which evapotransporation occurred was hypothesized to be three meters. Recharge of water to the sand-and-gravel aquifer was calculated as follows: Titi Creek's average discharge near Crestview is 134 ft^3/s (3.79 m^3/s) and its drainage area is 62.9 mi^2 (1.63×10^8 m^2) (69:25). Dividing the area from the discharge gave a discharge rate of 2.33×10^{-8} m/s. The average rainfall rate for Crestview is 63.94 in/yr (5.15×10^{-8} m/s) (69:22). Subtracting the discharge rate form the rainfall rate yielded a recharge rate of 2.82×10^{-8} m/s. Even though this value was based on data from the 1960's, it served as a good value for the level of detail in this model.

Well data from TA C-64C was used to calibrate the model (Section B.2). The six wells at this TA are located in grid block (10, 8) as indicated in Figure B.9. The average

or mean hydraulic head value from the wells was calculated to be 43.7 meters (Table B.13) (i.e., an unbiased point estimate). The parameters varied to calibrate the model were the initial head values of the creek nodes (i.e. the boundary value). The initial topography used for models two and three is shown in Table B.14. The bold values are the constant head values representing the assumed creek stages. Adjusting these creek values produced a direct impact on the resulting model output at block (10, 8) (calibrating it with the actual head reading of 43.7 m). In other words, the model was very sensitive or was dictated by the choice of the constant head values.

Six monitoring wells at TA C-64C				
Well	Dist. to GW from surf. in **ft**	Surf. elev.	hydraulic head **ft.**	head in **m**
1	92.3	227	134.7	41.1
2	99.5	227	127.5	38.9
3	96.2	227	130.8	39.9
4	56.8	227	170.2	51.9
5	75.4	227	151.6	46.2
6	80.7	227	146.3	44.6
			Average	**43.7**

Table B.13 Calculation of Actual Head Value at Block (10,8)

Furthermore, adjusting only the recharge rate and the evapotransporation rate led to a poor calibration at this block due to the model's lack of sensitivity to these parameters. The calibrated initial values used for model four (including the boundary values) are shown in Table B.15. The constant head values representing the creeks are in bold.

All values in Table B.15 are identical to the initial values used for model two and three except for Bull and Ramer Creek head values. These values were modified for calibration with the well hydraulic head. The Bull and Ramer Creek nodes closest to Titi

Sand-and-Gravel head values (m)		1	2	3	4	5	6	7	8	9	10
From Topographic map	1	45	45	40	40	45	50	50	50	40	45
	2	45	45	40	45	40	45	50	45	40	45
Approximate Location of	3	45	45	45	45	40	40	45	40	40	40
Target Butt: ■	4	45	50	55	50	45	45	40	45	45	50
	5	45	50	55	50	50	50	45	40	45	50
Calibration Location:	6	45	50	55	55	55	55	50	45	45	50
	7	50	45	50	55	55	55	55	50	45	50
Greater TA C-64 location:	8	50	45	50	55	55	55	55	50	45	50
	9	50	45	50	55	55	55	55	55	45	50
	10	50	45	50	55	55	60	60	60	50	45
	11	45	50	50	55	55	60	60	55	50	45
	12	50	45	50	55	60	60	55	55	55	50
	13	55	50	45	50	55	55	55	55	55	55
	14	50	50	50	45	50	55	55	55	55	55
	15	45	50	55	45	50	55	55	55	55	55

Table B.14 Initial Head Values for Model 2 and 3

Sand-and-Gravel head values (m)		1	2	3	4	5	6	7	8	9	10
From Topography map	1	45	45	40	40	45	50	50	50	40	45
	2	45	45	40	45	40	45	50	45	40	45
Approximate Location of	3	40	40	45	45	40	40	45	40	40	40
Target Butt: ■	4	40	50	55	50	45	45	40	45	45	50
	5	40	50	55	50	50	50	45	40	40	50
Calibration Location:	6	40	50	55	55	55	55	50	45	40	50
	7	50	40	50	55	55	55	55	50	40	50
Greater TA C-64 location:	8	50	40	50	55	55	55	55	50	40	50
	9	50	40	50	55	55	55	55	55	42.5	50
	10	50	40	50	55	55	60	60	60	50	45
	11	40	50	50	55	55	60	60	55	50	45
	12	50	40	50	55	60	60	55	55	55	50
	13	55	50	42.5	50	55	55	55	55	55	55
	14	50	50	50	45	50	55	55	55	55	55
	15	45	50	55	45	50	55	55	55	55	55

Table B.15 Adjusted Model 4 Initial Head Values

Creek were reduced by five meters (from 45 to 40), and an intermediate value of 42.5 m was used as a transition between 40 m and 45 m nodes. The values in Table B.15 match the topographic map of the test area fairly well. The major assumption was that these constant head values representing the creeks portray the actual creek stages. The simplicity of this representation reduced uncertainty, and the model validation with the well data provided greater confidence in the model results.

After calibration, the discrepancy between the model and the actual head value for block (10, 8) was: $|43.483m - 43.7m| = 0.217$ m or 0.497% absolute error. The calibrated groundwater model achieved a low 0.05% cumulative volumetric budget (analogous to mass balance) percent error between total inflow and outflow of water into the modeled system. This indicated good solution validity for the entire simulation (48:3-18). The remaining input into MODFLOW® for model four is presented in Table B.16.

The piezometric level output of model four is shown in the contour plot of Figure B.10. The contour plot indicated that groundwater flows toward the intersection of Titi, Bull and Ramer Creek as expected (direction of decreasing hydraulic head values). If DU leached into the groundwater system and traveled with the groundwater, then it would migrate towards the inverted "U" shaped boundary defined by the three creeks.

The decrease in piezometric level between the initial head values and the final head values after two years of simulation is shown in the drawdown contour plot in Figure B.11. This figure clearly indicates the zero drawdown at the constant head blocks representing the creeks (verifying that the model was working properly). The high

Model 4											
No	**Input**					**Value**					
1	Layers					1					
2	No. of Rows					15					
3	No. of Columns					10					
4	Stress Periods					1					
5	Wells					None					
6	River Nodes					None					
7	Evapotransporation					top layer only					
8	Recharge					top layer only					
9	Boundaries					constant head boundaries (river blocks)					
	-1 = constant head		**1**	**2**	**3**	**4**	**5**	**6**	**7**	**8**	**9**	**10**
	0 = in active	**1**	1	1	-1	-1	1	1	1	1	1	1
	1 = active	**2**	1	1	-1	1	-1	1	1	1	-1	1
	X = calibration cell location	**3**	-1	-1	1	1	-1	-1	1	-1	-1	-1
		4	-1	1	1	1	1	1	-1	1	1	1
		5	-1	1	1	1	1	1	1	-1	-1	1
		6	-1	1	1	1	1	1	1	1	-1	1
		7	1	-1	1	1	1	1	1	1	-1	1
		8	1	-1	1	1	1	1	1	1	-1	1
		9	1	-1	1	1	1	1	1	1	-1	1
		10	1	-1	1	1	1	1	1	X	1	-1
		11	-1	1	1	1	1	1	1	1	1	-1
		12	1	-1	1	1	1	1	1	1	1	1
		13	1	1	-1	1	1	1	1	1	1	1
		14	1	1	1	-1	1	1	1	1	1	1
		15	-1	1	1	-1	1	1	1	1	1	1
10	Layer I					active					
11	HNOFLOW					999					
13	Simulation					Steady State					
14	Layer I					unconfined					
15	Wet to dry (active)					50					
16	Anisotropy ratio					1					
17	Delta X (meters)					250					
18	Delta Y (meters)					250					
19	Hydraulic Conductivity (K)					0.001 m/s (28)					
20	Aquifer Bottom elevation (meters)					28.35					
21	Length of stress period					2 year					
22	No. of time steps in stress period 1					24					
23	Evapotransporation Surface Elevation					Same as topography					
24	Max. E-T rate from U.S.G.S.					36 in/year $\Rightarrow$ 2.8976 X 10^{-8} m/s					
25	E-T extinction depth modification					3 m					
26	Recharge rate (average)					(rain fall - stream dis. (Titi)) $\Rightarrow$ 2.82 X 10^{-8} m/s					

Table B.16 Model 4 Input for MODFLOW®

drawdowns represent the active cells of the superficial land mass. Calculating the average linear groundwater velocity between TA C-64 and the closest neighboring creek node was straight forward. TA C-64 was incorporated in nine grid blocks (4,4), (4,5), (4,6), (5,4), (5,5), (5,6), (6,4), (6,5), and (6,6). The average head value for these nine grid blocks is 40.706 meters. Center this value at block (5,5). The closest creek node is at block (5,3) with a head value of 40 meters. The calculated average linear velocity (specific discharge divided by porosity) of the groundwater flow between these two blocks for a porosity range of 0.2 to 0.5 (The porosity of the sand-and-gravel aquifer lies within this range specified by the sand and gravel constituents. (28:37)) was between 7.06 X 10^{-6} m/s to

2.82 X 10^{-6} m/s respectively. This indicated that the average linear groundwater velocity
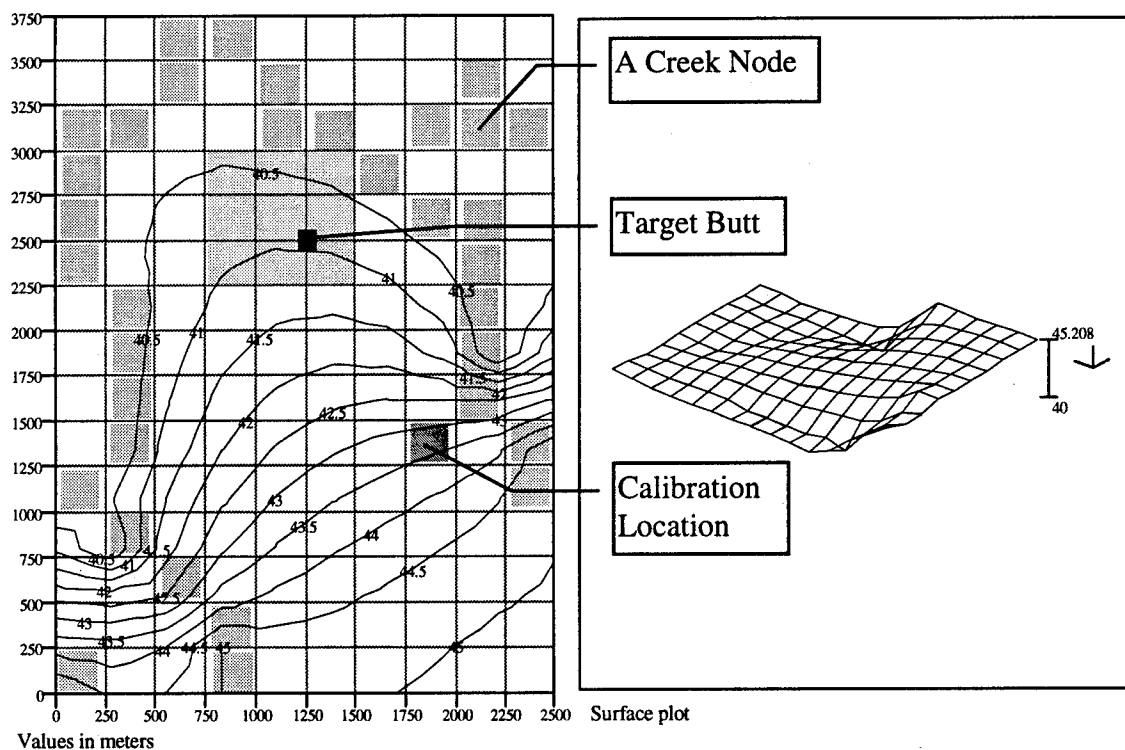
Figure B.10 Head level contour and surface plot - Sand-and-Gravel Aquifer
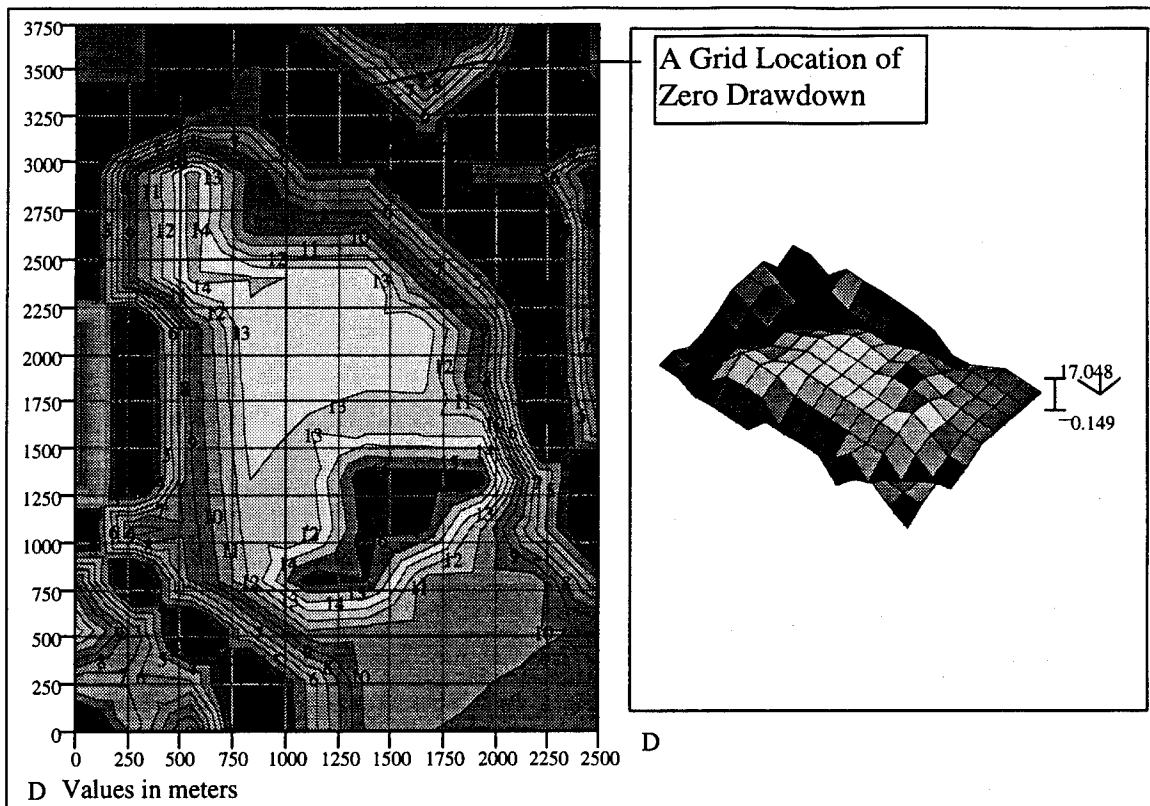
Figure B.11 Drawdown contour and surface plot of TA C-64 and vicinity

and porosity (the volume of void divided by the total volume of soil) are inversely

proportional.

Furthermore, these velocities are only applicable to laminar flow, since Darcy's

law is valid only for the Reynolds number range between 1 and 10 (28:73). In either case,

the groundwater moved considerably slow compared to surface water flow, so any

leached DU contaminant will also migrate slowly (excluding dispersion, sorption and rate

reaction effects).

The general nature of DU movement horizontally in the sand-and-gravel aquifer

can be determined through a particle tracking analysis. MODPATH®, a simple particle

tracking program, uses tracer particles to track groundwater flow from specified blocks. One particle was placed at the center of each of the nine blocks (hypothetically representing point sources of a contaminant). The program was executed for porosity values between 0.2 and 0.5 in increments of 0.1. This covers the porosity range of the sand-and-gravel aquifer as indicated in the previous paragraph. Also, for worst case no evapotransporation of the tracer particles was assumed. Furthermore, the particles were only stopped at strong sinks or depressions in the piezometric (head) level. MODPATH® results are depicted graphically in Figure B.12.

As seen in Figure B.12, all nine particles stop at the creek constant head blocks. This, clearly indicated that any contaminant from the test area would migrate northward towards the intersection of the three creeks. The time for the tracer particles to reach their endpoints is shown in Table B.17.

The time for the center of mass of leached DU contaminant to reach the endpoint was also tabulated (in Table B.17) for the corresponding calculated retardation factors of 43.40, 25.73, 16.90 and 11.60 (for the various porosities). The equation used to calculate retardation factor (R_d) is (Equation B.4):

$$R_d = \frac{\overline{\upsilon}}{\overline{\upsilon}_c} = 1 + \frac{(1-n)}{n}\rho_s K_d \qquad (B.4)$$

K_d is the distribution coefficient. K_d for uranium in tuff matrix (assumed similar to sand and gravel) is 4 ml/g. (23:442) ρ_s is the particle mass density of the soil, generally assumed to be 2.65 g/cm^3 (28:337). $\overline{\upsilon}$ and $\overline{\upsilon}_c$ are the average linear groundwater velocity and the velocity of the retarded contaminant at the center of mass respectively.
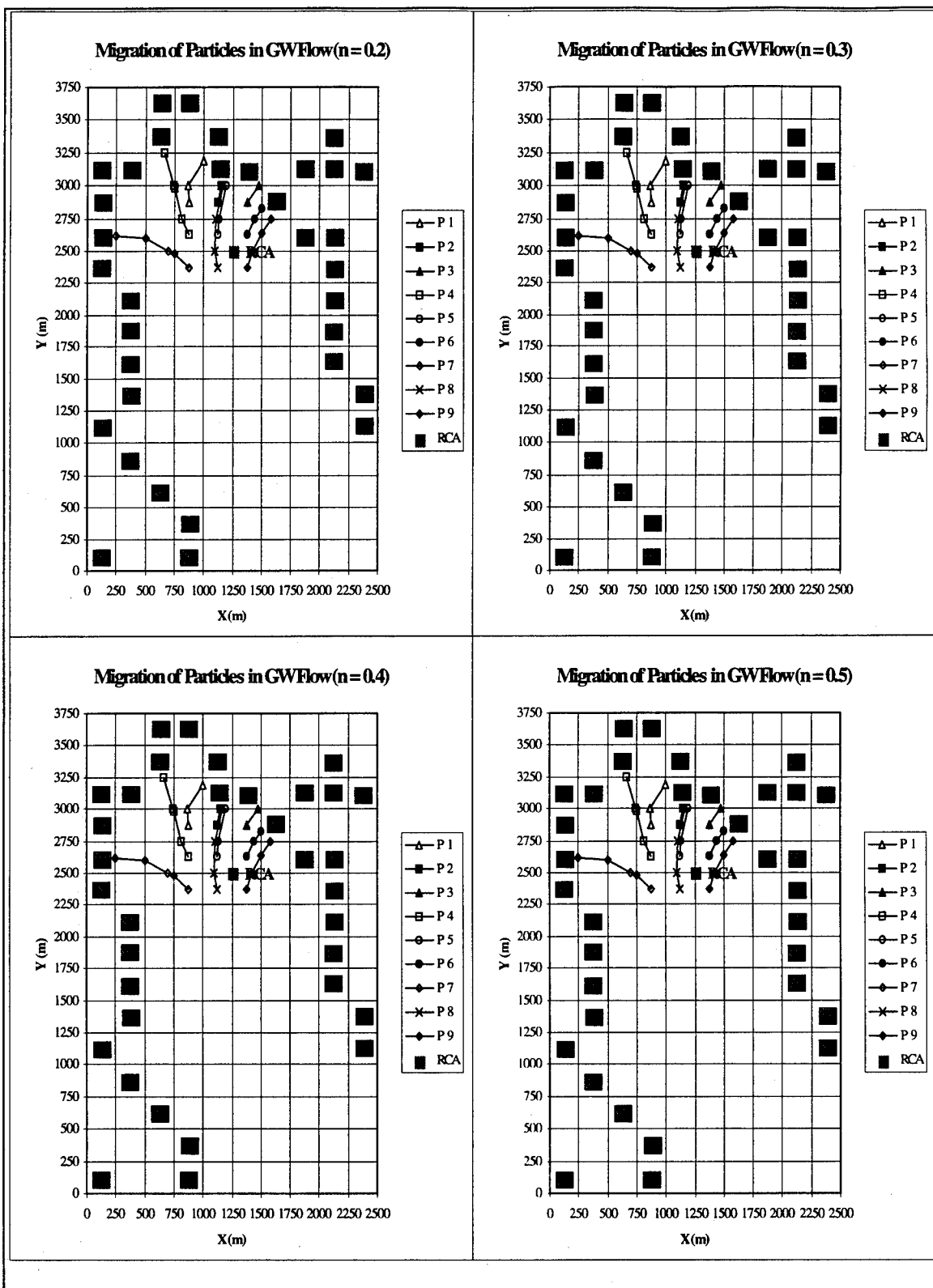
Figure B.12 Particle Tracking Output

B-42

Time to Reach Finishing Location (yrs)

Particle	At GW velocity	Retarded		
1	7.59	329.25	n	0.20
2	1.68	72.70	ps	2.65
3	2.08	90.12	Kd for Tuff	4.00
4	15.27	662.91	Rd	43.40
5	5.61	243.51		
6	2.95	127.99		
7	13.47	584.49		
8	9.85	427.45		
9	5.19	225.15		

Time to Reach Finishing Location (yrs)

Particle	At GW velocity	Retarded		
1	11.38	292.83	n	0.30
2	2.51	64.66	ps	2.65
3	3.11	80.15	Kd for Tuff	4.00
4	22.91	589.59	Rd	25.73
5	8.42	216.58		
6	4.42	113.84		
7	20.20	519.85		
8	14.77	380.17		
9	7.78	200.25		

Time to Reach Finishing Location (yrs)

Particle	At GW velocity	Retarded		
1	15.17	256.42	n	0.40
2	3.35	56.62	ps	2.65
3	4.15	70.19	Kd for Tuff	4.00
4	30.55	516.28	Rd	16.90
5	11.22	189.65		
6	5.90	99.68		
7	26.94	455.20		
8	19.70	332.90		
9	10.38	175.35		

Time to Reach Finishing Location (yrs)

Particle	At GW velocity	Retarded		
1	18.97	220.01	n	0.50
2	4.19	48.58	ps	2.65
3	5.19	60.22	Kd for Tuff	4.00
4	38.19	442.96	Rd	11.60
5	14.03	162.72		
6	7.37	85.53		
7	33.67	390.56		
8	24.62	285.62		
9	12.97	150.44		

Table B.17 Time to Reach Endpoint

Using these values R_d was calculated. The retardation factor modeled only the sorption of DU (the retardation of the center of mass of the contaminant moving from the nine assumed point sources relative to the bulk mass of water). (28:404) Note, this transport did not take into account dispersion, chemical rate reaction, and sorption with respect to concentration of contaminant.

The first particle to reach its endpoint, Particle 2, arrived at Titi creek between 1.7 to 4.2 years (n = 0.2 to n = 0.5). If this particle was retarded like DU, then (for worst case: n = 0.5) it would reach the creek in 48.6 years. The last particle, Particle 4, arrived at the Titi and Bull Creek intersection between 15.3 to 38.2 years (n = 0.2 to n = 0.5) or for worst case (n = 0.5): 443 years (if retarded like DU).

Thus, the main results from MODFLOW® indicated that the groundwater in the sand-and-gravel flows towards the three creeks as better illustrated in Figure B.13.

MODFLOW's® numeric output is shown in Table B.18. Therefore, DU contaminant particles that have leached into the groundwater would eventually travel to those creeks. For more conclusive results, actual field and experimental data on aquifer and depleted uranium interaction characteristics are required to perform proper contaminant transport modeling using programs such as MT3D.

MODFLOW® Groundwater Model Sensitivity Analysis. The sensitivity of the MODFLOW® groundwater model to key input parameters was tested. The changes in the model output (due to input parameter variation) in block (10,8) was observed. The input parameters varied were: recharge rate; max evapotransporation rate; evapotransporation extintion depth (48:10-1); hydraulic conductivity; and constant (initial) head boundary at block (9,9) and (13,3). The parameters were varied individually. The default parameters

	1	2	3	4	5	6	7	8	9	10
1	40.3	40.2	40.0	40.0	40.1	40.2	40.3	40.2	40.1	40.2
2	40.2	41.1	40.0	40.1	40.0	41.1	40.2	41.1	40.0	40.1
3	40.0	40.0	40.2	40.2	40.0	40.0	40.1	40.0	40.0	40.0
4	40.0	40.2	40.4	40.5	40.4	40.3	40.0	40.1	40.1	40.2
5	40.0	40.3	40.6	40.7	40.8	40.7	40.4	40.0	40.0	40.2
6	40.0	40.3	40.6	40.9	41.1	41.0	40.8	40.5	40.0	40.3
7	40.1	40.0	40.7	41.1	41.4	41.4	41.3	40.8	40.0	40.6
8	40.1	40.0	40.8	41.4	41.7	41.9	41.8	41.4	40.0	41.3
9	40.1	40.0	41.0	41.6	42.1	42.4	42.5	42.5	42.5	43.1
10	40.1	40.0	41.2	42.0	42.6	43.0	43.2	43.5	43.9	45.0
11	40.0	40.4	41.5	42.4	43.0	43.5	43.8	44.1	44.5	45.0
12	40.9	40.0	41.8	42.9	43.5	43.9	44.2	44.5	44.8	45.0
13	42.4	42.2	42.5	43.7	44.1	44.4	44.6	44.8	44.9	45.1
14	43.8	43.7	44.0	45.0	44.7	44.8	44.9	45.0	45.1	45.2
15	45.0	44.4	44.5	45.0	44.9	44.9	45.0	45.1	45.2	45.2

- Approximate Location of Target Butt: ■
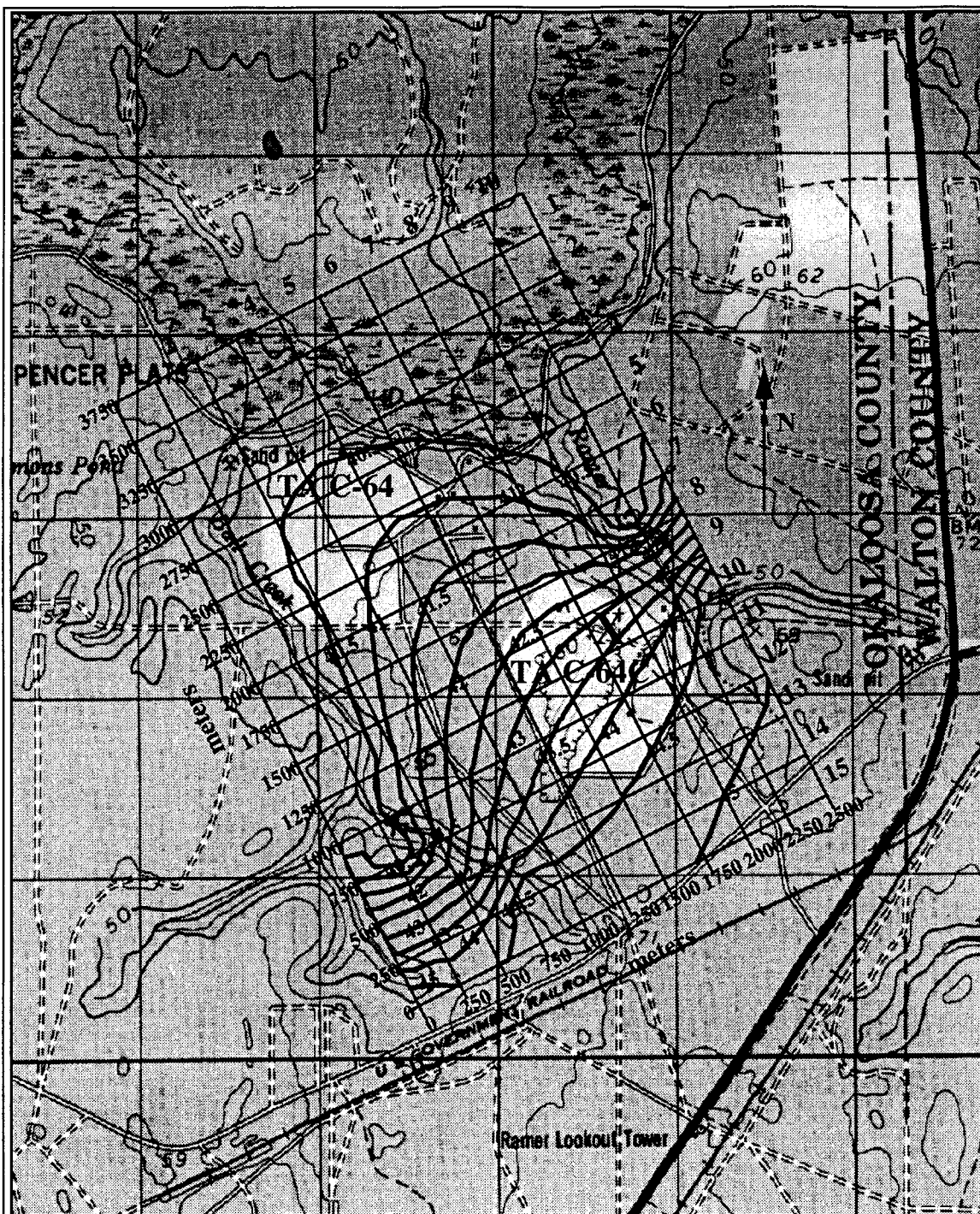- Calibration Location: ▨
- Greater TA C-64 location: ▢

Table B.18 Model 4 Output Head Values in meters

were: Recharge Rate = 2.82 E-8 m/s; E-T Rate = 2.90E-8 m/s; E-T depth = 3 m; K = 1E-3 m/s; Initial Head = 42.5 m.

The results of the analysis indicated that the model output was most influenced by the adjustment of the constant head values representing the creeks. The evapotransporation rate did not have any effect on the output, because the active head values were drawn down well below the 3 m E-T extinction depth (due to the constant head boundaries of the creek). The individual sensitivity plots are shown in Figure B.14. Note as the E-T depth is increased, the default E-T rate starts to have an impact on the output at test cell (10,8), whose calibrated value is 43.483 m.

Unsaturated Region Groundwater Flow. Unsaturated soil is a region where the void space of the soil is partially filled with water and partially with air. Appendix B.5 includes a more complete description of the unsaturated groundwater flow equations including capillary head, ϕ_c; water saturation, S; moisture content, θ; and specific discharge, q, for both air and water. To characterize the unsaturated groundwater flow region around the TA, a program from the International Ground Water Modeling Center (IGWMC) was used. The program, Infil, was originally developed in 1979 by M. Vauclin and others and was modified in 1983 by Aly I. El-Kadi (see Appendix B.5 for a more in-depth description of the program and solution method) (38).

The data used to evaluate the unsaturated groundwater flow was from, "Contaminant Transport In Unsaturated Flow", by Charbeneau and Daniel in chapter 15 of the, *Handbook of Hydrology,* edited by Maidment. The parameters were for the Brooks and Corey solution to the Richard's equation for fine sand. The fine sand fitted parameters

Legend:
- Map Grid Block: 1000 m by 1000 m
- Model Grid Block: 250 m by 250 m
- Location: Longitude (between 86 15' and 30') and Latitude (between 30 30' and 45')
- X -- Calibration block (10,8)
- Contour Lines Indicate MODFLOW® Hydraulic Head Output Values in meters

Figure B.13 Hydraulic Head Contour Plot Output, Sand-and-Gravel Aquifer
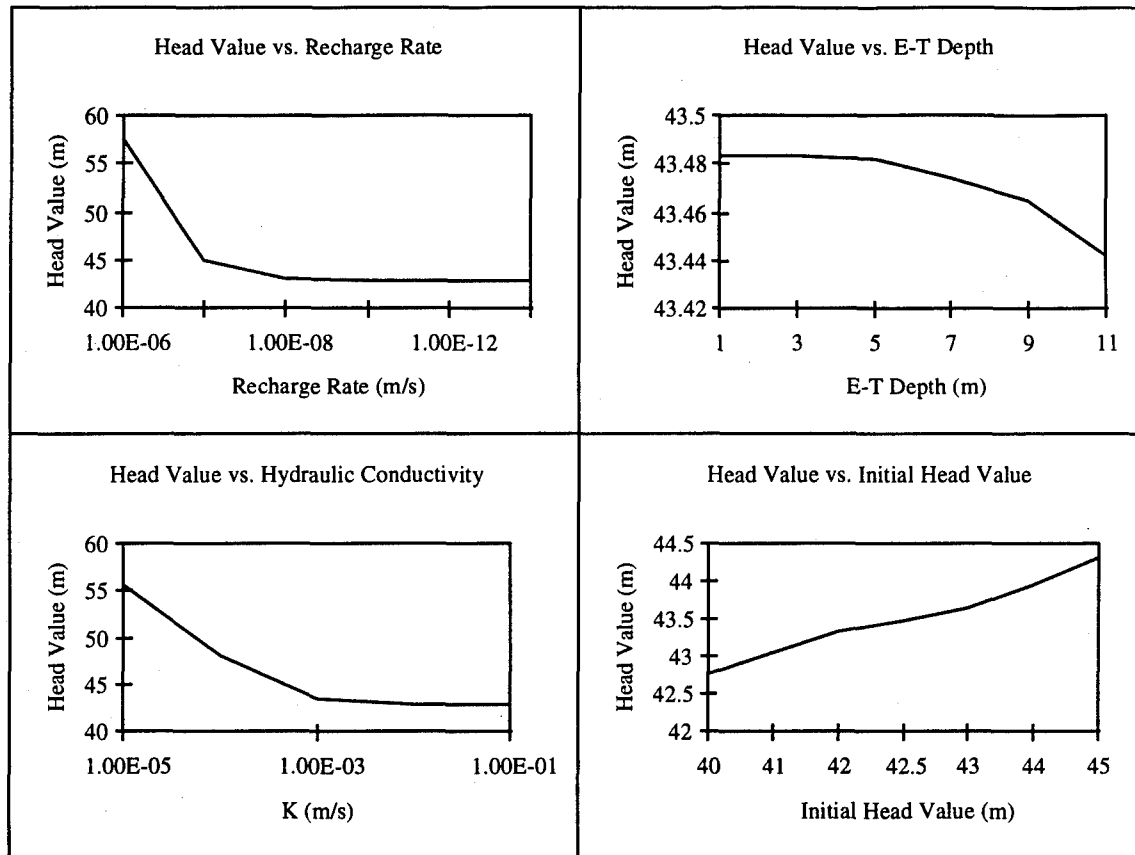
Figure B.14 Sensitivity Plots at Block (10, 8)

were porosity, n = 0.36, irreducible water content, θ_r = 0.06, pore size distribution index, λ = 3.74, bubbling capillary pressure head, ψ_b = 41 cm, and saturated hydraulic conductivity, K_s = 2.8e-3 cm/s (45:15.7).

The Infil program assumed a constant head at the surface of the unsaturated region and was used for this problem just to get a general idea of the time it takes standing surface water to seep through the unsaturated region into the sand-and-gravel aquifer. From the Infil output, at a time of 36 hours the infiltration amount has reached 23.58 meters (see Appendix B.6 for Infil printed output). This showed that the standing surface

water reaches the sand-and-gravel aquifer around 36 hours. This value was just a rough order of magnitude and does not represent the actual water infiltration rate of TA C-64, but does provide a reference time frame for water infiltration in fine sand.

For the level of data available for the groundwater leakage between aquifers, horizontal sand-and-gravel aquifer groundwater flow, DU concentrations in the groundwater, and groundwater infiltration rate, all solutions obtained must be viewed as providing a general idea of the groundwater flow around TA C-64. When uranium concentration or transport calculations were required, an effort was made to provide the worst case analysis for the lack of better data. A more detailed analysis of groundwater flow would be required to reduce the uncertainty and provide a more representative description of the groundwater flow around TA C-64. A more detailed analysis may or may not be required for risk management and would require additional laboratory and field work to provide actual soil characteristics. The benefits gained by additional analysis may not be the most cost effective method to reduce the health risk and should be evaluated in the health risk assessment and risk management sections.

B.5   Groundwater Modeling Theory

   Basics of Groundwater Modeling. Groundwater modeling is essential for

understanding hydrogeologic systems, forecasting future conditions and focusing

environmental remediation programs on key contaminant transport pathways.

Groundwater modeling is a human's representation of nature's hydrogeologic system,

therefore, calibration and validation of groundwater modeling output with field data is

very important in performing proper characterization and obtaining pertinent results. To

understand how depleted uranium particles from TA C-64 might be transported if it

infiltrated the groundwater system, requires site specific characterization of the

groundwater system under TA C-64 and vicinity. Analysis of this system allows for

proper health risk assessment & remediation, and will serve as a basis for future in-depth

studies in this field with respect to the test area. To fully grasp the insights gained by

groundwater modeling requires a knowledge of the basic concepts.

   A groundwater flow equation is required to determine the characteristics of

groundwater flow. Three main components lead into the groundwater flow equation as
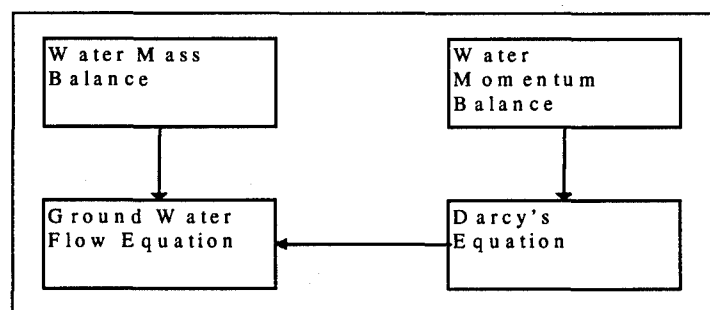
Figure B.15 Components of the Groundwater
Equation (40)

shown in Figure B.15. In the following paragraphs these major components will be explained briefly.

The ground in modeling sense is broken up into two primary regions: an aquifer and an aquitard. The former is a saturated permeable geologic unit which can transport a sizable amount of water under ordinary hydraulic gradients or pressure. The latter is a less permeable region that acts as a confining layer to the aquifer. Since the laws of nature dictate a path of least resistance, groundwater flow will tend to flow along an aquifer. However, natural hydraulic pressure through time, forces water to penetrate the aquitard. A simple hydrogeologic system is shown in Figure B.16.
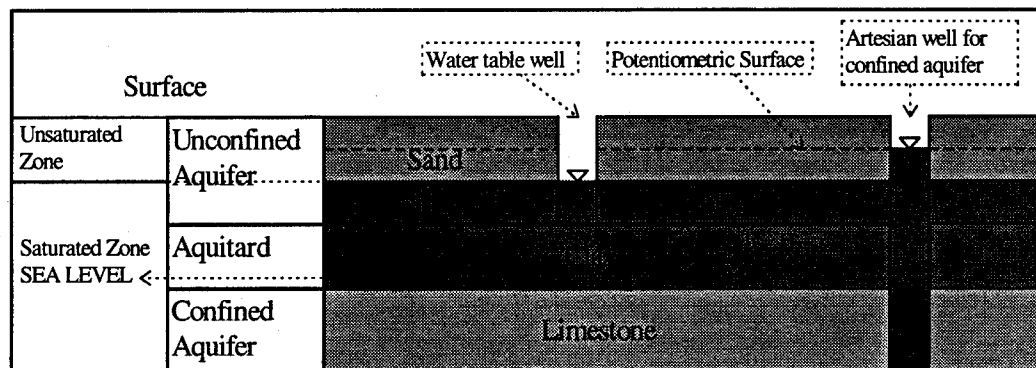
Figure B.16 Simple Hydrogeologic System

Fluid flows from a high potential to a low potential. To determine fluid potential, Bernoulli's equation can be derived from the conservation of linear momentum. Bernoulli's equation for steady frictionless incompressible flow along a streamline is used for groundwater purposes (Equation B.5).

$$\Phi = gz + \frac{v^2}{2} + \frac{p - p_0}{\rho}$$
(B.5)

where: Φ is the fluid potential, v is the velocity of the fluid (in this case water), p is the variable pressure, p_0 is the atmospheric pressure, and ρ is the constant density of an incompressible fluid. Since, groundwater flows very slowly, the velocity term is small and assumed to be approximately zero (v $\approx$ 0). Also, through derivation, it can be shown that Φ = gh, where h is the hydraulic head. In groundwater hydrology it is common to work with gauge pressure (p = ρgH), in which case the atmospheric pressure is set equal to zero. Performing this simplifications lead to Equation B.6.

$$h = z + H \tag{B.6}$$

Hydraulic head (h) is the sum of the elevation head (z) and pressure head (H).

The main output of groundwater modeling programs are the hydraulic head values to characterize a particular site. From the hydraulic head values and contour plots, one can obtain groundwater velocity values and corresponding flow field lines (28). These lines indicate the direction and magnitude of groundwater flow in an hydrogeologic system.

The pressure head and the elevation head are the two components of hydraulic head. The pressure head is induced by natural forces (e.g., gravity) pushing the water up a well tapped into the aquifer. The elevation head is the distance from a datum point (e.g., sea level) to the point where the pressure head H is determined. Groundwater flows in the direction of decreasing hydraulic head (piezometric level). The rate of groundwater flow depends on the hydraulic gradient (change of head per unit distance). This gradient can be calculated when piezometric levels are available from at least two wells tapped into the same aquifer. To calculate groundwater velocity from the hydraulic head data requires characterization of the particular aquifer medium.

In 1856, a French hydraulic engineer named Henry Darcy performed an experiment to analyze the flow of water through sand. The quantification of his experiments lead to a generalized empirical law, named after him (28). The concept of Darcy's experiment is illustrated in Figure B.17. In this figure, water flows in with a
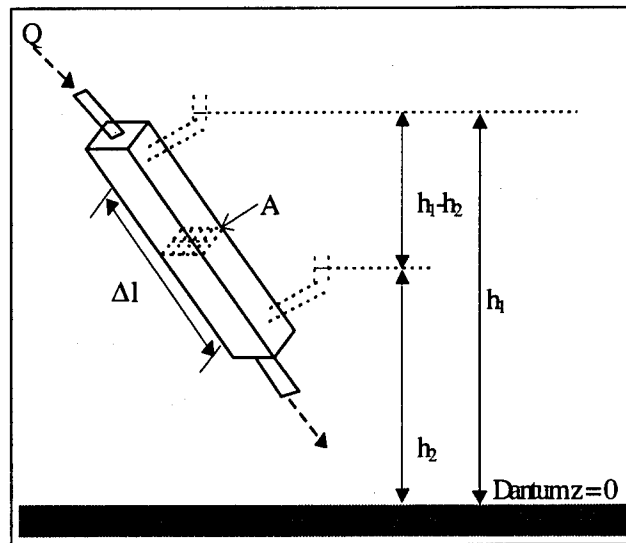
Figure B.17 Darcy's Experiment

volume rate Q at the top of the tube, until the sand in the tube (e.g., emulates a confined sand aquifer) is completely saturated. An arbitrary datum point to measure elevation is set (usually sea level, $z = 0$). The elevation of the water line (hydraulic head) in the upper and lower manometers are h_1 and h_2 respectively, and the distance between the two manometers is Δl.

Specific discharge υ (units of velocity) is defined as Q/A, where A is the cross-sectional area of the tube. Even though specific discharge has the units of velocity, it is not the true velocity of the groundwater flow. In reality the true velocity or microscopic

velocity is associated with the flow of water between each grain of sand (impossible to measure directly) (28). Specific discharge is macroscopic velocity which is the simplification or the "average" of all the microscopic velocities.

Darcy's experiment showed that specific discharge is directly proportional to $h_1 - h_2$ when Δl is held constant, and inversely proportional to Δl when $h_1 - h_2$ ($-\Delta h$) is held constant. The quantification of Darcy's experiment lead to the following empirical law (Equation B.7):

$$\upsilon = -K\frac{\Delta h}{\Delta l} \tag{B.7}$$

K is an empirical constant of proportionality known as hydraulic conductivity. It has high values for sand and gravel, and low values for clay and many rocks. K has the dimension of velocity (Length/Time). K is directly proportional to the permeability of the medium and inversely proportional to the viscosity of the fluid flowing through the medium. Field studies or laboratory analysis is required to quantify K. To make it easier for general analysis, many hydrogeologic books have K tabulated for various geologic material.

Conservation of mass (or mass balance) is the third key equation from which the groundwater flow equation is derived. An elemental control volume (CV) for flow through porous media is shown in Figure B.18. The continuity (conservation of mass) equation requires that the net rate of fluid mass flow into a CV must equal the time rate of change of fluid within the CV. This can be stated as follows with respect to the fluid: (mass leaving CV - mass entering CV) = (final mass in CV - initial mass in CV). The mass leaving the elemental CV is $[(Q\rho_{x+\Delta x}) + (Q\rho_{y+\Delta y}) + (Q\rho_{z+\Delta z})]$. Q is the volume rate

flow (length^3/time) and ρ (mass/length^3) is the density of the fluid in the x, y, and z

directions respectively. Similarly for the mass flow entering the CV: [(Qρ_x) + (Qρ_y) +

(Qρ_z) + (Rρ Δx Δy Δz)]. R is the volumetric injection rate per unit volume (e.g., from a

well). If the well is extracting fluid, then R will be negative (40). The final and initial

mass of fluid in the CV is modeled as a compaction of the soil or change in soil porosity

(n), and a change of fluid density ρ between the final and initial time. So, the final fluid

mass minus the initial fluid mass in the CV is: [(n$\rho_{t+\Delta t}$) - (nρ_t)] Δx Δy Δz. Combining

these parts results in the mass balance equation (Equation B.8).
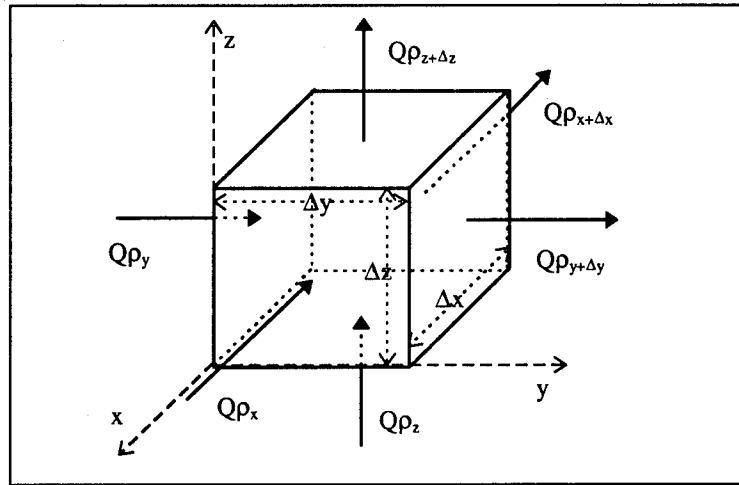
Figure B.18 Elemental control volume

$$\left[[(Q\rho)_{x+\Delta x} + (Q\rho)_{y+\Delta y} + (Q\rho)_{z+\Delta z}] - [(Q\rho)_x + (Q\rho)_y + (Q\rho)_z + R\rho\Delta x\Delta y\Delta z] \right]\Delta t$$
$$+ [n\rho_{t+\Delta t} - n\rho_t]\Delta x\Delta y\Delta z = 0 \tag{B.8}$$

The change in density and porosity with respect to time occur due to a change in

hydraulic head. The volume of water produced by the change in density and porosity due

to a unit decline in hydraulic head is called specific storage, (S_s; 1/length) (28:65). So, $[(n\rho_{t+\Delta t}) - (n\rho_t)]$ can be stated as $\rho S_s \Delta h$. Letting the fluid be water (incompressible), one can assume the density to be constant. Now, Equation B.8 can be expressed as (B.9):

$$-\left[[Q_{x+\Delta x}+Q_{y+\Delta y}+Q_{z+\Delta z}]-[Q\rho_x+Q_y+Q_z]\right]\frac{1}{\Delta x \Delta y \Delta z}+R=S_s\frac{\Delta h}{\Delta t} \qquad \text{(B.9)}$$

The specific discharge through each surface of the CV is: $\upsilon_x = Q_x/\Delta y\,\Delta z$, $\upsilon_y = Q_y/\Delta x\,\Delta z$, $\upsilon_z = Q_z/\Delta x\,\Delta y$. Using this and writing Equation B.9 in differential form yields:

$$-\left[\frac{\upsilon_x}{\partial x}+\frac{\upsilon_x}{\partial y}+\frac{\upsilon_x}{\partial z}\right]+R=S_s\frac{\partial h}{\partial t} \qquad \text{(B.10)}$$

Substituting the differential form of Darcy's equation ($\upsilon = -K\,dh/dl$) results in the groundwater flow equation (Equation B.11).

$$\frac{\partial}{\partial x}\left(K_{xx}\frac{\partial h}{\partial x}\right)+\frac{\partial}{\partial y}\left(K_{yy}\frac{\partial h}{\partial y}\right)+\frac{\partial}{\partial z}\left(K_{zz}\frac{\partial h}{\partial z}\right)+R=S_s\frac{\partial h}{\partial t} \qquad \text{(B.11)}$$

Some useful simplifications of the groundwater flow equation are: for steady state processes, dh/dt equals zero; and for isotropic processes, hydraulic conductivity is, $K_{xx} = K_{yy} = K_{zz} = K$. For a confined aquifer (with the latter characteristics) of thickness b (two dimensional flow), the hydraulic conductivity K is equal to T/b, where T is the transmissivity of the aquifer. Similarly for the same type of aquifer, the specific storage is equal to S/b, where S is the storativity of the aquifer.

The groundwater flow equation is used in groundwater modeling programs to determine the change in hydraulic head temporally and spatially from initial piezometric levels due to changing environmental conditions (e.g., recharge, evapotransporation, river

or stream interaction...). Furthermore, groundwater modeling programs spatially

propagate disconnected well hydraulic head measurements so that a continuous head

surface plot can be attained to examine groundwater flow in intermediate locations

between wells. The resulting continuity achieved increases one's understanding of the

true behavior of the aquifer and its interaction with its surroundings. But like any model,

careful calibration of the results with respect to real world data is required for proper

validation and trust in the model.

Numerical groundwater modeling. Groundwater modeling programs use either finite

difference (FD) or finite element (FE) numerical methods to model a grided area required

to be analyzed (40). The former centers the data points in the grid block, while the latter

places the data points at the corners of the grid block. The objective of both of these

methods is to transform the problem from partial differential equations (PDE) to one

having an algebraic representation. The general concept is shown in Figure B.19. The

method most commonly used in groundwater modeling is the finite difference approach,

since it provides the most direct route towards the solution.

To perform the FD method requires the translation of physical aquifer

characteristics to partial differential equations. The three most common groundwater

flow types modeled are: confined artesian conditions; leaky artesian conditions; and

water table conditions (40:36-39). In the first case, the modeled aquifer is confined by an

aquitard on both the top and the bottom. No leakage through the aquitard in assumed.

Furthermore, the hydraulic head measured from a tightly cased well is higher than the top

of the modeled aquifer (indicating an artesian condition). Assuming a two dimensional

Concepts of the physical system

Translate to

PDE, boundary and initial conditions

Finite-element approach

Finite-difference approach

Transform to

Integral equation

Subdivide region into a grid and apply FD approximations to space and time derivatives

Subdivide region into elements and integrate

First-order differential equations

Apply FD approximation to time derivative

System of algebraic equations

Solve by direct iterative methods

Solution

Figure B.19 Numerical Methods (40)

flow, the aquifer parameters required are the transmissivity, storativity, thickness, porosity and hydraulic conductivity. In the second case, the modeled aquifer is confined by a leaky aquitard which allows the seepage of water from the aquifer above it. In this case, the aquitard parameters are also required: its vertical hydraulic conductivity and thickness. The third case models an unconfined aquifer whose hydraulic head measurements indicate the water table. For example, the sand and gravel aquifer at TA C-64 is an unconfined aquifer. For these aquifers, a constant saturated thickness cannot be assumed, therefore, the hydraulic conductivity and specific storage (or specific yield) need to be measured. Most three dimensional groundwater modeling programs combine all three types of flow to simulate a multi-layer aquifer system.

Any grided aquifer area requires boundary conditions to define its limits. Three types of boundary conditions used in groundwater modeling are (40:40): constant

hydraulic head, specified flux, and value dependent flux. Constant hydraulic head boundaries include lakes, large rivers and constant stream stages. Specified flux boundaries include wells, drains, impermeable rock and groundwater divide. Value dependent flux include hydraulic head dependent leakage through an aquitard.

In addition to boundary conditions, initial conditions are required for each node in a finite difference mesh. Current hydraulic head measurements from wells serve as good initial conditions. For general analysis, regional piezometric level contour plots provide a rough approximation of initial conditions.

Once the aquifer system is characterized and the initial & boundary conditions are known, finite differencing is used to obtain algebraic equations from the groundwater flow equation. Finite differencing allows for the formulation of the groundwater flow problem in terms of a general matrix equation: $[A] (h) = (d)$, where A is a matrix representing storage & transmissivity, h is a vector of unknown head values at node points, and d contains the source terms and the known parts of storage. There are two methods of solving for h: the direct and the iterative method (39:2-26). Direct methods include solution by determinants, solution by successive elimination of unknowns, and matrix inversion. Iterative methods involve a systematic way of converging at the solution through guessing. There are numerous iterative methods used in groundwater modeling: successive over-relaxation, alternative direction implicit (ADI), iterative alternating direction implicit, strongly implicit procedure (SIP), and conjugate gradient (PCG) (40). In general groundwater modeling computer programs use iterative methods because it is efficient in terms of storage and computation time (especially for large

models). However, iterative methods require initial estimates, iteration parameters & tolerance levels, and the matrix must be well conditioned for adequate convergence upon the solution.

Basics of Contaminant Transport. The final hydraulic head output from the groundwater modeling feeds into contaminant transport. Contaminant transport is a useful tool for determining how under ground plume distributions spread spatially with respect to time. This insight helps in the development of remedial actions, and provides guidance for additional data collection and study.

The four major transport processes are: advection, dispersion, chemical reaction, and sorption (39). Advection is the transport of solute in the subsurface induced by the groundwater flow. Dispersion is the spreading of solute over a greater region than would be predicted solely from macroscopic groundwater velocity. Chemical reactions take into account radio active decay, biodegradation, and hydrolysis. Sorption is the mass transfer process between the contaminants dissolved in groundwater (solution phase) and the contaminants sorbed on porous media (solid phase). This includes the absorption of the solution phase into the porous media (i.e., the aquifer), the adsorption of the solution or the attraction of the solution to a surface, and ion exchange. Modeling these four major processes requires complete and thorough characterization of the initial contaminant plume and the quantification of complex chemical reactions.

The primary theory behind advection and dispersion is the conservation of mass with respect to contaminants. The statement for an elemental volume is: [net rate of change of mass of solute within the element] = [flux of solute out of the element] - [flux

of solute into the element] ± [loss or gain of solute mass due to reactions] (28:389). In

terms of the elemental CV (Figure B.20):
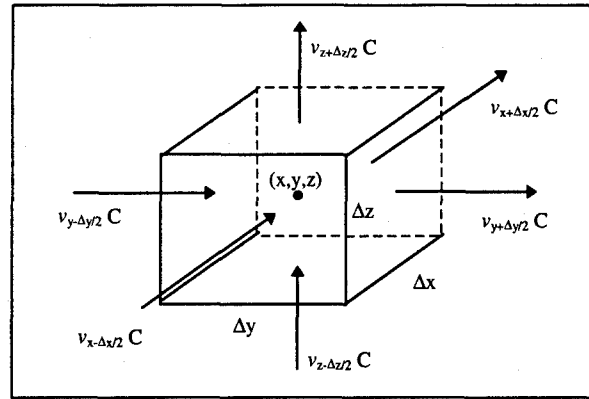
Figure B.20 Control Volume

for non reactive dissolved constituents in saturated, homogeneous, isotropic, materials,

under steady state flow conditions is (Equation B.12):

$$\frac{\partial C}{\partial t} = \left[D_x \frac{\partial^2 C}{\partial x^2} + D_y \frac{\partial^2 C}{\partial y^2} + D_z \frac{\partial^2 C}{\partial z^2} \right] - \left[\bar{v}_x \frac{\partial C}{\partial x} + \bar{v}_y \frac{\partial C}{\partial y} + \bar{v}_z \frac{\partial C}{\partial z} \right] \qquad (B.12)$$

C is the concentration of the contaminant (mass/unit volume of solution), D is the

dispersion coefficient, and v is the velocity of advective transport (specific

discharge/porosity). The first bracketed term on the right hand side is the transport due to

dispersion and the other bracketed term is the transport due to advection; Freeze and

Cherry provides a detailed derivation (28:550-551). The problem posed is to solve for the

contaminant concentration with respect to space and time, given the groundwater average

linear velocities and dispersion characteristics. Again, transport modeling programs such

as MT3D use finite difference techniques to transform the PDE into a series of algebraic equations for solution.

Dispersion is the sum of mechanical dispersion and molecular diffusion. Mechanical dispersion is the spread of solute as a result of the deviation of actual groundwater velocity from average "macroscopic" groundwater velocity (calculated by Darcy's law). To determine the characteristics of this dispersion requires experimental analysis of actual versus predicted velocities through the introduction of tracer dies into the groundwater. Molecular diffusion is the spread of solute as a result of only concentration variations. This is illustrated in Figure B.21.
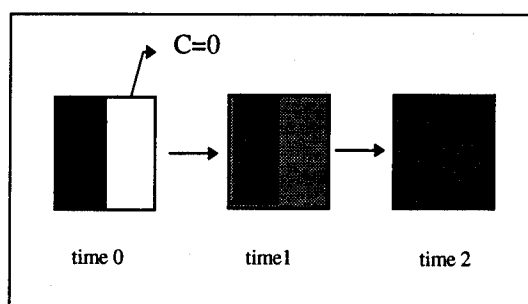
Figure B.21 Molecular Diffusion

The addition of dispersion allows one to model contaminant transport more realistically. Contaminant plumes do not propagate in sharp fronts with a set concentration (advection). They are more likely to propagate with a diffused concentration front with "fingering" produced by heterogeneity in the soil hydraulic conductivity (advection plus dispersion). Figure B.22 illustrates the latter point.
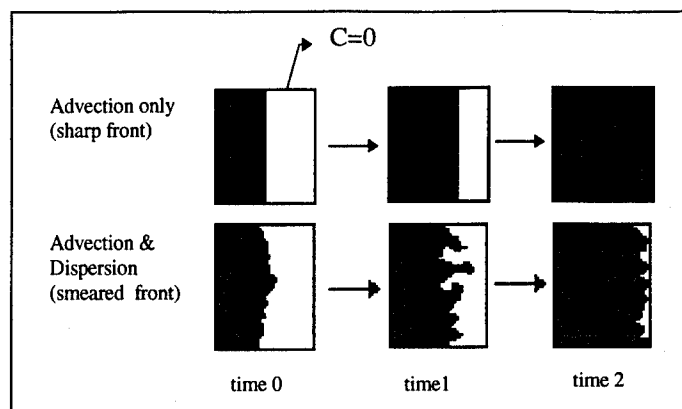
Figure B.22 Effect of Dispersion

Sorption plays a key part in a retarding or an advancing contaminant plume. In both cases, sorption has a retarding effect on the contaminant plume (28:402, 404). Advancing contaminant plumes are retarded because dissolved contaminants are sorbed on to the porous materials, leaving less contaminant mass to be transported. Retreating contaminant plumes are retarded because sorbed contaminants are desorbed into the dissolved phase, leaving more mass behind. The sorption term is incorporated into the advection-dispersion equation as flows (Equation B.13):

$$\frac{\partial C}{\partial t} = Dispersion + Advection - \frac{\rho_b \partial S}{n \partial t} \qquad \text{(B.13)}$$

The sorption term acts like a sink/source term where ρ_b is the bulk density of the porous media, and S is the mass of the chemical contaminant sorbed on the solid part of the porous medium pre unit mass of solid (mass of contaminant/ mass of solid porous media). dS/dt is the rate at which the contaminant is sorbed (units: 1/time). Empirical equations have been formulated to calculate S. The Freundlich isotherm equation states that: $S = (K_d C^a)$. K_d is the distribution coefficient (28:403). C is the solute

concentration. The superscript a characterizes the relationship between S and C on a log-log plot (e.g., a = 1 for a linear isotherm). The distribution coefficient is obtained empirically and represents the mass of the solute (i.e., contaminant) on the solid phase per unit mass of the solid phase divided by the concentration of the solute in the solution (units: length^3/mass). The concentration C is obtained from "known" initial conditions, and updated every time step in transport modeling programs.

Chemical reaction is also modeled in transport programs. Various empirical formulas have been formulated to capture major contaminant reactions with the porous media. The rate reaction term is incorporated into the transport model equation with the addition of the following term (Equation B.14):

$$\frac{\partial C}{\partial t} = Dispersion + Advection + Sorption - \left(\lambda_1 C + \lambda_2 \frac{\rho_b S}{n} \right) \qquad \text{(B.14)}$$

λ_1 and λ_2 are rate reaction constants for the sorbed and solid phase of the porous media (e.g., sand) respectively. For linear sorption, the rate constants are equal ($\lambda_1 = \lambda_2$). For radioactive decay $\lambda = \ln(2)/t_{1/2}$, where $t_{1/2}$ is the half life of the radioactive contaminant.

The formulation of the contaminant transport equation is complete. It incorporates dispersion, advection, sorption and chemical rate reaction. More detailed models exist for the transport of specific types of contaminants, but for general contaminant transport modeling Equation B.14 suffices.

The MT3D contaminant transport modeling program uses Equation B.14 as its basis for the finite difference formulation of transport problems. MODFLOW® groundwater flow output (valid only in saturated region) is used as the input into MT3D®.

MT3D needs this data for the propagation of the plume with respect to the flow field.
The link between groundwater modeling and transport modeling is now complete.

Unsaturated Groundwater Flow. As described in Bear and Verruijt (10),
unsaturated groundwater flow is characterized by the void space of the soil which is
partially filled with water and partially with air and is a region of two fluids, gas and
liquid, in the soil. As such, the moisture content, θ, and water saturation, S, can be
written as θ_w and S_w for the liquid (water) fluid and θ_a and S_a for the gas fluid (air).
Where θ_w and S_w as defined as

$$\theta_w = \frac{\text{Volume of water in Representitive Elementry Volume (REV)}}{\text{Volume of REV}}; \ 0 \leq \theta_w \leq n$$

$$S_w = \frac{\text{Volume of water in Representitive Elementry Volume (REV)}}{\text{Volume of Voids in REV}}; \ 0 \leq S_w \leq 1$$

and θ_a and S_a similarly defined for air.

The air-water interface creates free interfacial energy between them due to the
difference in attraction between air and water on the interface versus water-water or air-
air attractions on the interior of the fluids. This energy difference gives rise to interfacial
tension (surface tension) and a contact angle between the two fluids. This angle can be
readily seen after a car has just been waxed. The water beads up because the water
molecules have little attraction for air or the waxed surface of the car and greater
attraction for other water molecules. Wettability is a measure of the contact angle
between the two fluids and solids. If $\theta < 90$ the fluid is called the wetting fluid and if $\theta >$
90° the fluid is a non-wetting fluid.

Three ranges of water saturation between 0% and 100% can occur in an air-water-soil system. They are pendular saturation, funicular water saturation, and insular saturation

Pendular saturation is characterized by a saddle shape water-air interface where no water flow is possible because the water phase is not continuos. For funicular water saturation, the water and air phases are continuos and water flow is possible. Finally, for insular saturation only the water phase is continuos, flow is possible, and the air phase forms bubbles which may or may not be able to move.

Because of the different forces of attractions between air and water in unsaturated flow, a difference of pressure exists between them. The difference in pressure is called capillary pressure and is denoted, $P_c = P_{air} - P_{water}$. This gives rise to a new definition of piezometric head for unsaturated flow often called capillary head (ϕ_c).

$$\phi_c = z + P_w/\gamma_w = z - P_c/\gamma_w = z - h_c$$

Where h_c is the capillary pressure head, and γ_w is the volumetric weight of water. Additionally, suction, ψ, is defined as the negative of the pressure head.

In unsaturated flow the retention of water in the soil during drainage generates a retention cure (or desorption curve) and shows how capillary forces hold water in the soil against gravity. In addition, to water retention, the filling of water into the void space gives rise to wetting curves (or sorption curves). The difference in wetting and drying curves is termed hysteresis.

Other terms used in unsaturated groundwater flow are field capacity and specific yield. Field capacity, as defined by Bear and Verruijt, is that value of water content remaining in a volume of soil after downward gravity drainage has ceased, or materially done so, after a period of rain or excess irrigation (10:135). Bear and Verruijt define specific yield as the volume of water drained from a soil column of the unit horizontal area extending form the water table to the ground surface, per unit lowering of the water table.

Now that the ground work has been laid for the motion equations for the air and water phases in unsaturated flow are given as

$$q_w = -\frac{k_w(S_w)}{\mu_w}\gamma_w \cdot \nabla\phi_w = -K_w(S_w) \cdot \nabla\phi_w$$

$$q_a = -\frac{k_a(S_a)}{\mu_a}\gamma_a \cdot \nabla\phi_a = -K_a(S_a) \cdot \nabla\phi_a$$

where K_w and K_a are the effective hydraulic conductivities. Finally for vertical water flow (the area of concern for this study)

$$q_{wz} = -D_w(\theta_w)\frac{\partial\phi_w}{\partial z} - K_w(\theta_w) \qquad \text{where} \quad D_w(\theta_w) = -K_w(\theta_w)\frac{d\psi}{d\theta_w}$$

B.6 Infil Program

Infil is a water infiltration program from the international groundwater modeling center (IGWMC) originally developed by M. Vauclin (38) and provided in both FORTRAN and BASIC computer language formats. The original version of Infil has been modified by Aly I. El-Kadi in 1983. El-Kadi has added two addition sets of soil properties from Brutsaert and Brooks and Corey. Below is a description of the Infil program including equations from Aly I. El-Kadi's modified program.

The Infil program is based on three functional solutions to the Richard's equation

$$C(h)\frac{\partial h}{\partial t} = \frac{\partial}{\partial z}\left[K(h)\left(\frac{\partial h}{\partial z} - 1\right)\right]$$

where C(h) is $d\theta/dh$, moisture capacity, θ is volumetric water content, h is pressure head, t is time, z is the vertical coordinate (positive downward), and K is unsaturated hydraulic conductivity. The three functions are based on Philip's solution in 1957 of the Richard's equation (38):

$$z(\theta,t) = \sum_{m=1}^{M} f_m(\theta) \cdot t^{m/2}$$

where M is the number of terms in the series solution and the function $f_m(\theta)$ can be solved by a number of differential equations. The functions used by Aly I. El-Kadi for the Philip's solution of the Richard's equation are

Vauclin et. al.

$$C(h) = \frac{d\theta}{dh} = \frac{\alpha\left(\theta_s - \theta_r\right)\beta\left[\ln(|h|)\right]^{\beta-1}}{h\left(\alpha + \left[\ln(|h|)\right]^{\beta}\right)^2}$$

B-67

$$K = K_s \frac{A}{A + |h|^B}$$

$$\theta = \frac{\alpha \left(\theta_s - \theta_r\right)}{\alpha + \left[\ln(|h|)\right]^\beta} + \theta_r \qquad\qquad \text{for h < -1 cm}$$

$$\theta = \theta_s \qquad\qquad \text{for h} \geq \text{-1 cm}$$

Where θ is the water content at section h, θ_s is the saturated residual water content, θ_r is the residual water content, K is the unsaturated hydraulic conductivity, K_s is the saturated hydraulic conductivity, and α, β, A and B are soil parameters.

Brutsuert

$$C(h) = \frac{d\theta}{dh} = \frac{ab\left(\theta_s - \theta_r\right)|h|^{b-1}}{\left(a + |h|^b\right)^2}$$

$$K = K_s \left[\frac{a}{a + |h|^b}\right]^N$$

$$\theta = \frac{a\left(\theta_s - \theta_r\right)}{a + |h|^b} + \theta_r \qquad\qquad \text{for h < 0}$$

$$\theta = \theta_s \qquad\qquad \text{for h} \geq 0$$

Where a, b, and N are parameters of the Brutsaert model.

Brooks and Corey

$$C(h) = \frac{d\theta}{dh} = \lambda\left(\frac{h_p}{h}\right)^{\lambda'} \frac{1}{h}\left(\theta_s - \theta_r\right)$$

$$K = K_s \left(\frac{h_p}{h}\right)^\eta$$

$$\theta = \left(\frac{h_p}{h}\right)^{\lambda'} (\theta_s - \theta_r) + \theta_r, \qquad\qquad \text{for } h > h_p$$

$$\theta = \theta_s \qquad\qquad \text{for } h \leq h_p$$

Infil Output. Below is the output of the Infil program with the parameters outlined in the implementation section of Chapter B Groundwater.

```
C-64 Infiltration Problem

INPUT DATA ARE: AKS= 10.08
WCS= .5    WCR= .06
WCI= .1    WC1= .5
NO. OF WATER CONTENT INCREMENTS= 44
TOTAL TIME OF SIMULATION= 36

PARAMETERS OF THE BROOKS & COREY FUNCTIONS ARE:
    HP= 41    F11= 3.74

SOLUTION CONVERGENCE:

 NO. OF ITERATIONS              ERROR

        1                   -161.01364
        2                     42.96512
        3                    -44.72661
        4                     44.97097
        5                   -127.24707
        6                    131.76306
        7                    -15.09120
        8                      4.03303
        9                     -1.14880
       10                      0.34635
       11                     -0.10238
       12                      0.03053
       13                     -0.00918


           ------------------
           SIMULATION RESULTS
           ------------------


 SORPTIVITY= 4.718328   S1= 5.236188   S2= 3.171824
                             S3= 1.123465

HYDRAULIC PROPERTIES OF SOIL:

    TETA     PRESS     CONDUC     DIFU     CAP
```

```
0.491    41.230    9.36291    239.531    0.03909
0.482    41.465    8.68316    228.226    0.03805
0.473    41.708    8.03954    217.225    0.03701
0.464    41.957    7.43088    206.528    0.03598
0.455    42.213    6.85599    196.131    0.03496
0.445    42.477    6.31370    186.034    0.03394
0.436    42.749    5.80290    176.234    0.03293
0.427    43.029    5.32242    166.729    0.03192
0.418    43.319    4.87116    157.518    0.03092
0.409    43.617    4.44803    148.599    0.02993
0.400    43.926    4.05192    139.969    0.02895
0.391    44.246    3.68176    131.627    0.02797
0.382    44.576    3.33650    123.570    0.02700
0.373    44.919    3.01510    115.797    0.02604
0.364    45.275    2.71653    108.305    0.02508
0.355    45.644    2.43978    101.091    0.02413
0.345    46.029    2.18385     94.155    0.02319
0.336    46.429    1.94777     87.493    0.02226
0.327    46.846    1.73058     81.103    0.02134
0.318    47.281    1.53133     74.983    0.02042
0.309    47.737    1.34909     69.129    0.01952
0.300    48.214    1.18295     63.541    0.01862
0.291    48.714    1.03202     58.214    0.01773
0.282    49.240    0.89542     53.147    0.01685
0.273    49.794    0.77230     48.336    0.01598
0.264    50.379    0.66182     43.778    0.01512
0.255    50.998    0.56316     39.472    0.01427
0.245    51.655    0.47552     35.413    0.01343
0.236    52.353    0.39811     31.599    0.01260
0.227    53.100    0.33019     28.026    0.01178
0.218    53.899    0.27101     24.691    0.01098
0.209    54.759    0.21985     21.590    0.01018
0.200    55.688    0.17601     18.720    0.00940
0.191    56.696    0.13883     16.076    0.00864
0.182    57.798    0.10764     13.656    0.00788
0.173    59.009    0.08183     11.453    0.00714
0.164    60.351    0.06079      9.465    0.00642
0.155    61.851    0.04394      7.687    0.00572
0.145    63.545    0.03074      6.112    0.00503
0.136    65.485    0.02066      4.736    0.00436
0.127    67.743    0.01320      3.553    0.00371
0.118    70.424    0.00790      2.557    0.00309
0.109    73.697    0.00433      1.739    0.00249
0.100    77.845    0.00210      1.093    0.00192
```

TIME= 3.2E-01   HOURS
INFILTATION AMOUNT= 5.005 CM
INFILTATION RATE= 12.819   CM/HR

WATER CONTENT PROFILE AT TIME= 3.2E-01 HOURS:

    Z (CM)   TETA   Z (CM)   TETA

Z (CM)	TETA	Z (CM)	TETA
0.000	0.500	2.648	0.491
4.566	0.482	5.977	0.473
7.034	0.464	7.842	0.455
8.476	0.445	8.984	0.436
9.404	0.427	9.760	0.418
10.068	0.409	10.342	0.400
10.588	0.391	10.813	0.382
11.022	0.373	11.216	0.364
11.399	0.355	11.571	0.345
11.733	0.336	11.887	0.327
12.032	0.318	12.170	0.309
12.300	0.300	12.424	0.291
12.540	0.282	12.651	0.273
12.755	0.264	12.854	0.255
12.946	0.245	13.034	0.236
13.116	0.227	13.194	0.218
13.267	0.209	13.336	0.200
13.401	0.191	13.462	0.182
13.520	0.173	13.574	0.164
13.627	0.155	13.677	0.145
13.727	0.136	13.779	0.127
13.840	0.118	13.935	0.109
13.586	0.100	0.000	0.000

```
TIME=   7.9E-01    HOURS
INFILTATION AMOUNT= 11.318   CM
INFILTATION RATE= 13.910   CM/HR
```

WATER CONTENT PROFILE AT TIME= 7.9E-01 HOURS:

Z (CM)	TETA	Z (CM)	TETA
0.000	0.500	9.567	0.491
15.668	0.482	19.485	0.473
21.809	0.464	23.170	0.455
23.922	0.445	24.300	0.436
24.457	0.427	24.494	0.418
24.473	0.409	24.435	0.400
24.401	0.391	24.384	0.382
24.389	0.373	24.418	0.364
24.468	0.355	24.538	0.345
24.624	0.336	24.722	0.327
24.829	0.318	24.943	0.309
25.060	0.300	25.178	0.291
25.297	0.282	25.413	0.273
25.526	0.264	25.635	0.255
25.740	0.245	25.841	0.236
25.936	0.227	26.026	0.218
26.111	0.209	26.192	0.200
26.267	0.191	26.339	0.182
26.407	0.173	26.472	0.164

```
      26.535    0.155              26.597    0.145
      26.661    0.136              26.734    0.127
      26.840    0.118              26.976    0.109
      25.972    0.100               0.000    0.000
```

TIME= 1.5E+00   HOURS
INFILTATION AMOUNT= 22.136 CM
INFILTATION RATE= 16.393 CM/HR

WATER CONTENT PROFILE AT TIME= 1.5E+00 HOURS:

Z (CM)	TETA	Z (CM)	TETA
0.000	0.500	26.550	0.491
42.106	0.482	50.618	0.473
54.697	0.464	56.062	0.455
55.840	0.445	54.756	0.436
53.274	0.427	51.678	0.418
50.136	0.409	48.742	0.400
47.539	0.391	46.539	0.382
45.737	0.373	45.117	0.364
44.657	0.355	44.334	0.345
44.126	0.336	44.011	0.327
43.970	0.318	43.987	0.309
44.047	0.300	44.139	0.291
44.253	0.282	44.381	0.273
44.516	0.264	44.656	0.255
44.794	0.245	44.930	0.236
45.062	0.227	45.188	0.218
45.308	0.209	45.422	0.200
45.530	0.191	45.634	0.182
45.733	0.173	45.830	0.164
45.928	0.155	46.030	0.145
46.144	0.136	46.294	0.127
46.562	0.118	46.751	0.109
44.259	0.100	0.000	0.000

TIME= 2.6E+00   HOURS
INFILTATION AMOUNT= 41.735 CM
INFILTATION RATE= 20.149 CM/HR

WATER CONTENT PROFILE AT TIME= 2.6E+00 HOURS:

Z (CM)	TETA	Z (CM)	TETA
0.000	0.500	66.160	0.491
102.623	0.482	120.401	0.473
126.716	0.464	126.275	0.455
122.117	0.445	116.172	0.436
109.637	0.427	103.224	0.418
97.330	0.409	92.150	0.400
87.751	0.391	84.121	0.382

```
81.207    0.373              78.931    0.364
77.208    0.355              75.951    0.345
75.079    0.336              74.518    0.327
74.205    0.318              74.084    0.309
74.107    0.300              74.236    0.291
74.440    0.282              74.694    0.273
74.977    0.264              75.276    0.255
75.579    0.245              75.878    0.236
76.168    0.227              76.447    0.218
76.711    0.209              76.963    0.200
77.202    0.191              77.431    0.182
77.653    0.173              77.873    0.164
78.099    0.155              78.344    0.145
78.633    0.136              79.032    0.127
79.790    0.118              79.910    0.109
74.063    0.100               0.000    0.000
```

TIME= 4.2E+00   HOURS
INFILTATION AMOUNT= 78.511   CM
INFILTATION RATE= 25.541   CM/HR

WATER CONTENT PROFILE AT TIME= 4.2E+00 HOURS:

Z (CM)	TETA	Z (CM)	TETA
0.000	0.500	156.247	0.491

TIME= 6.6E+00   HOURS
INFILTATION AMOUNT=149.456   CM
INFILTATION RATE= 33.213   CM/HR

WATER CONTENT PROFILE AT TIME= 6.6E+00 HOURS:

Z (CM)	TETA	Z (CM)	TETA
0.000	0.500	358.511	0.491

TIME= 1.0E+01   HOURS
INFILTATION AMOUNT=289.576   CM
INFILTATION RATE= 44.149   CM/HR

WATER CONTENT PROFILE AT TIME= 1.0E+01 HOURS:

Z (CM)	TETA	Z (CM)	TETA
0.000	0.500	809.723	0.491

TIME= 1.6E+01   HOURS
INFILTATION AMOUNT=572.003   CM
INFILTATION RATE= 59.812   CM/HR

WATER CONTENT PROFILE AT TIME= 1.6E+01 HOURS:

Z (CM)	TETA		Z (CM)	TETA
0.000	0.500		1813.445	0.491

TIME= 2.4E+01   HOURS
INFILTATION AMOUNT=%1151.373 CM
INFILTATION RATE= 82.377 CM/HR

WATER CONTENT PROFILE AT TIME= 2.4E+01 HOURS:

Z (CM)	TETA		Z (CM)	TETA
0.000	0.500		4044.420	0.491

TIME= 3.6E+01   HOURS
INFILTATION AMOUNT=%2358.015 CM
INFILTATION RATE=115.067 CM/HR

WATER CONTENT PROFILE AT TIME= 3.6E+01 HOURS:

Z (CM)	TETA		Z (CM)	TETA
0.000	0.500		9004.721	0.491

PROFILE AT INFINITY:

Z (CM)	TETA		Z (CM)	TETA
0.000	0.500		8.964	0.491
11.925	0.482		13.684	0.473
14.929	0.464		15.887	0.455
16.662	0.445		17.311	0.436
17.867	0.427		18.352	0.418
18.780	0.409		19.163	0.400
19.507	0.391		19.820	0.382
20.105	0.373		20.366	0.364
20.607	0.355		20.829	0.345
21.035	0.336		21.226	0.327
21.404	0.318		21.570	0.309
21.725	0.300		21.870	0.291
22.005	0.282		22.132	0.273
22.251	0.264		22.362	0.255
22.466	0.245		22.564	0.236
22.656	0.227		22.741	0.218
22.821	0.209		22.896	0.200
22.967	0.191		23.032	0.182
23.094	0.173		23.151	0.164
23.205	0.155		23.256	0.145
23.305	0.136		23.352	0.127
23.401	0.118		23.458	0.109
23.458	0.100		0.000	0.000

Appendix C.   Risk Analysis Appendix

C.1   Risk Equations

Residential Risk

Carcinogenic Risk

Soil Ingestion: Rs = (SFo)(Cs)(EF)[(0.08)(IRs$_{0-5}$)(ED$_{0-5}$) +
               (0.92)(IRs)(ED)], See Note 1

Water Ingestion: Rw = (SFo)(Cw)(IRw)(EF)(ED)

Irradiation: Re = (SFe)(Cs)(ED)(1-Se)(Te)

Inhalation: Ri = (SFi)(Cs)(IRi)(EFi)(ED)(ML)

Total Residential Risk: Rt = Rs + Rw + Re + Ri

Non-carcinogenic Hazard Index

Soil Ingestion HI = [(Cs)(EF)/(365 days)(360 pCi/micro-g)][(0.08)(IRs$_{0-5}$)/(BW$_{0-5}$) +
(0.18)(IRs)/(BW$_{6-18}$) + (0.74)(IRs)/(BW$_{19-75}$)]/(RfD), See Note 2

Water Ingestion HI = [(Cw)(EF)(IRw)/(365 days)(360 pCi/micro-g)][(0.08)/(BW$_{0-5}$) +
(0.18)/(BW$_{6-18}$) + (0.74)/(BW$_{19-75}$)]/(RfD)

Inhalation HI = [(Cs)(EFi)(IRi)(ML)/(365 days)(360 pCi/micro-g)][(0.08)/(BW$_{0-5}$) +
(0.18)/(BW$_{6-18}$) + (0.74)/(BW$_{19-75}$)]/(RfD)

Note 1: The 0.08 and 0.74 multipliers represent the percentage of the population that fall within the respective age categories. These percentages were determined from the 1990 Census for the county where the site is located (16).

Note 2: The 0.08, 0.18, and 0.92 multipliers represent the percentage of the population that fall within the respective age categories. These percentages were determined from the 1990 Census for the county where the site is located (16).

SFo = Oral cancer slope factor (risk/pCi)
SFe = External cancer slope factor (risk/yr per pCi/g)

SFi = Inhalation cancer slope factor (risk/pCi)
RfD = Reference dose (mg/Kg-day)
Cs = Radionuclide concentration in soil (pCi/g)
Cw = Radionuclide concentration in water (pCi/L)
Csrca = Radionuclide concentration in RCA soil (pCi/L)
OD = Occupational exposure duration (yrs)
OIRi = Occupational Inhalation rate (m^3/day)
OEF = Occupational exposure frequency (days/yr)
OEFi = Occupational inhalation exposure frequency (days/yr)
OTe = Occupational gamma exposure time factor (unitless)
OTerca = Occupational gamma exposure time factor in RCA (unitless)
ED = Exposure duration (yrs)
ED_{0-5} = Exposure duration for children 0 through 5 years (yrs)
IRs_{0-5} = Soil ingestion rate for children 0 through 5 years (g/day)
IRs = Soil ingestion rate for people 5 years and older (g/day)
IRw = Water ingestion rate (L/day)
IRi = Inhalation rate (m^3/day)
EF = Exposure frequency (days/yr)
EFi = Inhalation exposure frequency (days/yr)
Se = Gamma shielding factor (unitless)
Te = Gamma exposure time factor (unitless)
ML = Mass loading factor (g/m^3)
BW_{0-5} = Body weight for people 0 through 5 years (Kg)
BW_{6-18} = Body weight for people 6 through 18 years (Kg)
BW_{19-75} = Body weight for people 19 through 75 years (Kg)

Occupational Risk

Carcinogenic Risk

Soil Ingestion: Rs = (SFo)(Cs)(IR)(OEF)(OD)

Irradiation: Re = (SFe)[(Cs)(OTe) + (Csrca)(OTerca)](OD)(1-Se)

Inhalation: Ri = (SFi)(Cs)(OIRi)(OEFi)(OD)(ML)

Total Occupational Risk: Rt = Rs + Re + Ri

Non-carcinogenic HI

Soil Ingestion HI = [(Cs)(OEF)(IRs)/(365 days)(360 pCi/micro-g)(BW_{19-75})]/RFD

Inhalation HI = [(Cs)(ML)(OEFi)(IRi)/(365 days)(360 pCi/micro-g)(BW_{19-75})]/RFD

C.2   Probability Density Function

Explanation

Residential pdf's

Slope Factors (SF). All slope factors used in the calculations are taken directly from the 1992 HEAST as deterministic values. The HEAST values were derived from various studies on radiation effects on human populations. The full description of their method of derivation is discussed in the HEAST; however, the HEAST did not provide enough information to build a pdf of the slope factor. Since we considered all activity emanating from depleted uranium, we used a weighted average slope factor equivalent of 99.8% U-238 and 0.2% U-235.

Reference Dose (RfD). The RfD used was for uranium based soluble salts from a rabbit bioassay in the 1992 HEAST and is treated as a deterministic value.

Soil Concentration (Cs):

The soil concentration distribution generated from the soil modeling step is used as the pdf for the area outside the RCA. A risk assessment was performed for three different Cs pdf's -- background, mean, and maximum. Background uranium concentrations were measured between 1 and 3 pCi/g. We used a uniform pdf to model the background concentration, U[0,3] pCi/g. In the modeling step, kriging yielded different pdf's at each kriging node. The other two Cs pdf's were the mean and the maximum from the kriging nodes -- LN[27.5,17.75] and LN[35.3,7.8] respectively.

Water Concentration (Cw).   The water concentration was developed in the

modeling step and is U[0-61] pCi/L.

Exposure Durations (ED and ED$_{0-5}$).   ED is meant to characterize the duration

that people live at one residence, thus the time exposed to the hazard. The Exposure

Duration pdf is based on the 1983 Annual Housing Survey, a joint publication from the

U.S Department of Housing and Urban Development and the Bureau of the Census (61).

This report presents housing characteristics by dividing the United States into four

geographic regions -- west, midwest, northeast, and south. Since Eglin AFB is in Florida,

we used the data from the south region. The report further breaks down housing data

within regions by people residing in a central city and people residing outside a central

city. We assumed that the data of people residing outside a central city was more

appropriate because of the rural nature of the surrounding area. We fit this data using the

Weibull probability paper to determine if the data could be represented by a Weibull

distribution. A straight line went through the data almost perfectly. The shape parameter

was 1 and the scale parameter was 9. A Weibull distribution with shape parameter one is

just an exponential distribution with the scale parameter completely characterizing the

distribution. The 50th and 95th percentiles of the resulting distribution are 6.4 and 27

years respectively.

The same analysis was performed on the data presented in the EPA Exposure

Factors Handbook for the entire United States. These data also fit a straight line well and

had shape and scale parameters of 1 and 13 years respectively. The 50th and 90th

percentiles are 9 and 30 years respectively, as reported by the EPA. Since the EPA data

applies to the United States as a whole, we believe using region specific data was more appropriate. Exposure duration for people 0 through 5 years, ED_{0-5} is the same as ED, however it is truncated at 5 years.

Soil Ingestion Rates (IRs and IRs$_{0-5}$). This random variable is meant to characterize the daily amount of soil inadvertently ingested. Several studies have estimated the amount of soil ingestion. The range of soil ingestion from these studies are from zero to 10,000 mg/day. The studies focus on different age groups and different propensities of ingesting soil. The data indicate that children 0 to 5 years of age ingest much more soil than do people older than 5 years. Consequently, we found it impossible to develop a single pdf to characterize the entire population without being over or under conservative for the two age groups described above. Therefore, we decided to develop a different pdf for each. We decided to weight the risk due to soil ingestion of each age group by the proportion of people in the corresponding groups. Based on the 1990 census for Okaloosa county (county where TA-C64 is located), 8% of the population was made up of children 0 to 5 years of age. We also chose to use data from studies that focused on children with an intermediate tendency to ingest soil. Therefore, children who exhibit pica were not accounted for.

We decided to model the 0 to 5 year age group with a lognormal pdf because most of the data seemed to fall below 200 mg/day, but higher rates were recorded. A skewed lognormal has the ability to model this behavior. Another factor considered was the lognormal's requirement for a positive domain (no negative ingestion rates). The resulting pdf is LN[0.1,0.065] g/day

The data for second age group seemed to fall in-between 0 mg/day and 10 mg/day with equal probability. Therefore, we modeled the soil ingestion rate of this age group with a uniform pdf U[0,0.01] g/day.

Water Ingestion Rate (IRw). Water ingestion rate characterizes water consumed in the form of coffee, juices and other beverages containing tap water. The EPA's Exposure Factors Handbook gives an overview of water consumption studies by the National Academy of Sciences, the National Cancer Institute, the U.S. Department of Agriculture, the Food and Drug Administration, the International Commission on Radiological Protection, and several others (58). The adult drinking water consumption rate from these studies range from 0.26 L/day to 2.80 L/day, with the average being 1.4 L/day. Using the data from these studies, we developed a lognormal pdf, LN[1.4,0.25] L/day.

Inhalation Rate (IRi). For the daily inhalation rate, we chose to use the criteria described in the EPA Exposure Factors Handbook (1989) (58). In this study, the EPA estimated the average amount of time spent each day at different activity levels: resting, light, moderate, and heavy activity. The EPA also measured ventilation rate ranges for each of these activity levels according to different weight and sex classes. We considered the male adult, female adult, 6-year old, and 10-year old ventilation rates and matched them up with the average daily activity times to develop four different inhalation rate ranges. We found the children's inhalation rate did not differ significantly from the adults', so we used the adult male and female data to form our distribution. We assumed an equal number of males and females so that we could use the average between their two

inhalation ranges for our estimate. The females had an average inhalation rate of 11.8 m^3/day and the males had an average rate of 21 m^3/day. We decided to use 17 m^3/hr as our average. Both males and females had a variance of about 6.5 m^3/day so we used this for our variance. We decided to model this with a lognormal distribution, LN(17, 6.5) m^3/day. The ICRP (1981) recommends an average of 22 m^3/day while the USEPA (1985) suggests an average of 14 m^3/day. We believe our average of 17 m^3/day is a good representation of the studies done as well as a good compromise between these two recommendations.

Exposure Frequency (EF and EFi). The exposure frequency (EF) is a measure of how many days per year that people will be exposed to the hazard. We decided to treat this parameter as a deterministic value of 350 day/year. We thought it reasonable to assume most people will be a their residence most of the year, except vacations, business trips, and other miscellaneous reasons. For the inhalation exposure frequency (EFi), we wanted to use the days per year that did not have significant rainfall, since rainfall washes the particulate out of the air. We used the local weather data over a 10 year period from April 1981 to March 1991, and found that the average number of days with rainfall over .25 inches was 60 days. This leaves 305 days in a year that may have significant contaminant particulate in the air. Since the amount of rain in any particular year is variable, and the EPA default value is a high 350 days, we decided to model this frequency by a normal distribution N[305,15] days/yr. This puts our three sigma value at 350 days.

Gamma Shielding Factor (Se). Se refers to the attenuation of radiation fields due to shielding (by structures, terrain, etc.). Although we believe that it would vary considerably depending on the structures built on the contaminated area, we did not find any particular studies on this factor, so we decided to use the EPA Superfund default value of 0.2.

Gamma Exposure Time Factor (Te). Te refers to the fraction of the day that a person is exposed to the external radiation. For the residential case, we decided to assume exposure throughout the day, therefore Te value of 1.0.

Mass Loading (ML). This variable was determined in the air concentration modeling section. We will use a uniform distribution U[3.3E-5, 1.2E-4] g/m^3.

Body Weight (BW_{0-5}, BW_{6-18}, and BW_{19-75}). Body weight pdf's were developed from percentile data in the EPA 1989 Exposure Factors Handbook (58) for 0-5, 6-18, and 19-75 year groups. Male and female body weights were averaged for each age group. Lognormal distributions were fitted to the body weight percentiles for each age group -- 0-5 years LN[14.4,2.5] Kg, 6-18 years LN[43.4,2.5] Kg, and 19-75 years LN[70,12] Kg.

Occupational pdf's

Slope Factors (SF). Same as the residential case.

Reference Dose (RfD).   Same as the residential case.

Soil Concentration (Cs and Csrca). The Cs pdf's are the same as the residential case. The soil concentration within the RCA, Csrca, was modeled by calculating the sample mean and variance from measurements taken in the RCA over the years. A

lognormal distribution was assumed around the sample statistics giving us a distribution of LN[4246, 18821] pCi/g.

Occupational Duration (OD). This pdf was developed using the same methodology as the ED variable. Except we used the 1974-1985 Bureau of Labor statistics on the duration a worker stays at one job. The resulting pdf is a three parameter Weibull W[0.6,0.6,1], where the first, second, and third parameters are the shape, scale, and location parameters respectively.

Soil Ingestion Rate (IRs). Same as the residential case.

Occupational Inhalation Rate (OIRi). For an inhalation rate, we used the studies contained in the EPA Exposure Factors Handbook (58). These studies provided a low, average, and high range for inhalation rates for different age and sex groups, as well as the rates for different levels of activity. We chose to use the values for light activity for a male adult with an 8-hour workday duration. Light activity includes basic indoor activities and non-strenuous walking. We felt this corresponded with the type of physical activity at the site. We chose to use the adult male because only adults work at the site, almost all the people currently working at the site are male, and the male rates are a little more conservative than the female. We used the average male adult light activity inhalation rate as our mean and the high inhalation rate as our 99th percentile value and fit the data to a lognormal distribution of LN[6.6, 2.0] m^3/day.

Occupational Exposure Frequencies (OEF and OEFi). The occupational exposure frequency (OEF) for the site workers consists of the number of days they work at the site each year. The average work year has 260 days and about 30 days of this can

be excluded due to holidays and vacations. We decided to model this parameter with a point estimate of 230 days. Since particulate matter in the air is usually washed out by rain, we decided to model this occupational exposure frequency for inhalation (OEFi) by taking into account the number of rainy days at Eglin AFB. We obtained the climatic data on the area and found that it rained over 0.25 inches about 16% of the days. Since we determined the average number of working days is 230, we subtracted 16% of these working days and added a standard deviation of 15 days to account for variability in the number of rainy days. We used a normal distribution to model this to show equal probability of higher and lower values with the majority falling near our mean. The final distribution is N[192, 15] days/yr.

Gamma Shielding Factor (Se). Same as the residential case.

Occupational gamma exposure Time Factors (OTe and Oterca). This factor describes the fraction of the day a person is exposed to the irradiation from the soil. We spoke with a supervisor at the site to find good estimates as to the amount of time spent in the RCA and on the grounds around the RCA. From our conversation, the best estimates we could develop were 25% of the work time is spent on the grounds surrounding the RCA and 1.5% of the time in the RCA itself. Assuming an 8-hour work day, this gives us point estimates of 2/24 for Tes and 0.12/24 for Terca.

Mass Loading (ML). Same as the residential case.

Body Weight for people 19 through 75 years (BW$_{19-75}$). Same as the residential case.

C.3   Risk Assessment Output

This section contains the Crystal Ball® output for each risk assessment

calculation. For each run the following is included: a sensitivity chart of the risk

variables, summary statistics, cumulative distribution chart, and percentiles of the risk or
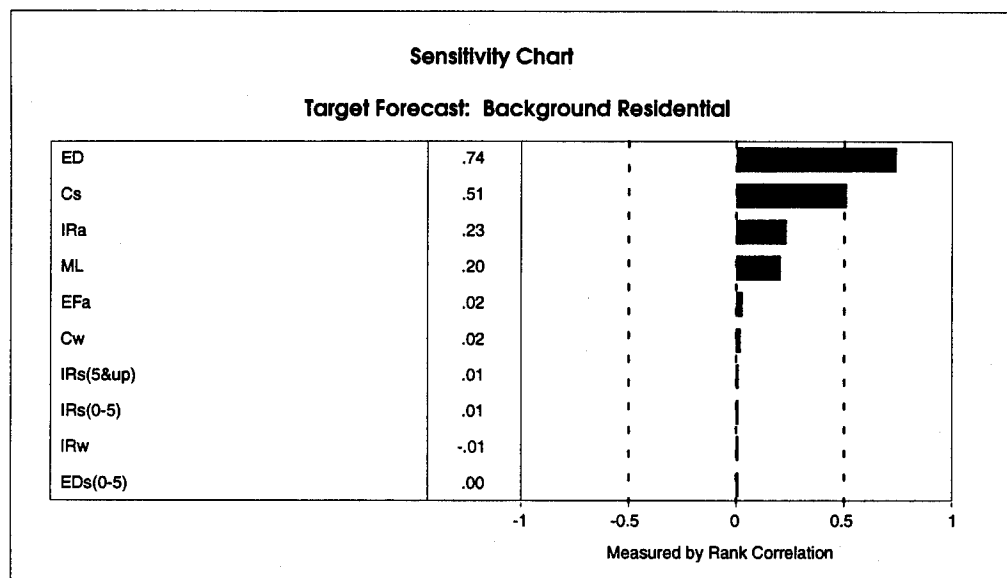
hazard.

Sensitivity Chart

Target Forecast: Background Residential

Variable	Value
ED	.74
Cs	.51
IRa	.23
ML	.20
EFa	.02
Cw	.02
IRs(5&up)	.01
IRs(0-5)	.01
IRw	-.01
EDs(0-5)	.00

Measured by Rank Correlation

Figure C.1 Sensitivity Chart: Background Residential

Forecast: Background Residential

Summary:
    Display Range is from 0.00E+0 to 7.00E-7 Risk/person
    Entire Range is from 5.66E-12 to 2.66E-6 Risk/person
    After 15,000 Trials, the Std. Error of the Mean is 1.64E-9

Statistics:	Value
Trials	15000
Mean	1.36E-07
Median (approx.)	6.40E-08
Mode (approx.)	1.33E-08
Standard Deviation	2.01E-07
Variance	4.04E-14
Skewness	3.53E+00
Kurtosis	2.19E+01
Coeff. of Variability	1.48E+00
Range Minimum	5.66E-12
Range Maximum	2.66E-06
Range Width	2.66E-06
Mean Std. Error	1.64E-09

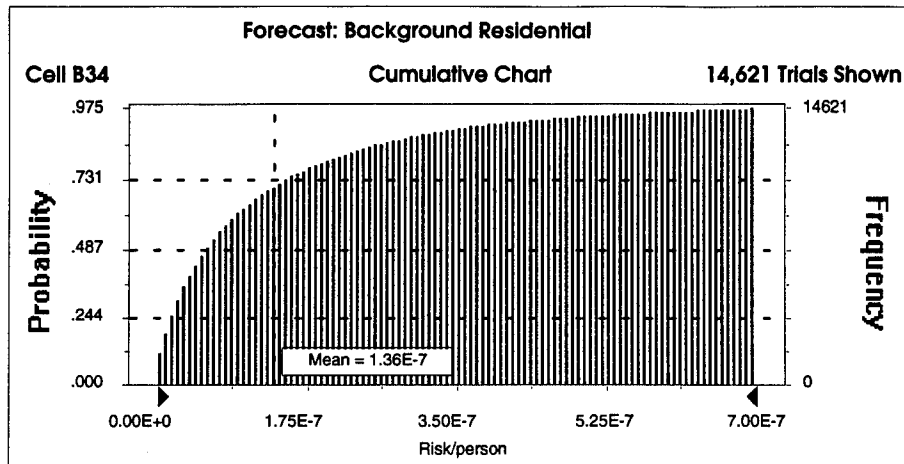Table C.1 Forecast: Background Residential

Figure C.2 Forecast: Background Residential (Cumulative)

Forecast: Background Residential (cont'd)	
Percentiles:	
Percentile	Risk/person (approx.)
0%	5.66E-12
10%	6.46E-09
20%	1.51E-08
30%	2.66E-08
40%	4.26E-08
50%	6.40E-08
60%	9.36E-08
70%	1.38E-07
80%	2.07E-07
90%	3.49E-07
100%	2.66E-06

Table C.2 Forecast: Background Residential (Percentiles)

Sensitivity Chart

Target Forecast: Average Residential

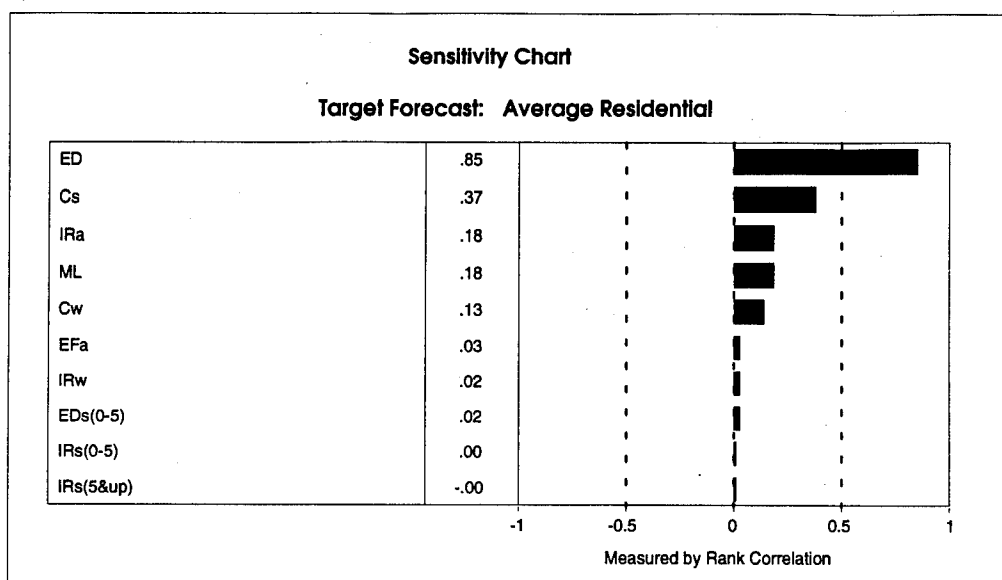|		
ED	.85	
Cs	.37	
IRa	.18	
ML	.18	
Cw	.13	
EFa	.03	
IRw	.02	
EDs(0-5)	.02	
IRs(0-5)	.00	
IRs(5&up)	-.00	

Measured by Rank Correlation

Figure C.3 Sensitivity Chart: Average Residential

Forecast: Average Residential

Summary:
Display Range is from 0.00E+0 to 1.50E-6 Risk/person
Entire Range is from 1.11E-10 to 1.68E-5 Risk/person
After 15,000 Trials, the Std. Error of the Mean is 3.79E-9

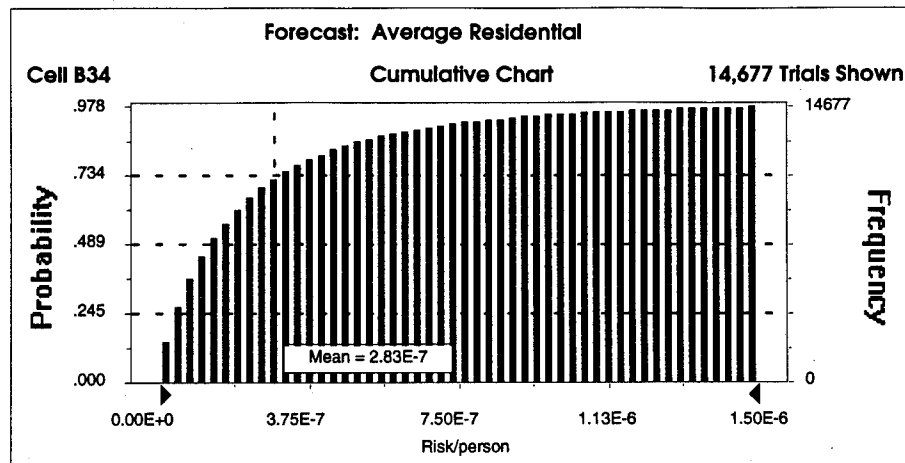| Statistics:	Value
Trials	15000
Mean	2.83E-07
Median (approx.)	1.47E-07
Mode (approx.)	1.68E-07
Standard Deviation	4.65E-07
Variance	2.16E-13
Skewness	9.06E+00
Kurtosis	2.07E+02
Coeff. of Variability	1.64E+00
Range Minimum	1.11E-10
Range Maximum	1.68E-05
Range Width	1.68E-05
Mean Std. Error	3.79E-09

Table C.3 Forecast: Average Residential

C-14

Figure C.4 Forecast: Average Residential (Cumulative)

Forecast: Average Residential (cont'd)	
Percentiles:	
Percentile	Risk/person (approx.)
0%	1.11E-10
10%	2.21E-08
20%	4.42E-08
30%	7.10E-08
40%	1.03E-07
50%	1.47E-07
60%	2.05E-07
70%	2.81E-07
80%	4.13E-07
90%	6.64E-07
100%	1.68E-05

Table C.4 Forecast: Average Residential (Percentiles)
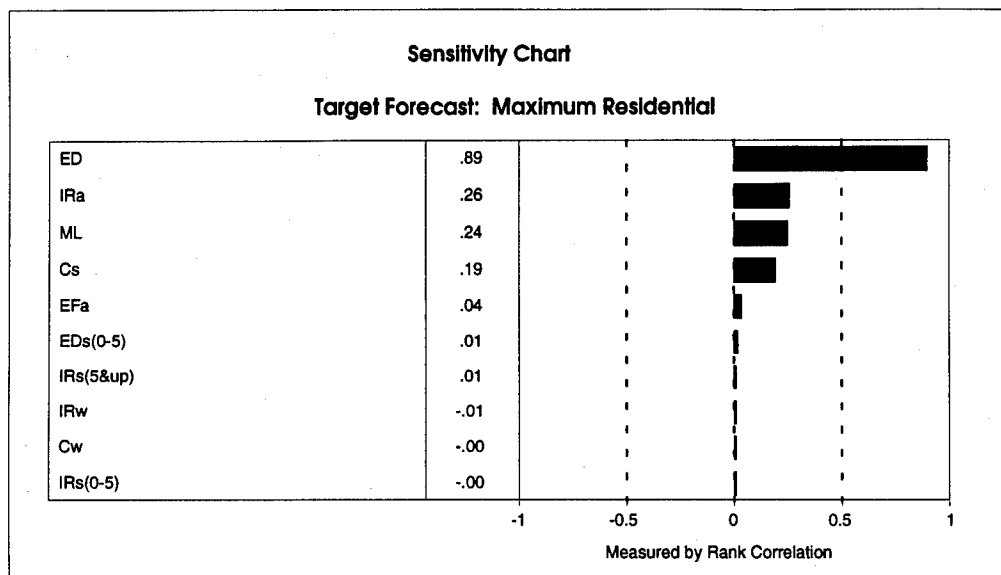
Figure C.5 Sensitivity Chart: Maximum Residential

Forecast: Maximum Residential

Summary:
   Display Range is from 0.00E+0 to 1.50E-5 Risk/person
   Entire Range is from 1.31E-9 to 8.65E-5 Risk/person
   After 15,000 Trials, the Std. Error of the Mean is 3.57E-8

Statistics:	Value
Trials	15000
Mean	3.42E-06
Median (approx.)	1.96E-06
Mode (approx.)	8.67E-07
Standard Deviation	4.37E-06
Variance	1.91E-11
Skewness	3.63E+00
Kurtosis	2.87E+01
Coeff. of Variability	1.28E+00
Range Minimum	1.31E-09
Range Maximum	8.65E-05
Range Width	8.65E-05
Mean Std. Error	3.57E-08

Table C.5 Forecast: Maximum Residential

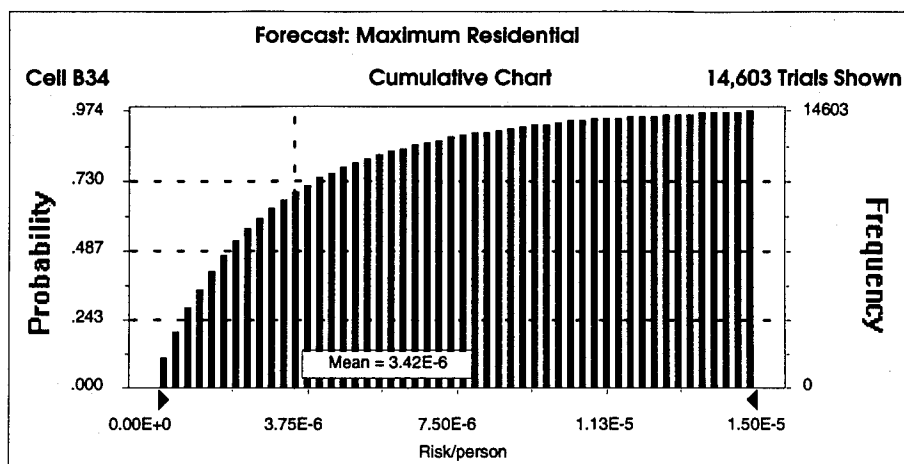Figure C.6 Forecast: Maximum Residential (Cumulative)

Forecast: Maximum Residential (cont'd)

Percentiles:

Percentile	Risk/person (approx.)
0%	1.31E-09
10%	2.81E-07
20%	5.85E-07
30%	9.68E-07
40%	1.41E-06
50%	1.96E-06
60%	2.70E-06
70%	3.70E-06
80%	5.25E-06
90%	8.31E-06
100%	8.65E-05

Table C.6 Forecast: Maximum Residential (Percentiles)

Sensitivity Chart

Target Forecast: Residential Soil Hazard Index

IRs(0-5)	.94	
BW 0-5	-.26	
IRs(5&up)	.15	
Bw 6-18	-.01	
BW 18&up	-.01	

-1   -0.5   0   0.5   1
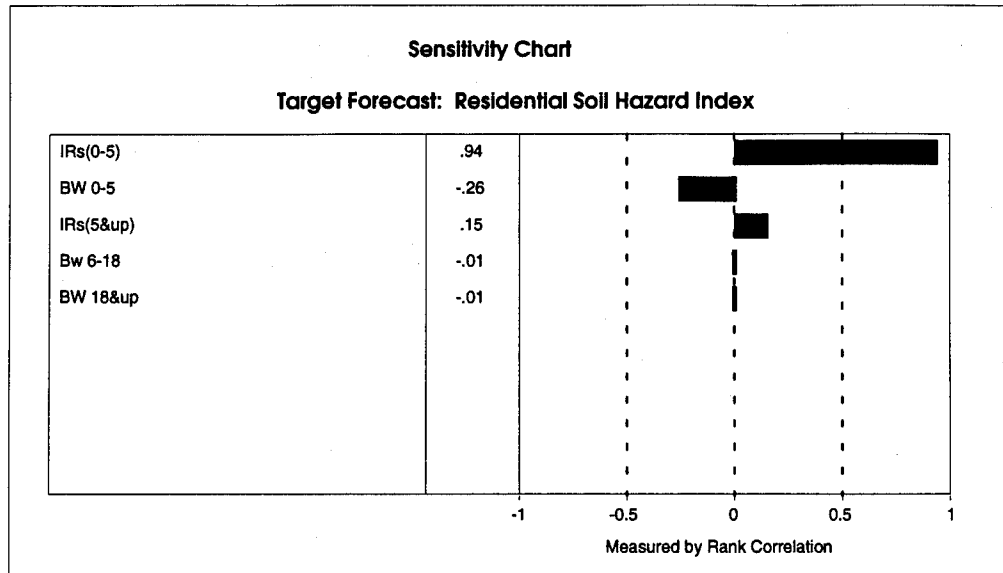
Measured by Rank Correlation

Figure C.7 Sensitivity Chart: Residential Soil Hazard Index

Forecast: Residential Soil Hazard Index

Summary:
    Display Range is from 0.000 to 0.045 Hazard Index
    Entire Range is from 0.001 to 0.104 Hazard Index
    After 15,000 Trials, the Std. Error of the Mean is 0.000

Statistics:	Value
Trials	15000
Mean	0.016
Median (approx.)	0.013
Mode (approx.)	0.009
Standard Deviation	0.009
Variance	0.000
Skewness	2.013
Kurtosis	9.674
Coeff. of Variability	0.598
Range Minimum	0.001
Range Maximum	0.104
Range Width	0.103
Mean Std. Error	0.000

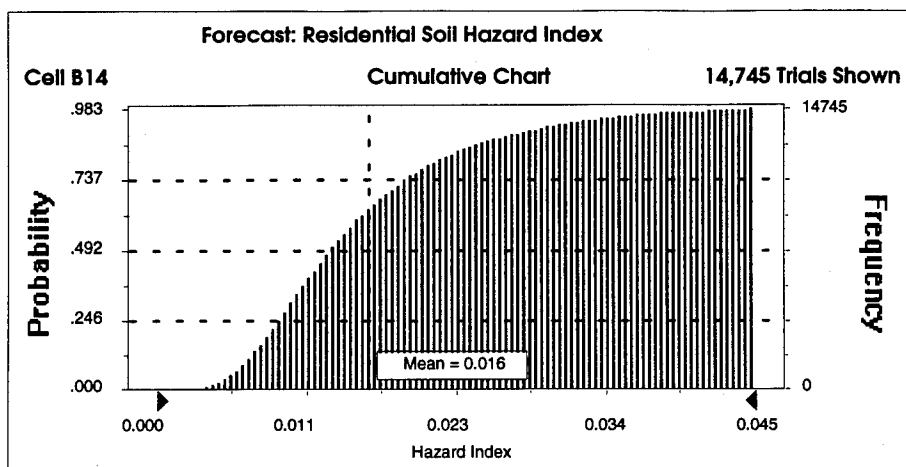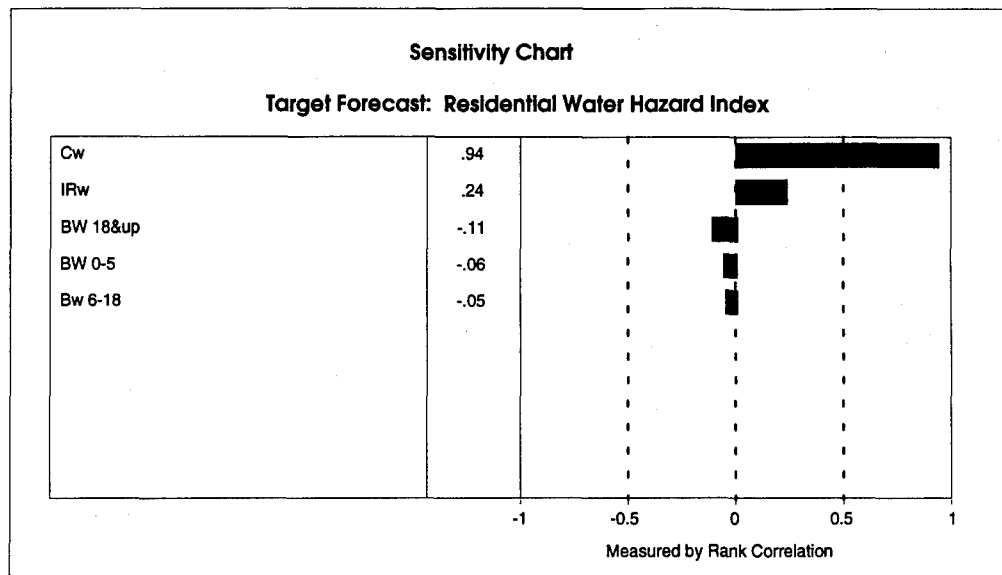Table C.7 Forecast: Residential Soil Hazard Index

Figure C.8 Forecast: Residential Soil Hazard Index (Cumulative)

Forecast: Residential Soil Hazard Index (cont'd)

Percentiles:

Percentile	Hazard Index (approx.)
0%	0.001
10%	0.007
20%	0.009
30%	0.010
40%	0.012
50%	0.013
60%	0.015
70%	0.018
80%	0.021
90%	0.028
100%	0.104

Table C.8 Forecast: Residential Soil Hazard Index (Percentiles)

Sensitivity Chart

Target Forecast: Residential Water Hazard Index

Cw	.94	
IRw	.24	
BW 18&up	-.11	
BW 0-5	-.06	
Bw 6-18	-.05	

Measured by Rank Correlation

Figure C.9 Sensitivity Chart: Residential Water Hazard Index

Forecast: Residential Water Hazard Index

Summary:
   Display Range is from 0.0000 to 0.0023 Hazard Index
   Entire Range is from 0.0000 to 0.0029 Hazard Index
   After 15,000 Trials, the Std. Error of the Mean is 0.0000

Statistics:	Value
Trials	15000
Mean	0.0008
Median (approx.)	0.0008
Mode (approx.)	0.0006
Standard Deviation	0.0005
Variance	0.0000
Skewness	0.3726
Kurtosis	2.4457
Coeff. of Variability	0.6234
Range Minimum	0.0000
Range Maximum	0.0029
Range Width	0.0029
Mean Std. Error	0.0000

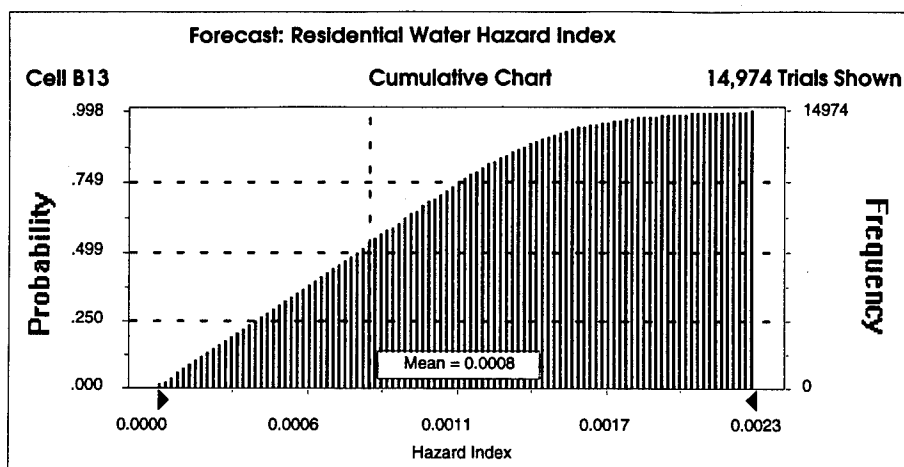Table C.9 Forecast: Residential Water Hazard Index

Figure C.10 Forecast: Residential Water Hazard Index

Forecast: Residential Water Hazard Index (cont'd)

Percentiles:

Percentile	Hazard Index (approx.)
0%	0.0000
10%	0.0002
20%	0.0003
30%	0.0005
40%	0.0006
50%	0.0008
60%	0.0009
70%	0.0011
80%	0.0012
90%	0.0015
100%	0.0029

Table C.10 Forecast: Residential Water Hazard Index (Percentiles)

Sensitivity Chart

Target Forecast: Background Occupational

OD	.77	
Cs	.53	
ML	.13	
IRa	.11	
EFa	.02	
IRs	-.00	

-1   -0.5   0   0.5   1

Measured by Rank Correlation
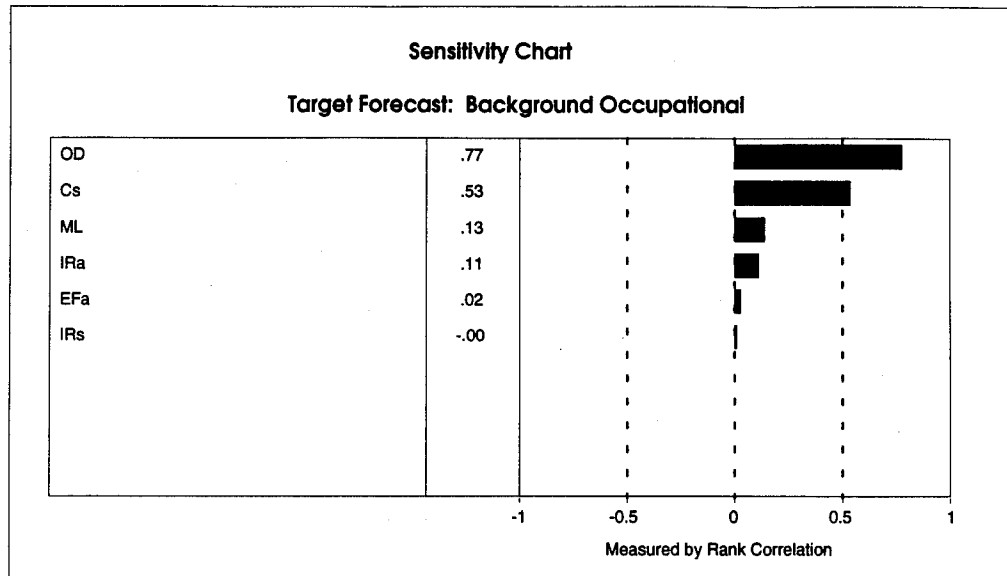
Figure C.11 Sensitivity Chart: Background Occupational

Forecast: Background Occupational

Summary:
Display Range is from 0.00E+0 to 8.00E-7 Risk/person
Entire Range is from 3.42E-12 to 7.08E-6 Risk/person
After 15,000 Trials, the Std. Error of the Mean is 2.00E-9

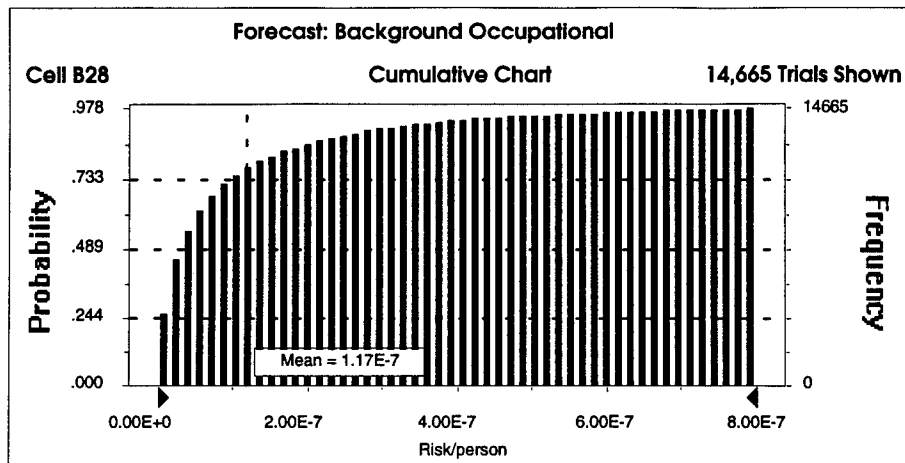| Statistics:	Value
Trials	15000
Mean	1.17E-07
Median (approx.)	4.05E-08
Mode (approx.)	7.08E-08
Standard Deviation	2.45E-07
Variance	5.98E-14
Skewness	6.95E+00
Kurtosis	9.52E+01
Coeff. of Variability	2.08E+00
Range Minimum	3.42E-12
Range Maximum	7.08E-06
Range Width	7.08E-06
Mean Std. Error	2.00E-09

Table C.11 Forecast: Background Occupational

Figure C.12 Forecast: Background Occupational (Cumulative)

Forecast: Background Occupational (cont'd)	
Percentiles:	
Percentile	Risk/person (approx.)
0%	3.42E-12
10%	6.39E-09
20%	1.28E-08
30%	1.92E-08
40%	2.76E-08
50%	4.05E-08
60%	5.90E-08
70%	8.98E-08
80%	1.49E-07
90%	2.91E-07
100%	7.08E-06

Table C.12 Forecast: Background Occupational (Percentiles)

Sensitivity Chart

Target Forecast: Average Occupational

OD	.78	
CsRCA	.41	
Cs	.30	
ML	.14	
IRa	.13	
EFa	.03	
IRs	.01	

-1   -0.5   0   0.5   1

Measured by Rank Correlation
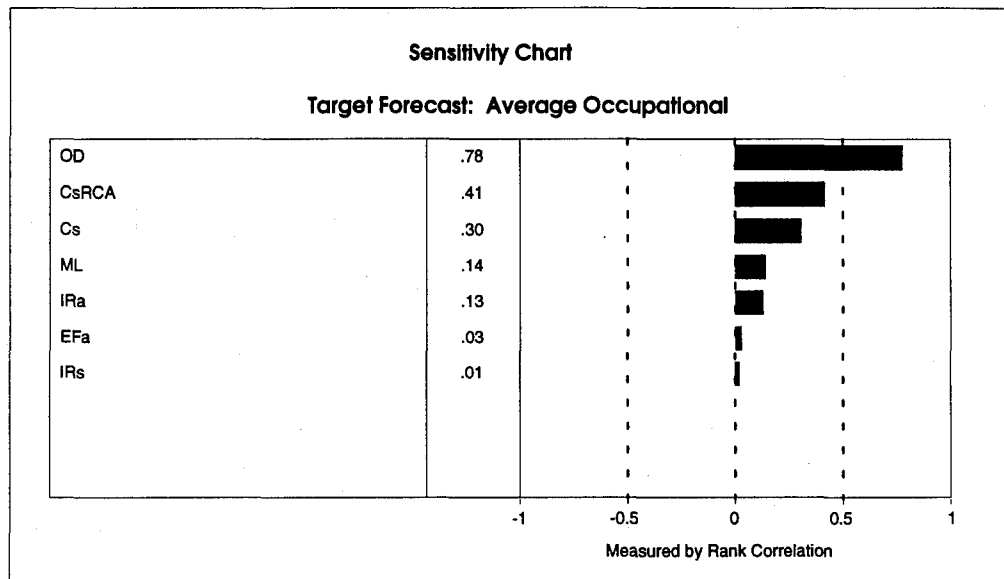
Figure C.13 Sensitivity Chart: Average Occupational

Forecast: Average Occupational

Summary:
    Display Range is from 0.00E+0 to 1.50E-6 Risk/person
    Entire Range is from 6.23E-10 to 2.37E-5 Risk/person
    After 15,000 Trials, the Std. Error of the Mean is 4.41E-9

Statistics:	Value
Trials	15000
Mean	1.43E-07
Median (approx.)	5.84E-08
Mode (approx.)	2.38E-07
Standard Deviation	5.41E-07
Variance	2.92E-13
Skewness	2.20E+01
Kurtosis	7.50E+02
Coeff. of Variability	3.77E+00
Range Minimum	6.23E-10
Range Maximum	2.37E-05
Range Width	2.37E-05
Mean Std. Error	4.41E-09

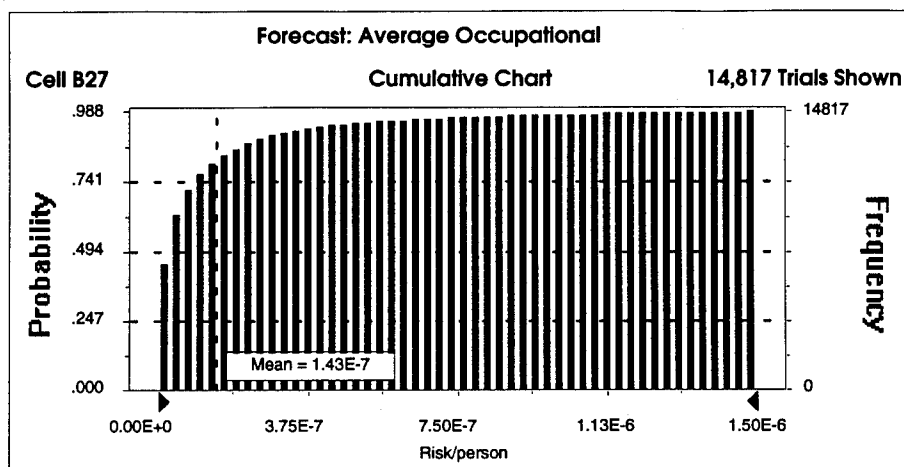Table C.13 Forecast: Average Occupational

Figure C.14 Forecast: Average Occupational (Cumulative)

Forecast: Average Occupational (cont'd)

Percentiles:

Percentile	Risk/person (approx.)
0%	6.23E-10
10%	1.22E-08
20%	2.37E-08
30%	3.53E-08
40%	4.68E-08
50%	5.84E-08
60%	6.99E-08
70%	8.94E-08
80%	1.50E-07
90%	3.01E-07
100%	2.37E-05

Table C.14 Forecast: Average Occupational (Percentiles)

Sensitivity Chart

Target Forecast: Maximum Occupational

OD	.91	
ML	.24	
IRa	.20	
Cs	.17	
CsRCA	.08	
EFa	.07	
IRs	.01	

-1   -0.5   0   0.5   1

Measured by Rank Correlation
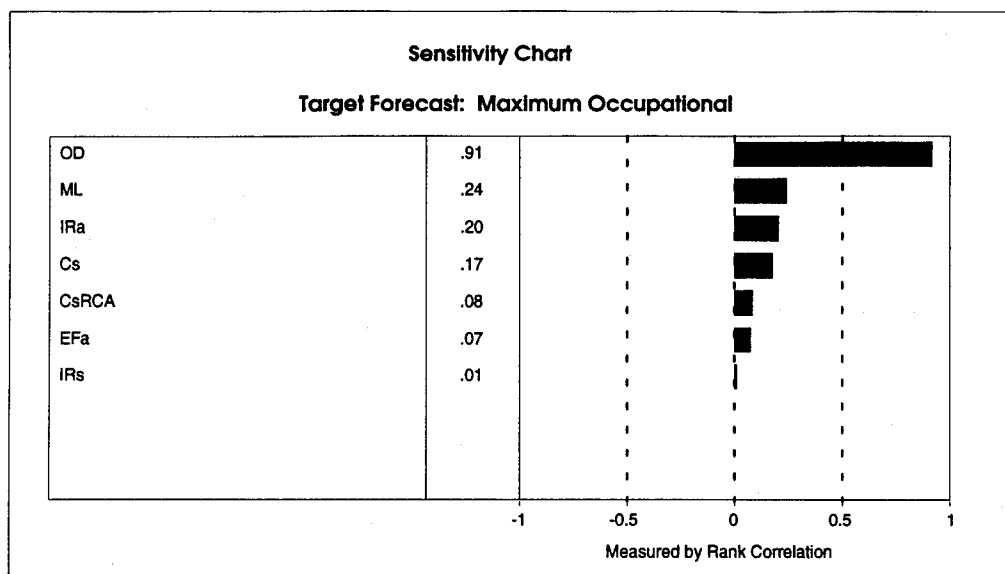
Figure C.15 Sensitivity Chart: Maximum Occupational

Forecast: Maximum Occupational

Summary:
　　Display Range is from 0.00E+0 to 6.00E-6 Risk/person
　　Entire Range is from 1.56E-8 to 5.18E-5 Risk/person
　　After 15,000 Trials, the Std. Error of the Mean is 1.54E-8

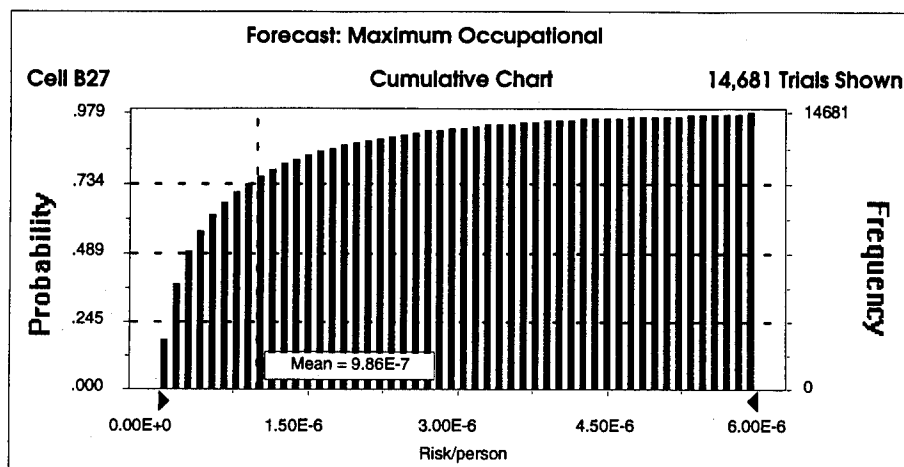| Statistics:	Value
Trials	15000
Mean	9.86E-07
Median (approx.)	3.71E-07
Mode (approx.)	5.34E-07
Standard Deviation	1.89E-06
Variance	3.57E-12
Skewness	7.59E+00
Kurtosis	1.19E+02
Coeff. of Variability	1.91E+00
Range Minimum	1.56E-08
Range Maximum	5.18E-05
Range Width	5.18E-05
Mean Std. Error	1.54E-08

Table C.15 Forecast: Maximum Occupational

Figure C.16 Forecast: Maximum Occupational (Cumulative)

Forecast: Maximum Occupational (cont'd)	
Percentiles:	
Percentile	**Risk/person (approx.)**
0%	1.56E-08
10%	7.12E-08
20%	1.27E-07
30%	1.83E-07
40%	2.73E-07
50%	3.71E-07
60%	5.44E-07
70%	8.25E-07
80%	1.31E-06
90%	2.43E-06
100%	5.18E-05

Table C.16 Forecast: Maximum Occupational (Percentiles)

Sensitivity Chart

Target Forecast: Occupational Soil Hazard Index

IRs(5&up)	.96	
BW 18&up	-.23	

-1   -0.5   0   0.5   1

Measured by Rank Correlation
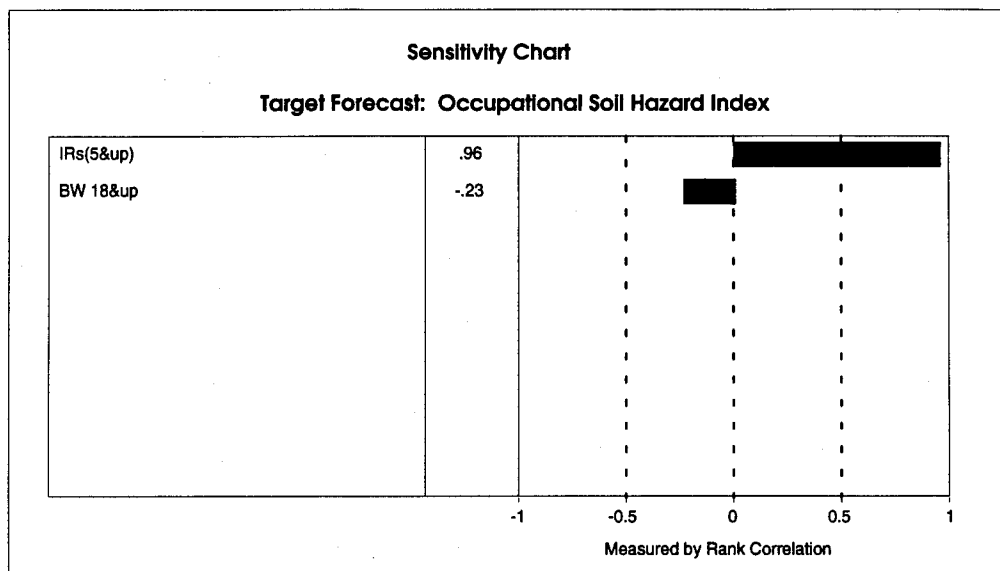
Figure C.17 Sensitivity Chart: Occupational Soil Hazard Index

---

Forecast: Occupational Soil Hazard Index

Summary:
     Display Range is from 0.0000 to 0.0035 Hazard Index
     Entire Range is from 0.0000 to 0.0038 Hazard Index
     After 15,000 Trials, the Std. Error of the Mean is 0.0000

Statistics:	Value
Trials	15000
Mean	0.0012
Median (approx.)	0.0011
Mode (approx.)	0.0006
Standard Deviation	0.0007
Variance	0.0000
Skewness	0.2754
Kurtosis	2.2633
Coeff. of Variability	0.6098
Range Minimum	0.0000
Range Maximum	0.0038
Range Width	0.0038
Mean Std. Error	0.0000

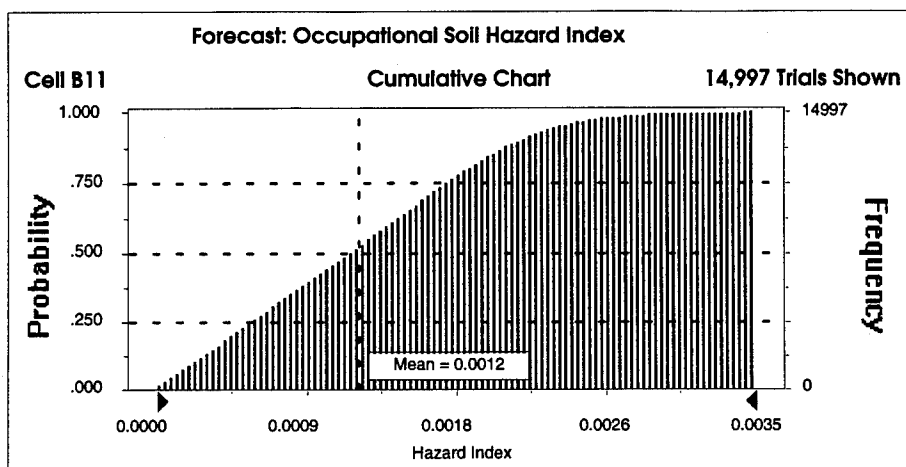Table C.17 Forecast: Occupational Soil Hazard Index

Figure C.18 Forecast: Occupational Soil Hazard Index

Forecast: Occupational Soil Hazard Index (cont'd)

Percentiles:

Percentile	Hazard Index (approx.)
0%	0.0000
10%	0.0002
20%	0.0005
30%	0.0007
40%	0.0009
50%	0.0011
60%	0.0014
70%	0.0016
80%	0.0019
90%	0.0022
100%	0.0038

Table C.18 Forecast: Occupational Soil Hazard Index (Percentiles)

Bibliography

1. Agency for Toxic Substances and Disease Registry. *Toxicological Profile for Uranium.* Series No. TP-90-29. Atlanta GA: U.S. Department of Health & Human Services, Public Health Services, December 1990.

2. Air Force Developmental Test Center. *AFDTC Technical Facilities, Volume II - Land Test Areas.* Eglin Air Force Base FL: AFDTC 3246 TESTW/EAST, December 1991.

3. Andrew, S.P., R.D. Caligiuri, and L.E.Eiselstein. "A Review of Penetrator Mechanisms and Dynamic Properties of Tungsten and Depleted Uranium Penetrators," *Tungsten and Tungsten Alloys -- Recent Advances.* Andrew Crowson and Edward S. Chen (Eds.). The Minerals, Metals & Materials Society, 1991.

4. Anspaugh, L.R. "The Use of NTS Data and Experience to Predict Air Concentrations of Plutonium Due to Resuspension of the Enewetak Atoll," *The Dynamics of Plutonium in Desert Environments*, P.B. Dunaway and M.G. White (Eds.), USAEC Report No. NVO-142. Nevada Operations Office: NTIS, 1974.

5. Arbuckle, J. Gordon. *Environemntal Law Handbook.* (12th Edition). Rockville MD: Governemnt Institues, Inc., 1993.

6. Arkin, W.M. "The Desert Glows---with Propaganda," *Bulletin of the Atomic Scientists*, Vol. 45 No. 4: 11-12+ (1993).

7. Athey, Thomas H. *Systematic Systems Approach: An Integrated Method for Solving Systems Problems.* Englewood Cliffs NJ: Prentice-Hall, Incorporated, 1982

8. Barr, D. E., A. Maristany and T. Kwader. *Water Resources of Southern Okaloosa and Walton Counties, Northwest Florida: Summary of Investigation.* Water Resources Assessment No. 81-1. Havana FL: Northwest Florida Water Management District, 1981.

9. Barr, D.E., L. R. Hayes and T. Kwader. *Hydrology of the Southern Parts of Okaloosa and Walton Counties, Northwest Florida, with Special Emphasis on the Upper Limestone of the Floridan Aquifer.* U.S. Geological Survey Water-Resources Investigations Report 84-4305. Tallahassee FL: U.S. Geological Survey, 1985.

10. Bear, J. and Verruijt A. *Modeling Groundwater Flow and Pollution.* Netherlands: D. Reidel Publishing Company, 1990.

11. Becker, Naomi M. Soil and sediment sample summary data. Unpublished memo. Los Alamos National Laboratory, Los Alamos NM, 9 April 1992.

12. Becker, Naomi M., Elizabeth B. Vanta, and Richard C. Crews. *Environmental Monitoring for Depleted Uranium at Eglin Air Force Base Test Areas C-64, C-64C, and C-74L, 1974-1988.* AFATL-TR-89-40. Eglin Air Force Base FL: Air Force Armament Laboratory, 1989.

13. Becker, Naomi M., Elizabeth B. Vanta, and Richard C. Crews. *Uranium Transport Investigation at Eglin Air Force Base*, Draft review copy. Eglin Air Force Base FL: Air Force Armament Laboratory, 1994.

14. Bramlitt, Edward T. and Nels R. Johnson. *The Segmented Gate Systems for the Volume Reduction of Plutonium-Contaminated Soil.* [Albuquerque NM: Thermal Analytical, Incorporated], unpublished.

15. Brown, S.M. et al. *Application of the Observational Method to Remediation of Hazardous Waste Sites.* Bellevue WA: CH2M Hill, April 1989.

16. Bureau of the Census. *1990 Census of Population and Housing.* Washington DC: U.S. Department of Commerce, 1994.

17. Burley, Gordon. *Transuranic Elements: Volume 1 - Elements of Radiation Protection.* Report No. EPA 520/1-90-015. Washington DC: Office of Radiation Programs, U.S. Environmental Protection Agency, June 1990.

18. Burmaster, David E. and Katherine Von Stackelberg. "Using Monte Carlo Simulations in Public Health Risk Assessments: Estimating and Presenting Full Distributions of Risk," *Journal of Exposure Analysis and Environmental Epidemiology, Vol. 1, No. 4*: 491-512 (1991).

19. Bush, P.W. and R.H. Johnston. *Ground-Water Hydraulics, Regional Flow, and Ground-Water Development of the Floridian Aquifer System in Florida and In Parts of Georgia, South Carolina, and Alabama.* U.S. Geological Survey Professional Paper 1403-C. Washington: GPO, 1988.

20. Clark, I. *Practical Geostatistics*, Essex England: Applied Science Publishers, 1979.

21. Copeland, Teri L. and others. "Comparing the Results of a Monte Carlo Analysis with EPA's Reasonable Maximum Exposed Individual (RMEI): A Case Study of a Former Wood Treatment Site," *Regulatory Toxicology and Pharmacology, Vol. 18*: 275-312 (1993).

22. *Crystal Ball Version 3.0 User's Manual: Forecasting and Risk Analysis for Spreadsheet Users*. Denver CO: Decisioneering, Inc, 1993.

23. Domenico, Patrick A. and Franklin W. Schwartz. *Physical and Chemical Hydrogeology*. New York: John Wiley & Sons, Incorporated, 1990.

24. Ebinger, M.H. and others. *Long-Term Fate of Depleted Uranium at Aberdeen and Yuma Proving Grounds Final Report, Phase I: Geochemical Transport and Modeling*. Los Alamos NM: Los Alamos National Laboratory, June 1990.

25. *Environmental Assessment for Depleted Uranium Waste Disposal at Eglin AFB, FL*. Oakridge TN: Oak Ridge National Laboratory, October 1986.

26. *Fernald Environmental Management Project FY 1992, Environmental Restoration and Waste Management Site Specific Plan*. PL-3010, Rev 0. Cincinnati OH: Westinghouse Environmental Management Company of Ohio, 11 September 1991.

27. Ficklin, Don L. TA C-64 Site Chief, Vitro Services Corporation. Personal interview. 21 June 1994.

28. Freeze, R. Allan and John A. Cherry. *Groundwater*. Englewood Cliffs NJ: Prentice-Hall, Incorporated, 1979.

29. Gianti, S. et al. *The Streamlined Approach for Environmental Restoration*. Reston VA: CH2M Hill, 1993.

30. Gianti, Samuel J. Environemntal Scientist, CH2M Hill, Herndon, VA. Personal interview. 1994.

31. Glickman, Joan. "A Superfund Retrospective: Past, Present, and..." *Public Management*: 4-8 (February 1994).

32. Hall, Arthur D. *A Methodology for Systems Engineering*. Princeton NJ: D. Van Nostrand Company, 1962.

33. Hall, Arthur D. "Three-Dimensional Morphology of Systems Engineering," *IEEE Transactions on Science and Cybernetics, Vol. SSC-5*: 156-160 (April 1969).

34. Hasofer, Abraham M. and Niels C. Lind. "Exact and Invariant Second-Moment," *Journal of the Engineering Mechanics Division, Vol. 100, No. EM1*: 111-121 (February 1974).

35. Healy, J.W. *A Proposed Interim Standard for Plutonium in Soils*. USAEC Report No. LA-5483-MS. Los Alamos NM: Los Alamos Scientific Laboratory, 1974.

36. Healy, J.W. "Review of Resuspension Models," *Transuranic Elements in the Environment: A Summary of Environmental Research on Transuranium Radionuclides Funded by the U.S. Department of Energy Through Calendar Year 1979*. Report No. DOE/TIC-22800. Springfield VA: U.S. Department of Energy Technical Information Center, 1980.

37. Hill, J.D. and J.N. Warfield. "Unified Program Planning," *IEEE Transactions on Systems, Man, and Cybernetics, Vol. SMC-2, No. 5*: 610-621 (November 1972).

38. International Ground Water Modeling Center. *INFIL*. Course notes. Golden CO: Colorado School of Mines, 1983.

39. International Ground Water Modeling Center. *Practical Modeling of Three-Dimensional Contaminant Transport and Remedial Designs Using Modular Flow and Transport Models (MODFLOW/MT3D)*. Course notes. Golden CO: Colorado School of Mines, 24-27 January 1994.

40. International Ground Water Modeling Center. *Principles and Applications of MODFLOW and Accompanying Modules*. Course notes. Golden CO: Colorado School of Mines, 22-25 March 1994.

41. *International Station Meteorological Climate Summary U.S. Navy - U.S. Air Force*. Version 2.0. Ashville: Federal Climate Complex, June 1992.

42. Jernigan, Robert W. *A Primer on Kriging*. Washington DC: U.S. Environmental Protection Agency, February 1986.

43. Johnson, Nels R. President, Thermo Analytical Inc, Albequerque, NM. Personal interview. October 1994.

44. Longest, H.L. *Total Quality Management (TQM) and Quality Assurance (QA) in Superfund*. Memorandum from Office of Emergency and Remedial Response. Washington DC: U.S. Environmental Protection Agency, 5 December 1990.

45. Maidment, David R. (Ed.) *Handbook of Hydrology*. New York: McGraw-Hill, Incorporated, 1992.

46. Mallory, Charles W., William S. Sanner, and John G. Funk. *Alternatives for Disposal of Depleted Uranium Waste*. Report No. AFATL-TR-85-78. Eglin Air Force Base FL: Air Force Armament Laboratory, November 1985.

47. *Mathcad 5.0® Plus User's Guide Windows Version.* Cambridge MA: Mathsoft Inc., 1994.

48. McDonald, Michael G. and Arlen W. Harbaugh. *Techniques of Water-Resources Investigations of the United States Geological Survey: A Modular Three-Dimensional Finite-Difference Ground-Water Flow Model.* Book 6, Chapter A1. Washington: GPO, 1988.

49. Mosard, Gil R. "A Generalized Framework and Methodology for Systems Analysis," *IEEE Transactions on Engineering Management, Vol. EM-29, No. 3*: 81-87 (August 1982).

50. Myrick, T. E., B. A. Bervin and F. F. Haywood. *State Background Radiation Levels: Results of Measurements Taken During 1975-1979.* ORNL/TM-7343. Oak Ridge TN: Oak Ridge National Laboratory, November 1981.

51. National Archives and Records Administration. *Protection of Environemnt.* 40 CFR Parts 300 to 399. Washington: Office of the Federal Register, 1 July 1993.

52. National Research Council Committee on the Biological Effects of Ionizing Radiation. *Effects on Population of Low Levels of Ionizing Radiation: 1980.* Washington: National Academy Press, 1980.

53. Neptune, Dean, Austin L. Moorehead, and Daniel I. Michael. *Streamlining Superfund Soil Studies: Using Data Quality Objectives Process for Scoping.* Technical Report No. RD-680. Washington: U.S. Environmental Protection Agency, undated.

54. Novak, Joseph D. and D. Bob Gowin. *Learning How to Learn.* New York: Cambridge University Press, 1984.

55. Office of Emergency and Remedial Response. *Data Quality Objectives Process for Superfund Interim Final Guidance.* pre-publication copy. Report No. EPA/540/G-93/071. Washington: U.S. Environmental Protection Agency, September 1993.

56. Office of Emergency and Remedial Response. *Health Effects Assessment Summary Tables, FY 1992 Annual.* Report No. OERR 9200.6-303 (92-1). Washington: U.S. Environmental Protection Agency, March 1992.

57. Office of Emergency and Remedial Response. *Risk Assessment Guidance for Superfund: Volume 1 - Human Health Evaluation Manual (Part B, Development of Risk-Based Preliminary Remediation Goals) (Interim).* Report No. EPA/540/R-92/003. Washington: U.S. Environmental Protection Agency, December 1991.

58. Office of Health and Environmental Assessment, Exposure Assessment Group. *Exposure Factors Handbook.* Report No. EPA/600/8-89/043. Springfield VA: National Technical Information Service, July 1989.

59. Office of Radiation Protection, U.S. Environmental Protection Agency. *Risk Assessment Methodology, Environmental Impact Statement for National Emissions Standards for Hazardous Air Pollutants (NESHAPS) Radionuclides: Volume 1 - Background Information Document.* Report No. EPA 520/1-89-005. Springfield VA: NTIS, September 1989.

60. Rao, Singiresu S. *Reliability-Based Design.* New York: McGraw-Hill, Incorporated, 1992.

61. Rau, John G. and David C. Wooten. *Environmental Impact Analysis Handbook.* New York: McGraw-Hill Book Company, 1980.

62. Royce, A. and others. *Geostatistics.* New York: McGraw-Hill, Incorporated, 1980.

63. Saaty, Thomas L. *The Analytic Hierarchy Process: Planning, Priority Setting, Resource Allocation.* (2nd Edition). Pittsburgh PA: RWS Publications, 1990.

64. Sage, Andrew P. "A Case for a Standard For Systems Engineering Methodology," *IEEE Transactions on Systems Man, and Cybernetics, Vol. SMC-7, No. 7:* 499-504 (July 1977).

65. Sage, Andrew P. *Methodology for Large-Scale Systems.* New York: McGraw-Hill, Incorporated, 1977.

66. Shleien, B. and others. *The Fernald Dosimetry Reconstruction Project, Tasks 1 through 5.* Neese SC: Radiological Assessments Corporation, May 1993.

67. Thompson, S.K. *Sampling.* New York: John Wiley & Sons, Incorporated, 1992.

68. Till, J. E. ed. and H. R. Meyer. ed. *Radiological Assessment: A Textbook on Environmental Dose Analysis.* NUREG/CR-3332. Washington: U.S. Nuclear Regulatory Commission, September 1983.

69. Trapp, Henry, Jr., C. A. Pascale, and J.B. Foster. *Water Resources of Okaloosa County.* U.S. Geological Survey Water-Resources Investigations 77-9. Tallahassee FL: U.S. Geological Survey, August 1977.

70. Williams, Cindy and Gordon Crawford. *The Analysis of Subjective Judgment Matrices*. Rand Report No. R2572-1-AF. Santa Monica CA: Rand Corporation, 1980.

Vita

Captain Charles M. Carter was born on 18 February 1961 in Buffalo, New York. He graduated from the University of Illinois at Urbana-Champaign with a Bachelor of Science in Aeronautical and Astronautical Engineering in 1989. He enlisted in the U.S. Air Force in 1979 and served as a Law Enforcement Specialist at Dyess AFB, Texas and Ft Lewis, Washington before entering a commissioning program in 1986. After completing his engineering degree and receiving a commission as an Air Force officer, Capt Carter worked as a Titan satellite launch engineer at Vandenberg Air Force Base from 1989 to 1993. Captain Carter entered the Graduate Systems Engineering Program, School of Engineering, Air Force Institute of Technology in May 1993. Capt Carter's immediate family includes wife Lela Joy Carter and children Christopher Michael, Brittany Marie, and Kyle Matthew.

Permanent Address: 1497 Love Road, Grand Island, New York   14072

Major Kristina M. Fortmann was born on 29 December 1958 in Springfield, Ohio. She graduated from the University of Washington with a Bachelor of Science in Aeronautical and Astronautical Engineering in June 1983. Maj Fortmann also attended the United States Test Pilot School course for engineers in 1987 and completed a Master of Aeronautical Science degree from Embry-Riddle Aeronautical University in 1993. She was assigned to the Air Force Flight Test Center as a flight test engineer and program manager for KC-135 aerial refueling and F-16 systems projects from 1983 to 1989. Maj Fortmann then worked at the Air Force Development Test Center as a flight test lead engineer on F-16 structural tests from 1989 to 1993. Maj Fortmann entered the Graduate Systems Engineering Program, School of Engineering, Air Force Institute of Technology in May 1993. Maj Fortmann's immediate family includes husband Troy Andrew Fortmann.

Permanent Address: 15210 163rd Place NE, Woodinville, Washington, 98072

Captain Stephen W. Hill was born on 16 April 1967 in Cincinnati, OH. He graduated from the Ohio Northern University with a Bachelor of Science in Electrical Engineering in May 1989. Capt Hill worked as a communications engineer for the 1912th Computer Systems Group at Langley Air Force Base from 1989 to 1993. Captain Hill entered the Graduate Systems Engineering Program, School of Engineering, Air Force Institute of Technology in May 1993. Capt Hill's immediate family includes wife Lorraine Allebach Hill and child Joshua Brandon.

Permanent Address: 188 Walnut Street, Cedarville, OH 45314

Captain Robert M. Latin was born on 25 August 1963. He graduated from the Ohio State University with a Bachelor of Science in Aeronautical and Astronautical Engineering in June 1989. The then Sgt Latin trained for and worked as an F-4E weapons control systems technician at Lowery, Seymour Johnson, and Ramstein Air Force Bases from 1982 to 1986. After completing his engineering degree and receiving a commission as an Air Force officer, he worked as a sensor engineer for the Defense Meteorological Satellite Program (1989-1990), as an engineer for the Non-Chemical Propulsion Laboratory Aerospace Corporation (1990-1991), and as a software manager for the Global Positioning System (1991-1993) at Los Angeles Air Force Station. Captain Latin entered the Graduate Systems Engineering Program, School of Engineering, Air Force Institute of Technology in May 1993. Capt Latin's immediate family includes wife Captain Anita E. Latin.

Permanent Address: FA 43 RD 3, Harrisburg, PA 17112

Captain Edward J. Masterson was born on 10 June 1966 in Boston, MA. He graduated from the Worchester Polytechnic Institute with a Bachelor of Science in Mechanical Engineering in May 1988. Capt Masterson worked as an aircraft design engineer for Wright Laboratory at Wright Patterson Air Force Base (WPAFB) from 1989 to 1991. He then worked as an F-16 structural loads engineer at the F-16 System Program Office from 1991 to 1993 at WPAFB. Captain Masterson entered the Graduate Systems Engineering Program, School of Engineering, Air Force Institute of Technology in May 1993.

Permanent Address: 31 Stratford Road, Natick, MA 01760

Captain Joseph A. Roh was born on 4 June 1965 in Seattle, Washington. He graduated from the United States Air Force Academy with a Bachelor of Science in Aeronautical Engineering in June 1988. Capt Roh worked as a test and evaluation manager for the Delta launch Vehicle and the Atlas Launch vehicle/payload integration loads at Los Angeles Air Force Station from 1988 to 1993. Captain Roh entered the Graduate Systems Engineering Program, School of Engineering, Air Force Institute of Technology in May 1993. Capt Roh's immediate family includes wife Dianne E. Roh.

Permanent Address: 5487 Corkhill Drive, Dayton, OH 45424

2nd Lieutenant Sujay R. Setlur was born on 24 August 1971 in Bangalore, India and became a naturalized United States citizen. He graduated from Worchester Polytechnic Institute with a Bachelor of Science in Mechanical Engineering in May 1993. 2nd Lieutenant Setlur entered the Graduate Systems Engineering Program, School of Engineering, Air Force Institute of Technology in May 1993.

Permanent Address: 51 Wilson Street, Framingham, MA 01701

REPORT DOCUMENTATION PAGE

Form Approved
OMB No. 0704-0188

1. AGENCY USE ONLY (Leave blank)	2. REPORT DATE	3. REPORT TYPE AND DATES COVERED
	December 1994	Master's Thesis

4. TITLE AND SUBTITLE

A SYSTEMS ENGINEERING APPROACH TO ENVIRONMENTAL RISK MANAGEMENT: A CASE STUDY OF DEPLETED URANIUM AT TEST AREA C-64 AT EGLIN AIR FORCE BASE, FLORIDA

5. FUNDING NUMBERS

6. AUTHOR(S)   Kris M. Fortmann, Major, USAF

Charles M. Carter, Capt, USAF   Stephen W. Hill, Capt, USAF
Robert M. Latin, Capt, USAF   Edward J. Masterson, Capt USAF
Joseph A. Roh, Capt, USAF   Sujay R. Setlur, 2Lt, USAF

7. PERFORMING ORGANIZATION NAME(S) AND ADDRESS(ES)

Air Force Institute of Technology, WPAFB OH 45433-6583

8. PERFORMING ORGANIZATION REPORT NUMBER

AFIT/GSE/ENY/94D-1

9. SPONSORING / MONITORING AGENCY NAME(S) AND ADDRESS(ES)

WL/MNSE, Environmental Assessment Branch
101 West Eglin Boulevard, Eglin Air Force Base
Florida 34542-6810

10. SPONSORING / MONITORING AGENCY REPORT NUMBER

11. SUPPLEMENTARY NOTES

12a. DISTRIBUTION / AVAILABILITY STATEMENT

Approved for public release; distribution unlimited

12b. DISTRIBUTION CODE

13. ABSTRACT (Maximum 200 words)

This case study used the systems engineering technique to determine human health risk and to provide risk management guidelines with respect to depleted uranium (DU) contamination at test area (TA) C-64 in Eglin Air Force Base, Florida. We applied a systems engineering methodology consisting of the following steps: defining the problem, setting objectives, developing alternatives, modeling alternatives, evaluating alternatives, selecting alternatives, and planning for implementation. We performed kriging on available soil data to determine the present state of DU contamination around the radiation control area. We used the results from this analysis to determine the probability of contaminant infiltration into the groundwater and air transport pathways. Using the TA site characterization, we performed Monte Carlo simulation analysis to determine residential and occupational health risks to humans with respect to present and future land use. Carcinogenic risks ranged from approximately 10E-5 to 10E-10; the non-carcinogenic risks were statistically insignificant. The main pathway of concern was the inhalation pathway for the residential and occupational land use scenarios. For residential land use, a remediation method using a soil cleaning technique including volume reduction was selected. For occupational land use, further air sampling was recommended to reduce the uncertainty in the analysis.

14. SUBJECT TERMS

15. NUMBER OF PAGES

327

16. PRICE CODE

17. SECURITY CLASSIFICATION OF REPORT	18. SECURITY CLASSIFICATION OF THIS PAGE	19. SECURITY CLASSIFICATION OF ABSTRACT	20. LIMITATION OF ABSTRACT
Unclassified	Unclassified	Unclassified	UL